UNIVERSITÉ PARIS DESCARTES

THESE

Ecole doctorale BioSPC

Spécialité Neurosciences

Présentée par

Mariana Ramos-Brossier

Pour obtenir le grade de

DOCTEUR DE L'UNIVERSITE PARIS DESCARTES

Unraveling the impact of *IL1RAPL1* mutations on synapse formation: towards potential therapies for intellectual disability

Sous la direction du **Dr. Pierre Billuart**

Soutenue le 9 octobre 2015, devant le jury composé de :

Dr. Barbara Bardoni	Rapportrice
Dr. Cyrille Vaillend	Rapporteur
Dr. Patricia Gaspar	Examinatrice
Dr. Yann Humeau	Membre invité
Dr. Pierre Billuart	Directeur de thèse

REMERCIEMENTS

Je remercie avant tout Pierre Billuart pour sa grande disponibilité et pour sa direction tout au long de cette thèse. Je lui suis reconnaissante de m'avoir fait confiance et m'avoir donné une grande liberté. Merci pour ces 4 années et tout ce qu'elles m'ont apporté scientifiquement et humainement.

Je remercie les docteurs Barbara Bardoni, Cyrille Vaillend et Patricia Gaspar pour le temps consacré à l'évaluation et à la critique de ce travail.

Un grand merci à tous les collaborateurs qui ont enrichi ce travail:

Yann Humeau à Bordeaux, pour ses commentaires et sa collaboration tout au long de ce travail de thèse, et pour m'avoir initié à l'électrophysiologie. Je remercie aussi les membres de son équipe, Xander, Etienne, Christelle, Marylin, Elizabeth pour leur aide précieuse et leur bonne humeur.

Ringrazio Carlo Sala e Caterina Montani a Milano per la loro collaborazione, che e stata une esperienza molto gratificante.

Hamid Meziane et Yann Hérault à Illkich, pour les études de comportement. Jozef Gecz and Anna Hacket in Australia, and Franck Kooy and Bart Loeys in Belgium, for their invaluable contribution to the genetics studies.

Un grand merci à l'Ecole des Neurosciences de Paris, non seulement pour le financement, mais aussi pour leur soutien logistique dès mon arrivé à Paris, et pour m'avoir offert l'opportunité d'appartenir à ce grand réseau. Merci particulièrement à Jean Antoine Girault, Yvette Henin, Andre Sobel, Laura et Deborah. Je remercie également la Fondation EDF, qui m'a permis de travailler une année de plus pour terminer mes travaux en cours.

Je remercie l'Université Paris Descartes, et à Michelle Pitte pour l'aide administrative.

Merci à tous les membres de l'Institut Cochin qui sourient (ou pas) dans les couloirs, et à Agnès Fouet pour sa bienveillance. Merci aux plateformes de l'Institut Cochin sans lesquelles ce travail n'aurait pas pu avoir lieu, spécialement la plateforme de microscopie (Béatrice, Thomas et Pierre) pour leur aide et expertise précieuse, ainsi qu'à l'animalerie.

Un énorme merci aux membres de l'équipe BiBi:

Jamel Chelly pour m'avoir accueilli dans son équipe et pour ses conseils précieux.

Olivier pour son conseil scientifique; Nicolas pour ses critiques toujours constructives et son aide précieuse; Chloé pour sa bonne humeur et son exemple de travail ; Yoann a pesar de que nuestra relación tuvo un inicio tormentoso, gracias por tu ayuda siempre.

Ainsi qu'à à tous les membres présents et passés du laboratoire : Thierry, Nadia, Laurence, Karine, Juliette, Giuseppe, Adelyn, Léa, Audrey, Loïc, Julia, Miriam, Christine, Adrienne, Devina, Justine, Matthieu, Laure Elise, Anne, Benjamin, Pang, France, Madison, Cécile, Remi, Bénédicte, Marine, Mélanie, Claire, Hamida, Sylvain…

Je voudrais remercier particulièrement les membres de la plateforme 5004 pour leur amitié et les bonbons partagés au rythme de radio latina: Rodrick, pour faire monter la température dans le bureau; Julie pour toutes les discussions et pour être toujours à l'écoute; Flora pour sa franchise et son énergie; Julien pour partager mes peines de neurones; et Laetitia pour sa grande gentillesse, repose en paix.

Pendant cette thèse j'ai eu l'opportunité d'encadrer Geoffroy Goujon, que je remercie pour son aide technique et son optimisme. C'était une grande expérience pour moi, et je lui souhaite beaucoup de réussite pour la suite.

Merci à Maryse pour son efficacité imbattable et sa bonne humeur, et à Josiane, Nathalie, Mireille et Annick pour l'animation dans les couloirs du 5ème.

Merci à Julie Dam, Ralph Jokers, Denis Hervé, Salah El Mestikawy, Diana Sakae et Bruno Ragazzon pour leur aide et conseils techniques.

Gracias a Magda Giordano y Ranulfo Romo por sus consejos, y por apoyarme y alentarme a venir a Francia.

Merci à toutes les personnes qui ont réaffirmé mon engagement envers la vulgarisation scientifique, et qui m'ont permis d'apprendre et de m'améliorer. A tous ceux qui ont subi les présentations, résumés, posters et explications, et qui ont survécu pour me dire ce qui n'était pas clair.

À mes parents, ma famille et à mes amis, au loin mais près au même temps, et à ceux qui m'ont entouré, motivé et inspiré depuis mon arrivée en France. A Ximena por estar ahí siempre, y en todos lados. A Benjas, Lalo y Nica por tantas risas. A Yavé, Maja, Ana, Gerardo, Inseparable, Oscar, Mag, Romu, Lily, Oriane, Benjamin, Olivia, à tous les Brossier et les Percoco. Merci aux salseros, joueurs et aux polyglottes pour les bons moments partagés. A Elisa que no deja de hacerme sentir orgullosa.

A Stefen, qui a cumulé 58,630,231 points-thèse grâce à son soutien constant et inconditionnel, indispensable à la réalisation de cette thèse. Merci d'être monté dans ce train et parcourir avec moi autant de kilomètres.

Para Stefen

ABSTRACT

Preserving the integrity of neuronal synapses is important for the development and maintenance of cognitive capacities. Mutations on a growing number of genes coding for synaptic proteins are associated with intellectual disability (ID), a neurodevelopmental disease characterized by deficits in adaptive and intellectual functions. The present work is dedicated to the study of one of those genes, *IL1RAPL1*, and the role of its encoding protein in synapse formation and function. IL1RAPL1 is a trans-membrane protein that is localized at excitatory synapses, where it interacts with the postsynaptic proteins PSD-95, RhoGAP2 and Mcf2l. Moreover, the extracellular domain of IL1RAPL1 interacts trans-synaptically with the presynaptic phosphatase PTPδ.

We studied the functional consequences of two novel mutations identified in ID patients affecting this IL1RAPL1 domain. Those mutations lead either to a decrease of the protein expression or of its interaction with PTPδ, affecting in both cases the IL1RAPL1-mediated excitatory synapse formation. In the absence of IL1RAPL1, the number or function of excitatory synapses is perturbed, leading to an imbalance of excitatory and inhibitory synaptic transmissions in specific brain circuits. In particular, we showed that this imbalance in the lateral amygdala results in associative memory deficits in mice lacking Il1rapl1. Altogether, the results included in this work show that IL1RAPL1/PTPδ interaction is essential for synapse formation and suggest that the cognitive deficits in ID patients with mutations on IL1RAPL1 result from the imbalance of the excitatory and inhibitory transmission. These observations open therapeutic perspectives aiming to reestablish this balance in the affected neuronal circuits.

Key-words: *intellectual disability, synapses, IL1RAPL1, excitatory/inhibitory balance*.

RESUME

L'intégrité des synapses neuronales est primordiale pour le développement et le maintien des capacités cognitives. Des mutations dans des gènes codant pour des protéines synaptiques ont été trouvées chez des patients atteints de déficience intellectuelle (DI), qui est une maladie neurodéveloppementale ayant des conséquences sur les fonctions intellectuelles et adaptatives. Ce travail de thèse porte sur l'étude de l'un de ces gènes, *IL1RAPL1*, dont les mutations sont responsables d'une forme non-syndromique de DI liée au chromosome X, et sur le rôle de la protéine IL1RAPL1 dans la formation et le fonctionnement des synapses.

IL1RAPL1 est une protéine trans-membranaire qui est localisée dans les synapses excitatrices où elle interagit avec les protéines post-synaptiques PSD-95, RhoGAP2 et Mcf2l. De plus, IL1RAPL1 interagit en trans- avec une protéine phosphatase présynaptique, PTPδ, via son domaine extracellulaire.

Nous avons étudié les conséquences fonctionnelles de deux nouvelles mutations qui affectent le domaine extracellulaire d'IL1RAPL1 chez des patients présentant une DI. Ces mutations conduisent soit à une diminution de l'expression de la protéine, soit à une réduction de l'interaction avec PTPδ affectant ainsi la capacité d'IL1RAPL1 à induire la formation de synapses excitatrices. En absence d'IL1RAPL1, le nombre ou la fonction des synapses excitatrices est diminué, ce qui mène à un déséquilibre entre les transmissions synaptiques excitatrice et inhibitrice dans des régions spécifiques du cerveau. Dans le cas particulier de l'amygdale latérale, nous avons montré que ce déséquilibre conduit à des défauts de mémoire associative chez la souris déficiente en Il1rapl1.

L'ensemble des résultats qui font partie de ce travail montre que l'interaction IL1RAPL1/PTPδ est essentielle pour la formation des synapses et suggère que les déficits cognitifs des patients avec une mutation dans il1rapl1 proviennent du déséquilibre de la balance excitation/ inhibition. Ces observations ouvrent des perspectives thérapeutiques visant à rétablir cette balance dans les réseaux neuronaux affectés.

Mots clés: *déficience intellectuelle, synapses, IL1RAPL1, balance excitation/inhibitio*

TABLE OF CONTENTS

ABBREVIATIONS 1

INTRODUCTION 3

1. Synapses – targets for intellectual disability 3

1.1. Synaptic functions are impaired in intellectual disability 6

1.1.1. Regulation of cytoskeleton dynamics 7

1.1.2. Presynaptic vesicle cycling and exocytosis 10

1.1.3. Organization of postsynaptic protein complexes 12

1.1.4. Trans-synaptic signaling 14

2. IL1RAPL1, a synaptic protein implicated in non-syndromic ID 15

2.1. Identification of IL1RAPL1 as a gene related to ID 15

2.2. IL1RAPL1 structure and expression 17

2.3. Molecular partners of IL1RAPL1 and effects on neuronal physiology 19

2.3.1. NCS-1 and calcium-regulated exocytosis 20

2.3.2. PSD-95 and excitatory postsynaptic organization 22

2.3.3. PTPδ and synaptogenesis 24

2.3.4. Regulators of Rho GTPases and neuronal morphology 31

2.3.4.1. RhoGAP2 and dendritic spine formation 32

2.3.4.2. Mcf2l and stabilization of glutamatergic synapses 33

2.3.4.3. Neurite branching 34

2.3.5. Other potential IL1RAPL1 interacting proteins 35

2.4. Phenotypic characterization of Il1rapl1 KO mouse 36

2.5. IL1RAPL1 is a member of IL1 receptor family 38

2.5.1. IL1β signaling in the brain and regulation of synaptic function 38

2.5.2. Regulation of cognitive functions by IL1R members 43

2.5.3. IL1 receptor family members involved in synaptogenesis 43

2.5.4. IL1β-induced signaling in neurons and astrocytes 44

RESULTS 48

1. Novel IL1RAPL1 mutations associated with intellectual disability impair synaptogenesis. 49

2. Target-specific vulnerability of excitatory synapses leads to deficits in associative memory in a model of intellectual disorder. 67

3. Unpublished work 85

3.1. Behavioral and cellular deficits in Il1rapl1 KO mouse are rescued by α5IA treatment 85

3.1.1. Context 85

3.1.2. Material and methods 88

3.1.3. Results 90

DISCUSSION AND CONCLUSIONS 94

1. Importance of IL1RAPL1 - PTPδ interactions for synapse formation 94

2. Role of IL1RAPL1 in synapse formation and in E/I balance 100

3. Towards a treatment for restoring E/I balance and improve cognitive deficits in ID mouse models 104

APENDIX 108

BIBLIOGRAPHY 112

LIST OF FIGURES

Figure 1. Neurons are polarized cells. 3

Figure 2. Chemical synapses are excitatory or inhibitory. 4

Figure 3. Regulation of small GTPases activity by GEFs and GAPs. 8

Figure 4. Regulators of small GTPases associated with ID. 10

Figure 5. Presynaptic proteins associated with ID. 11

Figure 6. Postsynaptic organization is affected in ID. 13

Figure 7. Cell adhesion is affected in ID. 15

Figure 8. Gene and protein organization of human IL1RAPL1. 18

Figure 9. IL1RAPL1 is present in excitatory but not inhibitory synapses. 19

Figure 10. IL1RAPL1 regulates N-type Ca2+ current through NCS-1. 21

Figure 11. IL1RAPL1 interacts with PSD-95 and regulates its targeting to excitatory postsynapses. 24

Figure 12. Pre and postsynaptic differentiation is mediated by different IL1RAPL1 protein domains. 25

Figure 13. PTPδ structure and trans-synaptic interaction with the extracellular domain of IL1RAPL1. 27

Figure 14. Mapping of the IL1RAPL1/PTPδ interaction. 29

Figure 15. IL1RAPL1 interacts with two regulators of small GTPases activity through its TIR domain, RhoGAP2 and Mcf2l. 32

Figure 16. Interleukin 1 receptor family of proteins regulate cytokines signaling. 39

Figure 17. IL1β induces different cellular signaling in different brain cell types. 45

Figure 18. Crystal structure of Il1rapl1 and Ptpδ interaction. 51

Figure 19. Excitatory/inhibitory balance is perturbed in the absence of Il1rapl1. 68

Figure 20. Effect of α5IA on contextual memory in wild-type and *Il1rapl1* KO mice.. 90

Figure 21. Gabra5 mRNA relative abundance in wild-type and *Il1rapl1* KO hippocampal neurons in culture. 91

Figure 22. c-Fos mRNA relative abundance in hippocampal neurons after bicuculline or α5IA treatment 92

Figure 23. Postsynaptic changes after α5IA treatment 93

Figure 24. Presynapses are not altered after α5IA treatment 93

Figure 25. Synaptogenesis period in rat hippocampus and in hippocampal neurons in culture. 95

Figure 26. Cerebellar circuits are affected during development in the absence of Il1rapl1. 102

Figure 27. Possible mechanism for α5IA-induced improvement in hippocampal-dependent tasks in Il1rapl1 KO mice 106

Table 1. Reported mutations on IL1RAPL1 in ID patients and their consequences for protein function 108

ABBREVIATIONS

α5IA	3-(5-methylisoxazol-3-yl)-6-[(1-methyl-1, 2, 3-triazol-4-yl) methyloxy]-1, 2, 4-triazolo [3, 4-a] phthalazine
AHC	adrenal hypoplasia congenital,
AMPA	α-amino-3-hydroxy-5-methylisoxazole-4-propionic acid
ASD	autism spectrum disorder
BRET	bioluminescence resonance energy transfer
CAMs	cell adhesion molecules
CNV	copy number variant
DCN	deep cerebellar nuclei
E/I	excitation/inhibition
ECD	extracellular domain
G	granule cells
GABA	γ-aminobutyric acid
GAP	GTPase-activating proteins
GDP	guanosine diphosphate
GEF	guanine nucleotide exchange factors
GKD	glycerol kinase deficiency
GTP	guanosine triphosphate
ID	intellectual disability
IEG	immediate early gene
Ig	immunoglobulin
IL1R1	interleukin 1 receptor
IL1RAcP	interleukin 1 receptor accessory protein
IL1RAcPb	interleukin 1 receptor accessory protein isoform b
IL1RAPL1	interleukin 1 receptor accessory protein like 1
IL1β	interleukin 1 beta
In	interneurons
IQ	intelligence quotient
JNK	c-Jun N-terminal kinase
KO	Knockout
LA	lateral amygdala
LTD	long-term depression
LTP	long-term potentiation

MAPK	Mitogen-activated protein kinases
MD	muscular dystrophy
meA/B	mini-exon A/B
mEPSCs	miniature excitatory postsynaptic currents
NCS-1	neuronal calcium sensor-1
NFκB	nuclear factor κB
NMDA	N-methyl-D aspartate
NPCs	neural precursor cells
NT	neurotransmitter
N-VGCC	N-type voltage-gated calcium channels
P	post-natal
PC	Purkinje cells
PSD	postsynaptic density
PSD-95	postsynaptic density protein 95
PTPδ	protein tyrosine phosphatase δ
SAPK	stress-activated protein kinases
SE	startle epilepsy
SEM	standard error of the mean
sIPSC	spontaneous inhibitory post-synaptic currents
SV	synaptic vesicle
VGlut1	vesicular glutamate transporter 1
WS	West syndrome
WT	wild-type

INTRODUCTION

1. Synapses – targets for intellectual disability

Synapses are the elementary units in the formation of the neural circuits that regulates all the functions of the nervous system. These specialized structures mediate the contact and communication between nerve cells, and in mammalian brains we can count several billions of synapses (~10^{15} of synapses in the human brain). Although electrical synapses occur in every brain region, the most common mechanism for signaling between neurons is the neurotransmitter-releasing chemical synapse. Throughout this text I will talk about chemical synapses, that are formed by the axon of a presynaptic neuron, and either the dendrites or the cell body of the target postsynaptic neuron (Figure 1).

Neurons are polarized cells extending neurites, dendrites and axon, away from their cell body in order to contact other nerve cells.

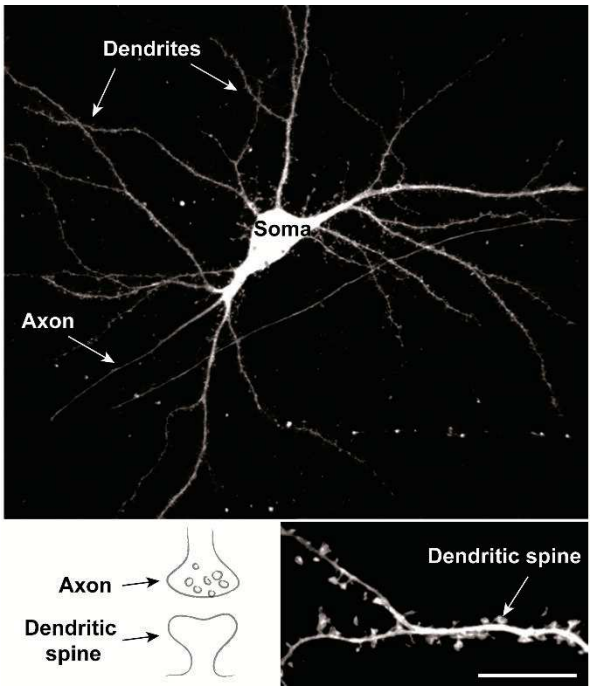

Figure 1. Neurons are polarized cells. An hippocampal neuron in culture was transfected with a plasmid carrying GFP fluorescent protein for visualization of neurites (dendrites and axons) and dendritic spines. The inset in the right shows a dendrite and dendritic spines. Synapses are mainly formed between axons and dendrites, as shown in the left inset. Scale bar 10 μm.

The morphology of neurites affects synaptic signaling, integration, and connectivity, and their diversity reflects the complexity and specificity of neural circuits. Neurites formation begins shortly after neurons complete their migration during brain development, and synapse formation, or synaptogenesis in the human brain occurs between gestational age week 20 until the adolescence (Tau & Peterson 2010). Scaffolding cells and molecular gradients are important in the assembly of synaptic connections, which will be constantly refined and modified throughout life. Synapses consist of two asymmetrically components separated by the synaptic cleft (about 20 nm): a presynaptic and a postsynaptic specialization that differ in their chemical, structural and functional characteristics. Even if large evidence of the participation of non-neuronal (glial) brain cells on synapse physiology, like microglia and astrocytes, I will only focus on the neuronal pre and postsynaptic partners.

Two major classes of chemical synaptic transmission are present in the central nervous system, excitatory and inhibitory (Figure 2). The differences arise from the type of neurotransmitter released (glutamate or γ-aminobutyric acid (GABA), respectively) and

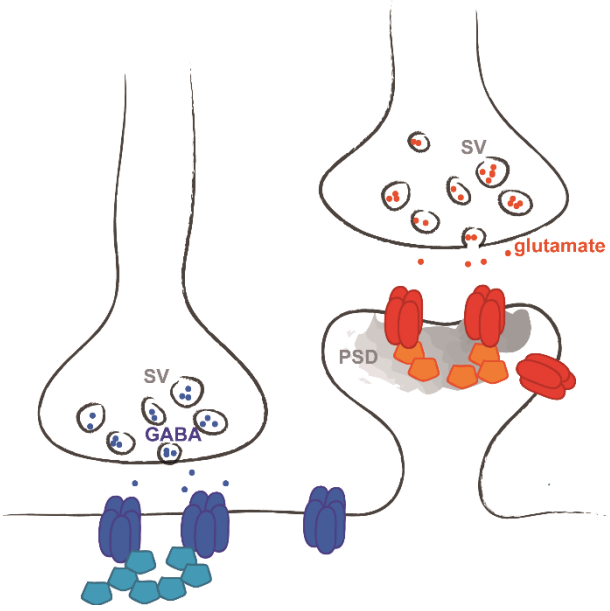

Figure 2. Chemical synapses are excitatory or inhibitory. Excitatory glutamatergic (red) are housed on dendritic spines, and inhibitory GABAergic (blue) synapses on dendritic shafts or neuronal soma. Each type of synapse is characterized by different neurotransmitter (NT), receptors (dark blue and red) and scaffolding proteins (light blue and orange). SV: synaptic vesicle. PSD: postsynaptic density.

from the molecular components (receptors, scaffolding proteins, effectors) that are present in them. The total number of synapses formed and the ratio of excitatory/inhibitory synaptic inputs that a neuron receives determine its excitability. Most excitatory synapses are housed on dendritic spines, small actin-rich protrusions extending from dendrites, and inhibitory synapses are formed on the dendritic shaft and on the cell soma. Excitatory synapses are characterized by a morphological and functional specialization of the postsynaptic membrane called the postsynaptic density (PSD), which is usually located at the tip of the dendritic spine. The PSD contains the glutamate receptors, as well as a large diversity of associated signaling and structural molecules.

Synapses have a high degree of molecular complexity, with elements acting as neurotransmitter receptors, adhesion molecules, signaling effectors, scaffolds, kinases and phosphatases, translation factors, cytoskeleton, ion channels, modification enzymes… Comparative studies between different species have suggested that the evolutionary diversification of the synapse components underlies the complexity in signal processing and behavior (Emes et al. 2008; Bayés et al. 2012).

Communication at chemical synapses involves the release of neurotransmitters (NT) from the presynaptic terminals in response to electrical impulses (action potentials), diffusion of the NT across the synaptic clefts, and NT binding to postsynaptic receptors. The postsynaptic compartment converts these chemical signals back into action potentials, allowing their propagation. The presynaptic terminals contain synaptic vesicles (SV) filled with neurotransmitters and a dense matrix of cytoskeleton and scaffolding proteins, the active zone, that contains all the machinery to release SV into the synaptic cleft. Diverse cell-adhesion molecules hold pre and postsynaptic specializations together through trans-synaptic interactions. On the postsynaptic specialization, glutamate and GABA receptors interact with the neurotransmitter and transduce its binding into electrical excitation or inhibition of the postsynaptic cell. These receptors form large signaling complexes, which send downstream signals into the postsynaptic cell and mediate feedback regulation of synaptic transmission. Dynamic regulation of function and localization of glutamate and GABA receptors mediate many forms of postsynaptic plasticity, including long-term potentiation (LTP) and long-term depression (LTD) of synaptic strength (two processes considered as representing the cellular basis of learning and memory), as well as the coupling of

synaptic activity to regulation of gene expression (Vithlani et al. 2011; Wang et al. 2012).

Given the crucial role of synapses on brain function, it's not surprising that disruption in key synaptic components lead to brain diseases. These synaptic diseases, or synaptopathies, have received particular interest in recent years (Grant 2012).
Since large scale screening of genetic information is available, the understanding of synapse pathology is increasing by systematically examining mutations in genes coding for all proteins in the synapse. Using this approach, it has been estimated that mutations on genes coding for synaptic proteins may play a role in around 133 brain diseases, including neurodegenerative diseases, motor disorders, epilepsy and cognitive disorders such as intellectual disability (ID) (Bayés et al. 2011).
To date, a large amount of genes encoding for synaptic proteins were associated with intellectual disability, the principal interest of the present work. Throughout this manuscript, I will focus on one of these genes, interleukin 1 receptor accessory protein-like 1 (*IL1RAPL1*) and address the consequences of mutations on this gene on synaptic formation and function.

1.1. Synaptic functions are impaired in intellectual disability

Intellectual disability (ID) is a common neurodevelopmental disorder characterized by an intelligence quotient (IQ) of 70 or below, and by impairments in adaptive behaviors including conceptual, social and practical areas (American Psychiatric Association 2000). This disorder was formerly known as mental retardation, but the term was changed in October 2010, when Rosa's law was signed in the United States as an effort to change the stigma among ID patients. The prevalence of ID is between 1 and 3% and is present in every social class and culture. ID was formerly classified in the basis of the IQ (from mild to profound severity) or into syndromic and non-syndromic depending on the presence of other clinical or morphological features. Recently, the DSM-5 rather set the severity in function of the adaptive behavior. Moreover, the classification of non-syndromic ID is debated because even if it has been traditionally defined by the presence of intellectual disability as the sole clinical feature, it is difficult to rule out the presence of more subtle neurological anomalies and psychiatric disorders in these patients.

ID can be caused by environmental and/or genetic factors. However, for up to 60% of cases there is no identifiable cause. Environmental exposure to certain teratogens, viruses or radiation can cause ID, as can severe head trauma or injury causing lack of oxygen to the brain. Genetic causes accounts for 25–50% of ID cases, although this number increases with ID severity. Among the genetic causes, chromosome abnormalities, large deletions and pathogenic copy number variants (CNV) have been found to be associated with ID in a large number of studies, and have contributed to the discovery of many ID-associated genes. Down syndrome, caused by human trisomy 21, and Fragile X syndrome due to mutations in the *FMR1* gene, are the most frequent genetic form of ID (Ropers 2010). A significant number of ID genes code for synaptic proteins, and it is noteworthy that many of them converge into common cellular pathways, allowing to determine the specific pathways perturbed in ID.

ID is considered as part of broad spectrum of neurodevelopmental disorders, including autism spectrum disorders (ASD). Clinically and genetically, these disorders are difficult to separate clearly, and the majority of ASD and ID genes share common cellular pathways. In this section I will describe briefly some of the synaptic features affected by genes whose mutations were described in patients with ID, associated or not with ASD or with other syndromes. These synapse-related ID proteins are involved in different cellular pathways but I will focus on those ID-related proteins involved in cytoskeleton dynamics, presynaptic vesicle cycling and exocytosis, organization of postsynaptic complexes and trans-synaptic signaling. This lets apart important processes underlying synaptic physiology like the regulation of transcription, protein synthesis and degradation that are also regulated by ID genes (Vaillend et al. 2008; Humeau et al. 2009; van Bokhoven 2011; Verpelli et al. 2013; Kroon et al. 2013; Srivastava & Schwartz 2014; Maurin et al. 2014; Volk et al. 2014).

1.1.1. Regulation of cytoskeleton dynamics

In mature neurons, the dendritic spines, small actin-rich protrusions extending from dendrites, house most excitatory synapses. Dendritic spines undergo marked changes in shape and number during development and in response to environmental stimuli. Changes in the number and morphology of spines and neurites are observed in several

neurodevelopmental diseases, including Rett syndrome, Fragile X syndrome, and ID (Xu et al. 2014; Castets et al. 2005; Khelfaoui et al. 2007).

Dynamic rearrangements of actin filaments, the predominant cytoskeletal element in dendritic spines (12% of total PSD proteins), regulates the formation and reorganization of dendritic spines (Matus 2000; Sheng & Kim 2011). Small GTPases are important regulators of the actin cytoskeleton that play essential roles in the development and remodeling of dendritic spines. These proteins account for the 8% of total PSD proteins and their activity is sensitive to synaptic transmission and can regulate activity-induced maturation of the synapse. This superfamily of proteins comprises several subfamilies like RhoA. The members of RhoA small GTPases subgroup include Ras homolog gene family member A (RhoA), Ras-related C3 botulinum toxin substrate (Rac1) and cell division cycle 42 (Cdc42). In neurons, Rac1, Ras and Cdc42 activity promote the formation, growth and maintenance of spines, whereas RhoA induces spine retraction and loss.

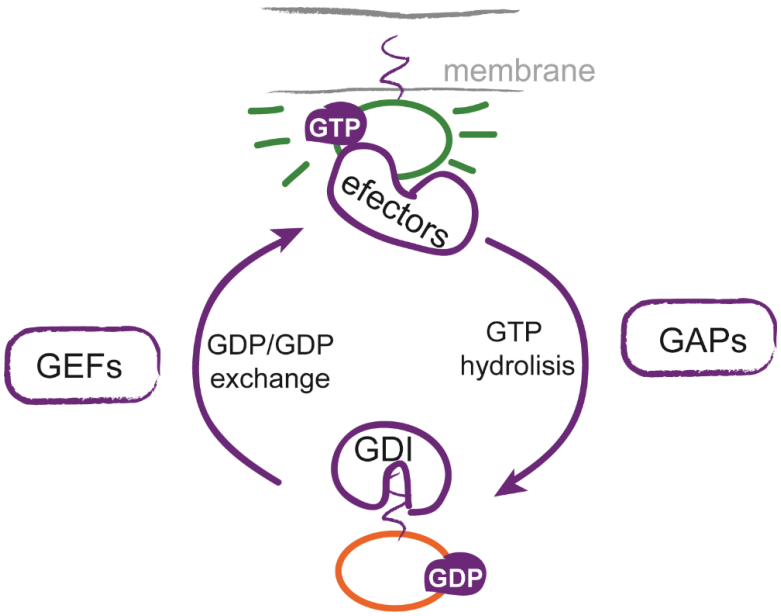

Figure 3. Regulation of small GTPases activity by GEFs and GAPs. In their GDP-bound state, small GTPases are maintained in an inactive form by GDIs and are located in the cytoplasm. GEFs catalyze the exchange of GDP for GTP and release small GTPases from the GDI complex. Active small GTPases translocate to the membrane, where they interact with their effectors. Small GTPases return to the inactive state by GAP-mediated GTP hydrolysis.

Spatial and temporal regulation of Rho GTPases activity is achieved by guanine nucleotide exchange factors (GEFs) and GTPase-activating proteins (GAPs) that activate and inhibit Rho GTPases activity respectively (Figure 3). In the inactive GDP-bound form, RhoA is locked in the cytosol by guanine dissociation inhibitors (GDIs). RhoGEFs catalyze the exchange of GDP for GTP to activate RhoA, by releasing it from the RhoA-GDI complex. Activated RhoA translocates to plasma membrane where it interacts with different effectors to transduce the signal. RhoA activation is turned off by RhoGAPs that induce the hydrolysis of GTP to GDP (Sasaki & Takai 1998). Other subfamilies of small GTPases, like Ras, Arf and Rab, similarly regulated by specific GAPs and GEFS, are also linked to cytoskeleton dynamics in neurons.

Mutations in regulators and effectors of the Rho GTPases have been found to underlay various forms of ID (syndromic written in **green**, and non-syndromic in **blue**) and are shown in Figure 4 (Newey et al. 2005; Ba et al. 2013). For example, the RhoGAPs **oligophrenin 1** (*OPHN1*) and **MEGAP** (*SRGAP3*), the Rac and Cd42GEF **αPIX** (*ARHGEF6*) and FGD1 (***FGD1***), as well as the RhoGTPases effector p21-activating kinase 3 **PAK3** (*PAK3*), are involved in regulating changes in spine morphology (Billuart et al. 1998; Endris et al. 2002; Lebel et al. 2002; Bienvenu et al. 2000; Boda et al. 2004). Spine morphogenesis is also regulated by **CNKSR2/CNK2** (*CNKSR2*) that interacts principally with the Rac and Cdc42 GAP ARHGAP33 (also known as Vilse) but also with βPIX and the scaffolding protein PSD-95 (Tarpey et al. 2009; Houge et al. 2012; Lim et al. 2014; Hu et al. 2015). **Preso** (*FRMPD4*) is another PSD-95-interacting ID protein (Hu et al. 2015) that also associates with actin filaments and βPIX, and is a positive regulator of spine density (Lee et al. 2008). A member of the Ras superfamily, the small GTPase ADP-ribosylation factor 6 (*ARF6*) is also known to impact actin dynamics in the brain, and is regulated by the ID-related protein **IQSEC2/BRAG2** (*IQSEC2*) (Shoubridge et al. 2010; Raemaekers et al. 2012). **SYNGAP** (*SYNGAP*) is a RasGAP that regulates spine maturation (Hamdan, Gauthier, et al. 2009; Hamdan, Daoud, et al. 2011; Clement et al. 2012). These examples strongly link ID with defects of actin dynamics that underlies defects in spine formation and morphology.

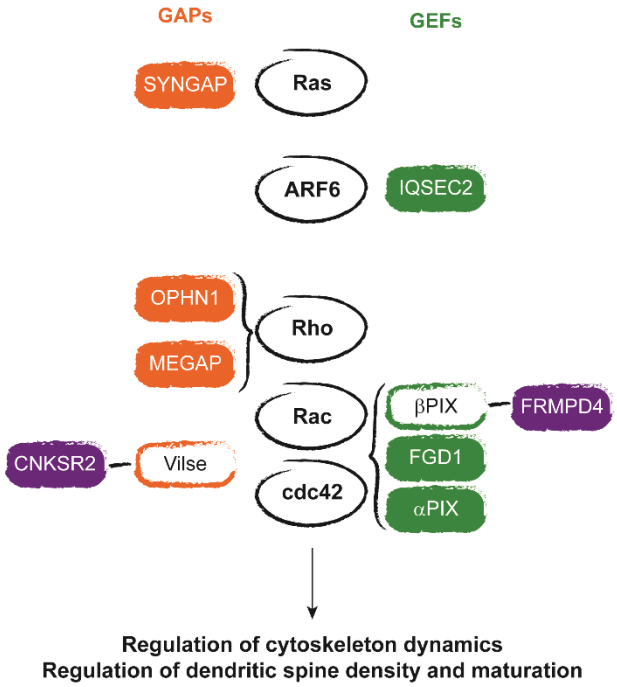

Figure 4. Regulators of small GTPases associated with ID. Proteins activating small GTPases (GAPs) are shown in orange, and GEFs are represented in green. Empty rectangles indicates proteins not associated with ID. Protein represented in violet interact with GAPs or GEFs and with the scaffolding protein PSD-95 found in excitatory postsynapses.

1.1.2. Presynaptic vesicle cycling and exocytosis

Neurotransmitters are stored in synaptic vesicles at presynaptic terminals. Several presynaptic proteins involved in the regulation of synaptic vesicle release, including vesicle docking, priming, fusion, endocytosis and recycling are found to be defective in syndromic (written in **green)** and non-syndromic (in **blue**) ID (Figure 5). Synaptic vesicle exocytosis is restricted to a small section of the presynaptic membrane called the active zone. This zone is composed of evolutionarily conserved proteins (the core is composed of RIM, Munc13, RIM-BP, liprin-α, and ELKS proteins) and performs the principal functions of neurotransmitter release: docks and primes synaptic vesicles, recruits calcium (Ca^{2+}) channels to the docked and primed vesicles, tethers the vesicles and Ca^{2+} channels to synaptic cell-adhesion molecules, and mediates presynaptic plasticity (Südhof 2012). Because Ca^{2+} entry governs neurotransmitter release, regulation of the Ca^{2+} channel is an important control point for synaptic transmission on the presynapses. Upon stimulation, the synaptic vesicles are translocated to the active zone, anchored to the presynaptic membrane and made ready for fusion. In response to Ca^{2+} influx, docked vesicles undergo exocytosis and

release neurotransmitters into the synaptic cleft, where neurotransmitter can bind to their receptors in the postsynaptic element. The synaptic vesicle fusion machinery for exocytosis is mediated by the SNARE (soluble N-ethymalemide sensitive factor attachment protein receptor) complex composed of three SNARE proteins (syntaxin, SNAP-25, and synaptobrevin) and **Munc18** (*STXBP1*), that was found mutated in patients with severe ID (Saitsu et al. 2008; Hamdan, Piton, et al. 2009). **Synaptophysin** (*SYP*) is also an ID protein found in synaptic vesicles that interacts with synaptobrevin, an essential component of SNARE complex (Tarpey et al. 2009; Gordon & Cousin 2013).

The synaptic vesicles are covered with Rab proteins, principally Rab3a, a subgroup of the Ras superfamily, which regulates vesicle trafficking and neurotransmitter release. **Rab39B** (*Rab39B*) and some proteins regulating this signaling pathway have been associated with ID: **αGDI** (*GDI1*), **Rab3GAP1** (*Rab3GAP1*) and the calcium/calmodulin-dependent serine protein kinase **CASK** (*CASK*) (Giannandrea et al. 2010; D'Adamo et al. 1998; Aligianis et al. 2005; Hackett et al. 2010). Both, αGDI and Rab3GAP1 causes Rab3a to remain inactive by maintaining it in its GDP-bound form. CASK is a member of the membrane associated guanylate kinase (MAGUK) family of scaffolding proteins that interacts with rabphilin3a, an effector of Rab3a, which stabilizes Rab3a in its active state on the vesicle (Zhang et al. 2001).

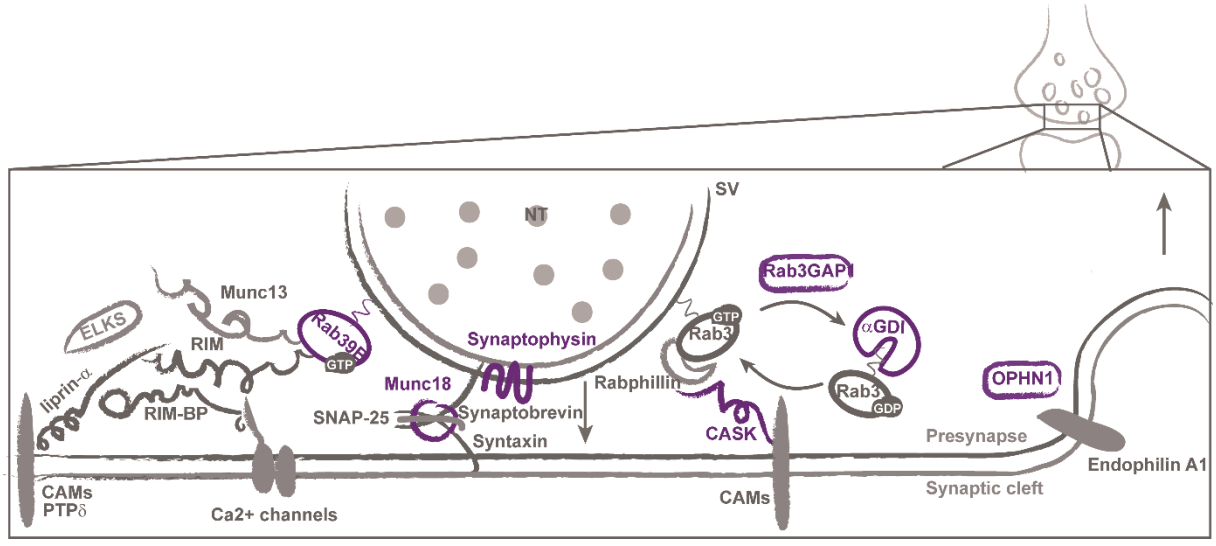

Figure 5. Presynaptic proteins associated with ID. Protein members of the active zone and SNAREs are shown in the left. The ID presynaptic proteins involved in synaptic vesicles (SV) exocytosis and endocytosis (right) are shown in violet. CAMs: cell-adhesion molecules.

Loss of **oligophrenin 1** signaling at presynapses has been shown to impair synaptic vesicle cycling at hippocampal synapses by forming a complex with endophilin A1, a protein implicated in several stages of synaptic vesicle endocytosis (Khelfaoui et al. 2009; Nakano-Kobayashi et al. 2009).

1.1.3. Organization of postsynaptic protein complexes

Disruption of signaling pathways in excitatory glutamatergic or inhibitory GABAergic synapses contributes to the cognitive impairment and behavioral anomalies in ID. However, most of the studies of the synaptic role of ID-associated proteins have been focused on excitatory synapses.

The integrity and composition of postsynaptic density (PSD) protein complexes is crucial for proper excitatory synaptic function. Two main types of ionotropic glutamate receptors are found in glutamatergic synapses: the N-methyl-D aspartate (NMDA) that transmits signals, and the α-amino-3-hydroxy-5-methylisoxazole-4-propionic acid (AMPA) receptors that triggers long-term changes in synaptic transmission. Both receptors are composed of different subunits that determine the signaling properties of the receptor, like channel conductance, signaling, localization, and interaction partners. Synaptic strength, or plasticity, is determined by the number of AMPA receptors that are inserted in the postsynaptic membrane, a process regulated by multiple mechanisms (phosphorylation of receptor subunits, for example). Mutations in genes encoding subunits glutamate receptors have been linked to syndromic (written in **green**) and non-syndromic (in **blue**) ID (Figure 6). Examples of this are the AMPA receptor subunit **GluA2** (*GRIA2*) and **GluA3** (*GRIA3*), and the NMDA receptor subunits **GluN1** (*GRIN1*), **GluN2A** (*GRIN2A*), and **GluN2B** (*GRIN2B*) (Tzschach et al. 2010; Gécz et al. 1999; Wu et al. 2007; Hamdan, Gauthier, et al. 2011; Reutlinger et al. 2010; Endele et al. 2010).

Among the ID–associated proteins that regulates AMPA receptor trafficking and stabilization to the membrane (and thus excitatory synaptic function) are **SynGAP** (*SYNGAP1*), the MAGUK protein **SAP102** (*DLG3*), **oligophrenin 1** and **TSPAN7** (*TM4SF2*) (Kim et al. 2005; Tarpey et al. 2009; Elias et al. 2008; Nadif Kasri et al. 2009; Zemni et al. 2000; Abidi et al. 2002; Bassani et al. 2012). Homer and Shank proteins are among the most abundant scaffolding proteins in the PSD, and form a network

structure serving as an assembly platform for other PSD proteins. ***SHANK2*** and ***SHANK3*** were found mutated in ID patients (Berkel et al. 2010; Durand et al. 2007).

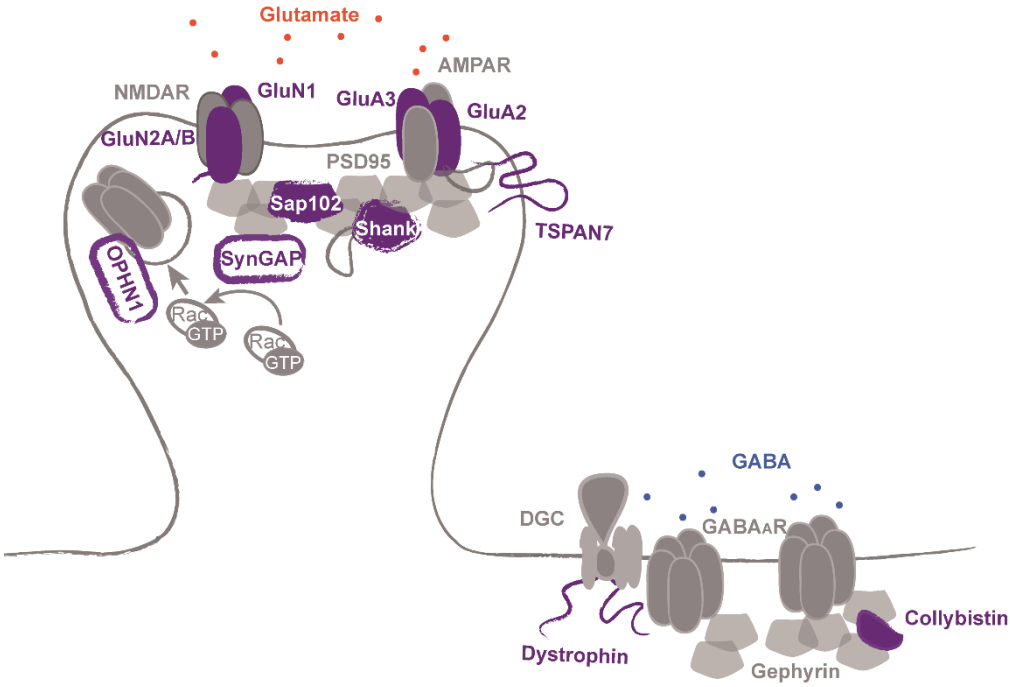

Figure 6. Postsynaptic organization is affected in ID. ID-related proteins involved in excitatory (left) or inhibitory (right) postsynaptic organization and neurotransmitter receptor stabilization to the membrane are shown in violet.

Unlike excitatory ones, inhibitory synapses are mostly formed on the dendritic shaft or in the cell soma. In those synapses, there are two classes of GABA receptors: ionotropic $GABA_A$ and metabotropic $GABA_B$, but most of the actions of GABA are mediated via $GABA_A$ receptors. $GABA_A$ receptors are anchored postsynaptically by gephyrin, a scaffolding protein that interacts with the cytoskeleton and with multiple signaling molecules. Modification of gephyrin clustering properties enable structural and functional regulation of inhibitory neurotransmission (Tyagarajan & Fritschy 2014). Mutations in *ARHGEF9*, coding for **collybistin**, a Cdc42 GEF essential for the clustering gephyrin, have been associated with ID (Marco et al. 2008; Lesca et al. 2011; Tyagarajan & Fritschy 2014). **Dystrophin** (*DMD*) is part of the dystroglycan complex (DGC), a large, membrane-spanning protein complex that links the cytoskeleton to the extracellular matrix. At inhibitory synapses this complex stabilizes $GABA_A$ receptors clusters (Perronnet & Vaillend 2010).

1.1.4. Trans-synaptic signaling

Cell-adhesion molecules (CAMs) play critical roles in brain development by ensuring proper synapse formation bridging the pre- and postsynaptic compartments, as well as during the maturation and maintenance of synapses (Yogev & Shen 2014). These proteins represent 7% of the PSD proteins (Sheng & Kim 2011). It has been suggested that CAMs might have overlapping functions or act together at synaptic sites, as no single pair of synaptic adhesion molecules seems to be sufficient to accomplish all aspects of synaptic development. Mutations in several CAMs are associated with syndromic (written in **green**) and non-syndromic (in **blue**) ID (Figure 7). The majority of CAMs at synaptic clefts are members of the cadherin, immunoglobulin and integrin families, as well as neurexins and neuroligins. CAMs provide anchors for scaffolding proteins like members of the MAGUK family, and several SH3 and multiple ankyrin repeat domain proteins (Shanks) (Südhof 2008).

Presynaptic neurexins and postsynaptic neuroligins are Ca^{2+}-dependent cell adhesion molecules that participate in the formation of both excitatory and inhibitory synapses. Neurexins encode two major isoforms, α (long) and β (short), differing in their extracellular domains. Trans-synaptic binding of neurexins to neuroligins is mediated by the sixth LNS (laminin, neurexin, sex-hormone-binding globulin) domain of α-neurexin, and the single LNS-domain of β-neurexin. Through their cytoplasmic tail, neuroligins bind to intracellular class-I PDZ-domains such as those contained in PSD-95, a postsynaptic MAGUK protein, whereas neurexins contain a binding site for class-II PDZ- domains that binds to the PDZ-domain of CASK and related proteins. Thanks to gene promoter diversity and complex alternative splicing, neurexins can be found in thousands of different isoforms, which contributes to the diversity and specificity of synapses in the nervous system (Südhof 2008).

The genes encoding **neurexin 1** (*NRXN1*) and **neuroligins 3 and 4** (*NLGN3* and *NLGN4*) were associated with ID, as well as **CASPR2** (*CNTNAP2*) a neurexin-related protein that contains additional extracellular domains not found in α-neurexins (Jamain et al. 2003; Laumonnier et al. 2004; Zweier et al. 2009). DGC complex (see below) was shown to bind to neurexins at inhibitory synapses (Reissner et al. 2014). Similarly to neurexin/neuroligins system, **IL1RAPL1** (*IL1RAPL1*) associates trans-synaptically with the receptor tyrosine phosphatase PTPδ, and binds to PSD-95. These interactions will be discussed in detail later on.

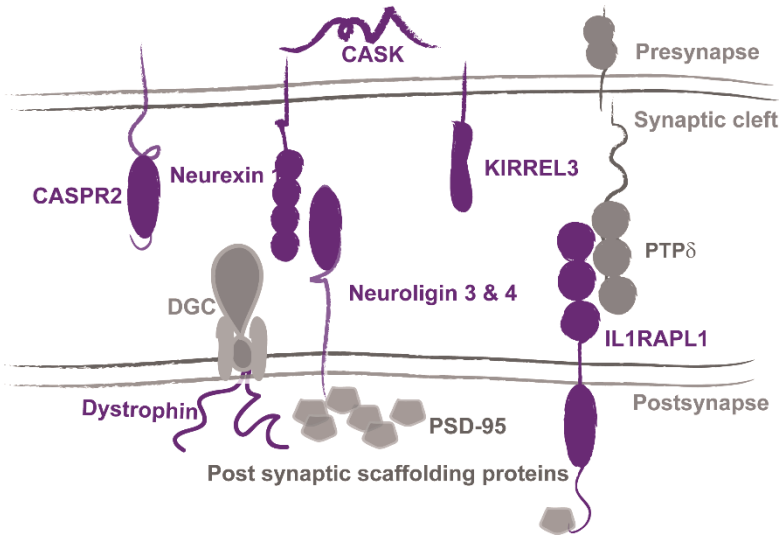

Figure 7. Cell adhesion is affected in ID. Cell adhesion molecules or their interacting proteins that are associated with ID are shown in violet.

CASK binds to the cytoplasmic tails of the presynaptic cell adhesion molecules **neurexin 1** and **KIRREL3/NEPH2** (*KIRREL3*), a member of immunoglobulin superfamily (Hata et al. 1996; Bhalla et al. 2008). These observations suggest that CASK may participate in the translation of extracellular interactions of cell-surface proteins into an intracellular response.

2. *IL1RAPL1, a synaptic protein implicated in non-syndromic ID*

Among the ID related genes coding for synaptic proteins, particular importance will be given to *IL1RAPL1* that is the main subject of this thesis work. This gene is located in X chromosome so is called an X-linked gene. An increasing number of functions and molecular partners for this protein have been found, and since its first description in 1999, investigating the physiopathology of *IL1RAPL1* has been one of the interests of our research team.

2.1. Identification of IL1RAPL1 as a gene related to ID

The interleukin 1 receptor accessory protein-like (*IL1RAPL*) gene was described as an ID gene by Carrie and collaborators in 1999. The Xp22.1–21.3 locus on the X chromosome was first identified by linkage analysis of large families, and *IL1RAPL* gene was identified through the detection of two inherited overlapping micro deletions

in this region associated exclusively with non-syndromic ID (Carrié et al. 1999). *IL1RAPL* gene is composed of 11 exons of which 10 are coding. The two *IL1RAPL* mutations characterized by Carrié and collaborators were a nonsense mutation (c.1377C>A, Y459X) and deletion of exons 3-5. Shortly after, Jin and collaborators reported the deletion of *IL1RAPL* exons 9 to 11 as responsible of the ID in a patient that also presented muscular dystrophy, glycerol kinase deficiency, and adrenal hypoplasia (Jin et al. 2000). Those pathologies are explained by the deletion of *GK* and *DAX-1* genes and the last exon of dystrophin gene, in addition to the deletion found in *IL1RAPL*. In that study, a gene homologous to *IL1RAPL* in Xq22 was identified. Following this observation, the protein product of the first described gene was named IL1RAPL1 and the homologous one IL1RAPL2, but they are also known as TIGIRR-2 (three immunoglobulin domain-containing IL1 receptor-related) or IL1R8, and TIGIRR-1 or IL1-R9, respectively (Born et al. 2000; Sana et al. 2000).

Since then, several mutations on *IL1RAPL1* gene were reported, and they are listed in Table 1 (Appendix). Most of them are large deletions including several exons (Carrié et al. 1999; Nawara et al. 2008; Piton et al. 2008; Whibley et al. 2010; Behnecke et al. 2011; Mikhail et al. 2011; Franek et al. 2011; Youngs et al. 2012; Barone et al. 2013; Mignon-Ravix et al. 2014; Tucker et al. 2013; Redin et al. 2014) or nonsense mutations leading to truncated proteins (Kozak et al. 1993; Carrié et al. 1999; Tabolacci et al. 2006). However, there are some reports of duplications of X chromosome regions encompassing several genes including *IL1RAPL1* in patients presenting ID or developmental delay and autistic features ((Honda et al. 2010; Utine et al. 2014), J. Lauer and F. Kooy personal communication). Surprisingly, most deletions involve one or more of the first 7 exons, and some authors suggested that this is probably due to the particular recombination potential of this region (Leprêtre et al. 2003; Tabolacci et al. 2006). This suggestion is supported by the reports of two patients with chromosome inversions with the breakpoint in *IL1RAPL1* intron 2 (Bhat et al. 2008) and exon 6 (Leprêtre et al. 2003).

In agreement with the X chromosome-linked recessive transmission, patients with mutations in *IL1RAPL1* gene are males, whereas females are identified as carriers in these families. However, some of these carriers show less severe phenotypes, like learning impairment or mild ID (Tabolacci et al. 2006; Bhat et al. 2008; Leprêtre et al. 2003; Piton et al. 2008). This may be due to the X chromosome inactivation that some

studies assessed in patient's fibroblasts, but no clear correlation between X chromosome inactivation in those cells and patients' phenotype has been established (Tabolacci et al. 2006; Nawara et al. 2008; Behnecke et al. 2011; Franek et al. 2011). Most of the mutations on this gene are associated with non-syndromic ID (Allen-Brady et al. 2011) but some studies have also associated *IL1RAPL1* with mild dysmorphic features (Leprêtre et al. 2003), autism spectrum disorder (ASD) (Piton et al. 2008; Bhat et al. 2008; Butler et al. 2015), or startle epilepsy (Dinopoulos et al. 2014). As mentioned before, when large deletions in *IL1RAPL1* region include contiguous genes, ID can be associated with muscular dystrophy, metabolic and hormonal diseases such as glycerol kinase deficiency and adrenal hypoplasia (Jin et al. 2000; Sasaki et al. 2003; Zhang et al. 2004).

2.2. IL1RAPL1 structure and expression

Two different transcripts were described for *IL1RAPL1* gene, one of ~9.5 kb and another of ~6.5 kb (Carrié et al. 1999; Born et al. 2000). The longer transcript is present in both adult and fetal tissue, whereas the short is only present in adult brain. The larger transcript produces a 696 amino acid protein, whereas the shorter transcript may result from alternative splicing and should lead to the first 259 amino acids identical to larger isoform differing only in the last 2 amino acids. No experimental evidence has been provided for the existence of the shorter protein.

IL1RAPL1 codes for a transmembrane protein sharing structural domains with members of interleukin 1 (IL1) receptor family (Carrié et al. 1999; Jin et al. 2000). For this reason it was named after its similarity with human interleukin 1 accessory protein (IL1RAcP), and it was speculated that interleukin 1 signaling could have a role in the pathophysiology of ID.

As represented in Figure 8, IL1RAPL1 includes a signal peptide with a predicted cleavage site between Ser18 and Leu19, an extracellular domain (357 amino acids), composed of three immunoglobulin-like (Ig-like) domains (Schreuder et al. 1997); a short transmembrane domain (21 amino acids), and an intracellular domain (318 amino acids) composed of a TIR (Toll/IL1 receptor (Rock et al. 1998)) domain and a 138 amino acid C-terminal tail. The extracellular domain of this protein is N-glycosylated at sites Asn63, 122, 138, 213, 264 and 331 (Yamagata, Yoshida, et al.

2015). Some proteins interacting with intra- and extra-cellular domains of IL1RAPL1 have been identified. Their characterization and function is mentioned below.

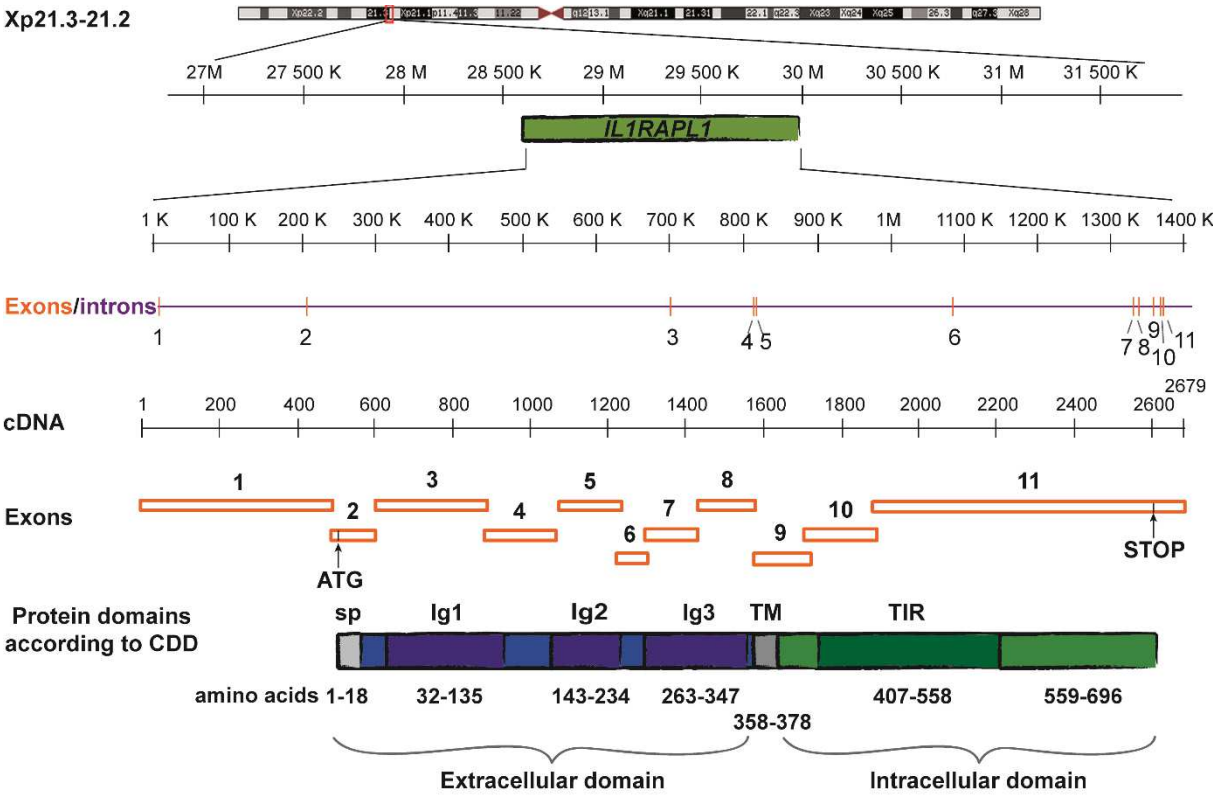

Figure 8. Gene and protein organization of human IL1RAPL1. CDD: NCBI's conserved domain database (Marchler-Bauer et al. 2014). Modified from Pavlowsky 2009.

In the mouse, *Il1rapl1* transcript is expressed in the brain, principally in the hippocampus, the olfactory bulb and mammillary bodies (Carrié et al. 1999; Houbaert et al. 2013). *Il1rapl1* transcript is expressed in neurons at 18 days *in vitro* (DIV) as well as in astrocytes derived from primary cultures (unpublished observations). As shown in Figure 9, overexpression of IL1RAPL1 showed that this protein is located in excitatory synapses, since it co-localizes with VGlut1 and PSD-95, excitatory pre and postsynaptic markers, respectively. In the other hand, IL1RAPL1 does not co-localize with inhibitory synapses markers, like VGat and gephyrin.

In the next section I will address the known roles of the ID-associated synaptic protein IL1RAPL1.

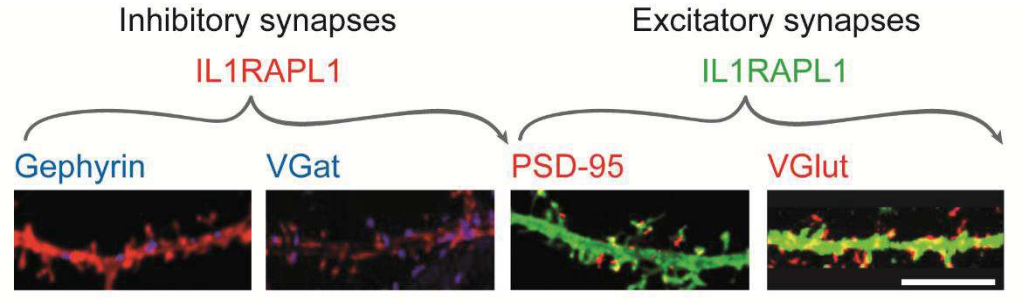

Figure 9. IL1RAPL1 is present in excitatory but not inhibitory synapses. Overexpressed IL1RAPL1 co-localizes with excitatory (PSD-95 and VGlut) but not inhibitory (Gephyrin and VGat) post and presynaptic markers. From Pavlowsky and collaborators (2010), and unpublished observations. Scale bar 10 µm.

2.3. Molecular partners of IL1RAPL1 and effects on neuronal physiology

Since its homology to interleukin 1 receptor family, it could be expected that IL1RAPL1 participates in interleukin 1 signaling. Until now, there is no direct evidence to support this cellular function (see hereafter) but it was suggested instead that IL1RAPL1 and its homologous IL1RAPL2 could have completely different signaling capacities in the nervous system.

A crystallographic study suggested that the TIR domain of human IL1RAPL1 forms dimers (Khan et al. 2004). Evidence of this could be observed in cells overexpressing IL1RAPL1 (Bahi et al. 2003), but until now the biological role of this dimerization is not clear. Evidence of IL1RAPL1 localization in presynaptic compartment has been provided in the zebrafish, where overexpressed Il1rapl1b is located in axons terminals of olfactory sensory neurons and co-localizes with the presynaptic protein synaptobrevin (Yoshida & Mishina 2008). The overexpression or down regulation of *il1rapl1b* in olfactory sensory neurons increases or decreases respectively presynaptic vesicle accumulation (Yoshida & Mishina 2008), a process in which the C-terminal domain of Il1rapl1b is required.

In mammals, most of the studies have addressed the postsynaptic role of IL1RAPL1, and even if there is some evidence of its role as a presynaptic protein (Bahi et al. 2003), this was observed in a cell line and remains to be confirmed in neurons. We have observed less or no IL1RAPL1 staining in the axons of mouse cultured neurons and that was also reported by others (Yoshida et al. 2011), supporting why most of the studies consider IL1RAPL1 as a postsynaptic protein.

Several studies have addressed the question of the interactions of IL1RAPL1 with other proteins (Bahi et al. 2003; Pavlowsky, Gianfelice, et al. 2010; Valnegri et al. 2011; Yoshida et al. 2011; Hayashi et al. 2013). Until now only the role of some of these IL1RAPL1 partners is known, and others remain to be validated and elucidated. Below I will address each of the known IL1RAPL1 partners, and how these interactions regulate several aspects of synapse and neuron physiology.

2.3.1. NCS-1 and calcium-regulated exocytosis

As mentioned above, the C-terminal domain of zebrafish Il1rapl1b is required for synaptic vesicle accumulation (Yoshida & Mishina 2008). This ~140 amino acid C-terminal of IL1RAPL1 is unique to this protein, which may confer some specific signaling characteristics that could be explained by interactions with partners through this tail. Bahi and collaborators used the IL1RAPL1 intracellular domain as a bait in a yeast two-hybrid screen and found the neuronal calcium sensor-1 (NCS-1) as an interacting protein (Bahi et al. 2003). In that study, they also identified the interacting region of IL1RAPL1 (amino acids 549-644), which spans the last 20 amino acids of the TIR domain and the half of the C-terminal specific domain, and defined the conserved Leu606 amino acid as critical for binding. On the other hand, NCS-1 interacts with IL1RAPL1 via the amino acids 174–190 on its C-terminal domain. This interaction was confirmed *in vitro* by GST pull down assays and *in vivo* by co-immunoprecipitation assays in HeLa cells, and was shown to be calcium-independent. Moreover, the same study showed that in IL1RAPL1-overexpressing PC12 cells the secretion of growth hormone induced by ATP is reduced. A mutation on NCS-1 gene (Arg102Gln) was found in patient with ASD, but it does not affect its binding to IL1RAPL1 (Piton et al. 2008; Handley et al. 2010).

Altogether, this data suggests that IL1RAPL1, through interaction with NCS-1, is a negative regulator of exocytosis, which could in part explain the increase of synaptic vesicles stained by synaptobrevin after Il1rapl1b overexpression (Yoshida & Mishina 2008). The mechanism of exocytosis regulation by NCS-1/IL1RAPL1 interaction was elucidated by Gambino and collaborators. By overexpressing IL1RAPL1 and down regulating NCS-1 in PC12 cells, they showed that IL1RAPL1, through NCS-1, silences the activity of N-type voltage-gated calcium channels (N-VGCC). The down regulation

of the activity of this channel by IL1RAPL1 inhibits secretion of growth hormone in PC12 cells, as shown in Figure 10 (Gambino et al. 2007).

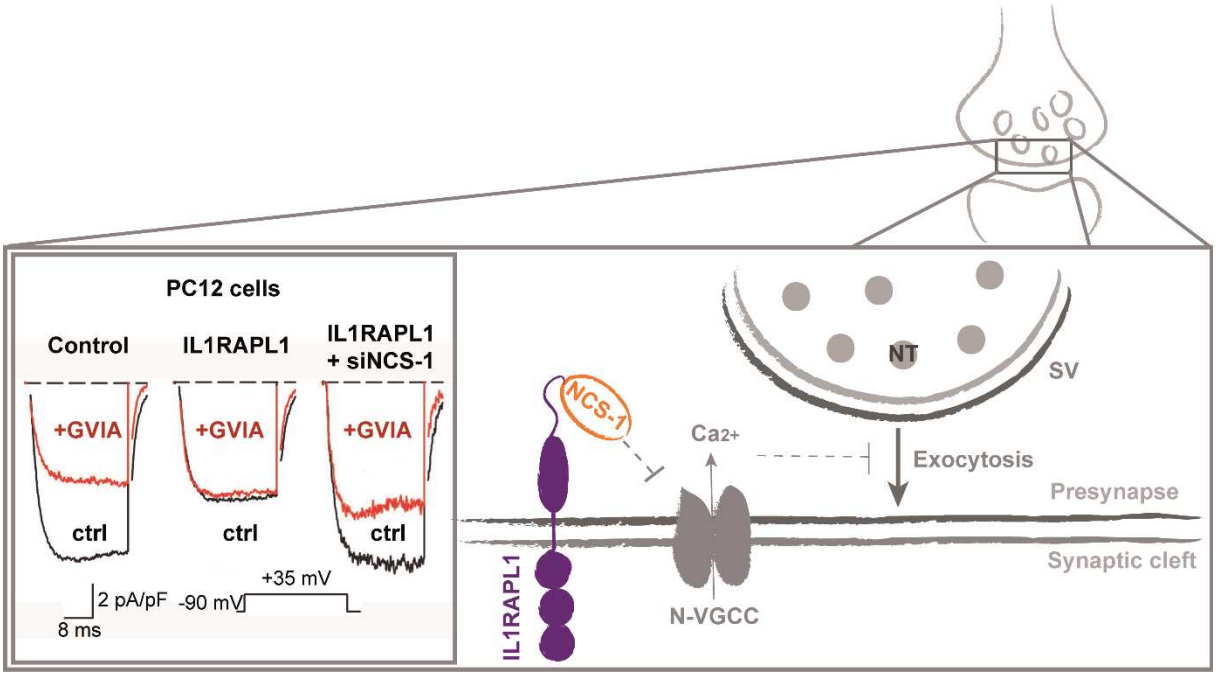

Figure 10. IL1RAPL1 regulates N-type Ca2+ current through NCS-1. Left: Overexpression of IL1RAPL1 abolishes N-type Ca^{2+} current in PC12 cells, which is not observed when NCS-1 is down regulated in IL1RAPL1-overexpressing cells (IL1RAPL1 + siNCS-1). Black traces indicate Ca^{2+} currents under control conditions (ctrl), and red traces indicate Ca^{2+} currents in the presence of 1 μM ω-conotoxin (GVIA), a specific antagonist of N-type voltage gated Ca^{2+} channels (N-VGCC). Right: The IL1RAPL1-NCS-1 interaction at presynapses could regulate synaptic vesicle (SV) exocytosis by inhibiting N-VGCC, as observed for growth hormone secretion in PC12 cells by Gambino and collaborators in 2007. NT: neurotransmitter.

NCS-1, found from yeast to humans, is a member of a family of calcium-binding proteins called neuronal calcium sensors (NCS), which include neurocalcin, visinin-like protein (VILIP), hippocalcin, recoverin, guanylate cyclase activating protein (GCAP), and K+ channel interacting protein (KChIP). These sensors are mainly expressed in the nervous system where they are involved in a number of calcium signaling pathways. In particular, NCS-1 is widely expressed in the brain, and there is evidence of its role in pre and postsynaptic compartments (Jinno et al. 2002; Martone et al. 1999; Jo et al. 2008).

In addition to the impact on secretion, the down regulation of N-VGCC by IL1RAPL1 and NCS-1 inhibits NGF-induced neurite elongation in PC12 cells. The negative regulation of NCS-1 in neurite outgrowth has been observed in different cell lines and

in neurons from *Drosophila melanogaster* (Chen et al. 2001; Hui et al. 2006). The roles of the NCS-1 fly homologue, Frequenin, in secretion and in neurite elongation are independent: Chronic expression of an interfering Frequenin C-terminal peptide affects both neuromuscular axon terminal branching, or structural complexity, and neurotransmitter release, while acute application of the same peptide produces a reduction of neurotransmitter release without an effect on axon morphology (Romero-Pozuelo et al. 2007).

At the presynaptic terminal, NCS-1 has been shown to regulate voltage gated calcium channels, including P/Q-, L- and N-type, as formerly mentioned. Those calcium channels group to the presynaptic membrane a large signaling complex containing SNARE proteins (see Figure 5), Ca^{2+}-binding proteins (including NCS-1), calcium-dependent kinases and scaffolding proteins. For example, presynaptic P/Q type CaV2 channels, whose Ca^{2+}-dependent inactivation is regulated by its interaction with NCS-1 in superior cervical ganglion neurons, provide a rapid and spatially limited Ca^{2+} entry that initiates synaptic transmission (Yan et al. 2014). Through interactions with SNARE proteins and scaffolding proteins, these Ca^{2+} channels bring docked synaptic vesicles close to the source of Ca^{2+} entry, allowing them to respond efficiently to the Ca^{2+} increase. Through specific interactions with Ca^{2+}-binding proteins and kinases like CaMKII, the activity of Ca^{2+} channels can be regulated to mediate forms of synaptic plasticity. The regulation of voltage gated Ca^{2+} channels (in particular N-type) by IL1RAPL1 through NCS-1 suggests a role for IL1RAPL1 in presynaptic function. Up to now, there is no direct evidence of the function of this protein in synaptic vesicle exocytosis in neurons.

2.3.2. PSD-95 and excitatory postsynaptic organization

The first evidence of the presence of IL1RAPL1 at the synapse was provided by a study by Pavlowsky and collaborators where, using subcellular fractionation, endogenous IL1RAPL1 protein was found enriched in postsynaptic density (PSD) fractions (Pavlowsky, Gianfelice, et al. 2010). By overexpressing this protein in mouse neurons in culture they observed that IL1RAPL1 co-localizes with excitatory pre (VGlut1) and post (PSD-95 and Shank) synaptic markers (Figure 9). Moreover, using the entire C-terminal domain of IL1RAPL1 (amino acids 390 – 696) as a bait for a two hybrid yeast system, Pavlowsky and collaborators found a direct interaction with PSD-95, SAP-97 and PSD-93. These are all members of the PSD-95 like subfamily of the

MAGUK family of scaffolding proteins (Cho et al. 1992), but only the interaction with PSD-95 was further characterized.

PSD-95 is the prototypical member of MAGUK family of proteins and constitutes a signaling hub that promotes formation and maturation of dendritic spines (El-Husseini et al. 2000). PSD- MAGUKs share a common organization with three N-terminal PSD-95/Dlg/ZO-1 (PDZ) domains, a Src-homology 3 (SH3) domain, and a C-terminal guanylate kinase (GK) domain catalytically inactive. PSD-MAGUKs are required for synaptic targeting of different glutamate receptors and their role is finely regulated during development (Elias et al. 2006).

PSD-95 interacts via its first two PDZ domains (PDZ1 and PDZ2) with a non-canonical PDZ binding domain within the last 8 amino acids of the C- terminal tail of IL1RAPL1 (Pavlowsky, Gianfelice, et al. 2010). IL1RAPL1 overexpression in mouse or rat hippocampal neurons largely increases PSD-95 cluster number. This increase is not observed when IL1RAPL1 lacking the last 8 amino acids (Δ8) is overexpressed, showing that interaction with PSD-95 is necessary for the IL1RAPL1-induced increase of PSD-95 clusters (Pavlowsky, Gianfelice, et al. 2010).

Besides PSD-95, IL1RAPL1 overexpression also increases VGlut1 staining and dendritic spine number, suggesting a global increase in excitatory synapse number. This was confirmed by increases miniature excitatory postsynaptic currents (mEPSC) in neurons overexpressing IL1RAPL1. In addition, VGlut1 staining and dendritic spine number are also increased in neurons overexpressing Δ8 IL1RAPL1 mutant, suggesting that these are events independent of IL1RAPL1/PSD-95 interaction (Pavlowsky, Gianfelice, et al. 2010). Accordingly, hippocampal neurons from *Il1rapl1* knockout (KO) mouse show ~25% less PSD-95 clusters number compared with wild-type neurons, and this was congruent with a decrease of miniature excitatory postsynaptic currents (mEPSCs) frequency.

IL1RAPL1 overexpression induces a significant increase of PSD-95 phosphorylation on Ser295 (Figure 11). This increase is dependent on IL1RAPL1 interaction with this scaffolding protein because Δ8 IL1RAPL1 mutant is not able to increase PSD-95 phosphorylation (Pavlowsky, Gianfelice, et al. 2010). According to the fact that phosphorylation on Ser295 by c-Jun N-terminal kinase (JNK) is important to target PSD-95 to synapses (Kim et al. 2007; Thomas et al. 2008), the increase/decrease of

PSD-95 at the synapse observed after overexpressing or knocking down *Il1rapl1*, respectively, may result from the changes in PSD-95 and JNK phosphorylation. Indeed, phosphorylation of PSD-95 and JNK is reduced in *Il1rapl1* KO cortical neurons. The mechanism of phosphorylation regulation could involve the PP1/2A phosphatases, as their pharmacological inhibition partially rescued the phosphorylation deficits in *Il1rapl1* KO neurons (Pavlowsky, Gianfelice, et al. 2010).

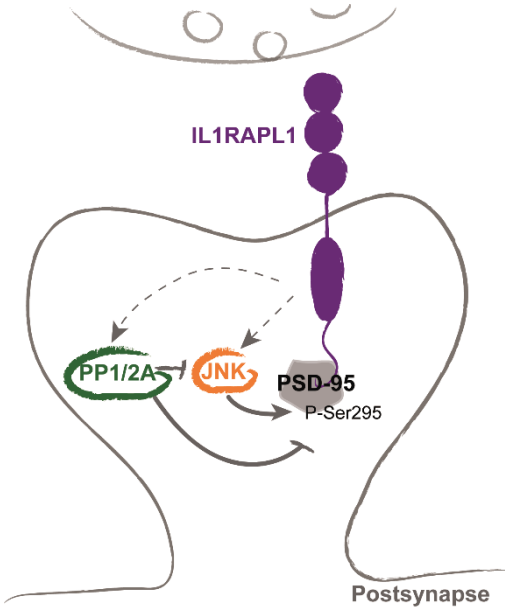

Figure 11. IL1RAPL1 interacts with PSD-95 and regulates its targeting to excitatory postsynapses. In addition to interacting with PSD-95, IL1RAPL1 regulates the phosphorylation at Ser295 of this scaffold protein. This process is regulated by direct or indirect activation of JNK and/or PP1/2A.

2.3.3. PTPδ and synaptogenesis

Synapse formation is initiated at contact sites between axon terminals and dendrites (see Figure 1). There, pre and postsynaptic adhesion molecules form trans-synaptic complexes to induce pre and postsynaptic differentiation (Figure 7).

In mouse hippocampal and cortical neurons in culture, overexpression of IL1RAPL1 induces excitatory presynaptic differentiation and dendritic spine formation (Pavlowsky, Gianfelice, et al. 2010; Valnegri et al. 2011; Yoshida et al. 2011). Interestingly, although IL1RAPL1 extracellular domain is sufficient for inducing this presynaptic differentiation, both extracellular and intracellular TIR domains are required for postsynaptic changes (Figure 12) (Valnegri et al. 2011; Yoshida et al. 2011).

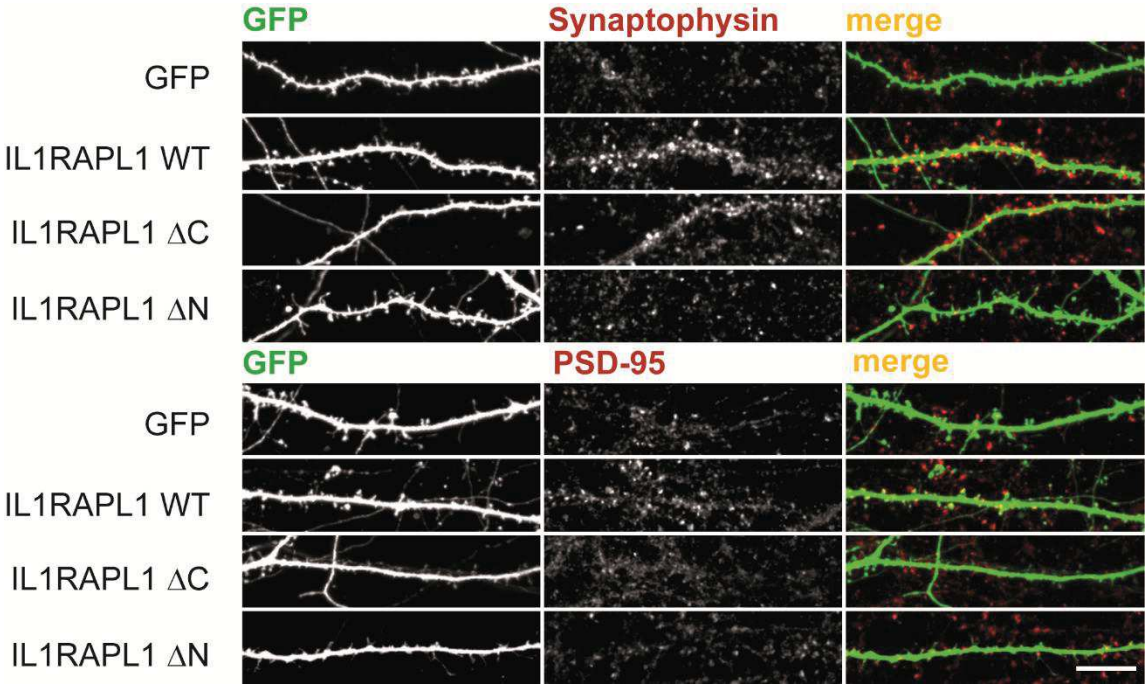

Figure 12. Pre and postsynaptic differentiation is mediated by different IL1RAPL1 protein domains. Pre (Synaptophysin, up) and post (PSD-95, down) synaptic markers are increased in mouse hippocampal mature neurons transfected with IL1RAPL1 (WT). In the absence of the C-terminal domain (ΔC), only synaptophysin increase is observed. On the other hand, in the absence of the two first Ig-like domains (ΔN), neither pre nor postsynaptic markers are increased.

These observations suggest a differential role of each IL1RAPL1 extra and intracellular domains in synaptic differentiation. These observations were also the starting point for the exploration aiming at finding partners of IL1RAPL1 extracellular domain, which may exert its synaptogenic activity by interacting with presynaptic proteins.
Using affinity chromatography, two research groups identified simultaneously protein tyrosine phosphatase δ (PTPδ) as a binding partner of IL1RAPL1 extracellular domain (Valnegri et al. 2011; Yoshida et al. 2011).

PTPδ is a member of the 2A subfamily of receptor-like protein tyrosine phosphatases (Tonks 2006). This family of proteins is composed of three members in vertebrates, leukocyte common antigen-related (LAR, which gives the name of the family), PTPσ, and PTPδ, that share overall 66% of amino acid identity (Pulido, Serra-Pagès, et al. 1995). mRNAs encoding the three family proteins show overlapping and differential distribution patterns in mouse brain (Kwon et al. 2010). In human tissue, PTPδ mRNA is predominantly detected in brain and, to a lesser extent, in heart, placenta, and kidney (Pulido, Serra-Pagès, et al. 1995). In the mouse brain, PTPδ mRNA is found in

hippocampus, in the reticular thalamic area, and is more present in the cortical layer IV of cortex compared with other layers (Kwon et al. 2010).
Some *de novo* deletions, duplications and single nucleotide polymorphisms (SNPs) in the 5'UTR of *PTPRD* gene are associated with attention-deficit hyperactivity disorder (ADHD) (Elia et al. 2010), autism spectrum disorder (ASD) (Pinto et al. 2010), bipolar disorder (Malhotra et al. 2011), and restless syndrome (Schormair et al. 2008; Elia et al. 2010; Yang et al. 2011). Recently, Choucair and collaborators identified an inherited homozygous deletion with breakpoints in *PTPRD* gene in a patient with ID, growth retardation, hearing loss, trigonocephaly and scaphocephaly (malformation of the skull) (Choucair et al. 2015).

As the other members of the LAR family, PTPδ contains extracellular typical cell adhesion immunoglobulin-like (Ig) and fibronectin III (FN) domains modified by alternative splicing, which mediate diverse extracellular protein interactions (Figure 13). The intracellular domain involves two intracellular protein tyrosine phosphatase (PTP) domains: a membrane-proximal D1 domain with robust catalytic activity and a membrane-distal D2 domain with residual or no catalytic activity (Takahashi & Craig 2013). Up to three endoprotease cleavage sites are located 81-87 amino acids N-terminal from the transmembrane domain, constitutively generating an extracellular subunit that remains non covalently bound to the phosphatase domain subunit (Pulido, Krueger, et al. 1995). However, the functional significance of this modification is not clear.
Ptprd deficient mice are semi lethal, since they have difficulties in taking food, but they have a normal brain morphology (Uetani et al. 2000). They exhibit impaired hippocampal-dependent learning and, although the hippocampus is histologically normal, the hippocampal LTP is increased. These data support the important role of PTPδ on hippocampal function, but unlike *Il1rapl1* KO mice (see later), the LTP does not correlate positively with the impaired learning ability in the absence of PTPδ (Uetani et al. 2000).
PTPδ extracellular domain promotes neurite growth in chicken neurons (Wang & Bixby 1999) and acts as an attractant for growing axons (Sun et al. 2000), but no PTPδ interacting proteins were yet associated with these effects. PTPδ was first shown to have homophilic interactions (Wang & Bixby 1999), but besides IL1RAPL1, postsynaptic binding partners in trans-synaptic complexes identified so far are netrin-

G ligand-3 (NGL-3) (Kwon et al. 2010), Slit and Trk-like family member 1-6 (Slitrk1-6) (Takahashi et al. 2012; Yim et al. 2013; Yamagata, Sato, et al. 2015), and interleukin 1 receptor accessory protein (IL1RAcP) (Yoshida et al. 2012).

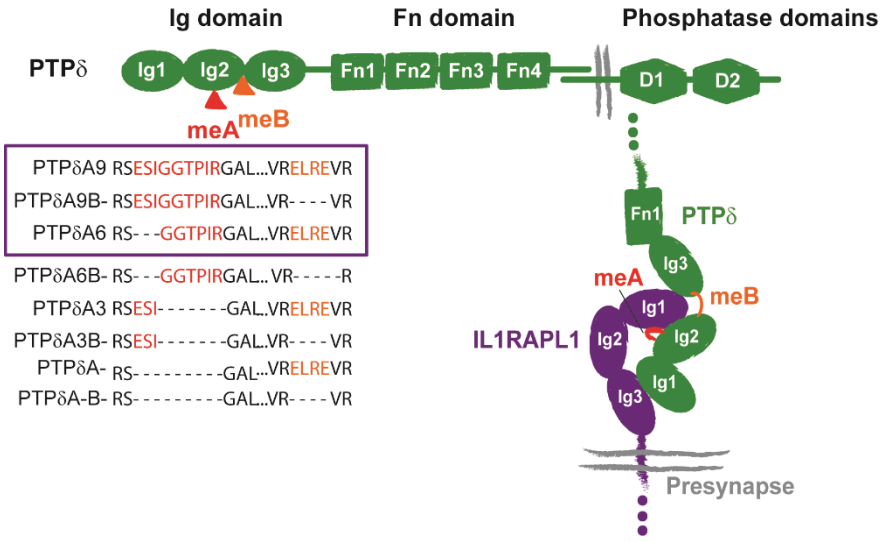

Figure 13. PTPδ structure and trans-synaptic interaction with the extracellular domain of IL1RAPL1. Up: Structure and domain of PTPδ. The isoforms generated by meA and meB splicing are shown, and those contained in the violet rectangle correspond to the ones interacting with IL1RAPL1. Right: Schematic representation of the interaction between IL1RAPL1 extra cellular domain and PTPδ Ig domain. Modified form Yoshida et al., 2011 and Yamagata, Yoshida et al., 2015.

Like other members of LAR family and their postsynaptic partners, IL1RAPL1/PTPδ interaction has three general functions in synaptic organization:

The first one is to **mediate cell–cell adhesion at synapses**. Wang and Bixby first described PTPδ as an adhesion molecule, and trans-synaptic adhesion mediated by PTPδ is highly selective, diverse and organized. This is clearly supported by two recent studies that show the crystal structures of PTPδ interacting with three of its partners, IL1RAPL1, IL1RAcP and Slitrk2 (Yamagata, Yoshida, et al. 2015; Yamagata, Sato, et al. 2015).

The diversity of trans-synaptic partners lead to a specific regulation of inhibitory and excitatory synaptogenesis. For example, interaction of PTPδ with IL1RAPL1 or Slitrk2 function selectively in excitatory synaptic organization, whereas interaction with Slitrk3 in inhibitory synaptic organization (Takahashi et al. 2012; Yim et al. 2013). However, despite its synaptogenic activity, Slitrk2 has not been found enriched in PSD fraction samples (Yim et al. 2013). As discussed further, PTPδ-IL1RAcP interaction induces

not only excitatory synapse formation *in vitro*, but can also mediate inhibitory synapses formation (Yoshida et al. 2012).

Multiple isoforms of LARs are generated by tissue-specific alternative splicing of four mini-exons (meA–meD) encoding short amino acid peptides (Pulido, Krueger, et al. 1995; Pulido, Serra-Pagès, et al. 1995). In PTPδ, the meA insert is located in the second Ig domain (Ig2), presumably affecting the length of a loop region between the D and E β-strands of Ig2, whereas the meB insert with four residues is located at the end of Ig2 (Figure 13). The most abundant form of PTPδ in the brain contains both meA and meB peptides, but several isoforms result from alternative splicing in both mini-exons (Yoshida et al. 2011). meA peptide (Glu-Ser-Ile-Gly-Gly-Thr-Pro-Ile-Arg) is derived from two exons encoding 3 amino acids (Glu-Ser-Ile) and 6 amino acids (Gly-Gly-Thr-Pro-Ile-Arg). As a result of alternative splicing on these exons, there are three variations in meA, a three-residue peptide Glu-Ser-Ile (meA3), a six-residue peptide Gly-Gly-Thr-Pro-Ile-Arg (meA6) and their tandem combination (Glu-Ser-Ile-Gly-Gly-Thr-Pro-Ile-Arg), but meA can also be totally absent. meB comprises four residues, Glu-Leu-Arg-Glu and can be either present or absent. The length and sequence of meA are important for PTPδ binding to IL1RAPL1 (Yoshida et al. 2011; Yamagata, Yoshida, et al. 2015). Only PTPδ variants containing meA9 and meA6 can bind to IL1RAPL1 (Figure 13, violet rectangle). The meB insertion increases binding of the meA9-containing variant, whereas the meA6-containing variant absolutely requires the combination with meB (Yamagata, Yoshida, et al. 2015). This interaction was shown to be specific, because LAR and PTPσ isoforms failed to show any significant binding for IL1RAPL1 (Yoshida et al. 2011).

As shown in Figure 14, the interface between the Il1rapl1 Ig1 and PTPδ Ig2 domains comprises interactions occurring on two β-strands containing Arg181– Ser187 and Arg196–Glu202 in the Ig2 domain of PTPδ (Figure 14, brown), between which meA is inserted. Trp34 of Il1rapl1 interacts with Leu153, Ala198 and Leu185 of PTPδ and this is essential for binding between both proteins. PTPδ Arg196 also participates in this hydrophobic interaction by forming a hydrogen bond with Asp37 of Il1rapl1, which is further stabilized by a hydrogen bond with Tyr59 of Il1rapl1. In addition, Ser187 and Glu188 in meA bind with Il1rapl1 Tyr59 and Gly58, respectively. Perturbing PTPδ Arg 196 and Il1rapl1 Asp37 decreases the affinity 11- and 16-fold, respectively (Yamagata, Yoshida, et al. 2015).

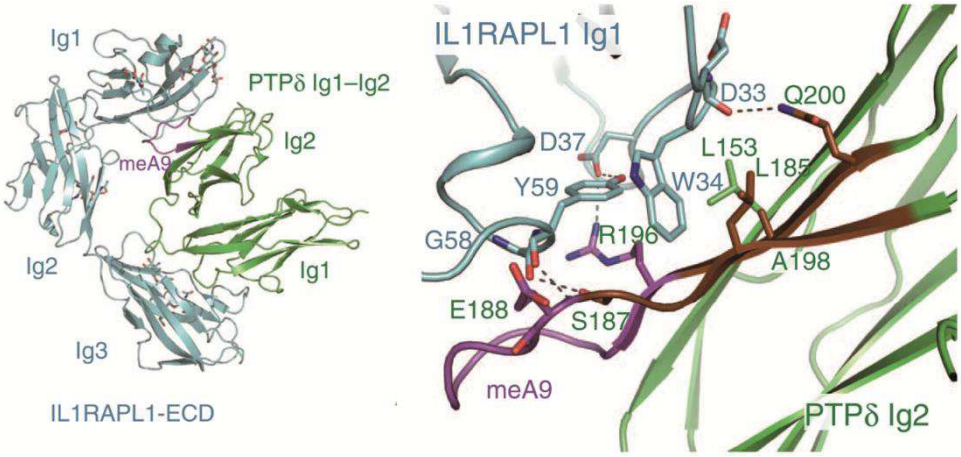

Figure 14. Mapping of the IL1RAPL1/PTPδ interaction. Left: Overall structure of the PTPδ Ig1–Ig2 and IL1RAPL1-extracellular domain (ECD) complex. PTPδ is represented in green and IL1RAPL1 in cyan. The meA insertion is highlighted in violet. N-linked glycans are shown as sticks. Right: Closer view of the interaction between the Ig1 domain of IL1RAPL1 and the Ig2 domain of PTPδ. IL1RAPL1-Ig1-interacting β-strands of PTPδ are represented in brown. Residues involved in the interactions are shown as sticks and hydrogen bonds are indicated by dotted lines. From Yamagata, Yoshida and collaborators (2015).

The second role of IL1RAPL1/PTPδ interaction in synapse organization is to **mediate presynaptic differentiation**, recruitment of synaptic vesicles, release and recycling machinery. This can be considered as a form of retrograde synaptogenic signaling triggered by binding of the postsynaptic partner to presynaptic PTPδ.

Using a co-culture system, Yoshida and collaborators showed that IL1RAPL1 requires PTPδ for induction of presynaptic differentiation. The increase of the presynaptic markers Bassoon and Synapsin I in cortical neurons induced by IL1RAPL1 overexpression in HEK293 cells is abolished in cortical neurons from *Ptprd* KO mouse. This observation is supported by *in vivo* data showing that overexpression of IL1RAPL1 in mouse cortex increases VGlut1 staining, and that this is not observed when overexpressed in *Ptprd* KO mouse cortex (Yoshida et al. 2011). Accordingly, delivering soluble PTPδ meA- meB- extra cellular domain (that cannot interact with IL1RAPL1) fails to suppress the stimulatory effect of IL1RAPL1 on synapse formation.

The extracellular domain of IL1RAPL1 is necessary and sufficient for the presynaptic induction. This was shown by overexpressing IL1RAPL1 lacking either extra or intracellular domains in hippocampal neurons in culture (Valnegri et al. 2011). IL1RAPL1 lacking the entire intracellular domain (ΔC) still increases the presynaptic

marker VGlut1, whereas IL1RAPL1 lacking the first two Ig-like domains (ΔN) is not able to do so (Figure 12).

PTPδ induces excitatory presynaptic differentiation by interacting with NGL-3 *in vitro* (Kwon et al. 2010), but unlike IL1RAPL1, no postsynaptic differentiation is induced by this interaction. The functional relevance of this interaction is questioned, because NGL-3 synaptogenic effect is maintained in cells lacking PTPδ (Yoshida et al. 2011).

Takahashi and collaborators (2010) suggested that PTPδ containing full meA and meB inserts is the presynaptic receptor by which Slitrk3 induces inhibitory presynaptic differentiation. Since this isoform can also bind to other Slitrks and to IL1RAPL1 to regulate excitatory presynaptic differentiation, perhaps with different affinity, it is possible that differential splicing of PTPδ in GABAergic and glutamatergic axons contributes to selectivity in postsynaptic partner binding and function.

Among the mechanisms proposed to regulate PTPδ-induced presynaptic differentiation, is the interaction between the membrane distal D2 domain of LARs and liprin-α, also known as LAR interacting protein 1 (see Figure 5) (Pulido, Serra-Pagès, et al. 1995). Although liprin-α is located in both pre and postsynaptic specializations, this protein is part of the core of presynaptic active zone, and has a primordial role for synaptic vesicle release. Even if there are few studies of liprins in vertebrates and their presynaptic role, studies on *Drosophila* and *C. elegans* point out the involvement of this protein and LAR members in generating a spatial synaptic organization that provides the most efficient arrangement for synaptic transmission (Ackley et al. 2005).

A study in mouse hippocampal neurons suggested that liprin-α2 organizes presynaptic ultrastructure and controls synaptic output by regulating synaptic vesicles pool size through the control of the dynamics of two other components of the of presynaptic active zone, RIM1 and CASK (Figure 5) (Spangler et al. 2013).

The third mechanism regulated by IL1RAPL1/PTPδ interaction in synapses is to **trigger postsynaptic differentiation**, recruitment of neurotransmitter receptors, scaffolds, and signaling proteins.

Overexpression of IL1RAPL1 in HEK293 cells co-cultured with cortical neurons, induced an increase of the number of dendritic protrusions and of the excitatory postsynaptic scaffold protein Shank2, but not of the inhibitory postsynaptic scaffold gephyrin (Yoshida et al. 2011). This effect was not observed when IL1RAPL1 overexpressing neurons were co-cultured with *Ptprd* KO cortical neurons, and was

blocked by soluble IL1RAPL1 extracellular domain. Additionally, interfering with IL1RAPL1/PTPδ interaction by injecting the soluble IL1RAPL1 extracellular domain into the developing cerebral cortex of wild-type mouse decreases the spine density of cortical neurons (Yoshida et al. 2011). This effect was abolished in PTPδ KO mice, which suggests that IL1RAPL1 requires PTPδ for induction of dendritic protrusions and postsynaptic differentiation *in vivo* and *in vitro*. On the other hand, the capacity of PTPδ to induce excitatory postsynaptic differentiation was reduced to ~50% in cultured cortical neurons from *Il1rapl1* KO mice (Yasumura et al. 2014), indicating that PTPδ organizes postsynaptic differentiation by the interaction with IL1RAPL1 and other proteins.

Unlike IL1RAPL1-induced presynaptic differentiation, both domains extra and intracellular are required for postsynaptic induction: Overexpression of IL1RAPL1 lacking either extra or intracellular domains fail to increase dendritic spine formation (Valnegri et al. 2011). Moreover, not every part of the intracellular domain is implicated in the IL1RAPL1-dependent postsynaptic phenotypes. Swapping the TIR domain of IL1RAPL1 by the one of other IL1 receptor family abolishes the dendritic spine increase, while swapping the C-terminal domain has no effect on spines. On the other hand, swapping any of the TIR or C-terminal domains enables IL1RAPL1 to increase Shank2 staining. Thus, the TIR domain is responsible for the regulation of dendritic protrusions, while both the TIR and C-terminal domains are required for the accumulation of postsynaptic Shank2 (Yoshida et al. 2011).

2.3.4. Regulators of Rho GTPases and neuronal morphology

Neurons' morphology accompanies functional changes during development, learning, aging, and disease. This diverse neuronal morphology includes a dendritic arborization and dendritic spines formation. As mentioned before, small GTPases are important regulators of the actin cytoskeleton that play essential roles in the development and remodeling of dendritic spines (Figures 3 and 4). Rac1 and Rho, and in a minor extent Cdc42, have been implicated in the cytoskeletal dynamics that induce structural change of excitatory spines (Newey et al. 2005). Two independent studies identified two small GTPases regulators as interacting with IL1RAPL1 intracellular domain, which suggests that IL1RAPL1 could regulate dendritic spine formation by affecting cytoskeleton dynamics.

Along with its role in pre and postsynaptic differentiation, IL1RAPL1 regulates dendritic spine formation. In cortical and hippocampal neurons from *Il1rapl1* KO mouse, there is a decrease in the number of dendritic spines (Pavlowsky, Gianfelice, et al. 2010; Yasumura et al. 2014). Some of the possible mechanisms of spine regulation by IL1RAPL1 include different partners interacting with the intracellular domain of this protein. Those partners, RhoGAP2 and Mcf2l, are regulators of small GTPases activity, which are closely related to cytoskeleton changes (Figure 15).

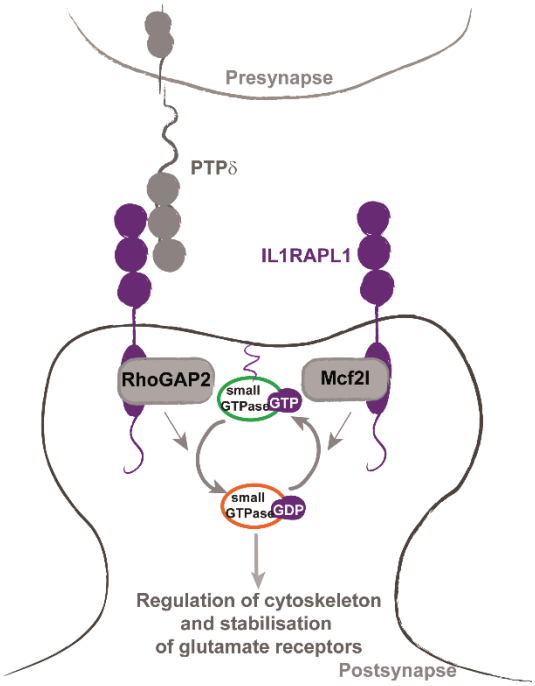

Figure 15. IL1RAPL1 interacts with two regulators of small GTPases activity through its TIR domain, RhoGAP2 and Mcf2l. IL1RAPL1/RhoGAP2 interaction is dependent on IL1RAPL1/PTPδ complex and negatively regulates Rac. IL1RAPL1/Mcf2l regulates RhoA activity, resulting in glutamate receptor stabilization to membrane.

2.3.4.1. RhoGAP2 and dendritic spine formation

With the aim of finding an interacting protein responsible for the postsynaptic induction, Valnegri and collaborators used the intracellular C-terminal tail of IL1RAPL1 (amino acids 390–696, comprising both the TIR and the C-terminal domains) as bait for a yeast two-hybrid screening. They found that RhoGTPase-activating protein II (RhoGAP2) interacts through its C-terminal domain with the TIR, and possibly the C-terminal tail of IL1RAPL1. RhoGAP2, also known as ARHGAP22, is localized in excitatory synapses, and its overexpression induces both excitatory synapse and

dendritic spine formation (Valnegri et al. 2011). This phenotype is in line with the fact that RhoGAP2 is known to inactivate Rac.

IL1RAPL1 overexpression increases the endogenous postsynaptic RhoGAP2 staining, but this was not observed after the over expression of IL1RAPL1 ΔC, unable to bind to RhoGAP2, or IL1RAPL1 ΔN, unable to bind to PTPδ. Moreover, incubation of neurons overexpressing IL1RAPL1 with the purified soluble extracellular domain of IL1RAPL2 (which interferes with IL1RAPL1/PTPδ binding, as described below), reduces the RhoGAP2 increase.

Overexpression of IL1RAPL1 ΔC, which does not interact with RhoGAP2, induces changes in the shape of dendritic spines which become filopodia-like shaped, a sign of spine immaturity. This suggests that the RhoGAP2 activity on dendritic spines is regulated by the interaction with IL1RAPL1/PTPδ trans-synaptic complex.

2.3.4.2. Mcf2l and stabilization of glutamatergic synapses

An independent study identified by affinity chromatography the RhoGEF protein Mcf2l as another interacting partner of IL1RAPL1 intracellular domain (Hayashi et al. 2013). As this protein interacts specifically with the TIR domain of IL1RAPL1, it is a good candidate for regulating the increase of dendritic protrusions mediated by this domain. Mcf2l (also known as Dbs or Ost) is a RhoGEF that activates RhoA and Cdc42, and binds to active Rac1 (Horii et al. 1994).

Knocking down Mcf2l in neurons prevents the IL1RAPL1-dependent increase of dendritic spines. The same phenotype was observed when an inhibitor of ROCK (the downstream kinase of RhoA) was used to interfere with Rho activity.

In the same line, knockdown of endogenous Mcf2l expression or inhibiting ROCK activity also suppresses IL1RAPL1-dependent stabilization of excitatory synapses. This was assessed by measuring the frequency of insertion of AMPA receptors containing different subunits to surface after IL1RAPL1 overexpression in cortical neurons. Synaptic delivery of GluA1- containing AMPA receptors occurs in an activity-dependent manner. This is followed by a constitutive and slow synaptic AMPA receptor replacement process that consists of removal of AMPA receptors containing long cytoplasmic tail subunits (as GluA1) and synaptic refill with AMPARs containing only short cytoplasmic tail subunits (GluA2/GluA3) (McCormack et al. 2006). Expression of IL1RAPL1 for 2 to 3 days reduces the newly insertion frequency of GluA1 subunit, but

increases the insertion rates of GluA2 and GluA3- containing AMPA receptors. This observation corresponds to the IL1RAPL1-induced increase in spine numbers and suggests that the replacement of AMPA receptors containing different subunits may reflect the switch from newly formed synapses to stable excitatory synapses (Hayashi et al. 2013).

The interaction of IL1RAPL1 with two small GTPases regulators, RhoGAP2 and Mcf2l, provides a link between IL1RAPL1 and its postsynaptic effect, like dendritic spine formation. As not much is known about the targets of these two regulators, to date is hard to conclude about the mechanism of IL1RAPL1-dependent spine remodeling.

2.3.4.3. Neurite branching

Dendrite morphology is a hallmark of neurons and has important functional implications in determining the signals that a neuron receives and how these signals are integrated. RhoGTPases as well as a variety of cell adhesion molecules are involved in the regulation of dendritic arbor morphology (Jan & Jan 2010), and these cellular pathways happen to be related to IL1RAPL1 (Figure 15). Alterations in dendrite morphology including changes in dendrite branching patterns, fragmentation of dendrites and retraction or loss of dendrite branching are observed in several neurological and neurodevelopmental disorders including ID (Kulkarni & Firestein 2012).

As mentioned before, expression of IL1RAPL1 in PC12 cells decreases neurite outgrowth by inhibiting N-type voltage- gated calcium channels via its interaction with NCS-1 (Gambino et al. 2007). In contrast, IL1RAPL1 overexpression in hippocampal neurons in culture does not affect neurite outgrowth at 3-5 DIV (Piton et al. 2008). This could be explained by the fact that, unlike PC12 cells, hippocampal neurons endogenously express IL1RAPL1.

On the other hand, down regulating IL1RAPL1 expression in hippocampal neurons increases dramatically the number and length of neurites (Piton et al. 2008). This phenotype is rescued by the overexpression of full length IL1RAPL1, but not by IL1RAPL1 mutant I367SfsX6, that lacks part of the transmembrane domain as well as the entire cytoplasmic domain. Contrastingly, in hippocampal and cortical neurons from *Il1rapl1* KO mouse, we did not observed any difference in neurite number or length at 2, 4, 5, 10 and 18 DIV (Pavlowsky 2009 and unpublished observations).

Similar to NCS-1, down regulation of *il1rapl1b* in zebrafish olfactory sensory neurons suppresses the morphological remodeling of their axon terminals. A point mutation (Pro455His) on Il1rapl1b TIR domain is also able to abolish the axon terminal remodeling (Yoshida & Mishina 2008). As predicted by homology to other TIR domains, this mutation is located in a conserved loop linking a β-sheet and an α-helix without disturbing TIR structure but is supposed to suppress the recruitment of adaptor molecules (Xu et al. 2000). However this mutation does not affect axon extension and projection. These observations suggest that TIR domain-mediated signaling is necessary for morphological remodeling of axon terminals, but the involvement of IL1RAPL1/NCS-1 interaction in this process is unknown, since the well conserved interaction domain is located in the C-terminal tail (Bahi et al. 2003).

Regulation of dendritic arborization by IL1RAPL1 is currently under investigation. However, branching regulation by IL1RAPL1 appears to be brain region-specific (Caterina Montani, unpublished observations). Some of the IL1RAPL1 partners, like NCS-1 and regulators of small GTPases, are differentially distributed in the brain. For example in human, NCS-1 mRNA is more expressed in cortex than in hippocampus (Chen et al. 2002), and in mouse the NCS-1 protein appears to be slightly more expressed in the hippocampus (Olafsson et al. 1997). The expression differences of the molecular partners could account for the phenotypes observed in different brain regions in the absence of IL1RAPL1.

2.3.5. Other potential IL1RAPL1 interacting proteins

The C-terminal domain of IL1RAPL1 was shown to interact with several proteins by affinity chromatography. Some of the published potential interacting proteins are PLCβ1, SNIP, Rasal1, PKCε, spectrin α1 and β2, and Bat3 (Hayashi et al. 2013), but some of those interactions are probably not physiological. For example, Bat3 (BAG6, protein implicated in the control of apoptosis) is located in the nucleus, while IL1RAPL1 is not.

Like Mcf2l and RhoGAP2, PKCε interacts with the TIR domain of IL1RAPL1. The implication of PKCε in dendritic spine regulation is discarded because this protein is known to interact with the TIR domains of many IL1/Toll receptor family proteins, and swapping the IL1RAPL1 TIR domain with the one of IL1R1 does not regulate spine

morphogenesis (Yoshida et al. 2011). PLCβ1, SNIP and Rasal1 bind to the C-terminal domain of IL1RAPL1, but the functional consequences of these interactions are still unexplored. Phospholipase-C β1 (PLCβ1) is expressed in the brain, where it has an important role in regulating G protein-coupled receptors calcium signaling, and it is present in mouse and human cortical synapses. Snap-25 interacting protein (SNIP, also known as p140Cap) was first described as a protein present in the presynaptic compartment, where it participates in Ca^{2+}-dependent vesicle fusion for exocytosis (Chin et al. 2000; Ito et al. 2008). Further study of this IL1RAPL1-interacting protein will be interesting since the recruitment of SNIP is important for SNAP-25 – regulated spine formation (Tomasoni et al. 2013). Indeed, this protein is also present at postsynapses, where it regulates spine density and morphology (Jaworski et al. 2009). Ras protein activator like 1 (Rasal1) is a regulator of Ras GTPases present in cortical synapses with not known function in the nervous system. As all these proteins may have important roles in spines formation and function, it will be interesting to explore their physiological interaction with IL1RAPL1 at synapses.

Another reported IL1RAPL1 interacting protein is the cystic fibrosis transmembrane conductance regulator (CFTR), a multi domain cAMP-regulated chloride channel found in the apical membrane of polarized epithelia lining many tissues (Wang et al. 2006). Defective folding and export of this protein from the endoplasmic reticulum is the cause of cystic fibrosis, an inherited childhood disease. The interaction of CFTR protein with IL1RAPL1 was observed in a human intestinal cell line, in a study aiming to define the global protein interactions of CFTR required for its folding, trafficking, and function. However, the biological relevance of the direct or indirect IL1RAPL1/CFTR interaction in the brain remains to be explored.

2.4. Phenotypic characterization of Il1rapl1 KO mouse

Most of the *IL1RAPL1* mutations found in ID patients result in the loss of function of IL1RAPL1 (see Table 1 in appendix section). For this reason the *Il1rapl1* knockout (KO) mouse is a valuable tool to explore the consequences of IL1RAPL1 function beyond the cellular level.

The first *Il1rapl1 KO* mouse was generated in Jamel Chelly's laboratory (Gambino et al. 2009) through a strategy based on the genomic deletion of *Il1rapl1* fifth exon, leading to a premature STOP codon after transcription and splicing of exon 4–6. If

produced, the resulting Il1rapl1 protein after the deletion would only contain the first Ig-like domain. A second *Il1rapl1* KO mouse was recently generated in Japan (Yasumura et al. 2014), and was obtained after replacing *Il1rapl1* exon 3 with a neomycin phosphotransferase gene cassette. This strategy leads to the complete absence of Il1rapl1 protein. *Il1rapl1* KO has no lethal consequences, as mice grow and mate normally, and no major structural brain defects are observed (Gambino et al. 2009; Yasumura et al. 2014). Both *Il1rapl1* KO mouse model are interesting tools for evaluating of the impact of Il1rapl1 deficiency in ID patients, especially those having a deletion of the whole *IL1RAPL1* gene.

Different studies have described how the function and plasticity of some neuronal circuits are impaired in absence of *Il1rapl1*, in particular in the cerebellum and the hippocampus (Gambino et al. 2009; Pavlowsky, Gianfelice, et al. 2010). More recently two studies (one of them being part of this thesis) characterized another brain structure affected in *Il1rapl1* KO mouse, the amygdala (Houbaert et al. 2013; Zhang et al. 2014). Overall, these observations lead to the conclusion that the absence of Il1rapl1 produces an imbalance of excitatory/inhibitory synaptic transmission that is translated into deficits in different types of learning and memory.

One of the phenotypes reported in *Il1rapl1* KO mice is hyperactivity ((Yasumura et al. 2014) and H. Meziane unpublished observations). This behavioral trait has also been observed in some patients with deletions in *IL1RAPL1* gene (Nawara et al. 2008; Franek et al. 2011; Youngs et al. 2012).

Il1rapl1 KO mice show consistent impairments of cognitive functions in several learning and memory tests (Zhang et al. 2014; Yasumura et al. 2014; Houbaert et al. 2013) (see also unpublished results). The acquisition of spatial reference memory is slower in *Il1rapl1* KO than in wild-type mice, but the KO mice can perform the task if they are trained for long enough. Furthermore, *Il1rapl1* KO mice have a difficulty to retain the remote memory, as well as spatial working memory. Cued and contextual fear conditionings are also impaired in those mice. Autistic-like features observed in some patients with *IL1RAPL1* mutations, were also present in *Il1rapl1* KO mice (stereotypies and behavioral flexibility). Unexpectedly, social interaction and motor coordination were enhanced and anxiety behavior was reduced (Yasumura et al. 2014). No differences were observed in the hot plate, acoustic startle response and paired pulse

inhibition tests between wild-type and *Il1rapl1* KO mice, indicating that sensory and motor responses are not impaired in the absence of Il1rapl1 (Yasumura et al. 2014).

Altogether, these observations suggest that *Il1rapl*1 KO mice model mimics the cognitive impairment of ID patients with *IL1RAPL1* mutations.

2.5. IL1RAPL1 is a member of IL1 receptor family

As mentioned earlier, IL1RAPL1 is a member of interleukin 1 (IL1) receptor family of proteins. IL1 receptor family members as well as their ligands have critical and well-described roles in immune system, but the objective of this section is to address the known roles of this family of proteins in the brain.

2.5.1. IL1β signaling in the brain and regulation of synaptic function

Cytokines are small signaling molecules that mediate cell-to-cell communication, ranging from immune response to a variety of physiological and pathological processes. These molecules are secreted by different cell types and present at low concentrations in the nervous system under physiological conditions but increase up to hundreds of times their basal concentrations in pathological conditions.

The interleukin 1 (IL1) family consists of 11 cytokines, but I will focus on the principal members, which are IL1α and IL1β. Interleukin 1α and interleukin 1β display high sequence homology, and both exist as inactive forms until they are cleaved by calpain and caspase-1, respectively. In the brain, IL1β has been more extensively studied than IL1α, even if some studies have reported that both have almost the same signaling effect at least in mixed glial cells cultures (Andre, Pinteaux, et al. 2005). Several studies have demonstrated that IL1β has roles not only on inflammatory conditions but also in physiological conditions, like learning and memory (Goshen et al. 2007; Avital et al. 2003). IL1β affecting directly the brain may have two origins: it can be produced elsewhere in the body and access to the brain through the brain blood barrier, or it can be produced by brain cells, mainly by microglia. However all receptors needed to transduce IL1β signaling are present in virtually all brain cell types (Ban et al. 1993; Blasi et al. 1999; Pinteaux et al. 2002; Andre, Lerouet, et al. 2005).

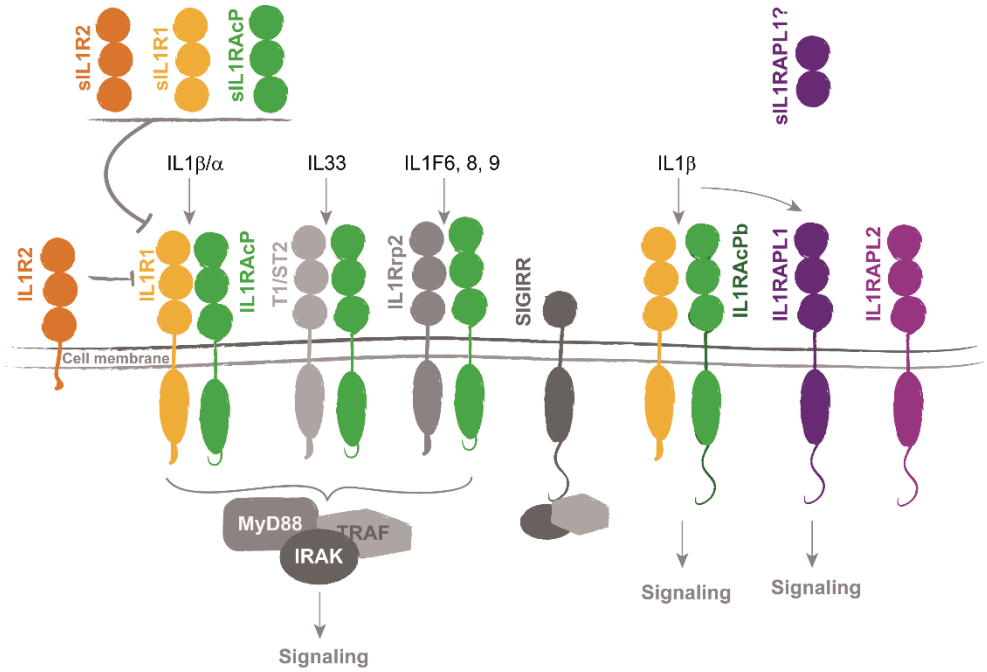

Figure 16. Interleukin 1 receptor family of proteins regulate cytokines signaling. Cytokines bind to the receptors, allowing the recruitment of accessory proteins and adaptor proteins that mediate intracellular signaling. Soluble or decoy isoforms can interfere with this signaling through different mechanisms as explained in the text.

The cellular signaling of IL1 family of cytokines is mediated through a group of closely related receptors, in which the defining structure is the Toll–IL1R (TIR) domain (Figure 16). Binding of each IL1 family cytokine to its receptor, IL1 receptor type I (IL1R1) in the case of IL1β and IL1α, initiates the signaling (Sims et al. 1988). The interaction of the cytokine and the IL1 receptor allows the recruitment of an accessory protein, IL1R accessory protein (IL1RAcP) (Cullinan et al. 1998). There are five receptors for IL1 family cytokines (IL1R1, IL1R2, T1/ST2, IL18Rα, IL1Rrp-2), and IL1RAcP is shared by four of them (all but IL18Rα).

Formation of the cytokine-receptor-accessory protein heterodimer and juxtaposition of the two TIR domains enables the recruitment of signaling intermediates including myeloid differentiation primary response protein 88 (MyD88), IL1R-associated kinase 4 (IRAK4) and TNFR-associated factor 6 (TRAF6) (O'Neill 2000).
Regulation of IL1 signaling is very complex and includes different mechanisms:

- Blocking the interaction of IL1 with IL1R1 by IL1Ra, a natural antagonist. IL1Ra is a protein highly homologous to IL1α and IL1β in its amino acid sequence, three-dimensional folding and gene structure. This antagonist can bind to IL1R1

with the same affinity than the other ligands, tough in a different manner, but does not allow the recruitment of IL1RAcP, sequestering the activating receptor into an inactive ligand–receptor complex.

- Blocking the recruitment of IL1RAcP to IL1/IL1R1 complex by IL1R2, that contains only an extracellular domain without being able to trigger TIR-mediated intracellular signaling (Symons et al. 1995). IL1R2 binds to IL1α and IL1β with high affinity and forms a complex with IL1 and IL1RAcP, sequestering IL1RAcP. In contrast, IL1R2 binds IL1Ra with low affinity (Symons et al. 1995).
- Interfering with IL1R1 and IL1RAcP through soluble proteins that consist on the extracellular domain of IL1R1, IL1RAcP or IL1R2 (see Figure 16). These soluble proteins are generated by alternative splicing (sIL1R2, sIL1RAcP), or by protein cleavage (sIL1R1, sIL1R2) (Elzinga et al. 2009). The generation of soluble forms is tissue specific, at least for IL1RAcP isoforms (Jensen et al. 2000; Jensen & Whitehead 2004). As an example of negative regulation, sIL1R2 can interact with IL1β precursor and prevent its cleavage (Symons et al. 1995). Other mechanisms of regulation by these soluble proteins are not fully elucidated at the physiological level. However, soluble proteins have been used as treatment for an autoimmune model of rheumatoid arthritis or as experimental tools to interfere with IL1R1/IL1RAcP signaling (Yoshida et al. 2012; Yoshida et al. 2011; Smeets et al. 2005).

IL1R1, IL1R2 and IL1RAcP are present in neurons and glial cells (Smith et al. 2009). In the brain, IL1RAcP exists in two membrane bound isoforms generated by alternative splicing: the more widely expressed IL1RAcP and the brain-specific IL1RAcPb also known as IL1RAcP687 (Smith et al. 2009; Lu et al. 2008). The IL1RAcPb isoform is principally expressed in neurons and is observed at low levels in astrocytes (Smith et al. 2009; Nguyen et al. 2011; Huang et al. 2011). IL1RAcPb contains 140 extra amino acids at the C-terminal, which may confer particular signaling properties since the IL1β -mediated response mediated by this isoform is considerably different from that of IL1RAcP as mentioned further in this section (Smith et al. 2009; Huang et al. 2011).

When first described, IL1RAPL1 was related to this family of proteins because of its similarity with IL1RAcP (51%) (Carrié et al. 1999). However, no experimental evidence of its function as a receptor or accessory protein has been provided. Like IL1RAcPb,

IL1RAPL1 also contains ~140 amino acids on its C-terminal tail, but the similarity of this region between the two proteins is quite low. IL1RAPL1 C-terminal tail was predicted to have little secondary structure (Sana et al. 2000).

IL1RAPL2 and *IL1RAPL1* genes are the only members of the family located in the X chromosome. IL1RAPL2 share the same domains, the same exon–intron organization and a high degree of similarity at the protein level (63%) with IL1RAPL1 (Sana et al. 2000). This protein also contains a long C-terminal domain (140 amino acids long) but it shares only 43% of identity with IL1RAPL1. The C-terminal of IL1RAPL2 does not contain neither the NCS-1 interaction sequence nor the PDZ-binding domain present in IL1RAPL1. In situ RNA hybridization studies show that *Il1rapl2* is specifically expressed in the mouse nervous system from embryonic day 12.5 (Ferrante et al. 2001) and a RNA transcript of 5.5 kb was detected in human brain fetal tissue (Sana et al. 2000). *Il1rapl2* mRNA is present in astrocytes, microglia and oligodendrocytes, but is not detectable in cortical neurons (Andre, Lerouet, et al. 2005). On the contrary, we were able to detect *Il1rapl2* transcripts in hippocampal neurons, but barely in astrocytes (unpublished observations).

In addition to IL1RAPL1 and IL1RAPL2, there is another member of IL1R family with not known ligand nor accessory activity: Single Ig IL1 related receptor (SIGIRR) is considered as a negative regulator of IL1 signaling, since it can interact with IRAK and TRAF-6 (Qin et al. 2005; Wald et al. 2003). Although there is only a single IgG domain in the extracellular domain, the intracellular part contains a TIR domain and a 95 amino acids long C-terminal domain (Thomassen et al. 1999). In mice deficient in SIGIRR there is more inflammation compared with wild-type control mice, which suggests that it is an inhibitor of inflammation (Wald et al. 2003). In the brain, this protein is expressed in cortical neurons, astrocytes and microglia (Andre, Lerouet, et al. 2005).

Some of the IL1R family transcripts are regulated in brain in response to focal cerebral ischemia and to lipopolysaccharide treatment, known for inducing a strong immune response (Wang et al. 1997; Andre, Lerouet, et al. 2005), but also after IL1 β treatment (Gayle et al. 1997). IL1β mRNA is induced after fear conditioning and LTP protocols (Goshen et al. 2007; Schneider et al. 1998). These observations suggest that this family of proteins have a role in brain inflammation, but not only, as I will address hereafter.

Besides IL1RAPL1, the presence at synapses of some members of this family is not clear, and there are just few reports. In one of them, it was shown by subcellular fractionation of adult hippocampus that IL1R1 is enriched in PSD fractions, together with specific markers like PSD-95 and glutamate receptors subunits (Gardoni et al. 2011). However in the same study, only traces of IL1RAcP were observed in this fraction. Furthermore, the analysis of co-localization with PSD-95 protein in cultured hippocampal neurons showed that IL1R1 is present in dendrites and highly co-localizes with PSD-95, whereas IL1RAcP is rather present at cell bodies and hardly co-localizes with PSD-95 in dendrites. In contrast to the subcellular fractionation study, Yoshida and collaborators (2012) observed IL1RAcP at synapses. As this was carried out by overexpression, it is not clear if endogenous protein is located at synapses, and no proper synaptic markers were used to address this issue.

The presence of IL1R proteins at synapses raises the question of which are their signaling partners at these sites. The NMDA glutamate receptor subunit GluN2B interacts with the intracellular domain of IL1R1, and interestingly, NMDA and IL1β treatment of neurons in culture increases the amount of IL1R1 to synapses (Gardoni et al. 2011). IL1β treatment increases NMDA receptor function and NMDA-mediated calcium influx in hippocampal neurons in culture, a response specifically mediated by IL1RAcPb (Viviani et al. 2003; Lai et al. 2006; Huang et al. 2011). Regulation of glutamate receptors by IL1β is not exclusive of NMDA receptors, since it was also observed that IL1β down regulates the surface expression of AMPA receptors by phosphorylating GluA1 subunit (Lai et al. 2006). IL1β increases GABAergic transmission in cortical synaptoneurosomes (subcellular preparation containing pre and postsynaptic structures), indirectly indicating the presence of at least IL1R1 in this preparation (Miller et al. 1991). However, the effects of this cytokine on GABA currents are not clear since inhibition of these current by IL1β was also reported in cultured hippocampal neurons (Wang et al. 2000).

These studies show that in addition to its role in infection and immunity, IL1β is able to modulate both glutamatergic and GABAergic transmission. Besides, IL1β exposure decreases dendrite complexity and length, which can impact the function of the neuronal networks (Gilmore et al. 2004).

2.5.2. Regulation of cognitive functions by IL1R members

IL1RAPL1 is the only member of IL1R family implicated in ID. Up to now, there are no mutations in IL1RAPL2 associated with ID, but some studies suggest its implication in ASD and developmental delay (Yamamoto et al. 2014; Shimojima et al. 2011).

Several studies reported a negative effect of IL1β treatment on LTP in hippocampal slices (Katsuki et al. 1990; Bellinger et al. 1993; Ross et al. 2003). Interfering with IL1 signaling in mice, by overexpressing IL1Ra or knocking down *Il1r1*, impairs hippocampal-dependent memory, but not hippocampal independent behavior (Avital et al. 2003). Interestingly, IL1β appears to have a dual role in hippocampal function, by impairing or improving hippocampal-dependent memory and LTP at high or low doses of IL1β, respectively. The hippocampal memory impairment produced by high doses is also observed by inhibiting IL1β action using IL1Ra (Goshen et al. 2007; Ross et al. 2003). This demonstrates that in inflammatory conditions, the high IL1β level has a negative effect on hippocampal function, while in physiological conditions this cytokine participates in the hippocampal plasticity (Pugh et al. 2001; Goshen et al. 2007). The specificity of IL1β effects on hippocampus may be due to the fact that IL1R1 and IL1RAcP are mainly expressed in this brain region (Allen Mouse Brain Atlas, http://www.brain-map.org). An interesting observation is that learning and memory impairments in *Il1r1* deficient mouse are rescued by the local injection of astrocytic precursor cells expressing IL1R, providing evidence for the importance of IL1 signaling in the different brain cell types for hippocampal function (Ben Menachem-Zidon et al. 2011).

2.5.3. IL1 receptor family members involved in synaptogenesis

In neurons, IL1β treatment produces the loss of excitatory synaptic connections (Mishra et al. 2012). This raises relevant questions about which IL1β receptors mediate this synaptic remodeling, and if a competition between the classical cellular response and synaptic response to IL1β exists.

Like IL1RAPL1, the two IL1RAcP isoforms have synaptogenic activity and interact with PTPδ with a KD of 0.7μM, showing less affinity than IL1RAPL1 (KD 0.3 μM) (Yoshida et al. 2012). Binding of PTPδ to IL1RAcP/AcPb is significantly enhanced by the presence of both meA and meB, independently of the meA variation (Yamagata, Yoshida, et al. 2015). In a lesser extent, IL1RAcP/AcPb interact with PTPσ and LAR

proteins (Yoshida et al. 2012). The latter could have a functional relevance since IL1RAcP-dependent presynaptic induction is only partially abolished in co-cultures of HEK293 cells over expressing the accessory protein and *Ptprd* KO neurons.

As observed for IL1RAPL1, knocking down *Il1racp* in cortical neurons decreases pre and postsynaptic differentiation (Yoshida et al. 2012). This defect is also observed in of *Il1rap* KO mice, where a decrease on dendritic spine density in the cortex and the hippocampus was observed. Overexpression of both IL1RAcP isoforms can induce excitatory presynaptic differentiation but only IL1RAcPb can also promote dendritic spine formation (Yoshida et al. 2012). This indicates that the different domains of this protein regulate different processes, and suggests that its C-terminal tail confers IL1RAcPb brain-specific characteristics to the protein. Indeed, IL1RAcPb terminates in a consensus type II PDZ domain binding sequence but no interacting partner has been described yet. Interestingly and in contrast to IL1RAPL1, little but significant inhibitory presynaptic induction was observed in neurons overexpressing IL1RAcP (Yoshida et al. 2012), opening the possibility of having non-explored partners at inhibitory synapses.

IL1RAPL2 overexpression is able to induce pre and postsynaptic differentiation in neuronal cultures (Valnegri et al. 2011). Its capacity of inducing dendritic spines increase is about the same than IL1RAPL1 effect, but the VGlut1 increase is less important. IL1RAPL2 interacts with PTPδ in a specific manner, like IL1RAPL1, since it does not bind to either PTPσ or LAR (Valnegri et al. 2011).

Besides IL1RAPL1, IL1RAPL2 and IL1RAcP/AcPb, other members of the IL1 receptor family do not have synaptogenic activity (Yoshida et al. 2012). All this evidence suggests that IL1RAcP may have two roles, one as an accessory protein with IL1R1 to mediate IL1β responses, and another interacting with PTPδ to regulate synaptic adhesion and synapse organization. In the same line, IL1RAcPb, IL1RAPL1 and IL1RAPL2 emerge as a new group of IL1R members with a role in synaptic organization and function.

2.5.4. IL1β-induced signaling in neurons and astrocytes

The best characterized IL1β-induced cellular signaling consists of the activation of the transcription factor nuclear factor κB (NFκB) and the mitogen-activated protein kinases

(MAPK). NFκB pathway controls the transcription of a large set of target genes with important roles in cell survival, inflammation, and immune response. MAPK are transducing proteins also involved in many facets of cellular regulation, linking signaling from membrane receptors to gene expression in neurons. They include p38, JNK and ERK1/2 kinases, whose function is activated by kinases-mediated phosphorylation and inactivated by phosphatases-mediated dephosphorylation. Throughout this text, the terms activation and phosphorylation of kinases are indistinctly used.

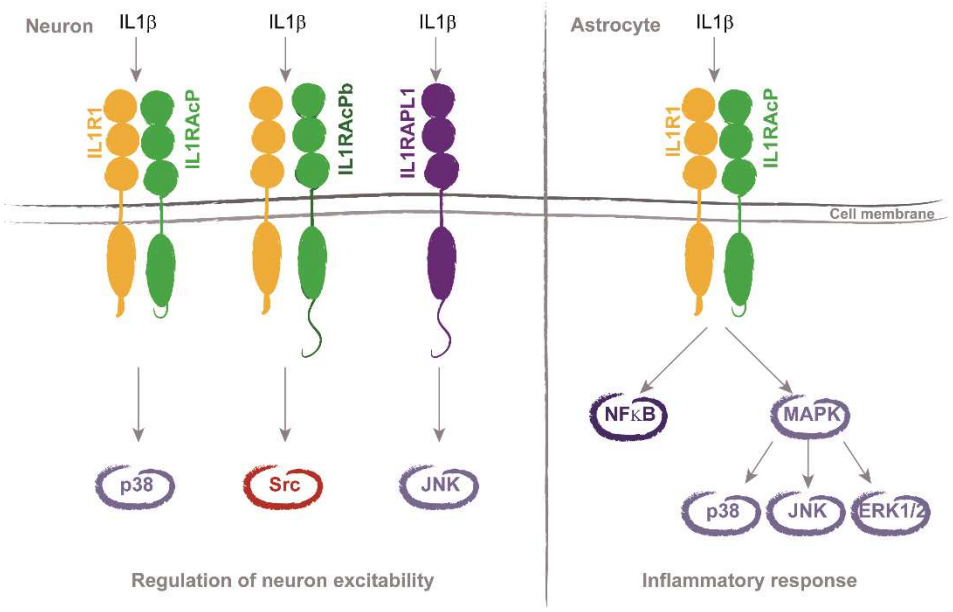

Figure 17. IL1β induces different cellular signaling in different brain cell types. The signaling mediated by IL1β in neurons is shown in the left, and in astrocytes in the right.

As shown in Figure 17, IL1β elicits different signaling in neurons and in astrocytes and its ability to trigger cellular signaling depends on the expression of IL1R1 and the appropriate accessory protein, and activation of specific intracellular signaling pathways. Different responses to IL1β were reported, depending of experimental procedures, like IL1β concentration, time of exposure, cell culture purity and brain structure. In the following section I will summarize the signaling pathways elicited by IL1β in two different brain cell types, neurons and astrocytes.

Neurons

IL1β modulates the electrophysiological state and excitability of neurons via distinct signaling pathways. In these cells, only IL1β-induced activation of Src and p38 was

consistently reported (Srinivasan et al. 2004; Tsakiri et al. 2008; Pavlowsky, Gianfelice, et al. 2010; Huang et al. 2011). However, a single study reported JNK activation in cortical neurons (Pavlowsky, Zanchi, et al. 2010), and NFκB in cerebellar neurons (Pizzi et al. 2002).

Src is a non-receptor-type protein tyrosine kinase, with known roles on synaptic activity regulation through the phosphorylation of different neurotransmitter receptors (Ohnishi et al. 2011). In neurons, IL1β-induced Src phosphorylation is regulated by IL1RAcPb (Huang et al. 2011; Smith et al. 2009), and is the consequence of the activation of neutral sphingomyelinase 2 (N-SMase2) and ceramide production (Davis et al. 2006). Moreover, IL1RAcPb-dependent phosphorylation of Src after IL1β treatment is responsible of NMDA receptor activation by phosphorylation of GluN2B, increasing the receptor currents and calcium influx as mentioned before (Huang et al. 2011; Viviani et al. 2003). IL1RAcPb was shown to interact with IL1R1 in an IL1β-dependent manner in two different cell lines (Smith et al. 2009; Lu et al. 2008), and this is supported by the fact that activation of neutral sphingomyelinase by IL1β is dependent on IL1R1 in neurons (Nalivaeva et al. 2000). However, the information about the capacity of IL1RAcPb to recruit the other components of the signaling complex, like MyD88, IRAK and Tollip, is contradictory (Smith et al. 2009; Lu et al. 2008). These interactions remain to be explored in neurons, including the ones mediated by the C-terminal tail. With this respect, Smith and collaborators (2009) showed that the presence or absence of this tail does not affect the inability of IL1RAcPb to mediate IL1β /IL1R signaling.

In neurons, the IL1β-induced phosphorylation of p38 MAPK is regulated by IL1RAcP. The activation of this MAPK was observed in cortical and hippocampal neurons from *Il1racpb* and *Il1rapl1* KO mice, but not in *Il1racp* KO neurons (Smith et al. 2009; Pavlowsky, Zanchi, et al. 2010). JNK activation by IL1β was shown to be dependent of Il1rapl1 in cortical neurons (Pavlowsky, Zanchi, et al. 2010). Moreover, JNK phosphorylation is decreased in the brain cortex of *Il1rapl1* KO mouse in basal conditions. Consequently, phosphorylation levels of PSD-95 Ser-295 is decreased, leading to a reduction of PSD-95 localization at the synapse (Pavlowsky, Gianfelice, et al. 2010). Both JNK and PSD-95 phosphorylation levels were reestablished in *Il1rapl1* KO neurons by treatment with okadaic acid, an inhibitor of PP1 and PP2B phosphatases. This suggests two possible mechanisms of IL1RAPL1-dependent JNK activation: one by the regulation of an upstream JNK activator, like Rac1, and the other

by the regulation of phosphatases activity (Pavlowsky, Gianfelice, et al. 2010). The capacity of IL1RAPL1 to activate JNK was observed by overexpression in different systems (Khan et al. 2004).

JUN amino-terminal kinases (JNK), also known as stress-activated protein kinases (SAPK), and are members of MAPK. They are encoded by 3 genes (JNK1-3) that together generate 10 isoforms of 54 and 46 kDa. JNKs have different roles in the brain, from regulation of cytoskeleton dynamics to synaptic plasticity by phosphorylation of synaptic targets (Coffey 2014). For example, in neurons JNK phosphorylates PSD-95 on Ser295, causing its enrichment at synapses, resulting in the enhancement of postsynaptic currents (Kim et al. 2007). In addition JNK phosphorylates the long splice form of the GluR2 AMPAR subunit (GluR2L) and facilitates its insertion at the cell surface in response to NMDAR stimulation (Thomas et al. 2008).

Opposed to IL1RAPL1, IL1RAPL2 is not able to activate JNK (Khan et al. 2004). IL1RAPL2 is not able to activate NFκB in non-neuronal cells (Born et al. 2000; Sana et al. 2000) nor to bind to IL1β (Bahi et al. 2003; Smith et al. 2000) and no evidence of function as accessory protein has been yet provided.

Astrocytes

IL1β is expressed at very low levels in the adult healthy brain and it is possible that in these conditions this cytokine exerts no pro-inflammatory actions on glial cells, including astrocytes. In contrast, when IL1 expression is dramatically increased by injury or inflammation, it acts on those cells to initiate the inflammatory response. The astrocytic response to IL1β includes the synthesis and release of cytokines, adhesion molecules, prostaglandins, nitric oxide (NO), and growth factors. Those responses are regulated by NFκB, p38, ERK1/2 and JNK, since IL1β-dependent activation of these proteins is abrogated in glial cells from *Il1r1* and *Il1racp* KO mice (Molina-Holgado et al. 2000; Parker et al. 2002; Huang et al. 2011). In the absence of Il1rapl1, JNK phosphorylation can be triggered by IL1β in both cortical and hippocampal astrocytes in culture (unpublished observations).

IL1β signaling in astrocytes is able to regulate other signaling pathways, like RhoGTPases, having an impact on the cell morphology changes induced by inflammation (John et al. 2004).

RESULTS

When I started my PhD, IL1RAPL1 was known to interact with NCS-1 to regulate calcium-mediated vesicle release in PC12 cells, with PSD-95 to regulate its targeting to the synapses, and to regulate JNK activity (Gambino et al. 2007; Khan et al. 2004; Pavlowsky, Gianfelice, et al. 2010; Pavlowsky, Zanchi, et al. 2010). Moreover, IL1RAPL1 was shown to be located at excitatory synapses and to have a strong synaptogenic activity. At that time another molecular partner of IL1RAPL1, PTPδ, was described by two different research groups. This discovery changed the perspectives for IL1RAPL1 protein function: it does not receive attention as a member of interleukin 1 receptor family anymore, but rather unravels a new trans-synaptic function in which each IL1RAPL1 domain, extra and intracellular, regulates different signaling during synaptogenesis.

The aim of my PhD work was to evaluate the consequences of ID-associated *IL1RAPL1* mutations impacting the extracellular domain of the protein on IL1RAPL1-dependent synaptogenesis. The extracellular domain of IL1RAPL1 interacts with PTPδ, and perturbing IL1RAPL1/PTPδ interaction could alter synaptogenesis and ultimately lead to cognitive deficits. This study was the object of the first article presented here.

Besides the localization of IL1RAPL1 in excitatory synapses, it was not known if all synapses in all brain regions were affected to the same extent in the absence of IL1RAPL1. This could be first assessed by the characterization of IL1RAPL1 localization in different brain regions and cell types. I participated in this description and the results were included in a publication leaded by Yann Humeau. Moreover, this study addressed the behavioral consequences associated with *Il1rapl1* loss of function in a particular brain region, the lateral amygdala, and provides the first published characterization of cognitive deficits in *Il1rapl1* KO mice.

Besides these published results, I also participated in other studies about IL1RAPL1 pathophysiology. One of them (included in the unpublished results section) aims to propose the negative regulation of $GABA_A$ receptors as way to improve the cognitive impairments in *Il1rapl1* KO mice.

1. Novel *IL1RAPL1* mutations associated with intellectual disability impair synaptogenesis.

To date, most of the *IL1RAPL1* mutations found in ID patients are deletions that can include large fragments of the gene. Some *IL1RAPL1* duplications have also been described, but their implication in the ID pathology is not well understood. When I started my PhD work, few mutations on *IL1RAPL1* other than copy number variation were described, and few information about their consequences for protein function was available. So far, two nonsense mutations in exon 11 (Y459X and W487X) leading to a frame shift of the open reading frame, and thus to premature termination of translation, were found in ID patients (Carrié et al. 1999; Kozak et al. 1993; Tabolacci et al. 2006). The predicted proteins produced by these frameshifts lack part of the IL1RAPL1 TIR domain and the entire C-terminal domain. A synthetic mutant lacking both the TIR and the C-terminal domain (ΔC) is able to increase presynaptic differentiation, but not to increase dendritic spines number (Pavlowsky, Gianfelice, et al. 2010; Valnegri et al. 2011). A nonsense mutation found in exon 9, I367SX6, is predicted to produce a protein lacking part of the trans-membrane domain as well as the entire intracellular domain (Piton et al. 2008). This probably leads to a loss of IL1RAPL1 function, since the produced protein it is not even targeted to the membrane. Another example is the in-frame deletion of *IL1RAPL1* exons 3-6 (p.28_259del), that is predicted to produce a short protein devoid of the two firsts Ig-like domains. A mutant lacking these two Ig-like domains, ΔN, does not increase dendritic spine density, nor increases functional excitatory synapses (Valnegri et al. 2011). However, it is likely that large *IL1RAPL1* deletions do not lead to protein production due to mRNA degradation by the nonsense-mediated decay system (Miller & Pearce 2014), and that truncated proteins loose completely their function or may be degraded (Caramelo & Parodi 2015).

In contrast to these *IL1RAPL1* deletions, a point mutation located in exon 3 [c.91T>C; p.(Cys31Arg)], was identified in an ID cohort by Patrick Tarpey in collaboration with Anna Hackett and Jozef Gecz in Australia, but its consequence was not further explored even if it was predicted to damage IL1RAPL1 protein function (Tarpey et al. 2009). In the framework of the diagnosis activity at Cochin Hospital, an inherited deletion of *IL1RAPL1* exon 6 was identified in some members of a French family

presenting with ID, studied by Delphine Heron and collaborators. This was an in-frame exon deletion predicted to have no impact on protein translation. Another genomic deletion of the same nature was described in an unrelated ID patient by R. Frank Kooy and Bart Loeys, in Belgium.

Both Cys31 and exon 6 are located in the coding regions for the extracellular domain of IL1RAPL1, the region known to interact with PTPδ (Figures 8 and 13). The characterization of these mutations is interesting from two points of view: one is to determine the consequences of these mutations on IL1RAPL1 protein production and function that could explain ID patient's phenotype, and the other to better understand the specific function of IL1RAPL1 extracellular domain. This characterization was the subject of the first article presented here, and was realized in collaboration with the teams of Carlo Sala and Yann Humeau.

By overexpressing C31R and Δex6 IL1RAPL1 in mouse neurons in culture, we showed that both mutants lead to the loss of the synaptogenic function of IL1RAPL1, but by different mechanisms. In one hand, C31R protein expression is not affected, it is targeted to the membrane and located at synapses, suggesting that this mutant protein has the potential to mediate the same signaling that the wild-type IL1RAPL1. However, C31R mutation abolishes the IL1RAPL1-mediated induction of pre and postsynaptic differentiation, and further analysis shows that this mutation decrease IL1RAPL1/PTPδ interaction. On the other hand, Δex6 mutant is located at the membrane, but it is not expected to lead to IL1RAPL1-dependent signaling, since its protein expression is dramatically decreased and it is not correctly targeted to synapses. Like C31R, Δex6 does not induce synapse formation and does not interact with PTPδ. But unlike C31R, this is probably due to its low expression and miss-localization. One interesting result was that both mutants are still able to increase JNK phosphorylation in non-neuronal cells. This observation dissociates two IL1RAPL1 functions, the synaptogenic and the JNK-regulating ones.

We evaluated also the functional impact of Ile643Val variant, found in healthy as well as in ID patients ((Piton et al. 2008) and unpublished observations). This missense mutation is located in the exon 11, that codes for the C-terminal tail. This IL1RAPL1-specific tail is predicted to have little secondary structure which can explain why amino acid changes in this domain appear to be tolerated by the protein (predicted by Polyphen2, (Adzhubei et al. 2010)) and several SNPs found in healthy patients are located in this region (Table 1 in appendix section).

Altogether, this study provides the evidence for IL1RAPL1 protein misfunction in patients carrying either C31R or Δex6 mutations that can explain their cognitive deficits. Moreover, we also suggest that Cys31 is a critical residue necessary for IL1RAPL1/PTPδ interaction, which was recently confirmed by crystallographic studies (Yamagata, Yoshida, et al. 2015). The location of C31 residue is shown in red in Figure 18.

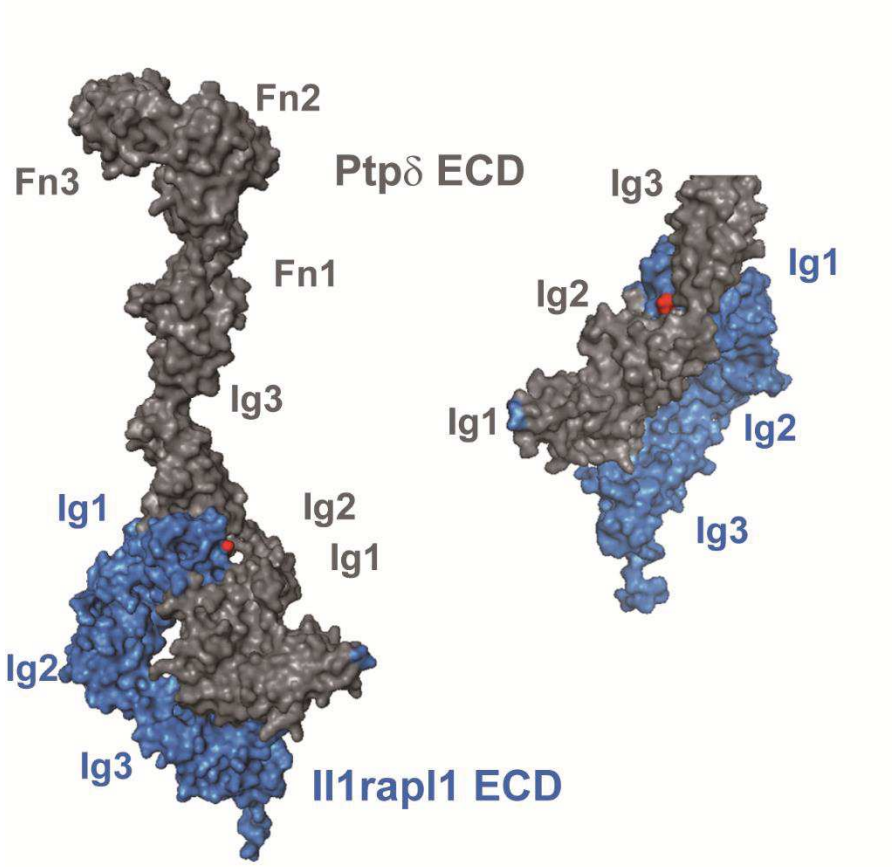

Figure 18. Crystal structure of Il1rapl1 and Ptpδ interaction. The extracellular domain (ECD) of Il1rapl1 is shown in blue, and the one of Ptpδ in grey. Red residue shows the location of IL1RAPL1 Cys31, whose change to R was found in an ID patient. This mutation lead to a decrease of interaction with PTPδ, and thus of IL1RAPL1-induced synaptogenesis. Image generated with PyMOL visualization system (https://www.pymol.org/), using as a template the crystallographic structure defined by Yamagata and collaborators (2015).

Human Molecular Genetics, 2015, Vol. 24, No. 4 **1106–1118**
doi:10.1093/hmg/ddu523
Advance Access published on October 9, 2014

Novel *IL1RAPL1* mutations associated with intellectual disability impair synaptogenesis

Mariana Ramos-Brossier[1,†], Caterina Montani[2,†], Nicolas Lebrun[1], Laura Gritti[2], Christelle Martin[3], Christine Seminatore-Nole[1], Aurelie Toussaint[4], Sarah Moreno[1], Karine Poirier[1], Olivier Dorseuil[1], Jamel Chelly[1,‡], Anna Hackett[5], Jozef Gecz[6], Eric Bieth[7], Anne Faudet[8], Delphine Heron[8], R. Frank Kooy[9], Bart Loeys[9], Yann Humeau[3], Carlo Sala[2] and Pierre Billuart[1,*]

[1]Institut Cochin, INSERM U1016, CNRS UMR8104, Université Paris Descartes, Paris 75014, France, [2]CNR Neuroscience Institute and Department of Medical Biotechnology and Translational Medicine, University of Milan, Milan 20129, Italy, [3]IINS, CNRS UMR5297, Université de Bordeaux, Bordeaux 33000, France, [4]Assistance Publique-Hôpitaux de Paris, Laboratoire de Biochimie et Génétique Moléculaire, Hôpital Cochin, APHP, Paris 75014, France, [5]Genetics of Learning Disability Service, Hunter Genetics, Waratah, NSW 2298, Australia, [6]School of Paediatrics and Reproductive Health, Robinson Institute, The University of Adelaide, Adelaide, SA 5006, Australia, [7]Service de Génétique Médicale, Hôpital Purpan, Toulouse 31059, France, [8]Genetics and Cytogenetics Department, GRC-UPMC, Pitié-Salpetrière CHU, Paris 75013, France and [9]Department of Medical Genetics, Faculty of Medicine and Health Sciences, University and University Hospital Antwerp, Antwerp 2610, Belgium

Received July 5, 2014; Revised and Accepted October 7, 2014

Mutations in interleukin-1 receptor accessory protein like 1 (*IL1RAPL1*) gene have been associated with non-syndromic intellectual disability (ID) and autism spectrum disorder. This protein interacts with synaptic partners like PSD-95 and PTPδ, regulating the formation and function of excitatory synapses. The aim of this work was to characterize the synaptic consequences of three *IL1RAPL1* mutations, two novel causing the deletion of exon 6 (Δex6) and one point mutation (C31R), identified in patients with ID. Using immunofluorescence and electrophysiological recordings, we examined the effects of IL1RAPL1 mutant over-expression on synapse formation and function in cultured rodent hippocampal neurons. Δex6 but not C31R mutation leads to IL1RAPL1 protein instability and mislocalization within dendrites. Analysis of different markers of excitatory synapses and sEPSC recording revealed that both mutants fail to induce pre- and post-synaptic differentiation, contrary to WT IL1RAPL1 protein. Cell aggregation and immunoprecipitation assays in HEK293 cells showed a reduction of the interaction between IL1RAPL1 mutants and PTPδ that could explain the observed synaptogenic defect in neurons. However, these mutants do not affect all cellular signaling because their over-expression still activates JNK pathway. We conclude that both mutations described in this study lead to a partial loss of function of the IL1RAPL1 protein through different mechanisms. Our work highlights the important function of the trans-synaptic PTPδ/IL1RAPL1 interaction in synaptogenesis and as such in ID in the patients.

INTRODUCTION

Intellectual disability (ID) is defined as an overall intelligence quotient (IQ) of <70 and limitations in adaptive behavior, with an onset before the age of 18. ID affects $\sim$3% of the population, and X-linked ID (XLID) is responsible for 10% of severe ID cases. To date, 116 of XLID genes have been identified. Mutations in one of these genes, interleukin-1 receptor accessory protein-like 1 (*IL1RAPL1*), are associated with cognitive impairment ranging from non-syndromic ID to autism spectrum disorder (ASD). Until now, described mutations include exon deletions and nonsense mutations that result in the absence of protein, in most of the cases (1–14).

*To whom correspondence should be addressed at: Pierre Billuart, INSERM U1016 – Institut Cochin, 24 rue du Faubourg Saint Jacques, Paris 75014, France. Tel: +33 144412486; Fax: +33 144412421; Email: pierre.billuart@inserm.fr
†The authors wish it to be known that, in their opinion, the first two authors should be regarded as joint First Authors.
‡Present address: IGBMC – UMR 7104 CNRS, Inserm U964, Université de Strasbourg, Strasbourg 67404, France.

IL1RAPL1 is a member of interleukin 1 receptor family and shares 52% of homology with the IL-1 receptor accessory protein (IL1RAcP) (1). It contains three extracellular immunoglobulin (Ig)–like domains, a single transmembrane domain, an intracellular Toll/IL-1R (TIR) domain and a C-terminal tail of 150 amino acids, that is not shared with other family members. IL1RAPL1 is expressed in the brain and is located on excitatory synapses with an enrichment at the postsynaptic compartment (15).

The importance of IL1RAPL1 in brain function was demonstrated by studies of *Il1rapl1* knockout mouse model (16). These mice show impaired associative learning and synaptic defects, including decrease in dendritic spines and synaptic plasticity in different brain regions (15,17).

Growing body of evidence underlines the importance of IL1RAPL1 on synapse physiology. Several IL1RAPL1-interacting proteins necessary for IL1RAPL1-induced pre- and post-synaptic differentiation have been identified. IL1RAPL1 interacts through its C-terminal domain with the calcium sensor NCS-1, regulating the activity of N-type voltage-gated calcium channel in PC12 cells (18,19). In neurons, IL1RAPL1 interacts with PSD-95, a major scaffolding protein of excitatory synapses, and modulates its synaptic localization by regulating JNK activity and PSD-95 phosphorylation (15). Interaction with RhoGAP2 and Mcf2l, two regulators of Rho GTPases activity, is required for IL1RAPL1 to induce dendritic spine formation and function (20,21). Hayashi *et al*. identified other proteins interacting with the intracellular domain of IL1RAPL1, like PKCε, PLCβ1 and Rasal1 (21). Trans-synaptic interaction with the protein tyrosine phosphatase PTPδ through the extracellular domain of IL1RAPL1 was also shown to be essential for synaptogenesis (20,22).

We identified two novel *IL1RAPL1* mutations, an in-frame deletion of exon 6 (Δex6), in two unrelated patients with ID. Unlike the majority of previously reported *IL1RAPL1* mutations, which primarily lead to loss of IL1RAPL1 protein, this deletion and one point mutation in exon 3 [c.91T>C; p.(Cys31Arg)] (23) are compatible with IL1RAPL1 protein synthesis but are predicted to affect the function of its extracellular domain. As part of this work, we explore the impact of these mutations on synapse formation and function and how this can explain the ID of the patients.

RESULTS

Clinical characterization of patients and identification of two novel mutations on IL1RAPL1

P72 family

The pedigree of family P72 is shown in Figure 1A. Patient II-2 (male, 30 years) presents moderate ID, autistic-like behavior,

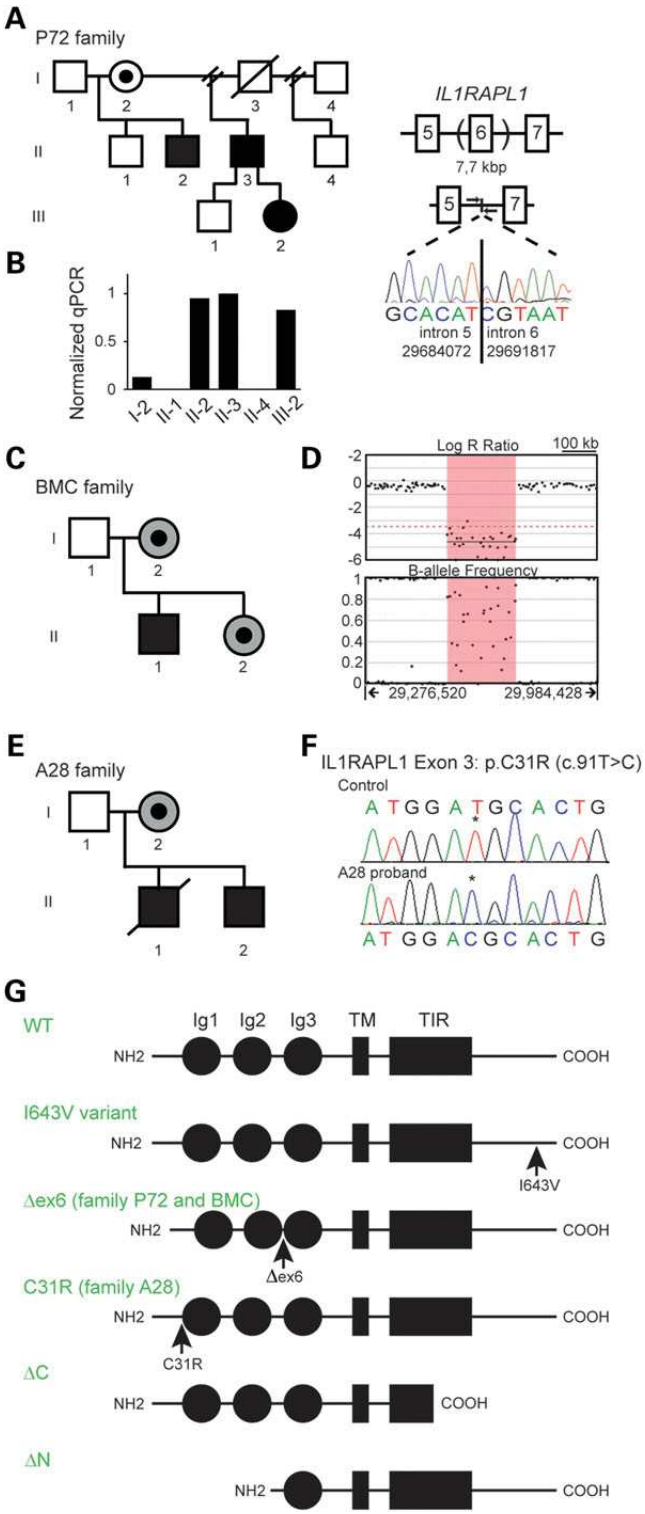

Figure 1. Identification of two novel mutations on *IL1RAPL1* associated with ID. (**A**) Pedigree of family P72, where II-2, II-3 and III-2 present moderate-to-mild ID. In those individuals, a ∼ 7-kb deletion on *IL1RAPL1* between intron 5 and 6 results in exon 6 deletion. This was confirmed by real-time PCR in fibroblast from the obligate carrier female I-2 and affected patients, using oligonucleotides flanking the deletion (**B**). This in-frame deletion leads to an IL1RAPL1 protein lacking 25 amino acids in the extracellular domain (**G**). (**C**) Pedigree of family BMC, where II-1 has ID. I-2 and II-2 (shaded in gray) have learning problems, but their developmental delay is less severe than that of the proband. (**D**) SNP array revealed a deletion of ∼200 kb between intron 5 and 6 of *IL1RAPL1* that results in the in-frame exon 6 deletion, as in family P72. (**E**) Pedigree of Family A28, where II-1 and II-2 present moderate-to-mild ID, and I-2 has learning problems (shaded in gray). (**F**) Both affected males inherited from I-2 a point mutation located in exon 3 of *IL1RAPL1* (c.91T>C), which results in an amino acid change C31R. [c.91T>C mutation in II-2 was initially reported by Tarpey *et al*. (23)]. This missense mutation is located before the first Ig-like domain (**G**). Structure of I643V variant and mutants are shown in (G). IL1RAPL1 protein (696 aa) contains three extracellular Ig-like domains (Ig1-3), a single transmembrane domain (TM), an intracellular toll/IL-1 receptor (TIR) domain and a 150-amino acid C-terminal tail. ΔC and ΔN mutants were used as controls in this study. The in-frame deletion of *IL1RAPL1* exon 6, found in P72 and BMC, is referred as Δex6.

is extraverted, aggressive and has language and motor delay. He has large hands, big ears, long face and synophrys. Patient II-3 (male, 43 years) presents mild ID and has no major behavioral problems. He also has autistic-like behavior and language and motor delay. He has facial dysmorphism, big ears and round face. Neurological examination was normal. The only clinical feature of III-2 (female, 10 years) is ID, needing special care.

During a search for mutations in *IL1RAPL1* gene in male patients with XLID, we found a deletion of exon 6 in genomic DNA from patient II-2. This deletion was also found in the affected brother II-3. Physical mapping of the deletion by CGH array and long-range PCR allowed us to characterize its size [7744 base pairs (bp)] and define the DNA breakpoints between intron 5 and 6 of *IL1RAPL1* (g.29684073_29691812del; c.1212_1286del; hg19/LOVD3 IL1RAPL1_000009). Using oligonucleotides flanking the deletion breakpoints, we studied by real-time PCR the segregation of the deletion in P72 family. As shown in Figure 1B, the deletion is present in II-2, II-3 and III-2 but not in II-1 and II-4 DNA isolated from blood; the low level of amplification in obligate carrier I-2 suggests somatic mosaicism. The in-frame deletion of *IL1RAPL1* exon 6 is predicted to lead to a protein lacking 25 amino acids in the extracellular domain, between immunoglobulin domain (Ig) 2 and 3 (p.(Ala235_Leu259del); Fig. 1G).

In order to elucidate whether III-2′s phenotype is due to a skewed X chromosome inactivation, we evaluated her X-inactivation pattern using the *AR*, *FMR1* or *FMR2* loci in her fibroblasts. Unfortunately, none of these markers was informative and given that *IL1RAPL1* expression in fibroblasts and blood cells is very low, we assessed the X-inactivation skewing by testing the expression of one SNP (single-nucleotide polymorphism) in the 3′ UTR of *APOO*, a gene located on the X chromosome at <5 kb from *IL1RAPL1*, in fibroblasts from III-2. Using this SNP (rs8680), we were able to differentiate her parent's contribution, and we found the expression of both alleles in III-2 cDNA suggesting random X-inactivation in her fibroblasts (Supplementary Material, Fig. S1).

BMC family

The proband II-1 (male, 27 months old) was born after an uneventful pregnancy as the second child of non-consanguineous parents (Fig. 1C). He had some delay of motor development, sitting at 9 months and walking at 25 months. At the age of 27 months, he only speaks three words and formal developmental testing confirmed delay. He was advised to start in special education. Family history is significant for learning difficulties in the mother; she attended special education. The proband has one sister with learning difficulties. Physical examination reveals height of 84 cm (below third percentile), weight of 12.7 kg (25th percentile) and head circumference of 48.4 cm (25th percentile). He has mild facial dysmorphism with a prominent forehead. He has generalized joint hyperlaxity, normal male genitalia and skin significant eczema. Brain MRI was normal.

Microarray analysis revealed a deletion of $\sim$200 kb with the proximal breakpoint in intron 5, and the distal breakpoint in intron 6 of *IL1RAPL1* (g.29517322_29746541del; c.703+99897_778+59920del; hg19/LOVD3 IL1RAPL1_000008) predicted to result in a deletion of the entire exon 6 (Fig. 1D). Additionally, a duplication on chromosome 19q13.41 of unknown clinical significance was observed (g.52860055_52996104dup; c.-41492_*76112dup; hg19, LOVD3 ZNF528_000001). The parents and sister of the proband were also tested, and both the deletion and duplication are inherited from the mother and present in the sister. Similarly to the above-described deletion of exon 6, this one is predicted to lead to the same IL1RAPL1 mutant protein lacking 25 amino acids in the extracellular domain, between immunoglobulin domain (Ig) 2 and 3 (p.(Ala235_Leu259del); Fig. 1G).

A28 family

The pedigree of family A28 is shown in Figure 1E. II-1 (male, now deceased) had moderate ID (IQ assessed as 36–51), gynecomastia, obesity, small testes, normal height (169 cm) and head circumference (54.5 cm), sexual deviant behavior (treated with an anti-androgen medication and necessitating living in care). II-2 (male, 57 years) presents mild ID, obesity, significant behavioral issues, normal head circumference, normal facial features, gynecomastia, normal hands and feet. The female obligate carrier I-2 is phenotypically normal, with normal height (153 cm) and head circumference (54.2 cm). She appeared to have low average intelligence.

A missense substitution in *IL1RAPL1* exon 3 (c.91T>C) (LOVD3 IL1RAPL1_000003) leading to an amino acid change p.(Cys31Arg) (C31R) was initially reported by Tarpey *et al*. in II-2 patient (23), but no clinical information about the family nor further characterization of this variant (i.e. if deleterious to IL1RAPL1 function or not) was studied. We first confirmed the segregation of this variant in the A28 family (Fig. 1F) and subsequently investigated its functional consequences. This point mutation is located in the extracellular domain of IL1RAPL1 protein before the first Ig domain (Fig. 1G). We assessed the pathogenicity of this variant by *in silico* analysis using the following software: Mutation taster (24), SIFT (25) and PolyPhen 2 (26). Mutation taster analysis predicted that this missense variant is a disease-causing mutation. PolyPhen analysis, which predicts possible impact of an amino acid substitution on the structure and function of a human protein using straightforward physical and comparative considerations, of the missense mutation also considered it to be 'probably damaging' (score 1.0). Finally, SIFT analysis predicted also the substitution at position 31 from Cys to Arg to affect protein function with a score of 0.00 (damaging). Alamut splicing predictions (Interactive Biosoftware) suggested no significant impact of this substitution on donor and acceptor splice sites.

Finally, a point mutation in *IL1RAPL1* exon 11 (c.1927A>G) leading to an amino acid change p.(Ile643Val) (I643V) was found in a male with ID, but was not observed in his affected brother potentially ruling out this variant as the genetic cause of the disease in this XLID family. This *IL1RAPL1* variant was reported before by Piton *et al*. (5) and is unlikely to be pathogenic because *in silico* analysis considered it to be tolerated by the protein. In our study, we use this variant as a control, as this single amino acid change is located in the intracellular domain (Fig. 1G), contrary to Δex6 and C31R mutations.

In this and previous studies (15,20), we used as controls two IL1RAPL1 mutant proteins, ΔC and ΔN, lacking a large part of intra- or extra-cellular domains, respectively (Fig. 1G and Table 1).

Table 1. Reported mutations on IL1RAPL1 gene in ID patients, and their consequences for protein function

Reference	Mutation/exons	Protein	Functional consequences
(1)	Deletion exon 3–5	Probably not produced	
(1)	Nonsense exon 11	Y459X predicted to lead to a protein lacking part of the TIR domain and the entire C-ter domain	ΔC (15,20) Does not increase dendritic spines number nor changes their length and width Increases the number of active pre-synaptic compartments Fails to target RhoGAP2 to synapses
(2,3)	Nonsense exon 11	W487X predicted to produce a protein lacking half of the TIR domain and the entire C-ter domain	
(4)	Deletion exons 3–6[a]	Probably not produced	
(5)	Nonsense exon 9	I367SX6 predicted to produce a protein lacking part of the trans-membrane domain as well as the entire C-ter domain	I367SX6 (5) Not targeted to the membrane Rescues neurite number and length phenotype after *Il1rapl1* knock down
(5)	Deletion exon 3–7	Frame shift A28EfxX15 predicted to produce a short protein containing only eight amino acids in addition to the signal peptide	
(5) and current report	Missense exon 11	I643V variant produces a full-length protein *In silico* analysis predicts it to be tolerated by the protein	I643V (current report) Induces dendritic spines formation and increase functional excitatory synapses Interacts with PTPδ and induces basal JNK activation
(6)	Deletion exon 3–5	The resulting protein should lack the first two Ig-like domains, but it is possible that synthesis stops after deletion	
(6)	Deletion exon 2	Probably not produced	
(7)	Deletion exons 3–5	Probably not produced	
(8)	Deletion exons 1–5	Probably not produced	
(8)	Deletion exons 3–6[a]	In-frame deletion (p.28_259del) predicted to produce a shorter protein devoid of the two first Ig-like domains	ΔN (20) Does not increase dendritic spine density nor changes spine length and width Fails to increase functional excitatory synapses Lacks interaction with PTPδ and fails to target RhoGAP2 to synapses
(9)	Deletion exons 2–6	Probably not produced	
(10)	Deletion exons 3–11	Probably not produced	
(11,13)	Deletion exon 3	Out-of-frame deletion leading to a premature stop codon A28EfxX7 Protein is probably not produced	
(12)	Deletion exon 3–5	Predicted to cause an in-frame deletion of 207 amino acids (N29_A235del)	
Current report	Deletion exon 6	In-frame deletion that results in a shorter extracellular domain Protein instability	Δex6 (current report) Induces protein instability Targeted to the membrane but mislocalized within dendrites Does not increase dendritic spines and functional excitatory synapses Induces basal JNK activation
(23) and current report	Missense exon 3	One amino acid change before the first Ig-like domain (C31R) *In silico* analysis predicts damage to the structure and function	C31R (current report) Targeted to the membrane and to dendritic spines Does not increase dendritic spines and functional excitatory synapses Decreases interaction with PTPδ but induces basal JNK activation
(14)	Deletion exon 7	Predicted to produce a truncated protein, containing only the first two Ig-like domains	

[a]Modified from original article, in accordance with hg38 assembly.

ΔC mutant corresponds to a nonsense *IL1RAPL1* mutation in exon 11 (c.1377C>A) observed in a patient with non-syndromic ID (1). The construct used in our study lacks the half of the TIR and the complete C-terminal domains (p.(Tyr459X)).

ΔN mutant protein lacks the first two Ig-like domains and corresponds to the deletion of exons 1 to 6 of *IL1RAPL1* (c.1_778del) (Fig. 1G and Table 1). Deletions of these exons were found in different patients with ID, but they probably lead to the absence of IL1RAPL1 expression (4,6–9).

IL1RAPL1 protein expression and localization is affected by mutations in its extracellular domain

In order to evaluate the effect of IL1RAPL1 mutations on protein stability, HEK293 cells were co-transfected with GFP and vectors bearing HA-tagged WT or mutant IL1RAPL1. Protein expression of mutants is significantly decreased [∼75% for Δex6 (∼108 KDa) and ∼60% for C31R (∼115 KDa), compared with the WT (∼115 KDa) protein] 24 h after transfection

as revealed by immunoblot (Supplementary Material, Fig. S2). The decrease in protein is not due to lower transfection efficiency (evaluated by GFP signal) suggesting that both mutations lead to decreased stability of the IL1RAPL1 protein in these cells. Protein expression of an IL1RAPL1 mutant lacking the half of the TIR and the complete C-terminal domains (ΔC, ∼62 KDa) is decreased to similar levels than Δex6 and C31R. Next, we studied the stability of the mutants in mouse hippocampal neurons. Whereas IL1RAPL1 protein expression in Δex6 transfected neurons is severely abolished to the background level, C31R mutant protein has similar expression level to WT protein (Fig. 2A and B). I643V variant is more abundant compared with WT protein, but there are probably no consequences because this excess of protein does not affect other analyzed parameters (see below). All IL1RAPL1 variants including Δex6 are correctly targeted to the membrane of neurons as measured by the ratio of surface HA per total HA signal, compared with WT IL1RAPL1 protein (Fig. 2C and D). As WT

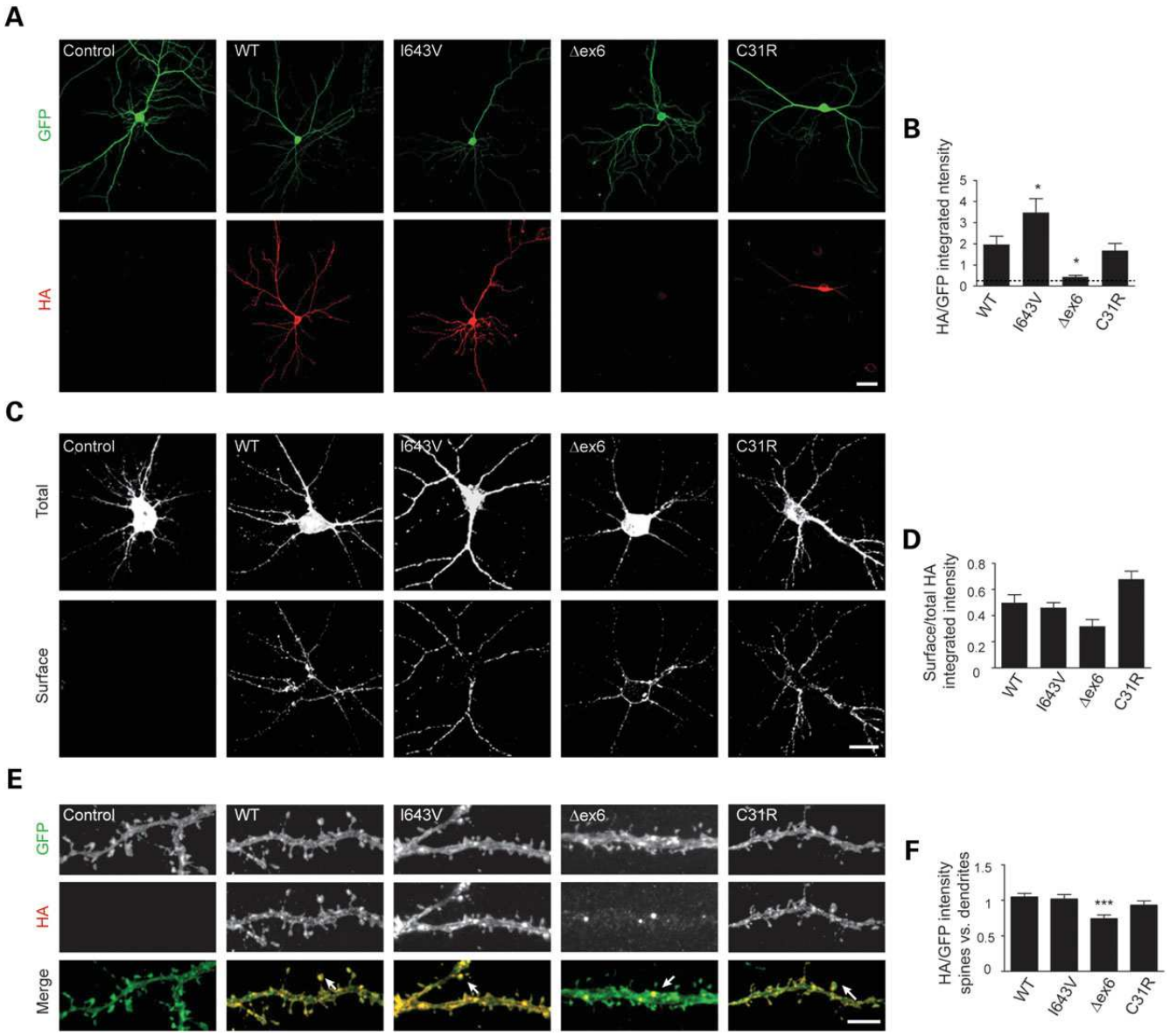

Figure 2. Protein expression and localization of Δex6 and C31R IL1RAPL1 mutants. (**A**) Protein detection by immunofluorescence in mouse hippocampal neurons co-transfected with different HA-IL1RAPL1 constructs and GFP. IL1RAPL1 proteins were revealed by an anti-HA tag antibody, and signal was normalized to GFP expression (scale bar 20 μm). (**B**) Bar graphs show the mean + SEM of HA-IL1RAPL1 to GFP expression ratio (at least 35 neurons per each condition from three independent experiments, $^{*}P < 0.01$ compared with WT). (**C**) Total (top panel) and surface (bottom panel) staining of HA-IL1RAPL1 proteins in mature hippocampal neurons using an anti-HA tag antibody (scale bar 20 μm). The ratio of integrated intensity of surface HA signal per total HA signal was measured for each neuron, and the mean + SEM is shown in (**D**). (**E**) Localization of total IL1RAPL1 within dendrites at DIV 18 in hippocampal neurons co-transfected with GFP (green) and the different HA-IL1RAPL1 constructs (red). Arrows in merge images show IL1RAPL1 localization to spines, or forming puncta on dendritic shafts when Δex6 is expressed (scale bar 5 μm). (**F**) Bars show the mean + SEM of the ratio of HA/GFP integrated density in spines and the HA/GFP integrated density in dendritic shafts ($^{***}P < 0.001$ compared with WT protein).

IL1RAPL1 protein is present in the dendrites and enriched at the postsynaptic site in the dendritic spines (15), we analyzed the subcellular localization of the variants by measuring the coefficient of variation of HA-IL1RAPL1 signal along dendrites (CV, see Materials and methods) and also the distribution of IL1RAPL1 signal in spines versus dendrites. Both C31R and I643V mutant proteins are distributed in dendritic shafts and are also enriched in spines similarly to WT (Fig. 2E and F). In contrast and despite its low abundance, Δex6 mutant is predominantly observed forming discrete puncta within dendritic shafts. Coefficient of variation analysis of Δex6 IL1RAPL1 signal along the dendritic shaft clearly shows more variations than WT and other mutated proteins [$^{***}P < 0.001$ compared with WT protein, $n = 14$ neurons (not shown)]. In addition, Δex6 mutant shows a decrease of IL1RAPL1 signal in dendritic spines of neurons compared with WT transfected neurons (Fig. 2F).

In conclusion, deletion of the region between Ig2 and Ig3 domains in Δex6 mutant is responsible for its instability and mislocalization in dendrite and spines. In contrast, these parameters are not altered by C31R mutation.

Impact of IL1RAPL1 mutations on excitatory synapse formation

Knocking-down or overexpressing IL1RAPL1 decreases or increases excitatory synapse formation, respectively (15,20,22,27). In order to evaluate the impact of the three newly described mutants on this IL1RAPL1-dependent synaptogenic phenotype, we co-transfected cultured hippocampal neurons with GFP and HA-tagged IL1RAPL1 constructs and their effect on pre- and post-synapse formation was evaluated using specific markers.

WT and I643V IL1RAPL1-transfected neurons at DIV18 present a large increase of the pre-synaptic marker synaptophysin that is not observed in neurons overexpressing Δex6 or C31R mutant (Supplementary Material, Fig. S3). As synaptophysin labels both excitatory and inhibitory pre-synapses, we stained transfected neurons with more specific markers using anti-VGLUT1 and anti-VGAT antibodies to label excitatory or inhibitory pre-synapses, respectively. We observed that IL1RAPL1 increases the excitatory pre-synaptic marker, an effect that is not observed after Δex6 or C31R mutant over-expression (Fig. 3A and B). Staining for the inhibitory pre-synaptic marker, VGAT is not affected after WT or mutants expression confirming the specific function of IL1RAPL1 in excitatory synapses (Supplementary Material, Fig. S4A).

Over-expression of both WT and I643V IL1RAPL1 induces an increase of the excitatory postsynaptic marker PSD-95 (Fig. 3C and D, ∼100 and ∼150%, respectively, no statistical differences between them) together with an increase in the number of dendritic protrusions (Fig. 3E, ∼20% in both cases), compared with control neurons. In agreement with these data and as previously reported, WT and I643V IL1RAPL1 overexpression increase the frequency (∼300% in both cases) but not the amplitude of spontaneous excitatory postsynaptic currents (sEPSC) (Fig. 3F and G). In contrast, none of the postsynaptic effects are observed in neurons overexpressing Δex6 or C31R mutants (Fig. 3C–E), suggesting that these mutants lose their synaptogenic properties. According to immunocytochemistry data, neither WT nor mutant protein altered the frequency and amplitude of spontaneous inhibitory postsynaptic currents (sIPSC, Supplementary Material, Fig. S4B).

Worth noting, ΔC mutant lacking part of intracellular domain is able to increase synaptophysin (Supplementary Material, Fig. S3) and VGLUT1 staining, but not to increase PSD-95 staining ($n = 16$ neurons per group from two independent experiments) or the number of dendritic spines (20). On the other hand, a mutant lacking part of the extracellular domain (ΔN in Fig. 1G) is also unable to increase pre- and post-synaptic differentiation (Supplementary Material, Fig. S3). These observations support the fact that pre-synaptic differentiation is dependent on IL1RAPL1 extracellular domain, whereas both extra and intracellular domains are important for postsynaptic differentiation (20,22). This suggests that extracellular domain of IL1RAPL1 is damaged in C31R mutant and that this could account for its synaptogenic deficit. In the case of Δex6 mutant, this deficit is probably due to the decrease in protein stability and mislocalization within dendrites as shown earlier.

Mechanism of synaptic deficits induced by IL1RAPL1 mutants

The synaptogenic activity of IL1RAPL1 is dependent on its interaction with a specific isoform of the tyrosine phosphatase PTPδ (20,22,28). This protein interacts with IL1RAPL1 extracellular domain and was shown to be specific as other members of the protein family, like LAR and PTPσ, are able neither to interact with nor to induce IL1RAPL1-dependent synaptogenesis.

As C31R mutant lacks synaptogenic activity, presumably because of changes in its extracellular domain structure, we hypothesized that this mutation perturbed the trans-synaptic interaction with PTPδ. In order to test this hypothesis, a group of HEK293 cells overexpressing either GFP or HA-IL1RAPL1 proteins and another group expressing Myc-PTPδ ectodomain were subjected to a cluster assay as previously described (20). After counting the number of red/green clusters (yellow in merge image in Fig. 4A), this assay revealed some but not significant interaction between C31R IL1RAPL1 mutant and PTPδ, compared with control cells and ΔN mutant that lacks the first two Ig-like domains (Fig. 4A). Similarly, the small amount of the Δex6 mutant expressed shows a severe reduction of clustering. However, compared with WT IL1RAPL1, both mutants show significant decrease of clustering efficiency, suggesting that the mutants reduce somehow the interaction with PTPδ (∼40% for both mutants). This deficit could contribute to the inability of C31R mutant to induce the formation of excitatory synapses.

To support this conclusion, we performed *in vitro* interaction tests by immunoprecipitating IL1RAPL1 from protein lysates containing both IL1RAPL1 and Myc-PTPδ proteins, and we evaluated by immunoblotting the presence of Myc- PTPδ ectodomain in the immunoprecipitate. Whereas WT or I643V efficiently interact with PTPδ, we observed a strong reduction of Myc staining after immunoprecipitation of both Δex6 and C31R mutants (Fig. 4B). However, decrease of Δex6 protein expression is likely to be also responsible for this observation (Supplementary Material, Fig. S2 and Fig. 4B, input 10% and immunoprecipitated IL1RAPL1 proteins).

Taken together, cell aggregation and immunoprecipitation assays lead us to conclude that C31R mutation decreases the interaction of IL1RAPL1 with PTPδ.

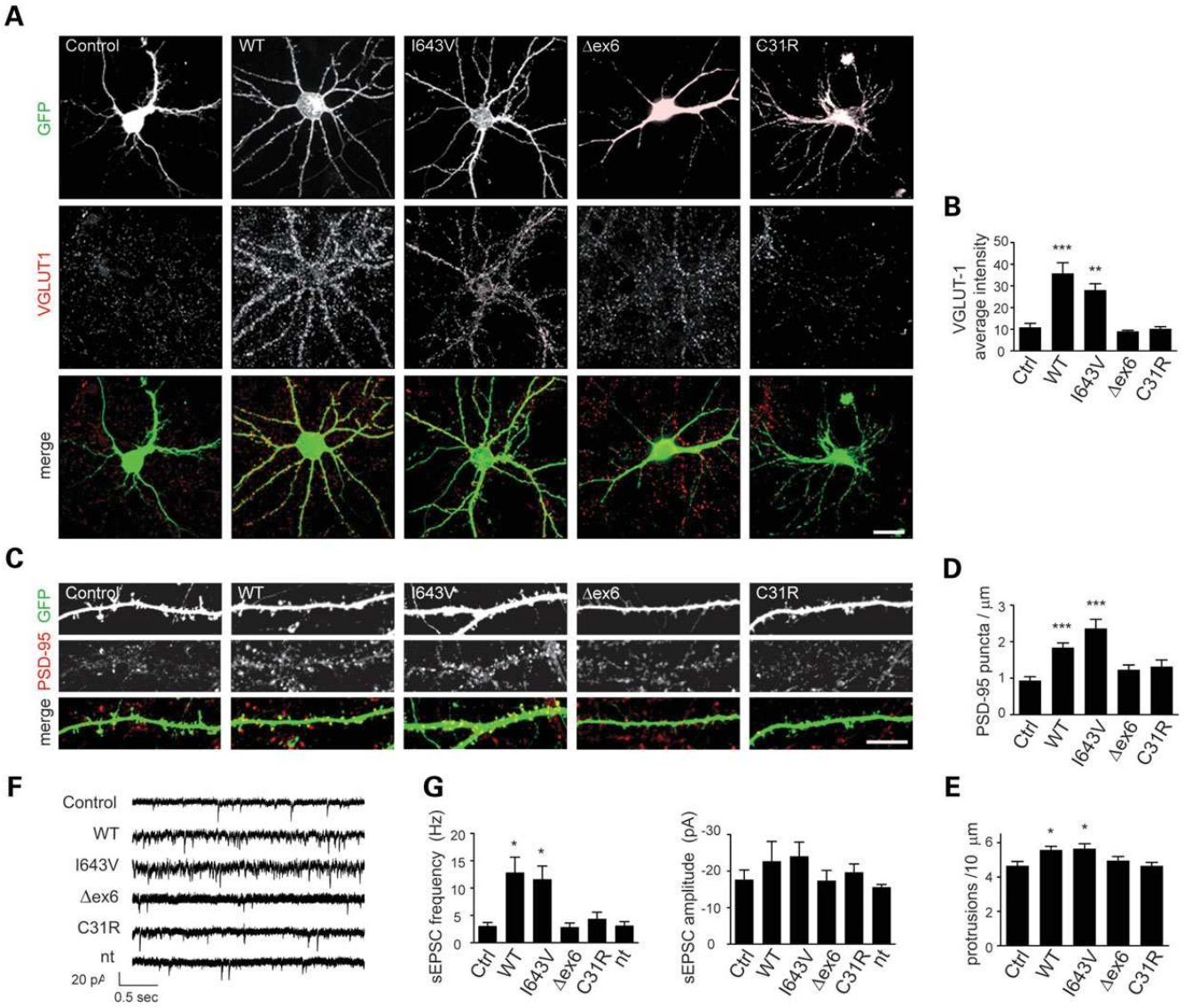

Figure 3. Consequences of IL1RAPL1 mutations on excitatory synapse formation. (**A**) Rat hippocampal neurons co-transfected with GFP and different HA-IL1RAPL1 constructs were stained with anti-VGLUT1 antibody to label excitatory pre-synapses. Each column of images shows double-labeling for GFP (top panel) and VGLUT1 (middle panel); the merged images are shown in the bottom panel (scale bar 20 μm). Quantification of VGLUT1 clusters intensity in neurons overexpressing IL1RAPL1 constructs is shown in (**B**). Bar graphs show the mean + SEM of VGLUT1 intensity (15 neurons from 3 independent experiments for each condition, $^{**}P < 0.005$, $^{***}P < 0.001$, compared with control neurons). (**C**) Mouse hippocampal neurons were co-transfected with GFP and the different IL1RAPL1 constructs and were stained at DIV18 with anti-PSD-95 antibody to label excitatory post-synapses. Each column of images shows double-labeling for GFP (top panel) and PSD-95 (middle panel); the merged images are shown in the bottom panel (scale bar 10 μm). Bar graphs in (**D**) show the mean + SEM of the PSD-95 clusters per micron in at least 26 neurons from 3 independent experiments ($^{*}P < 0.01$ $^{***}P < 0.001$, compared with control neurons). The number of protrusions along dendrites was assessed from at least 25 neurons from each condition as showed in (**E**) ($^{*}P < 0.01$, compared with control neurons). (**F**) Typical recording of sEPSC from mouse hippocampal neurons at 18–21 DIV transfected with different IL1RAPL1 constructs. The average frequency and amplitude of these events is represented in (**G**) (6 to 10 transfected neurons per condition and 32 non-transfected neurons (nt) $^{*}P < 0.01$, compared with control neurons).

Mutants regulate other IL1RAPL1-dependent signaling

Besides PTPδ, IL1RAPL1 interacts with NCS-1, PSD-95, RhoGAP2, Mcf2l, PKCε and PLCβ1 (15,18,20,21). These proteins interact with the intracellular domain of IL1RAPL1, suggesting that signaling independent from the extracellular domain could still be induced in neurons expressing IL1RAPL1 mutants with intact intracellular domains.

Even if there is no evidence for direct interaction with c-jun N-terminal kinase (JNK), the role of IL1RAPL1 on the regulation of activity of this kinase has been reported (15,29,30). Overexpression of IL1RAcP and IL1RAPL1 was shown to increase JNK basal activity in HEK293 cells (29,31). In order to evaluate the capacity of the mutants to activate JNK, we assessed by immunoblotting the basal activity of this kinase in HEK293 cells overexpressing different IL1RAPL1 constructs.

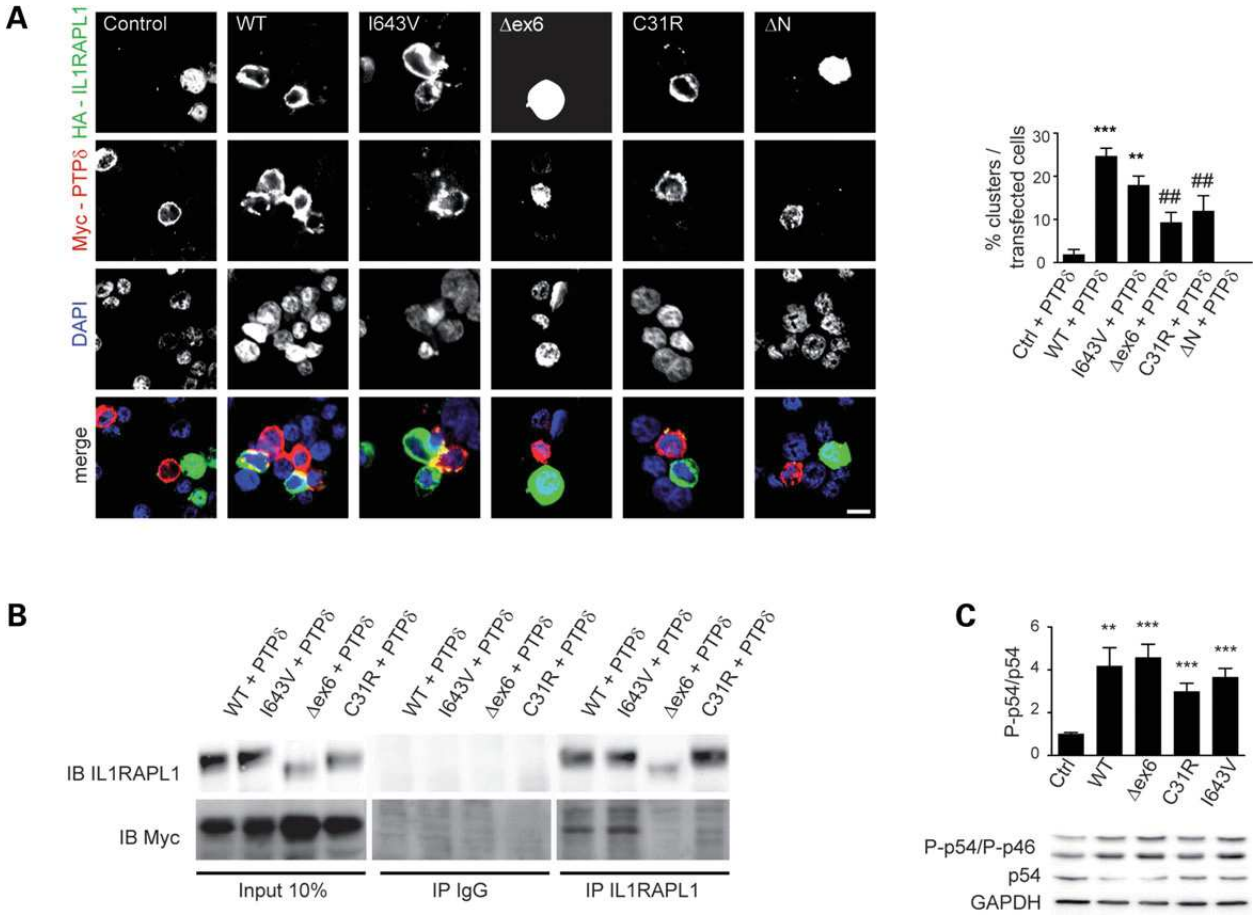

Figure 4. Molecular mechanism accounting for synaptic deficits induced by IL1RAPL1 mutants. (**A**) HEK293 cells expressing either GFP or HA-IL1RAPL1 constructs (green), and HEK293 cells expressing Myc-PTPδ ectodomain (red) were subjected to a cluster assay. Nuclei (blue) were stained with DAPI (scale bar 10 μm). Clustering was assessed by counting the number of green/red clusters (yellow in merge images) and normalizing by the number of transfected cells (green + red) ($^{**}P < 0.005$ $^{***}P < 0.001$ compared with control + PTPδ; $^{\#\#}P < 0.005$ compared with WT + PTPδ). ΔN mutant, which lacks the first two Ig-like domains, was used as negative control. (**B**) Lysates from HEK293 cells expressing the indicated HA-IL1RAPL1 constructs were mixed with lyzates from another group of cells expressing Myc-PTPδ ectodomain in a volume proportion of 1 (for IL1RAPL1) to 1.5 (for Myc-PTPδ) and subjected to an *in vitro* immunoprecipitation assay using IL1RAPL1 antibody. 10% of the mixed lyzates was loaded as control of IL1RAPL1 and Myc-PTPδ protein over-expression (left panel). IL1RAPL1 antibody immunoprecipitates were revealed after immunoblotting (IB) using IL1RAPL1 (K10) and Myc antibodies. Rabbit IgG antibody was used as a negative control (central panel). (**C**) Lysates from HEK293 cells transfected with different IL1RAPL1 constructs were probed by immunoblot with antibodies against total p54 and phospho-specific (Thr183/Tyr185) p46 and p54 JNK isoforms. Protein loading was normalized by GAPDH expression. Bar graphs show the mean + SEM of phospho/total ratio of p54 JNK isoform (six independent experiments, $^{**}P < 0.005$ $^{***}P < 0.001$ compared with control lysates).

We show that over-expression of IL1RAPL1 mutants in HEK293 cells increases the basal JNK phosphorylation, to levels comparable with the WT protein (Fig. 4C). Even if only p56 JNK isoform was quantified, phosphorylation of p46 isoform appears also to be increased after IL1RAPL1 over-expression. This result suggests that Δex6 and C31R mutants do not lose all signaling capacity, independently from synaptogenesis, and that even low expression of the IL1RAPL1 Δex6 mutant is able to induce this signaling.

DISCUSSION

There are hundreds of genes in which mutations are known to cause ID or ASD or both. As its discovery as a gene implicated in ID, several mutations of *IL1RAPL1* were found in patients with different severity of ID. As shown in Table 1, the majority of the described mutations include large deletions. It is of particular interest that they mostly involve the first exons coding for extracellular domain of IL1RAPL1 protein. Some authors suggest that because of the incidence of genomic rearrangements, such as pericentromeric inversions, this region must be particularly prone to recombination (3,32). Moreover, the majority of mutations likely results in the absence of the IL1RAPL1 protein or is predicted to lead to truncated proteins. Until now, only one frame shift mutation leading to a shorter IL1RAPL1 protein has been characterized functionally (5). The impact of mutations described so far on IL1RAPL1 protein production and function, when available, is summarized in Table 1.

Here, we report two novel mutations of *IL1RAPL1* related to non-syndromic ID and we characterize their functional consequences. Both mutations result in an in-frame deletion of exon 6, leading to a loss of 25 amino acids in the extracellular domain of

IL1RAPL1. These mutations were identified in two unrelated families (P72 and BMC) and have different DNA breakpoints. In both cases, the deletion co-segregates with the ID phenotype in an X-linked recessive manner. Besides exon 6 deletion, patient II-1 in family BMC presents also a duplication on chromosome 19 that includes *ZNF528* gene. Missense mutations of this gene were previously identified in two patients with mild ID (33). Owing to the fact that Δex6 mutation was also found in members of the P72 family presenting ID, we propose the deletion in *IL1RAPL1* as the major cause of ID in these two families, but we cannot rule out that the severity of cognitive impairment could be modulated by deletions or duplications in other genes, such as *ZNF528*.

We also characterized the functional consequences of a unique missense variant C31R previously reported, but not further investigated (23). This variant was predicted to be damaging to IL1RAPL1 protein, which can be due to the importance of this region for protein folding. To our knowledge, this is the only pathogenic *IL1RAPL1* missense variant described so far.

Several studies on XLID genes, including *IL1RAPL1*, raise the question of the role of X chromosome inactivation on female phenotype (3,4,6,8). In the present study, *IL1RAPL1* mutations were found in healthy as well as in affected females from the three families (Fig. 1). Females I-2 and II-2 (BMC family) and I-2 (A28 family) have some learning problems or low average intelligence. But, unlike III-2 from P72 family, they do not have ID. We speculate that, even if not observed in fibroblasts, the X chromosome inactivation pattern may be skewed in III-2′s brain or in particular subsets of neurons, resulting in a predominant expression of the mutant allele (34).

Together with Δex6, the C31R mutation allowed us to address the impact of relatively milder mutations, in comparison with large deletions or nonsense mutations, on IL1RAPL1 protein stability, localization and synaptic function. IL1RAPL1 is located at both pre- and post-synaptic compartments of excitatory synapses but is enriched in the postsynaptic membrane (15), and its over-expression is known to increase the formation of this type of synapses on hippocampal neurons (15,20,21). We showed that Δex6 mutation lead to decreased protein stability in neurons, mislocalization within dendrites and decreased presence in spines, even if mutant protein is correctly targeted to the membrane. In the other hand, C31R mutation does not affect IL1RAPL1 stability in neurons nor localization on dendritic spines and shafts. Our experiments clearly show that Δex6 and C31R were not able to increase excitatory synapse number, after evaluation of either pre- or post-synaptic markers. In the case of Δex6 mutant, the lack of synaptogenic effect can be explained by the severe decrease in IL1RAPL1 protein expression and its miss localization, as shown in Figure 2A–B and 2E–F. However, C31R mutant protein, whose expression is similar to WT, also fails to increase synaptic formation. This impairment was also observed in ΔN, which lack the majority of the IL1RAPL1 extracellular domain (Supplementary Material, Fig. S3 and Table 1). As previously shown (20), ΔC mutant with intact extracellular domain is able to increase the pre-synaptic marker synaptophysin establishing that this domain is essential for pre-synaptic differentiation (Supplementary Material, Fig. S3). We then hypothesized that C31R mutation affects this domain and the binding to interacting partners. PTPδ is the only partner known to interact with IL1RAPL1 extracellular domain, and this interaction was shown to be essential for IL1RAPL1-mediated synaptogenesis (20,22). In order to dissect the molecular mechanism underlying the synaptic deficits observed in neurons transfected with C31R, we evaluated mutant's capacity to interact with PTPδ. The cell aggregation and immunoprecipitation assays shown in Figure 4 allowed us to conclude that the decrease of interaction with this tyrosine phosphatase participates to the inability of C31R IL1RAPL1 mutant to increase the number of excitatory synapses.

Despite reduced expression (Δex6) and perturbed synaptogenesis (C31R), we hypothesized that some of the signaling could be preserved in cells transfected with Δex6 and C31R mutants. Indeed, we observed that both mutant proteins were able to induce JNKs basal activation. The capacity of IL1RAPL1 to regulate JNK activity was previously shown (15,29,30), even if the mechanism is still unclear. PSD-95 phosphorylation by JNK has been shown to regulate PSD-95 at the excitatory synapses, and we proposed that the reduction of excitatory synapses in *Il1rapl1* knockout neurons was secondary to reduced JNK activity (15,35). Our results suggest that Δex6 and C31R mutations decrease IL1RAPL1 synaptogenic activity while maintaining other signaling, like JNK activation, uncoupling the two events. Alternatively, JNKs belong to the MAPK family, and in neurons, they are involved in diverse roles including cell death, radial migration, neurite formation, metabolism regulation and behavioral control. JNK signaling has an impact on synaptic plasticity, as a regulator of AMPA receptors trafficking (36,37). The functional role of JNK regulation by IL1RAPL1, in particular in response to IL1β stimulation, is still under investigation (30).

Finally, the I643V variant was reported in ID patients as well as in controls. This together with *in silico* prediction suggests that this variant is not deleterious for IL1RAPL1 function. In this study, we evaluated the potential functional consequences of this amino acid change within the intracellular domain of IL1RAPL1 with the aim to assess whether it may act as a susceptibly variant to ID. We observed that I643V protein was significantly increased in transfected neurons, but the increase of excitatory synapse number was comparable with WT IL1RAPL1. These observations support the hypothesis that the functional interactions but not the quantity of IL1RAPL1 protein are important for synapse formation. This functional characterization strongly suggests I643V to be a neutral *IL1RAPL1* variant.

In conclusion, the cognitive deficits observed in patients carrying Δex6 mutations can be explained by the decrease of IL1RAPL1 protein stability in neurons, together with the fact that residual produced protein is mislocalized. In the other hand, deficits observed in patients with C31R mutation are caused by a decrease of the capacity to interact with PTPδ and thus to increase synaptogenesis. In addition, these mutations allowed us to rule out the functional involvement of JNK in the PTPδ-induced synaptogenic activity of IL1RAPL1.

MATERIALS AND METHODS

Genetic analysis

DNA was extracted from peripheral blood or skin fibroblasts using standard methods after parental and patients' consent was obtained.

The following intronic primers were used to investigate the exon 6 deletion in P72 family: TGAAAGTGAAAAATATTT

GGGAAA, and CACAATGTAACGAGAGCAGCA. Confirmation of the deletion was obtained by qPCR (LightCycler LC480, Roche) targeting exon 6 (CCCAAGCTTTTGTATCCTAT and ATGGATTTAGCTGCGAGTA) and exon 8 (ACATCAGAT TCGGATTCATC and GCGTGTCGACGTCCATT) was used as a reference.CGH array (NimbleGen's, Roche) and long-range PCR (TGTGAGTGAGTGTGCATATGTGTGTATAGGTG and CGTGGGGACTAGACCAGGAGTTG) was used to map exon 6 deletion in P72 family members. Germinal mosaicism of the deletion was explored by qPCR (TGCTTGACAGAAT TTTCCAAGGAGCA and GTTACCACTTTCATTTACCTTG GGATGA) where *COL6A5* expression was used as a reference (ACCACTGGCAGCTTCTGGCAA and CGCCCCTGGACA TCCTGCAA). The following primers were used to detect *APOO* polymorphism in patients' fibroblasts: genomic DNA (TCCCAACTGTCTGGTTCTAGCTTGT and TGGTTTGACC CTGTCCCCCAT) and cDNA (TGGGATTAGCTGCCTCCCT CT and ACTGACTTCTATGCCATTTTTCTGT). X-chromosome inactivation studies were performed using the *AR*-, *FMR1*- and *FMR2*-specific HpaII/PCR assay, to assess X-inactivation pattern.

SNP array analysis on BMC family members was performed using a HumanCytoSNP-12v2.1 beadchip following standard protocols as provided by the manufacturer on an iScan system (Illumina, San Diego, CA, USA). CNV analysis was performed using CNV-WebStore (38). Familial relationships were validated by comparing the SNP patterns of the patient with those of the parents.

Identification of c.91T>C (C31R) mutation II-2 member of family A28 is described elsewhere (23). Segregation studies were performed by PCR and Sanger sequencing.

Newly identified variants were submitted to Leiden Open Variation Database 3.0 (LOVD 3.0) (39) (IL1RAPL1_000008 and IL1RAPL1_000009).

cDNA constructs

HA-tagged human IL1RAPL1 described before (15) was modified using QuikChange II XL Site-Directed Mutagenesis Kit (Agilent Technologies) to generate Δex6, C31R and I643V constructs. Myc-tagged PTPδ, ΔC and ΔN were described elsewhere (20).

Antibodies

The following primary antibodies were used: rabbit anti-IL1RAPL1 (K10 (15)), goat anti-IL1RAPL1 (R&D), mouse anti-GFP (Roche and Abcam), rabbit anti-VGlut1 (Synaptic Systems), rabbit anti-VGAT (Synaptic Systems), rabbit anti-HA-tag (Santa Cruz Biotechnology), mouse anti-HA-tag (Roche), mouse anti-c-Myc (Santa Cruz Biotechnology), mouse anti-PSD-95 (Affinity Bioreagents), rabbit anti-synaptophysin (Cell Signaling), rabbit anti-P-Thr183/Tyr185 JNK (Cell Signaling), mouse anti-JNK (Cell Signaling)and mouse anti-GAPDH (Ambion). All fluorophore-conjugated secondary antibodies were purchased from Jackson ImmunoResearch Labs.

HEK293 cells culture, transfection and immunoblotting

HEK293 cells were grown in Dulbecco's modified Eagle's medium supplemented with 10% fetal bovine serum and penicillin/streptomycin (all Invitrogen). Cells were seeded at 60–70% of confluence and transfected with the different constructs using Lipofectamine 2000 (Life Technologies). Twenty-four hours after transfection, cells were lysed and an equal amount of protein was submitted to SDS–PAGE and transferred to nitrocellulose membrane. Membranes were incubated over night with HA tag, GFP, GAPDH or P-JNK antibodies. Total JNK was evaluated after stripping P-JNK signal. After incubation with HRP-conjugated secondary antibodies (Dako), Super Signal West Femto and ECL substrate (Pierce) were used for revelation. Acquisition was performed with LAS-4000 (General Electric), and quantification of band intensity was done with ImageJ software (Rasband, W.S., ImageJ, U. S. National Institutes of Health, Bethesda, Maryland, USA, http://imagej.nih.gov/ij/, 1997–2014). IL1RAPL1 abundance was evaluated in lysates from cells co-transfected with IL1RAPL1 constructs and GFP (control of transfection efficiency), by dividing HA intensity signal by GAPDH signal (protein loading control). JNK phosphorylation was measured by calculating the ratio between P-JNK (P-p54) and total JNK (p54). Statistical analysis was performed by one-way analysis of variance (ANOVA) followed by Tukey's *post hoc* test for multiple comparisons.

Cell culture and transfection of primary rat and mouse hippocampal neurons

Low-density rat hippocampal neuronal cultures were prepared from embryonic day (E) 18–19 hippocampi as previously described with minor modifications (40,41) and were grown in 12-well Petri dishes (Primo). Cultured mouse hippocampal neurons were prepared from E16.5 embryos, grown in 10-mm glass coverslips and maintained in Neurobasal B27-supplemented medium (Life Technologies). Neurons were transfected using Lipofectamine 2000 on Days In Vitro 11 (DIV11), and experiments were performed at DIV14–18. Experimental procedures on animals were approved by the local ethical committee.

Neuron surface staining

At DIV 14–15, live hippocampal neurons were labeled for 10 min at 37°C with anti-HA-tag rabbit antibody (10 μg/ml). After washing, neurons were fixed with paraformaldehyde (PFA) 4% plus 4% sucrose and incubated with anti-HA-tag mouse antibody in GDB [30 mM phosphate buffer, pH 7.4, 0.2% gelatin, 0.5% Triton X-100, 0.8 M NaCl (all Sigma–Aldrich)] for 3 h at room temperature. Cells were washed in 20 mM phosphate buffer containing 0.5 M NaCl and incubated with FITC- and Cy3-conjugated secondary antibodies.

Immunocytochemistry and image analysis

Cells were fixed in 4% PFA plus 4% sucrose at room temperature for 20 min, or 100% methanol at −20° for 10 min. Primary (1 : 100–1 : 800) and secondary (1 : 200) antibodies were applied in GDB buffer or in PBS (pH 7.4) containing 3% BSA and 0.2% Tween 20.

Confocal images were obtained using a Zeiss 510 confocal microscope (Carl Zeiss, a gift from Fondazione Monzino) or a Leica DMI6000 Spinning disk microscope. Quantification of synaptic protein staining was performed using MetaMorph

(Molecular Devices, Downingtown, PA, USA), and ImageJ software and NeuronJ plugin (42). Labeled, transfected cells were chosen randomly for quantification from six coverslips from three independent experiments for each condition, and image analysis was performed under blind condition.

Coefficient of variation of IL1RAPL1 staining was calculated by dividing the standard deviation of HA signal by mean pixel intensity within dendrites (43). The dendritic spine number was measured as described previously (41,44) with minor modifications. For each neuron, we measured the number of protrusions present in all the dendrites along their entire length. Then, we calculated mean and SEM (standard error of the mean) for the neurons transfected with the same construct.

Quantification of protein surface staining was performed using MetaMorph (Molecular Devices) and ImageJ software. The ratio of integrated intensity of surface rabbit anti-HA signal per total mouse anti-HA signal was measured for each neuron. Then, we calculated the mean and SEM for the neurons transfected with the same construct.

HA-IL1RAPL1 in spines and dendritic shafts was quantified using IMARIS 7.2 software and Filament Tracer wizard (Bitplane). Integrated density of HA signal was normalized by GFP integrated density in each compartment. The ratio of HA/GFP in spines and in dendritic shafts was assessed for each neuron, and mean + SEM was reported for neurons transfected with the same IL1RAPL1 construct.

Statistical analysis was performed by ANOVA followed by Tukey's *post hoc* test.

Electrophysiological recording on mouse hippocampal cultured neurons

Whole-cell patch-clamp recordings were made from GFP- or IL1RAPL1-transfected mouse hippocampal neurons at 18–21 DIV. Non-transfected cells from the same coverslip were also recorded as controls. Patch electrodes, fabricated from thick borosilicate glass, were pulled and fire-polished to a final resistance of 2–4 MΩ and filled with internal solution containing (in mM): 125 $CsMeSO_3$, 2 $MgCl_2$, 1 $CaCl_2$, 4 Na_2ATP, 10 EGTA, 10 HEPES, 0.4 NaATP and 5 QX314. Cultured neurons were superfused with an oxygenated external solution containing (in mM): 130 NaCl, 2.5 KCl, 2.2 $CaCl_2$, 1.5 $MgCl_2$, 10 HEPES and 10 D-Glucose. Neurons were voltage-clamped at −70 mV to record EPSCs and at 0 V to record IPSCs. All of the experiments were performed at room temperature. Inward synaptic currents at −70 mV and outward currents at 0 mV were automatically detected by an automatic template-based routine using pClamp 10.4 software (Molecular Devices). Recordings were performed under blind conditions. Typically, time periods of 120 s were used for analysis of synaptic events occurring at both membrane potentials.

Cell aggregation and immunoprecipitation assays

Two groups of HEK293 cells grown in 12-well plates were transfected, one with HA-IL1RAPL1 WT or mutants and the other with Myc-PTPδ ectodomain. Cells transfected with GFP were used as negative control. After 12 h, cells were detached and counted for the cell aggregation assay or lysated with 50 mM Tris–HCl, 200 mM NaCl, 1 mM EDTA, 1% NP40, 1% Triton X-100 and protease inhibitors (RIPA buffer), for the immunoprecipitation assay.

For the cell aggregation assay, cell suspension was transferred to microtubes and gently centrifuged (800 g, 5 min, RT) to eliminate PBS-EDTA. The pellets were resuspended in aggregation medium (AM) containing 1× HBSS, 1 mM $MgCl_2$ and 2 mM $CaCl_2$. The two groups of transfected cells were mixed together and rotated at room temperature for 30 min to allow cells to aggregate. Cell mixtures (4×10^6 cells) were added to 1 ml AM on poly-L-Lys-coated coverslips in multiwall (12 well) plate and let attach for some minutes at 37°C with 5% CO_2. Once attached, cells were fixed and stained. Image analysis was performed under blind conditions, and aggregation coefficient was calculated by the number of green + red clusters (yellow in merge images) divided by the number of total transfected (green + red) cells and expressed as percent.

For the immunoprecipitation assay, protein A Sepharose beads (GE Healthcare) were washed in RIPA buffer. Anti-IL1RAPL1 antibody [K10, (15)] was added to the beads at 5 μg/ml in RIPA buffer and incubated for 1 h. Lysates from the two groups of transfected cells in RIPA buffer were mixed in a volume proportion of 1 (for IL1RAPL1) to 1.5 (for Myc-PTPδ) and incubated overnight at 4°C with the beads/IL1RAPL1 antibody. The beads were washed three times with RIPA buffer, and elution was performed in sample buffer for SDS–PAGE (5 min at 100°C) and loaded to 10% SDS–PAGE. Protein detection was performed as described in immunoblotting section.

SUPPLEMENTARY MATERIAL

Supplementary Material is available at *HMG* online.

ACKNOWLEDGEMENTS

We thank Cherif Beldjord for X chromosome inactivation and segregation studies; Thierry Bienvenu for mutation analyzes and *in silico* prediction of genetic variant pathogenicity; Cellular imaging facility of Institut Cochin for image analysis advice.

Conflict of Interest statement. None declared.

FUNDING

This work was supported by the European Union's FP7 large scale integrated network Gencodys (http://www.gencodys.eu/, HEALTH-241995); by the French Research Agency (ANR-2010-BLANC-1434-03); by the European Union's EraNet program (ANR 2010-Neuro-001-01); by Institut national de la santé et de la recherche médicale (INSERM); by Ecole des Neurosciences de Paris (to M.R.-B.); by Comitato Telethon Fondazione Onlus [grant no. GGP13187 and GGP11095 (to C.S.)]; Fondazione CARIPLO project number 2012-0593; Italian Institute of Technology; Seed Grant; Ministry of Health in the frame of ERA-NET NEURON; PNR-CNR Aging Program 2012–2014 and Foundation Jérôme Lejeune (to C.S.).

REFERENCES

1. Carrié, A., Jun, L., Bienvenu, T., Vinet, M.C., McDonell, N., Couvert, P., Zemni, R., Cardona, A., Van Buggenhout, G., Frints, S. *et al.* (1999) A new member of the IL-1 receptor family highly expressed in hippocampus and involved in X-linked mental retardation. *Nat. Genet.*, **23**, 25–31.

2. Kozak, L., Chiurazzi, P., Genuardi, M., Pomponi, M.G., Zollino, M. and Neri, G. (1993) Mapping of a gene for non-specific X linked mental retardation?: evidence for linkage to chromosomal region Xp21.1-Xp22.3. *J. Med. Genet.*, **30**, 866–869.
3. Tabolacci, E., Pomponi, M.G., Pietrobono, R., Terracciano, A., Chiurazzi, P. and Neri, G. (2006) A truncating mutation in the IL1RAPL1 gene is responsible for X-linked mental retardation in the MRX21 family. *Am. J. Genet.*, **487**, 482–487.
4. Nawara, M., Klapecki, J., Borg, K., Jurek, M., Moreno, S., Tryfon, J., Bal, J., Chelly, J. and Mazurczak, T. (2008) Novel mutation of IL1RAPL1 gene in a nonspecific X-linked mental retardation (MRX) family. *Am. J. Med. Genet. A*, **146A**, 3167–3172.
5. Piton, A., Michaud, J.L., Peng, H., Aradhya, S., Gauthier, J., Mottron, L., Champagne, N., Lafrenière, R.G., Hamdan, F.F., Joober, R. *et al.* (2008) Mutations in the calcium-related gene IL1RAPL1 are associated with autism. *Hum. Mol. Genet.*, **17**, 3965–3974.
6. Behnecke, A., Hinderhofer, K., Bartsch, O., Nümann, A., Ipach, M.L., Damatova, N., Haaf, T., Dufke, A., Riess, O. and Moog, U. (2011) Intragenic deletions of IL1RAPL1: report of two cases and review of the literature. *Am. J. Med. Genet. A*, **155A**, 372–379.
7. Whibley, A.C., Plagnol, V., Tarpey, P.S., Abidi, F., Fullston, T., Choma, M.K., Boucher, C.A., Shepherd, L., Willatt, L., Parkin, G. *et al.* (2010) Fine-scale survey of X chromosome copy number variants and indels underlying intellectual disability. *Am. J. Hum. Genet.*, **87**, 173–188.
8. Franek, K.J., Butler, J., Johnson, J., Simensen, R., Friez, M.J., Bartel, F., Moss, T., DuPont, B., Berry, K., Bauman, M. *et al.* (2011) Deletion of the immunoglobulin domain of IL1RAPL1 results in nonsyndromic X-linked intellectual disability associated with behavioral problems and mild dysmorphism. *Am. J. Med. Genet. A*, **155A**, 1109–1114.
9. Mikhail, F.M., Lose, E.J., Robin, N.H., Descartes, M.D., Rutledge, K.D., Rutledge, S.L., Korf, B.R. and Carroll, A.J. (2011) Clinically relevant single gene or intragenic deletions encompassing critical neurodevelopmental genes in patients with developmental delay, mental retardation, and/or autism spectrum disorders. *Am. J. Med. Genet. A*, **155A**, 2386–2396.
10. Youngs, E.L., Henkhaus, R., Hellings, J.A. and Butler, M.G. (2012) IL1RAPL1 gene deletion as a cause of X-linked intellectual disability and dysmorphic features. *Eur. J. Med. Genet.*, **55**, 32–36.
11. Barone, C., Bianca, S., Luciano, D., Di Benedetto, D., Vinci, M. and Fichera, M. (2013) Intragenic ILRAPL1 deletion in a male patient with intellectual disability, mild dysmorphic signs, deafness, and behavioral problems. *Am. J. Med. Genet. A*, **161A**, 1381–1385.
12. Mignon-Ravix, C., Cacciagli, P., Choucair, N., Popovici, C., Missirian, C., Milh, M., Mégarbané, A., Busa, T., Julia, S., Girard, N. *et al.* (2014) Intragenic rearrangements in X-linked intellectual deficiency: results of a-CGH in a series of 54 patients and identification of TRPC5 and KLHL15 as potential XLID genes. *Am. J. Med. Genet. A*, **9999**, 1–7.
13. Tucker, T., Zahir, F.R., Griffith, M., Delaney, A., Chai, D., Tsang, E., Lemyre, E., Dobrzeniecka, S., Marra, M., Eydoux, P. *et al.* (2013) Single exon-resolution targeted chromosomal microarray analysis of known and candidate intellectual disability genes. *Eur. J. Hum. Genet.*, **22**, 792–800.
14. Redin, C., Gerard, B., Lauer, J., Herenger, Y., Muller, J., Quartier, A., Masurel-Paulet, A., Willems, M., Lesca, G., El-Chehadeh, S. *et al.* (2014) Efficient strategy for the molecular diagnosis of intellectual disability using targeted high-throughput sequencing. *J. Med. Genet.*, **51**, 724–736.
15. Pavlowsky, A., Gianfelice, A., Pallotto, M., Zanchi, A., Vara, H., Khelfaoui, M., Valnegri, P., Rezai, X., Bassani, S., Brambilla, D. *et al.* (2010) A postsynaptic signaling pathway that may account for the cognitive defect due to IL1RAPL1 mutation. *Curr. Biol.*, **20**, 103–115.
16. Gambino, F., Kneib, M., Pavlowsky, A., Skala, H., Heitz, S., Vitale, N., Poulin, B., Khelfaoui, M., Chelly, J., Billuart, P. *et al.* (2009) IL1RAPL1 controls inhibitory networks during cerebellar development in mice. *Eur. J. Neurosci.*, **30**, 1476–1486.
17. Houbaert, X., Zhang, C.L., Gambino, F., Lepleux, M., Deshors, M., Normand, E., Levet, F., Ramos, M., Billuart, P., Chelly, J. *et al.* (2013) Target-specific vulnerability of excitatory synapses leads to deficits in associative memory in a model of intellectual disorder. *J. Neurosci.*, **33**, 13805–13819.
18. Bahi, N., Friocourt, G., Carrié, A., Graham, M.E., Weiss, J.L., Chafey, P., Fauchereau, F., Burgoyne, R.D. and Chelly, J. (2003) IL1 receptor accessory protein like, a protein involved in X-linked mental retardation, interacts with Neuronal Calcium Sensor-1 and regulates exocytosis. *Hum. Mol. Genet.*, **12**, 1415–1425.
19. Gambino, F., Pavlowsky, A., Béglé, A., Dupont, J.L., Bahi, N., Courjaret, R., Gardette, R., Hadjkacem, H., Skala, H., Poulain, B. *et al.* (2007) IL1-receptor accessory protein-like 1 (IL1RAPL1), a protein involved in cognitive functions, regulates N-type Ca 2+ -channel and neurite elongation. *Proc. Natl. Acad. Sci. USA*, **104**, 2–7.
20. Valnegri, P., Montrasio, C., Brambilla, D., Ko, J., Passafaro, M. and Sala, C. (2011) The X-linked intellectual disability protein IL1RAPL1 regulates excitatory synapse formation by binding PTPδ and RhoGAP2. *Hum. Mol. Genet.*, **20**, 4797–4809.
21. Hayashi, T., Yoshida, T., Ra, M., Taguchi, R. and Mishina, M. (2013) IL1RAPL1 associated with mental retardation and autism regulates the formation and stabilization of glutamatergic synapses of cortical neurons through RhoA signaling pathway. *PLoS One*, **8**, e66254.
22. Yoshida, T., Yasumura, M., Uemura, T., Lee, S.J., Ra, M., Taguchi, R., Iwakura, Y. and Mishina, M. (2011) IL-1 receptor accessory protein-like 1 associated with mental retardation and autism mediates synapse formation by trans-synaptic interaction with protein tyrosine phosphatase δ. *J. Neurosci.*, **31**, 13485–13499.
23. Tarpey, P.S., Smith, R., Pleasance, E., Whibley, A., Edkins, S., Hardy, C., O'Meara, S., Latimer, C., Dicks, E., Menzies, A. *et al.* (2009) A systematic, large-scale resequencing screen of X-chromosome coding exons in mental retardation. *Nat. Genet.*, **41**, 535–543.
24. Schwarz, J.M., Rödelsperger, C., Schuelke, M. and Seelow, D. (2010) MutationTaster evaluates disease-causing potential of sequence alterations. *Nat. Methods*, **7**, 575–576.
25. Ng, P.C. and Henikoff, S. (2001) Predicting deleterious amino acid substitutions. *Genome Res.*, **11**, 863–874.
26. Adzhubei, I.A., Schmidt, S., Peshkin, L., Ramensky, V.E., Gerasimova, A., Bork, P., Kondrashov, A.S. and Sunyaev, S.R. (2010) A method and server for predicting damaging missense mutations. *Nat. Methods*, **7**, 248–249.
27. Yoshida, T. and Mishina, M. (2008) Zebrafish orthologue of mental retardation protein IL1RAPL1 regulates presynaptic differentiation. *Mol. Cell. Neurosci.*, **39**, 218–228.
28. Pulido, R., Serra-Pagès, C., Tang, M. and Streuli, M. (1995) The LAR/PTP delta/PTP sigma subfamily of transmembrane protein-tyrosine-phosphatases: multiple human LAR, PTP delta, and PTP sigma isoforms are expressed in a tissue-specific manner and associate with the LAR-interacting protein LIP.1. *Proc. Natl. Acad. Sci. USA*, **92**, 11686–11690.
29. Khan, J.A., Brint, E.K., O'Neill, L.A.J. and Tong, L. (2004) Crystal structure of the Toll/interleukin-1 receptor domain of human IL-1RAPL. *J. Biol. Chem.*, **279**, 31664–31670.
30. Pavlowsky, A., Zanchi, A., Pallotto, M., Giustetto, M., Chelly, J., Sala, C. and Billuart, P. (2010) Neuronal JNK pathway activation by IL-1 is mediated through IL1RAPL1, a protein required for development of cognitive functions. *Commun. Integr. Biol.*, **10**, 245–247.
31. Brint, E.K., Fitzgerald, K.A., Smith, P., Coyle, A.J., Gutierrez-Ramos, J.-C., Fallon, P.G. and O'Neill, L.aJ. (2002) Characterization of signaling pathways activated by the interleukin 1 (IL-1) receptor homologue T1/ST2. A role for Jun N-terminal kinase in IL-4 induction. *J. Biol. Chem.*, **277**, 49205–49211.
32. Leprêtre, F., Delannoy, V., Froguel, P., Vasseur, F. and Montpellier, C. (2003) Dissection of an inverted X(p21.3q27.1) chromosome associated with mental retardation. *Cytogenet. Genome Res.*, **101**, 124–129.
33. Schuurs-Hoeijmakers, J.H.M., Vulto-van Silfhout, A.T., Vissers, L.E.L.M., van de Vondervoort, I.I.G.M., van Bon, B.W.M., de Ligt, J., Gilissen, C., Hehir-Kwa, J.Y., Neveling, K., del Rosario, M. *et al.* (2013) Identification of pathogenic gene variants in small families with intellectually disabled siblings by exome sequencing. *J. Med. Genet.*, **50**, 802–811.
34. Wu, H., Luo, J., Yu, H., Rattner, A., Mo, A., Wang, Y., Smallwood, P.M., Erlanger, B., Wheelan, S.J. and Nathans, J. (2014) Cellular resolution maps of X chromosome inactivation: implications for neural development, function, and disease. *Neuron*, **81**, 103–119.
35. Kim, M.J., Futai, K., Jo, J., Hayashi, Y., Cho, K. and Sheng, M. (2008) Synaptic accumulation of PSD-95 and synaptic function regulated by phosphorylation of serine-295 of PSD-95. *Neuron*, **57**, 326–327.
36. Zhu, Y., Pak, D., Qin, Y., McCormack, S.G., Kim, M.J., Baumgart, J.P., Velamoor, V., Auberson, Y.P., Osten, P., van Aelst, L. *et al.* (2005) Rap2-JNK removes synaptic AMPA receptors during depotentiation. *Neuron*, **46**, 905–916.
37. Thomas, G.M., Lin, D.T., Nuriya, M. and Huganir, R.L. (2008) Rapid and bi-directional regulation of AMPA receptor phosphorylation and trafficking by JNK. *EMBO J.*, **27**, 361–372.

38. Vandeweyer, G., Reyniers, E., Wuyts, W., Rooms, L. and Kooy, R.F. (2011) CNV-WebStore: online CNV analysis, storage and interpretation. *BMC Bioinformatics*, **12**, 4.
39. Fokkema, I.F.A.C., Taschner, P.E.M., Schaafsma, G.C.P., Celli, J., Laros, J.F.J. and den Dunnen, J.T. (2011) LOVD v.2.0: the next generation in gene variant databases. *Hum. Mutat.*, **32**, 557–563.
40. Sala, C., Piëch, V., Wilson, N.R., Passafaro, M., Liu, G. and Sheng, M. (2001) Regulation of dendritic spine morphology and synaptic function by Shank and Homer. *Neuron*, **31**, 115–130.
41. Verpelli, C., Piccoli, G., Zibetti, C., Zanchi, A., Gardoni, F., Huang, K., Brambilla, D., Di Luca, M., Battaglioli, E. and Sala, C. (2010) Synaptic activity controls dendritic spine morphology by modulating eEF2-dependent BDNF synthesis. *J. Neurosci.*, **30**, 5830–5842.
42. Meijering, E., Jacob, M., Sarria, J.C.F., Steiner, P., Hirling, H. and Unser, M. (2004) Design and validation of a tool for neurite tracing and analysis in fluorescence microscopy images. *Cytometry A*, **58**, 167–176.
43. Lyles, V., Zhao, Y. and Martin, K.C. (2006) Synapse formation and mRNA localization in cultured Aplysia neurons. *Neuron*, **49**, 349–356.
44. Piccoli, G., Verpelli, C., Tonna, N., Romorini, S., Alessio, M., Nairn, A.C., Bachi, A. and Sala, C. (2007) Proteomic analysis of activity-dependent synaptic plasticity in hippocampal neurons research articles. *J. Proteomic Res.*, **6**, 3203–3215.

SUPPLEMENTARY INFORMATION

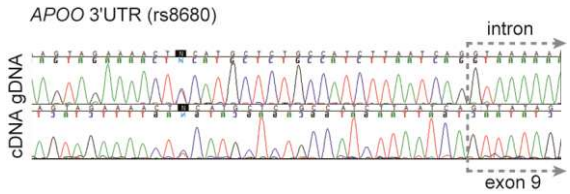

Supplementary figure 1. X-Chromosome inactivation study in III-2 patient (P75 family). Analyzes of genomic DNA (gDNA) from fibroblast by PCR and Sanger sequencing shows that female III-2 patient is heterozygous (C/T alleles) for the SNP (rs8680) in the 3'UTR of APOO gene. Amplification and sequencing of the APOO transcript using cDNAs from III-2 patient's fibroblasts reveals that both alleles are expressed at similar levels suggesting the absence of X-inactivation bias in patient's fibroblasts. The exon 8/intron 8 and exon8/exon9 boundaries of APOO gene and transcript respectively are indicated by grey dash lines with arrow.

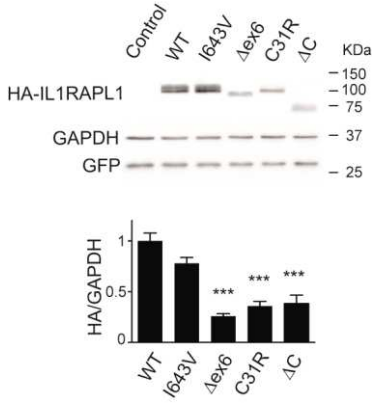

Supplementary figure 2. Protein expression of IL1RAPL1 mutants in HEK293 cells. Protein detection by immunoblot on lysates from HEK293 cells co-transfected with different HA-IL1RAPL1 constructs and GFP. IL1RAPL1 proteins were revealed by an anti-HA tag antibody, and signal was normalized to GAPDH expression. GFP is used as a control of transfection efficiency. Bar graphs show the mean + SEM of IL1RAPL1 protein expression normalized to the WT -transfected cells (6 independent experiments, *p <0.01 *** p <0.001).

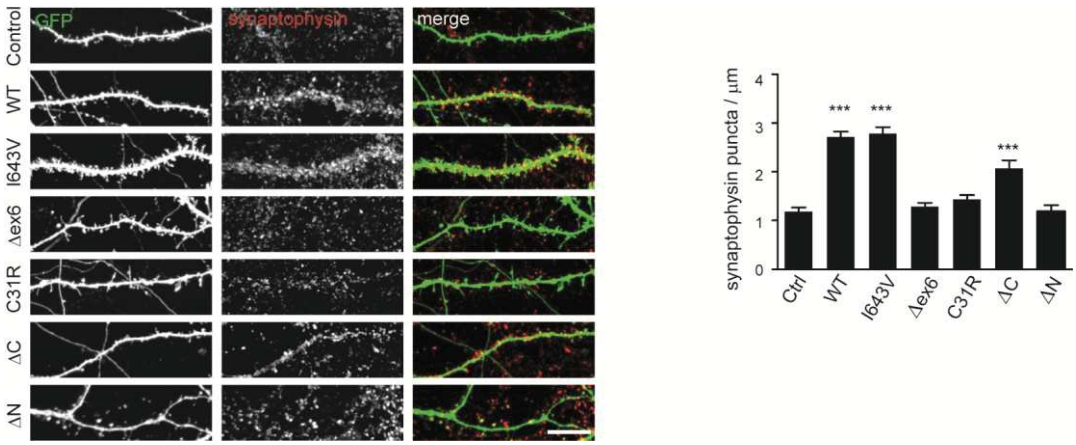

Supplementary figure 3. Consequences of IL1RAPL1 mutations on pre-synaptic formation. Mouse hippocampal neurons were co-transfected with GFP and the different IL1RAPL1 constructs, and were stained at DIV18 with synaptophysin antibody to label excitatory post-synapses. Each column of images shows double-labeling for GFP (top panel) and synaptophysin (middle panel); the merged images are shown in the bottom panel (scale bar 10 µm). Bar graphs show the mean + SEM of the synaptophysin clusters per micron in at least 50 neurons for each condition from 3 independent experiments (*** p < 0.001, compared to control neurons).

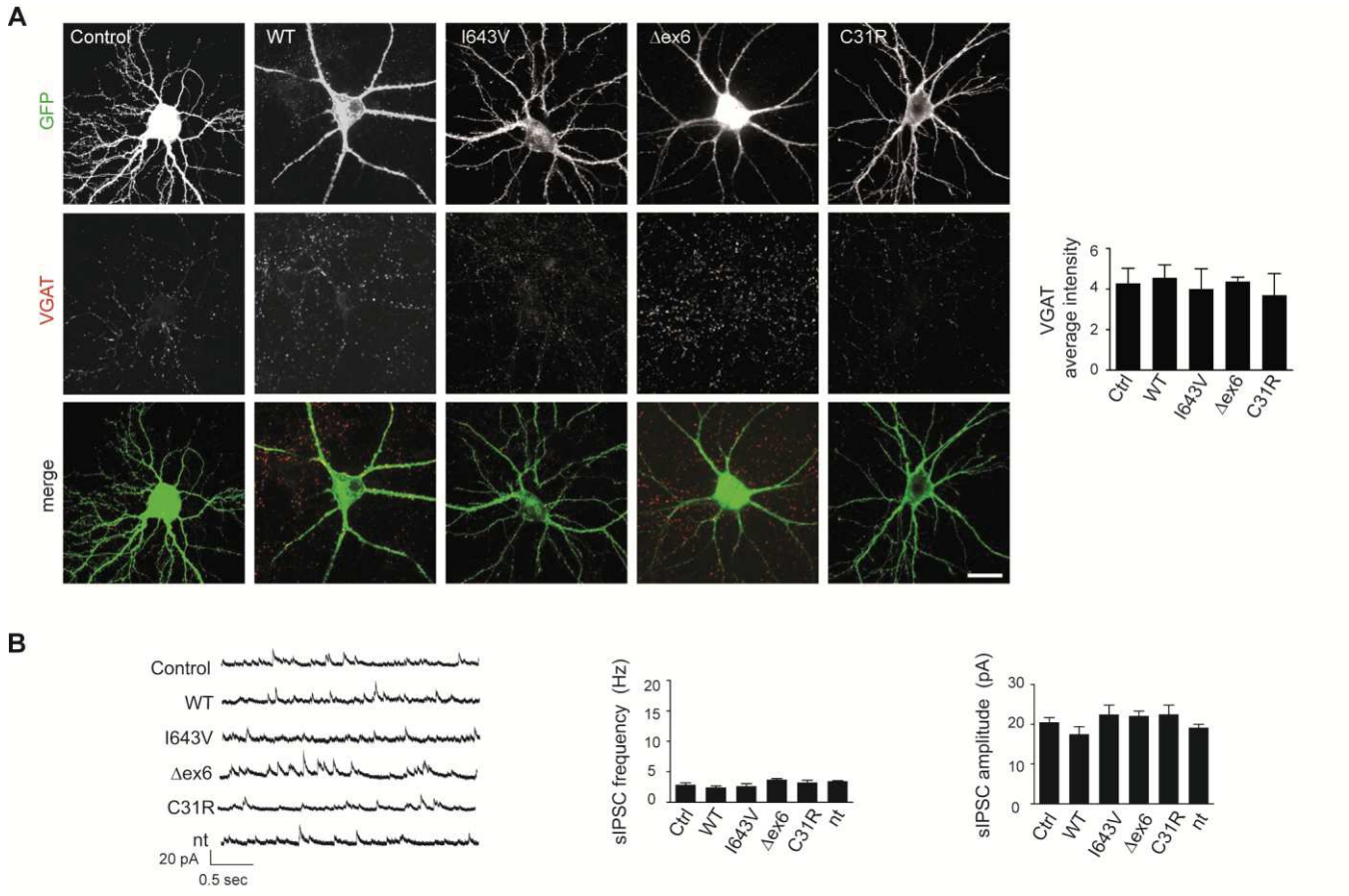

Supplementary figure 4. Consequences of IL1RAPL1 mutations on inhibitory synapse formation.
(A) Mouse hippocampal neurons co-transfected with GFP and different HA-IL1RAPL1 constructs were stained with anti-VGAT antibody to label inhibitory pre-synapses. Each column of images shows double-labeling for GFP (top panel) and VGAT (middle panel); the merged images are shown in the bottom panel (scale bar 20 μm). Bar graphs show the mean + SEM of VGAT intensity (15 neurons from 3 independent experiments for each condition). (B) Typical recording of sIPSC from mouse hippocampal neurons at 18-21 DIV transfected with different IL1RAPL1 constructs. Bars represent the average frequency and amplitude of these events (14 to 21 transfected neurons per condition and 61 non transfected neurons (nt)).

2. Target-specific vulnerability of excitatory synapses leads to deficits in associative memory in a model of intellectual disorder.

The vast majority of the mutations on *IL1RAPL1* associated with ID consist of the complete deletion of the gene, or of large deletions encompassing many exons that lead to the absence of the protein. This condition is fulfilled by the *Il1rapl1* KO mouse model, which make it a good tool for the study of IL1RAPL1 function on the establishment and function of brain circuits. When I started my PhD, the characterization of the cognitive consequences in the absence of IL1RAPL1 was lacking. Moreover, the endogenous brain expression pattern and cell distribution of IL1RAPL1 protein had not been described due to the lacking of proper tools to do so.
These two issues were addressed in a work published by our collaborators, the team of Yann Humeau at Bordeaux, and in which I participated.
In this study, taking advantage of the cellular network of the lateral amygdala and of a behavior associated with this brain structure, we described that IL1RAPL1 loss of function leads to deficits in the acquisition of associative memory. An initially neutral stimulus (a conditioned stimulus or CS) can acquire affective properties on repeated temporal pairings with a biologically significant event (the unconditioned stimulus or US). As the CS-US relation is learned, innate physiological and behavioral responses come under the control of the CS. In this study, if a mouse is given a tone (CS) followed by an electric shock (US), after a few tone-shock pairings a defensive response (freezing) will be elicited by the tone. The memory formed by fear conditioning (associative memory) is long lasting, can be easily assessed and has been observed in a wide range of organisms, from mice to humans (Ledoux 2000).
Fear conditioning is mediated by the transmission of information about the CS and US to the amygdala, and the fear reactions are controlled by the output projections from the amygdala to the brainstem. During CS/US associations, LTP is induced at the excitatory synapses between the thalamus and the principal cells of the lateral amygdala (Rumpel et al. 2005; Humeau et al. 2007).
Lateral amygdala is composed of GABAergic interneurons (~20%) and glutamatergic principal cells (PC) (~80%). Interneurons are activated by the same projections that activate PC, leading to a feed-forward inhibition mechanism, in a way that interneurons can control PC excitation and output.

We identified that in the fear conditioning circuit, only the synapses formed between the thalamus-projecting axons on PC, but not on interneurons, were affected by *Il1rapl1* loss (Figure 19). This leads to a decrease of excitatory inputs on PC, and thus a net increase of feed-forward inhibition. We propose that the perturbed E/I resulting ratio is the source of the behavioral deficits of *Il1rapl1* KO mice.

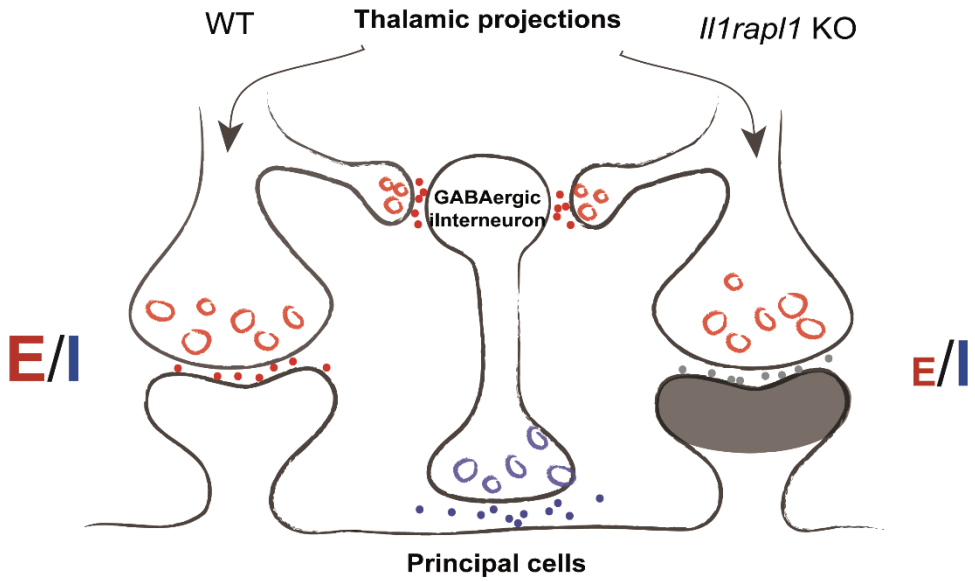

Figure 19. Excitatory/inhibitory balance is perturbed in the absence of Il1rapl1. In normal conditions (WT, left), thalamic projections (red) establish excitatory synapses with principal cells and interneurons in the lateral amygdala. Interneurons (blue) form inhibitory synapses on principal cells. In the absence of Il1rapl1 (right), the excitation on principal cells synapses is decreased, while synapses on interneurons are not affected. This results in an imbalance of E/I ratio in favor to inhibition in the lateral amygdala.

The fact that not all synapses are impaired in this system may be due to differences in IL1RAPL1 expression itself, or in the expression of IL1RAPL1 molecular partners on different synapses. However, our results suggest that *Il1rapl1* mRNA expression is not restricted to a particular cell type, thus the hypothesis of the different distribution of its partners seems to be plausible.

In the lateral amygdala, cued fear conditioning drives GluA1-containing AMPA receptors into the synapse of postsynaptic neurons and this subunit is essential for the LTP underlying this behavior (Rumpel et al. 2005; Humeau et al. 2007). Not all neurons types in all brain regions possesses AMPA receptors containing the same subunits. For example, the hippocampal GABAergic interneurons exhibit low levels of GluA2-containing AMPA receptors, and some hippocampal cells can express both GluA2—

containing and –lacking AMPA receptors that can be differentially targeted to synapses receiving distinct afferent inputs (Isaac et al. 2007; Tóth & McBain 1998). IL1RAPL1 was shown to regulate the membrane insertion of AMPA receptors subunits in cortical neurons in culture (Hayashi et al. 2013). Overexpression of IL1RAPL1 in these cells led to a decrease of the insertion to the membrane of GluA1-containing AMPA receptors, whereas the insertion of GluA2/GluA3-containing receptors is enhanced (Hayashi et al. 2013). These results were observed by overexpressing the different AMPA subunits, and may not reflect the physiological state of cortical neurons, but they suggest that IL1RAPL1 is able to regulate AMPA receptor dynamics in a subunit-dependent manner. Thus, one possible interpretation of our results in the lateral amygdala is that IL1RAPL1 regulates AMPA receptors trafficking at PC synapses, and that the subunit composition of AMPA receptors at interneuron synapses is less affected by IL1RAPL1.

Interestingly, the behavioral deficits of *Il1rapl1* KO mice were corrected by the local infusion of bicuculline, a $GABA_A$ receptors antagonist, and by the direct activation of PC using optogenetics. Both manipulations are thought to bypass E/I imbalance in *Il1rapl1* KO mice during the acquisition phase of cued fear conditioning, and thus lead to normal memory in those mice. These are encouraging results for a potential treatment for the cognitive deficits in the absence of IL1RAPL1.

Systems/Circuits

Target-Specific Vulnerability of Excitatory Synapses Leads to Deficits in Associative Memory in a Model of Intellectual Disorder

Xander Houbaert,[1]* Chun-Lei Zhang,[1]* Frédéric Gambino,[2] Marilyn Lepleux,[1] Melissa Deshors,[1,3] Elisabeth Normand,[3] Florian Levet,[4] Mariana Ramos,[5] Pierre Billuart,[5] Jamel Chelly,[5] Etienne Herzog,[1] and Yann Humeau[1]

[1]Team synapse in cognition, Institut Interdisciplinaire de Neuroscience, Centre National de la Recherche Scientifique CNRS UMR5297, Université de Bordeaux, 33077 Bordeaux, France, [2]Institut des neurosciences cellulaires et intégratives, Centre National de la Recherche Scientifique CNRS UPR3212, Université de Strasbourg, 67000 France, [3]Pole in vivo, Institut Interdisciplinaire de Neuroscience, Centre National de la Recherche Scientifique CNRS UMR5297, Université de Bordeaux, 33077 Bordeaux, France, [4]Team imaging the cell, Institut Interdisciplinaire de Neuroscience, Centre National de la Recherche Scientifique CNRS UMR5297, Université de Bordeaux, 33077 Bordeaux, France, and [5]Centre National de la Recherche Scientifique, Université Paris Descartes, Institut National de la Santé et de la Recherche Médicale, UMR8104, Institut Cochin, 75014 Paris, France

Intellectual disorders (IDs) have been regularly associated with morphological and functional deficits at glutamatergic synapses in both humans and rodents. How these synaptic deficits may lead to the variety of learning and memory deficits defining ID is still unknown. Here we studied the functional and behavioral consequences of the ID gene *il1rapl1* deficiency in mice and reported that *il1rapl1* constitutive deletion alters cued fear memory formation. Combined *in vivo* and *in vitro* approaches allowed us to unveil a causal relationship between a marked inhibitory/excitatory (I/E) imbalance in dedicated amygdala neuronal subcircuits and behavioral deficits. Cell-targeted recordings further demonstrated a morpho-functional impact of the mutation at thalamic projections contacting principal cells, whereas the same afferents on interneurons are unaffected by the lack of Il1rapl1. We thus propose that excitatory synapses have a heterogeneous vulnerability to *il1rapl1* gene constitutive mutation and that alteration of a subset of excitatory synapses in neuronal circuits is sufficient to generate permanent cognitive deficits.

Introduction

Learning-related forms of persisting synaptic plasticity (LTP) at excitatory synapses were initially discovered in the hippocampus (Bliss and Lomo, 1973). Although diverse in their molecular and cellular mechanisms, LTP has now been found in most brain areas, including amygdala (Rumpel et al., 2005). Meanwhile, >450 gene mutations have been identified as causing intellectual disorders (IDs) (van Bokhoven, 2011). Studies on human and animal models consistently reported that ID gene mutations primarily impact the morphology and/or function of excitatory synapses (Purpura, 1974). Remarkably, deficits in LTP in ID models remain poorly documented (Vaillend et al., 2008; Humeau et al., 2009), although an increasing number of ID gene products are involved in LTP-relevant signaling pathways (Pavlowsky et al., 2011).

In mammals, pairing an initially neutral stimulus (conditioned stimulus [CS]) with an aversive stimulus (unconditioned stimulus [US]) leads to the formation of a robust and long-lasting associative fear memory (Ledoux, 2000). During CS/US associations, long-lasting synaptic potentiation is induced at excitatory synapses impinging onto principal cells of the lateral nucleus of the amygdaloid complex (LA) (Rumpel et al., 2005; Humeau et al., 2007). Interestingly, the gating of this form of LTP is only possible in conditions lowering the influence of feedforward GABAergic inhibition (Bissière et al., 2003; Ehrlich et al., 2009), implying that a functional adaptation of the inhibition/excitation (I/E) balance is required to allow suprathreshold, postsynaptic depolarization during fear conditioning. Moreover, I/E balance alterations have been recurrently associated with neurological and ID animal models (Kleschevnikov et al., 2004; Dani et al., 2005; Baroncelli et al., 2011; Pizzarelli and Cherubini, 2011; Yizhar et al., 2011), including *il1rapl1* mutant mice (Gambino et al., 2009).

In humans, *il1rapl1* mutation leads to a spectrum of cognitive defects, ranging from nonsyndromic intellectual disorders to au-

Received April 3, 2013; revised July 20, 2013; accepted July 23, 2013.

Author contributions: J.C. and Y.H. designed research; X.H., C.-L.Z., F.G., M.L., M.D., E.N., P.B., and Y.H. performed research; F.L., M.R., and P.B. contributed unpublished reagents/analytic tools; X.H., C.-L.Z., F.G., M.L., and Y.H. analyzed data; E.H. and Y.H. wrote the paper.

This work was supported by Agence Nationale pour la Recherche (J.C., E.H., and Y.H.), the European Neuroscience Institutes Network (Y.H.), and the Gencodys FP7 program (Y.H. and J.C.). We thank Drs Shona Osborne, Cyril Herry, Andréas Lüthi, Julien Dupuis, and François Georges for their critical reading of the manuscript; Dr. Jiyun Peng for helping in the tracking of mouse activities; and the Pole In Vivo and animal facilities of the Bordeaux University for the animal care. The microscopy was done at the Bordeaux Imaging Center of the University of Bordeaux Segalen, with the help of Sébastien Marais and Magali Mondin.

The authors declare no competing financial interests.

*X.H. and C.-L.Z. contributed equally to this work.

Correspondence should be addressed to Dr. Yann Humeau, UMR5297 Institut Interdisciplinaire de Neuroscience, Centre de génomique fonctionnelle, 146 rue Léo Saignat, 33077, Bordeaux cedex, France. E-mail: yann.humeau@u-bordeaux2.fr.

F. Gambino's present address: Département des neurosciences fondamentales, CMU, Genève, Suisse.

DOI:10.1523/JNEUROSCI.1457-13.2013

 0270-6474/13/3313805-15$15.00/0

tistic spectrum disorders (ASDs) (Piton et al., 2008). Il1rapl1 is a member of a novel family of IL1/Toll receptors enriched at excitatory synapses (Pavlowsky et al., 2010). Il1rapl1 induces excitatory presynapse formation by interacting trans-synaptically with the protein tyrosine phosphatase δ (PTPδ) (Valnegri et al., 2011; Yoshida et al., 2011) but also interacts with some components of the postsynaptic density, such as PSD95, RhoGAP2, and Mcf2l (Pavlowsky et al., 2010; Valnegri et al., 2011; Hayashi et al., 2013), enabling morphological and functional maintenance of excitatory dendritic spines and glutamate receptor insertion (Hayashi et al., 2013). Il1rapl1 also regulates N-type voltage-gated calcium channel and neurite elongation in neuroendocrine cells through its interaction with the neuronal calcium sensor-1 (Gambino et al., 2007). Thus, current data support the notion that Il1rapl1 is important for the formation, maintenance, and function of excitatory synapses by converging presynaptic, postsynaptic, and trans-synaptic effects.

Yet, the consequences of *il1rapl1* deletion onto physiological properties of mature neuronal networks and related behavioral paradigms remain unexplored. Here we identified an I/E imbalance in the amygdala circuits of adult *il1rapl1* constitutive mutant mice, resulting from a heterogeneous vulnerability of excitatory synapses to Il1rapl1 removal. We then determined how these functional perturbations of amygdala circuit impact fear memory formation.

Materials and Methods

Animals

Most experiments were performed using male *il1rapl1* −*/y* and their control +*/y* littermates (2–3 months old, C57BL/6 background), housed in 12/12 LD with *ad libitum* feeding. Some crossings with GAD67-eGFP mice (Tamamaki et al., 2003) (kindly provided by A. Lüthi's laboratory, FMI, Basel, Switzerland) were made in house to allow visualizing amygdala interneurons. Every effort was made to minimize the number of animals used and their suffering. The experimental design and all procedures were in accordance with the European guide for the care and use of laboratory animals and the animal care guidelines issued by the animal experimental committee of Bordeaux Universities (CE50; A5012009).

Fear conditioning

Mice were housed individually in a ventilation area before the start of behavioral training. Animals were handled every day before the start of the experiment during a week. On day 1, animals were transferred to the conditioning context (Context A) for habituation. Both CS^+ (total CS duration of 30 s, consisting of 50 ms pips repeated at 0.9 Hz, pip frequency 7.5 kHz, 80 dB sound pressure level) and CS^- (30 s, consisting of white noise pips repeated at 0.9 Hz, 80 dB sound pressure level) were presented 4 times with a variable interstimulus interval (ISI). On day 2, we proceeded with the conditioning phase. The protocol consisted of 5 pairings of CS^+ with the US onset coinciding with the CS^+ offset (1 s foot shock, 0.6 mA, ISI 10–60 s). In all cases, CS^- presentations were intermingled with CS^+ presentations and ISI was variable over the whole training course. Cued memory was tested 24 h after conditioning by analyzing the freezing levels at the first CS^+ presentations in Context B (recall). Freezing behavior was quantified automatically in each behavioral session using a fire-wire CCD camera (Ugo Basile) connected to automated freezing detection software (ANY-maze, Stoelting). To test for animal exploration and activity, the animal displacement in the context was traced and analyzed with software programmed and provided by Dr. Jiyun Peng (Fudan, Shanghai, China).

Electrophysiology

Slice preparation. Standard procedures were used to prepare 300- to 330-μm-thick coronal slices from 4-week-old up to 2.5-month-old male wild-type or mutant mice following a protocol approved by the European and French guidelines on animal experimentation. Briefly, the brain was dissected in ice-cold artificial CSF (ACSF) containing the following (in mM): 124 NaCl, 2.7 KCl, 2 $CaCl_2$, 10 $MgSO_4$, 7 H_2O, 26 $NaHCO_3$, 1.25 NaH_2PO_4, 18.6 glucose, and 2.25 ascorbic acid; the brain was mounted against an agar block and sliced with a vibratome (Leica VT1200 s) at 4°C. Slices were maintained for 45 min at 37°C in an interface chamber containing ACSF equilibrated with 95% O_2/5% CO_2 and then for at least 45 min at room temperature before being transferred to a superfusing recording chamber. In the perfused ACSF, the $MgSO_4$ was decreased to 1.3 mM.

Recordings. Whole-cell recordings from LA principal neurons were performed at 30–32°C in a superfusing chamber as previously described (Humeau et al., 2005). Neurons were visually identified with infrared videomicroscopy using an upright microscope equipped with a 60× objective. Patch electrodes (3–5 MΩ) were pulled from borosilicate glass tubing and filled with a low-chloride solution containing the following (in mM): 140 Cs-methylsulfonate, 5 QX314 Cl, 10 HEPES, 10 phosphocreatine, 4 Mg-ATP, and 0.3 Na-GTP (pH adjusted to 7.25 with CsOH, 300 mOsm). For dedicated current-clamp experiments, Cs-methylsulfonate was replaced with equimolar K-gluconate. All LTP experiments were performed in the presence of picrotoxin (100 μM), except the no-PTX experiments shown in Figure 2. Monosynaptic EPSCs or EPSPs exhibiting constant 10–90% rise times and latencies were elicited by stimulation of afferent fibers with a bipolar twisted platinum/10% iridium wire (25 μm diameter). In all experiments, stimulation intensity was adjusted to obtain baseline EPSC amplitudes between 100 and 200 pA (CC mode) or 4–6 mV (IC mode). In some experiments, the capacitance of recorded cells was measured to evaluate the cell size. We used an exponential fit adjusted to the capacitive current generated by 100 ms/10 mV hyperpolarizing steps under the voltage-clampmode (see Fig. 4, seal tests).

LA interneuron classification. GAD-67-eGFP-expressing interneuron separation was based on the spiking patterns of recorded cells. To elicit spikes, cells were maintained at −70 mV in current-clamp mode and submitted to repeated, 400-ms-long, current steps of increasing intensity: −50, 50, 150, 250, and 350 pA, to explore a variety of potential response. In most cases, spiking inactivation was seen at the end of high intensity trains, indicating that the cell has reached its maximal spiking capacity. Otherwise, additional current injections of greater intensities were applied to reach spike inactivation. The last current step not inducing spike inactivation was retained for analysis. We analyzed neuronal discharge by measuring each spike amplitude and interspike intervals (ISI) observed during the train. IN classification was essentially based on the number of observed spikes (REG > BIM > ADA > SADA) and the degree of spike adaptation (last ISI/first ISI: BIM > ADA, SADA > REG). Occasionally, we also used spike half-width (REG < BIM < ADA, SADA) and the initial spike frequency (BIM > SADA, ADA, REG) to allow classifying some borderline cases.

Data acquisition and analysis. Data were recorded with a Multiclamp700B (Molecular Devices), filtered at 2 kHz and digitized at 10 kHz. Data were acquired and analyzed with pClamp10.2 (Molecular Devices). In all experiments, series resistance was monitored throughout the experiment; and if it changed by >15%, the data were not included in the analysis. Changes were quantified by normalizing and averaging EPSP slope during the last 5 min of the experiments relative to the 5 min of baseline before LTP induction or drug application.

Morphological analysis

In situ hybridization of il1rapl1 mRNA. This protocol was performed by a service company (Oramacell). Detection of each mRNA (VGLUT1, solute carrier family 17, member 7, slc17a7; NM_182993), glutamate decarboxylase 1 (gad1; NM_008077), and interleukin 1 receptor accessory protein-like 1 (il1rapl1; NM_001160403.1) was achieved by design of antisense oligonucleotides using Helios ETC oligo design software (Oramacell). For *il1rapl1* mRNA detection, two sets of oligonucleotides were designed: one specific for exon 5 (2 oligonucleotides) and one nonspecific of exon 5 (5 oligonucleotides). For slc17a7 and gad1 mRNA detection, a set of 3 oligonucleotides was designed for mRNA. Each oligonucleotide and a mix of two or three labeled oligonucleotides were tested for the hybridization step. Same results were obtained for each

mRNA for the four probes. *In situ* hybridization was performed as described previously (Moutsimilli et al., 2005). Briefly, oligonucleotides were labeled with [^{35}S]-dATP using terminal transferase to a specific activity of 5×10^8 dpm/μg. Experimental slides were fixed in 4% formaldehyde in PBS, washed with PBS, rinsed with water, dehydrated in 70% ethanol, and air-dried. Sections were then covered with 140 μl of a hybridization medium (Oramacell) containing 3–5 $\times 10^5$ dpm of the labeled oligonucleotide mix. Slides were incubated overnight at 42°C, washed, and exposed to a BAS-SR Fujifilm Imaging Plate for 15 d. The plates were scanned with a Fujifilm BioImaging Analyzer BAS-5000 and analyzed with MultiGauge software. Slides were then dipped in Kodak NTB emulsion, exposed for 6 weeks, developed and counterstained with toluidine blue.

Neurobiotin-based dendritic spine analysis. Amygdala-containing coronal sections (300 μm thick) in which LA principal cells were loaded with neurobiotin (0.02% in intracellular medium) for at least 20 min in open whole-cell configuration were first fixed in PFA 10% and then treated with PBS solution containing Triton 0.4% and 33 mM NaH_4Cl to block PFA aldehydic functions. Neurobiotin was then revealed using streptavidin-conjugated with AlexaFluor-568. Sections were then coverslipped with Vectashield, and *z*-stack images performed using confocal microscopy (Leica SP2, 63× oil-immersion objective) with a lateral resolution of ~200 nm. Spine number, spine length, spine head diameter, and spine type (mushroom, thin, stubby) were analyzed using Neuron Studio software (Rodriguez et al., 2008) (http://research.mssm.edu/cnic/tools.html). The first step consists of adjusting settings and software calibration to automatically detect dendritic spines. In all cases, automatic results were manually checked on the 3D reconstruction to delete false-positive and add nondetected spines. Values for each branch segment were expressed as spine number/μm.

Presynaptic and postsynaptic apposed clusters analysis. To prepare amygdala coronal sections, 3 and 3 *Il1rapl1* +/*y* and −/*y* mice were anesthetized with pentobarbital and fixed by intracardiac perfusion with 4% paraformaldehyde in PBS. The brains were dissected, postfixed during 24 h, and coronal, 50-μm-thick sections were obtained using a vibratome (Leica 1200 s). The brain sections were maintained in a blocking buffer (PBS solution containing 0.3% Triton X-100 and 2% gelatin) for 1 h at room temperature. Thereafter, sections were incubated at 4°C overnight with monoclonal antibody against PSD95 (1:600; Abcam, ab2723) and polyclonal antibodies against VGlut2 (1:10,000) from Millipore (AB2251) diluted in the blocking buffer. Slices were rinsed three times in PBS and incubated for 2 h at room temperature with Alexa488- and Alexa647-labeled goat anti-mouse or anti-guinea pig Ig G secondary antibodies (1:1000, Invitrogen), rinsed in PBS before being mounted with Vectashield.

Amygdala *z*-stacks were captured with confocal microscope (Leica SPE, 63× oil-immersion objective), at a constant depth from the surface. To compute apposition between the presynaptic and the postsynaptic staining, a plugin developed within ImageJ and based on wavelets transform was used to perform image processing and analysis. At first, each staining is segmented (by the use of "à trous" wavelets, see below) in a set of objects. Afterward, these two segmentations were used in a pixel-based technique to determine their appositions.

Segmentation. The input signal (i.e., the image) is analyzed by using the coefficients of a low-pass filter. Because wavelets are a multiresolution representation, the low-pass filter was stretched depending on the resolution level. As a result, each resolution level generated a different set of coefficients. To filter unwanted background noise while keeping details of interest, it was sufficient to directly set the threshold for the wavelet coefficient sub-bands in which the size of the filter is close to the size of the desired objects (in our case, there were the two first ones). Results of this filtering were two binary images (one for each staining) with clusters being identified as individual objects.

Apposition. To determine whether the presynaptic staining was apposed to the postsynaptic one at a given location, each cluster was tagged with a value: 0 for background, 1 for presynaptic, and 2 for postsynaptic clusters. A new image was created, which is the result of the addition of all the presynaptic and postsynaptic clusters. Once all the objects of this image were identified, we could easily determine whether there were apposed clusters. If an object was not composed of a single value (either 1 or 2), then it was an apposed cluster. Two cases were possible: if the two objects were touching themselves with no overlapping pixels, they were perfectly apposed. On the contrary, if some overlapping pixels were present, the objects were just apposed. In this study, all apposed events were counted. Because the technique is pixel-based, apposition was determined at the resolution level of the images.

Cannula implantation and drug administration

Cannula implantation. Stainless steel guide cannula (26 gauge; Plastics-One) were bilaterally implanted above amygdala under continuous anesthesia with isoflurane. Beforehand, mice were treated with buprenorphine (0.1 mg/kg, i.p) and positioned in a stereotaxic apparatus (David Kopf Instruments). The positions of bregma and λ points were defined and adjusted to the same horizontal level. Coordinates were as follows: LA, anteroposterior, −1.7 mm, mediolateral, ±3.1 mm, and dorsoventral, −2.8–3 mm. Cannula was secured to the skull using dental cement (Super-Bond, Sun Medical). In the end, the mice woke up on a 35°C heating pad, and a dummy cannula was inserted into the guide cannula to reduce the risk of infection.

Drug administration. To reduce stress during drug injection, the mice were trained with dummy cannula removal and insertion 1 week before use. To perform freely moving drug injection, the dummy cannula was replaced by an infusion cannula (33 gauge; connected to a 1 μl Hamilton syringe via polyethylene tubing) projecting out of the guide cannula with 1 mm to target LA. As previously described (Herry et al., 2008), the GABA-A receptor antagonist bicuculline (20 ng/200 nl in saline) was infused bilaterally at a rate of 0.1 μl/min in a volume of 200–250 nl per side by an automatic pump (Legato 100, Kd Scientific) 30–60 min before learning. To allow penetration of drug, the injector was maintained for an additional 3 min. After injection, mice were put back in the cages before behavioral testing. Importantly, no seizures were observed upon bicuculline treatment in all cohorts analyzed and presented here.

Controls. To analyze the location and extent of the injections, brains were injected with a fluorophore BODIPY TMR-X (Invitrogen; 5 mM in PBS 0.1 M, DMSO 40%). Then slices (60 μm) were imaged using a 5× epifluorescence microscope (Leica DM5000). The mice we considered for further analysis had at least one side precisely targeted above the LA and where each side was covered by >25% bodipy fluorescence.

Freely moving optical stimulation

AAV injections: adeno-associated viruses. AAV constructs and viruses were obtained from the U-penn Vector Core. We used AAV2/9 vectorsencodingforChR2-Venusexpression(AAV2/9.CAG.ChR2-Venus.W.SV40) (Addgene ref. 20071; 5.82E^{12} vector genomes, vg/ml). The injection of AAV-ChR2-virus was made through a guide cannula targeting the LA at least 2 weeks before behavioral testing (see above). Body weight and symptoms of sickness were monitored. One week before use, the mice were trained with dummy cannula removal and fiber insertion.

Optical stimulation and behavioral testing. To be tightly fixed to the guide cannula pedestal, an optical polymer fiber (200 μm of diameter, Prizmatix) was glued through an infusion cannula holder and assembled with a locking cap collar (Plastics One). The projection distance out of the guide cannula tip (1–1.5 mm) was set to allow positioning the fiber above the LA. One day before acquiring the associative fear, all the mice explored freely the Context A for 3 min and then habituated to tones. The following day, CS were delivered together with trains of blue light pulses (20 Hz, 30 s, 2 ms light pulses generated by pClamp10 software) produced by a 460 nm ultra high-power LED (UHP-460, Prizmatix) and terminated or not with US application (see Fig. 8). Then, mice were presented with CS$^+$ in another Context B (Recall), and the freezing response was analyzed.

Statistical analysis

Most data were analyzed using Student's *t* tests. However, when data were not following a normal distribution, we applied the Mann–Whitney rank-based statistical test. When studying the impact of two factors (genotype and treatment) in pharmacological rescue experiments (bicuculline), we used two-way ANOVA Student-Newman-Keuls *post hoc*

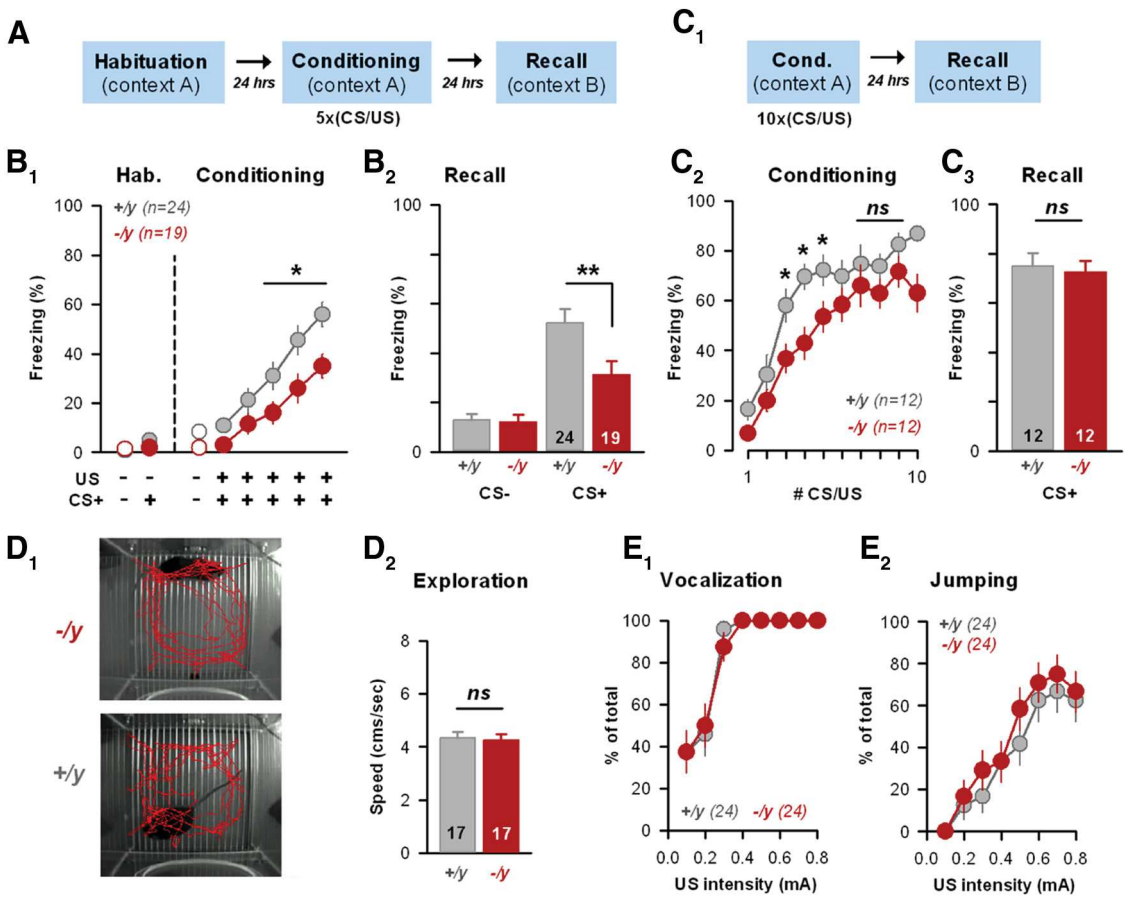

Figure 1. Deficits in cued fear learning in the absence of the ID-gene *il1rapl1*. ***A***, ***C*$_1$**, Behavioral paradigms. ***B***, ***C***, Freezing levels observed before and during CS/US pairings (***B*$_1$**,***C*$_2$**) or during the recall test (***B*$_2$**,***C*$_3$**) in *il1rapl1* WT (+/y, gray circles/bars) or KO (−/y, red circles/bars) mice submitted to normal (5 × CS/US) or reinforced (10 × CS/US) cued fear conditioning, respectively. The number of animals in each genotype is indicated. *$p < 0.05$. **$p < 0.01$. ns, Not significant. ***D***, Locomotor activity was tested in *il1rapl1* WT and KO mice during the exploration phase (first 2 min in the Context A) before CS presentations. No difference was detected between genotypes (***D*$_2$**). ***E***, Pain sensitivity was tested in WT and KO animals by scoring the vocalization (***E*$_1$**) and escaping responses (***E*$_2$**) for shocks of increasing intensities. WT and KO animals exhibited similar behavioral responses.

analysis to test for differences between groups of interest. Amplitude and frequency of spontaneous or miniature events were analyzed, and medians were directly compared as described above. Occasionally, cumulative distributions were compared using the nonparametric Kolgomorov–Smirnov test. Box plots in Figure 5 were done using SigmaPlot software (Systat Software).

Reagents

Picrotoxin was from Sigma-Aldrich, and QX-314 was from Alomone Labs. TTX was purchased from Latoxan and stock solution prepared in acetate buffer at pH 4.5. Bicuculline was purchased from Ascent Scientific.

Results

Deficits in cued fear learning in the absence of the ID-gene *il1rapl1*

Associative fear learning can easily be induced in rodents (Ledoux, 2000) and is classically monitored by measuring the degree of freezing reaction elicited upon subsequent presentations of the sole conditioning stimulus. We thus tested *il1rapl1*−/*y* and +/*y* littermates using a discriminative, associative fear learning/recall test paradigm (Fig. 1). After habituation in Context A, animals were submitted 5 times to 2 distinct tones: the CS^+ tone coupled to a foot shock (US) and an uncoupled CS^- tone (see Materials and Methods). The following day, in another context (Context B), animals were submitted to a single CS^+ presentation (Recall, Fig. 1*A*,*B*$_2$). We first noticed that *il1rapl1*−/*y* animals exhibited a significant delay in expressing the conditioned fear response to the last three CS presentations (Fig. 1*B*$_1$; $p < 0.05$). Accordingly, when tested, the recall of cued associative memory was also altered in KO mice: *il1rapl1*−/*y* mice exhibited a lower fear response than their WT littermates while hearing the first CS (*il1rapl1*+/*y*, 47 ± 5%; *Il1rapl1*−/*y*, 29 ± 5%, $p < 0.01$; Fig. 1*B*$_2$). To test for an eventual deficit in memory retention, animals were submitted to a reinforced conditioning session (10 CS/US pairings, Fig. 1*C*). Interestingly, under these strong learning conditions, *il1rapl1* KO mice did not exhibit any deficit in both the level of freezing at the last CS/US presentations ($CS/US_{7–9}$, $p > 0.05$) (Fig. 1*C*$_2$) and during the recall test (*il1rapl1*+/*y*, 75 ± 5%; *il1rapl1*−/*y*, 73 ± 5%, $p > 0.05$, Fig. 1*C*$_3$). This indicates that, once formed, cued fear memory is well retained, and also that the potency of learning is preserved in the absence of *Il1rapl1*.

To avoid confusion from potential locomotor hyperactivity, we analyzed the mean distance run by the mice during the habituation/exploration period, which did not differ between KO mice and their WT littermates (Fig. 1*D*). In addition, we challenged the mice for pain thresholds: *il1rapl1*−/*y* and +/*y* animals started vocalization (Fig. 1*E*$_1$) and escaping–jumping responses (Fig. 1*E*$_2$) for the same shock intensity, indicating that pain sensitivity was not altered in *il1rapl1* mutant animals. Together, these results suggest that information processing within the amygdala may be impacted by *il1rapl1* mutation.

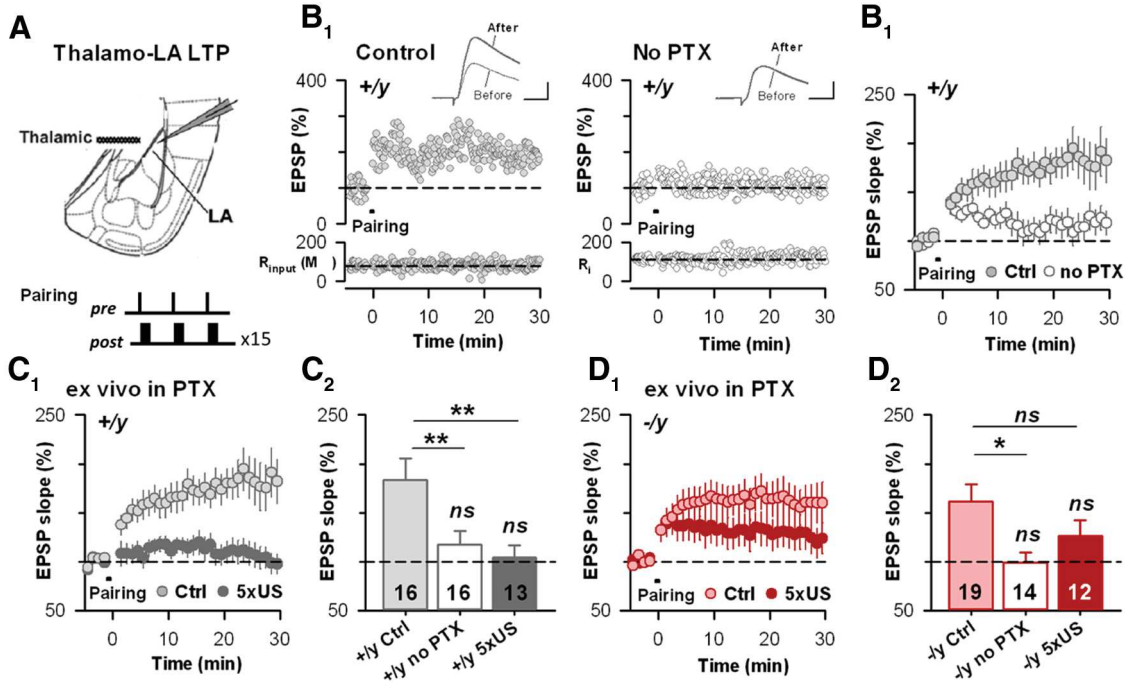

Figure 2. Constitutive *il11apl1* deletion impairs fear-learning associated LTP induction *in vivo*. ***A***, Scheme of the acute slice preparation with the positioning of recording and stimulating electrodes. The pairing protocol used to induce LTP is indicated. $\boldsymbol{B_1}$, Typical time course of EPSP slope in WT animals after associative STDP-pairing application in control and no PTX conditions. Insets, Typical EPSPs. Calibration: 4 mV, 5 ms. $\boldsymbol{B_2}$, Average time courses in both conditions in WT mice. ***C***, Fear learning mediates thalamo–LA LTP occlusion in *il1rapl1*+/*y* mice. $\boldsymbol{C_1}$, Time course of thalamo–LA EPSP slope before and after pairing in *il1rapl1*+/*y* naive (Ctrl) and conditioned (5 × US) adult mice. $\boldsymbol{C_2}$, Mean LTP in naive *il1rapl1*+/*y* in both control and no PTX conditions, and fear-conditioned *il1rapl1*+/*y* adult mice. $^{**}p < 0.01$. ***D***, Fear learning did not induce complete thalamo–LA LTP occlusion in *il1rapl1*−/*y* mice. $\boldsymbol{D_1}$, Time course of thalamo–LA EPSP slope before and after pairing in *il1rapl1*−/*y* naive (Ctrl) and conditioned (5 × US) adult mice. $\boldsymbol{D_2}$, Mean LTP in naive *il1rapl1*−/*y* in both control and no PTX conditions, and fear-conditioned *Il1rapl1*−/*y* adult mice. $^{*}p < 0.05$.

Constitutive *il1rapl1* deletion impairs fear associated LTP induction *in vivo*

Associative long-term synaptic plasticity at thalamo–LA synapses underlies the acquisition of fear conditioning (Rumpel et al., 2005; Humeau et al., 2007). Thus, the behavioral deficits observed in *il1rapl1*-deficient mice within the acquisition session must be linked to a decrease in the gating of amygdala associative synaptic plasticity. We therefore examined the induction of associative, postsynaptic LTP at thalamo–LA synapses *il1rapl1* KO and WT in acute brain slices (Fig. 2). At adult synapses, as in juveniles (Bissière et al., 2003), a robust LTP can be triggered by coincident bursts of preactivites and postactivities, but only in the presence of the GABAA-R antagonist PTX (100 μM) (Fig. 2*B*). Interestingly, when tested in these standard conditions, both *il1rapl1* WT and KO animals exhibited similar levels of LTP (*il1rapl1*+/*y*, 183 ± 23%; *il1rapl1*−/*y*, 161 ± 18%, $p > 0.05$; Fig. 2*C*,*D*), indicating that *il1rapl1* deletion did not alter the capability of thalamo–LA synapses to produce postsynaptic LTP.

Noteworthy, these experiments were conducted in the absence of ionotropic GABAergic transmission, therefore bypassing an eventual GABAergic modulation. Thus, to examine the occurrence of genuine thalamo–LA LTP *in vivo* during associative fear learning, we tested LTP levels in slices from fear-conditioned KO and WT animals. Indeed, it was previously reported that fear conditioning led to occlusion of thalamo–LA LTP in brain slices (Hong et al., 2011). *il1rapl1*−/*y* and +/*y* animals were first submitted to the associative fear conditioning described above (5 CS/US), and brain slices were prepared 24 h after the last CS/US presentation. Compatible with an effect of fear conditioning in both genotypes, LTP levels in conditioned animals were nonsignificant ($p > 0.05$ compared with baseline; Fig. 2*C*,*D*). However, while in conditioned WT mice, a pronounced occlusion of LTP was observed (*il1rapl1*+/*y* LTP_{naive}, 183 ± 23%; $LTP_{5CS/US}$, 104 ± 12%, $p < 0.01$) (Fig. 2*C*), LTPs obtained in naive and conditioned *il1rapl1* KO slices were not significantly different (*il1rapl1*−/*y* LTP_{naive}, 161 ± 18%; $LTP_{5CS/US}$, 126 ± 16%, $p > 0.05$). This indicates that fear-induced LTP occlusion is only partial in *il1rapl1* KO mice, probably because of a lower LTP induction *in vivo* during fear acquisition. We propose that this impairment of LTP induction could, at least partially, contribute for both the delay in fear acquisition and the deficit in the recall of cued fear memory observed in *il1rapl1*-deficient animals.

Increased I/E balance in LA principal cells is associated with *il1rapl1* mutation

Gating of AMPAR-mediated, NMDAR-dependent postsynaptic LTP requires the relief of the magnesium block of NMDA receptors through the firing of postsynaptic cells. Previous studies demonstrated the crucial role of local GABAergic interneurons in controlling the postsynaptic discharge (Pouille and Scanziani, 2001; Gabernet et al., 2005), thereby limiting the gating of synaptic plasticity through postsynaptic hyperpolarization (Bissière et al., 2003). Thus, we examined feedforward inhibition (FFI) in the LA of *il1rapl1* KO and WT mice after activation of major excitatory inputs (Fig. 3). To achieve that, LA principal cells were recorded at two different membrane potentials, −70 and 0 mV in physiological chloride, while stimulating thalamic excitatory fibers (Humeau et al., 2005; Gambino et al., 2010) (Fig. 3*A*). Through this electrophysiological manipulation of the membrane potential, we could isolate AMPAR-mediated excitation (EPSCs, at −70 mV) and GABAA-R-mediated inhibition (IPSCs, at 0 mV) based on their different reversal potential (Fig. 3A_2).

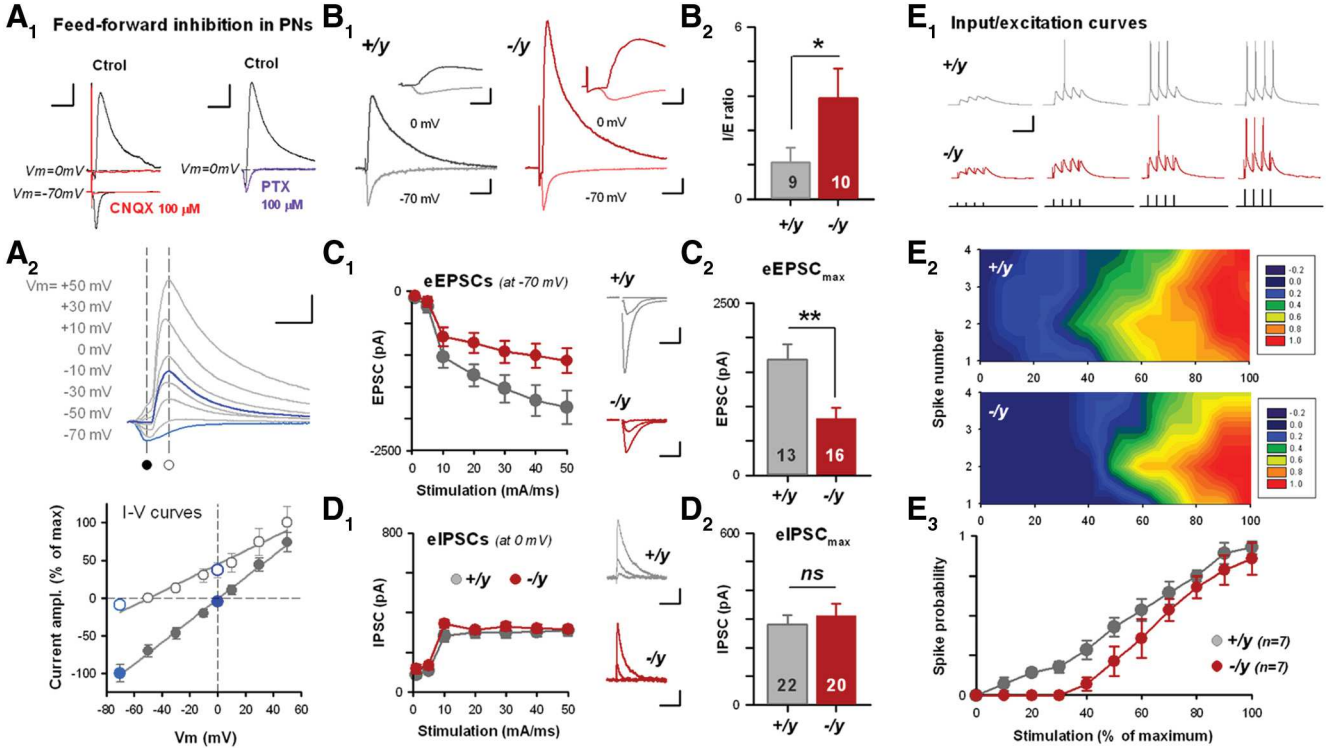

Figure 3. Increased I/E balance and lack of activation in LA principal cells are associated with *il1rapl1* mutation. ***A***, FFI measurements in LA principal cells. ***A*$_1$**, Pharmacological controls demonstrating that FFI is induced after thalamic fiber stimulations. ***A*$_2$**, AMPAR and GABAA-R-mediated PSCs can be isolated by their differential reversal potential. ***B***, FFI is increased in il1rapl1 KO mice (red traces). ***B*$_1$**, Typical FFI recordings using similar EPSC values. Calibration: top, 150 pA, 5 ms; bottom, 50 pA, 20 ms. ***B*$_2$**, Mean I/E ratio obtained at thalamo–LA synapses in +/*y* and −/*y* preparations. $*p < 0.05$. The number of recorded cells is indicated. ***C***, Evoked excitatory transmission at thalamo–LA synapses is affected by *il1rapl1* mutation. ***C*$_1$**, Left, average I/O curves. Right, Typical EPSCs recorded for 0.1, 1, and 10 mA stimulations in +/*y* and −/*y* preparations. Number of recorded cells is indicated. Calibration: 200 pA, 30 ms. ***C*$_2$**, Mean EPSC amplitude for 10 mA stimulations. $**p < 0.01$. ***D***, Same presentation as in ***C*** but describing thalamic-evoked IPSCs. Calibration: 100 pA, 60 ms. *ns*, Not significant. ***E***, Activation of LA principal cells by incoming thalamic excitation is decreased in *il1rapl1*-deficient mice. ***E*$_1$**, Typical recordings of LA-PNs V_m upon thalamic fiber stimulations of increasing intensity in +/y and −/y preparations. Calibration: 20 mV, 40 ms. ***E*$_2$**, Probability map of spike occurrence at each stimulation time point (1, 2, 3, or 4) and for each stimulation intensity (0–100%). Seven and seven cells were recorded in each genotype. ***E*$_3$**, Spike probability curve showing that LA cells are less efficiently activated by thalamic input in *il1rapl1*-deficient mice.

Accordingly, inward currents recorded at −70 mV were completely blocked by the AMPAR antagonist CNQX (100 μM; Fig. 3*A*$_1$, left), whereas the outward current recorded at 0 mV was sensitive to the GABAA-R antagonist picrotoxin (100 μM; Fig. 3*A*$_1$, right). Moreover, this last component was also sensitive to AMPAR blockade (Fig. 3*A*$_1$, left, at 0 mV), indicating the recruitment of local interneurons as a feedforward circuit (FFI). Importantly, I/V curves recorded in WT and KO preparations were similar and could be greatly approximated by a linear fit, indicating their correct measurements (data not shown).

To directly compare FFI in WT and KO preparations, we first elicited thalamo–LA EPSCs of comparable size in LA principal cells (at −70 mV, 130–60 pA, $p > 0.05$ between both groups) and compared the amplitude of the outward inhibitory current recorded at 0 mV (Fig. 3*B*). Strikingly, IPSCs were found to be significantly higher in KO preparations (Fig. 3*B*$_1$), and the I/E ratio was exacerbated in *il1rapl1* mutant mice (Fig. 3*B*$_2$). Theoretically, the increase of I/E balance (calculated here as a ratio) in *il1rapl1* KOs could result from an increase in inhibitory, or a decrease in the excitatory, transmission onto LA principal cells. To refine our observation, we compared eEPSC and eIPSC amplitudes for increasing stimulation intensities (Fig. 3*C*,*D*). As shown in Figure 3*C*, input/output (I/O) relationships of thalamo–LA eEPSCs were clearly impacted by *il1rapl1* mutation ($eEPSC_{max}$, $p < 0.01$). Thus, recurrent to some observations in pyramidal cells in hippocampus (Pavlowsky et al., 2010), the absence of Il1rapl1 led to a reduction of glutamatergic transmission in pyramidal cells. In stark contrast, inhibitory I/O curve was not modified by the mutation (Fig. 3*D*), indicating that the observed change in the I/E ratios (Fig. 3*B*) can be mostly attributed to a decrease in the excitatory component.

To assess for the functional consequences of these synaptic defects on amygdala output, we tested the ability of thalamic inputs to elicit spike discharges in LA principal neurons (Fig. 3*E*). Bursts of 4 presynaptic stimulations (at 20 Hz) were applied at various intensities and eventual postsynaptic spikes counted. Noteworthy, in KO preparations, the first generated spikes occur for greater stimulation intensities than in WT preparations (Fig. 3*E*), suggesting that *il1rapl1* mutation lowers LA-PN activation by incoming thalamic synaptic inputs.

Impact of *il1rapl1* deletion onto excitatory synaptic inputs to LA interneurons

Local interneurons of the LA account for ~20% of cell bodies (McDonald, 1982), tightly regulating principal cell excitability by providing strong feedforward inhibition (Szinyei et al., 2000; Chu et al., 2012). Moreover, accumulating evidence points for a role of GABAergic transmission in regulating fear conditioning (Ehrlich et al., 2009). To answer whether *il1rapl1* mutation had a specific impact on excitatory level reaching interneurons, we crossed *il1rapl1* mutant mice with GAD67-eGFP transgenic mice (Tamamaki et al., 2003), making it easy to visualize interneurons with fluorescence (Fig. 4*A*$_1$). Interneurons, although highly variable in their electrophysiological parameters and expression of specific

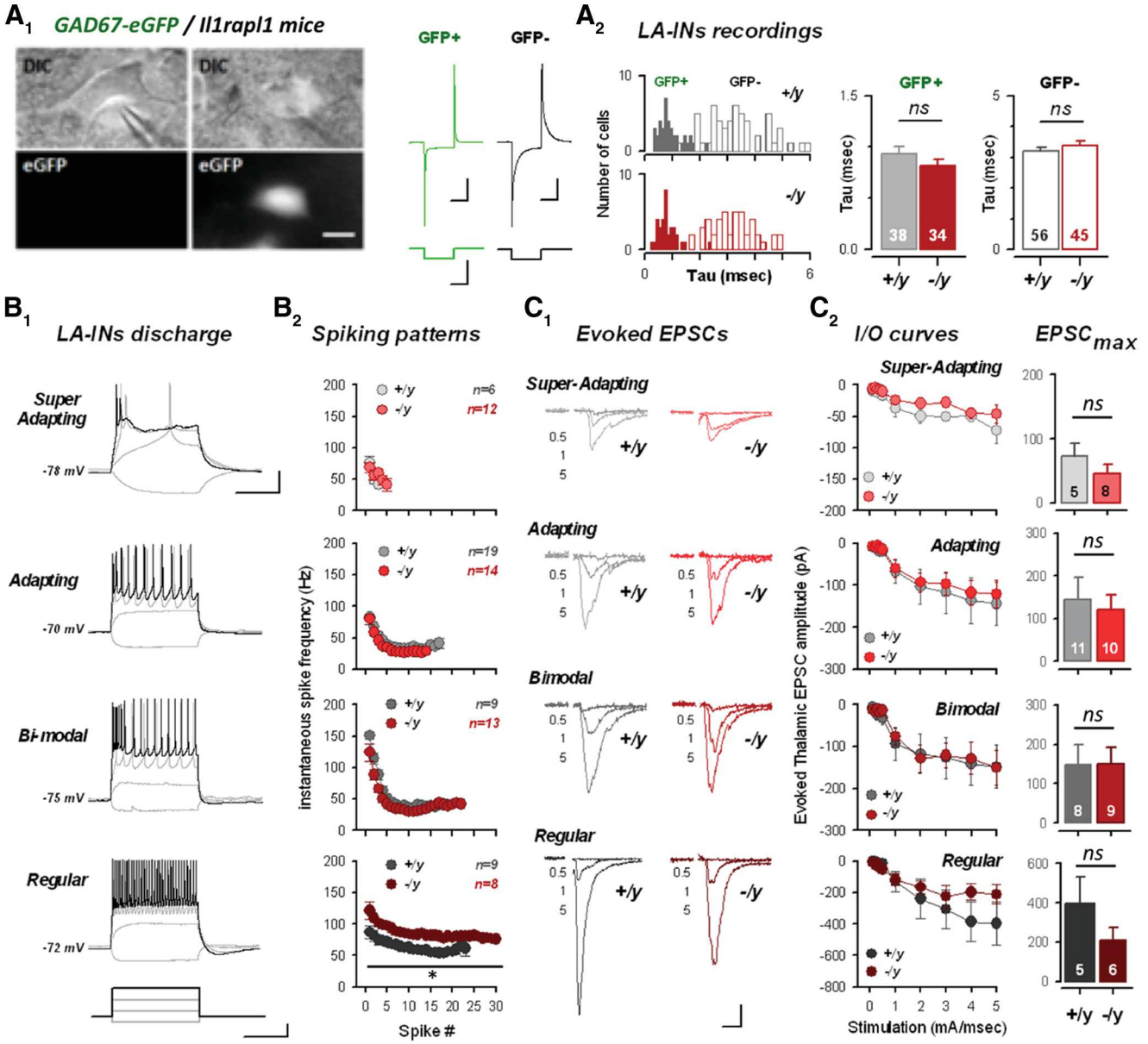

Figure 4. Excitatory transmission onto amygdala interneurons is preserved in *il1rapl1*-deficient mice. ***A***, Amygdalar GABAergic neurons were directly visualized and recorded by GFP fluorescence after crossing *il1rapl1* mutant mice with GAD67-eGFP mice (see Materials and Methods). ***A*$_1$**, Principal cells can be separated from interneurons by looking at cellular capacitance during the seal test. ***A*$_2$**, Density and capacitance of GABA-ergic (GFP $^+$) and principal (GFP $^-$) cells in Il1rapl1 WT and KO preparations. Number of recorded cells is indicated. ***B***, Spiking patterns of LA interneurons. ***B*$_1$**, LA interneurons were classified in four subclasses based on spiking behavior (for a detailed description of interneuron classification, see Materials and Methods). ***B*$_2$**, Mean spiking frequency against spike number for each subclass of interneuron. ***C***, Excitatory evoked transmission of LA interneurons after thalamic stimulation. ***C*$_1$**, Mean EPSC amplitude for 0.5, 1, and 5 mA stimulations in WT and KO interneurons. Calibration: 100 pA, 20 ms. ***C*$_2$**, Left, I/O curves of LA interneurons for a 5 mA stimulation in WT and KO interneurons. Right, Mean EPSC amplitude at 5 mA stimulation intensity for all LA interneurons. Number of recorded cells is indicated.

biological markers (Spampanato et al., 2011), could be distinguished from principal cells by cellular capacitance. Indeed, measurement of the exponential τ of the cellular response to a -10 mV voltage jump revealed a clear segregation with principal cells, a parameter that was not itself modified by *Il1rapl1* mutation for both cell populations (Fig. 4A_2). Interneurons were classified in different subclasses based on a previous study looking at diverse electrophysiological parameters of LA interneurons (Sosulina et al., 2010). Indeed, mRNA expression of different calcium binding proteins and neuropeptides was not very conclusive to further classify these populations (Sosulina et al., 2006). Thus, interneurons were assigned to a specific population looking solely at electrophysiological parameters (see Materials and Methods). To that end, we performed whole-cell patch-clamp recordings in current-clamp mode from GFP-expressing LA cells in *il1rapl1* KO and WT mice (Fig. 4*B*,*C*). Combined analysis of spiking pattern and other electrophysiological parameters allowed us to separate interneurons into four classes (Fig. 4B_1). Superadapting neurons showed a few spikes in the beginning of the depolarizing pulse before exhibiting spike failure/adaptation. Adapting neurons were characterized by a strong adaptation of spiking pattern during the depolarizing current step. Bimodal neurons, on the other hand, started spiking in a burst-fashion manner before adapting their firing pattern. Finally, regular spiking neurons were characterized by very low spike adaptation (Fig. 4B_1). Apart from superadapting neurons, all our subclasses share common

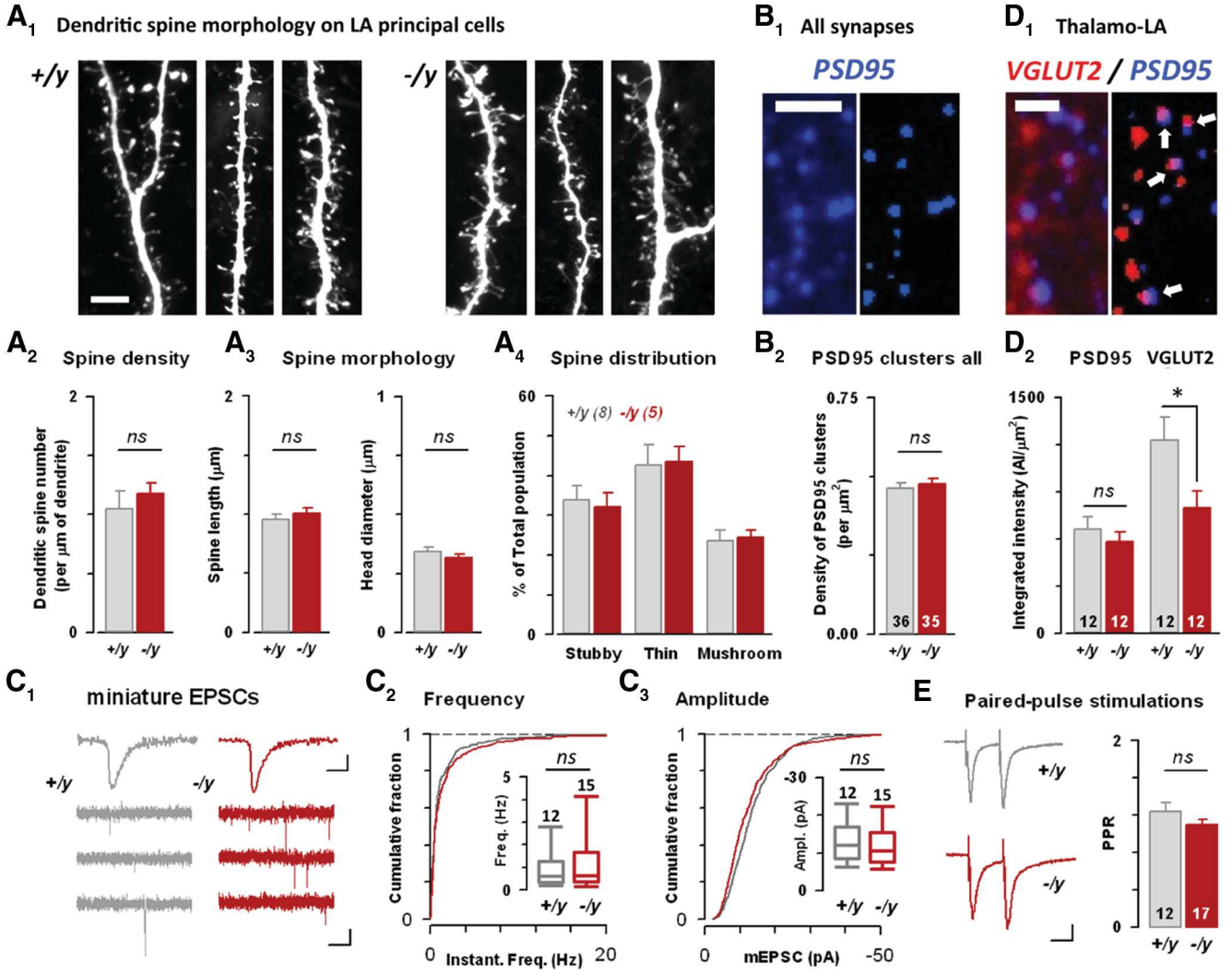

Figure 5. Morphology of LA excitatory synapses in constitutive *il1rapl1* mutant mice. ***A***, Morphology of LA principal cell dendrites is preserved in *il1rapl1*-deficient mice. A_1, Portions of neurobiotin-filled LA principal cell dendrites were analyzed and compared between genotypes. A_{2-4}, Analysis of spine density, morphology, and distribution of different spine types. ***B***, Morphological examination of LA synaptic contacts. B_1, Typical immunolabeling against PSD95. B_2, Density of PSD95 clusters for both genotypes. ***C***, Miniature EPSC recordings on LA principal cells for both genotypes. C_1, Representative trace of mEPSC recordings in both genotypes. C_{2-3}, Cumulative distribution of mEPSC frequency and amplitude for both genotypes. Insets, Medians of frequency and amplitude, respectively. ***D***, Putative synapses were identified as closely apposed VGLUT2/PSD95 clusters (see Materials and Methods). Scale bars, 2 μm. D_1, Typical immunolabeling showing apposed PSD95/VGLUT2 clusters. D_2, Integrated intensity of PSD95 and VGLUT2 in apposed clusters for both genotypes. *$p < 0.05$. ***E***, Paired pulse recordings for both genotypes. PPR was calculated as the ratio of the second response to the first one.

electrophysiological parameters with previously defined subtypes of LA interneurons (Sosulina et al., 2010). In both genotypes, plotting spiking frequency against spike number showed clear differences in the spiking behavior of these different populations (Fig. 4B_2); no differences were observed between genotypes, except for regular spiking neurons, which display a higher frequency in KO animals ($p < 0.05$). Next, we assessed excitatory signals reaching those categories by constructing I/O curves after thalamic stimulation (Fig. 4*C*). In stark contrast with the situation found in LA principal cells, none of the interneuron groups displayed significantly different I/O curves between WT and KO preparations (Fig. 4*C*). Noteworthy, superadapting and regular-spiking neurons exhibited a tendency to a decrease of thalamic EPSCs, which remained nonsignificant ($p = 0.093$ and $p = 0.217$, respectively). We raise two major conclusions from these genetically driven recordings: (1) the lack of impact of *il1rapl1* mutation onto excitatory transmission in LA interneurons may largely contribute to the increase of FFI described above (Fig. 3); and (2) Il1rapl1 may play a functional role in the postsynaptic compartment, as LA recordings involving the same presynaptic but different postsynaptic compartments exhibited or not a functional impact of the mutation (see also Discussion).

Morphological and functional characterization of excitatory synaptic inputs to LA principal neurons in *il1rapl1* WT and KO mice

We next performed morphological analysis of dendritic spines from LA principal cells to determine whether Il1rapl1 plays a role in synapse formation and/or maturation in the amygdala (Fig. 5). We filled LA principal cells with neurobiotin during whole-cell patch-clamp recordings and thoroughly analyzed dendritic spine density and morphology after fixation (see Materials and Methods) (Fig. 5*A*). Using this method, we could not find any differences between genotypes (Fig. 5*A*), which was in good line with two other observations. First, global analysis of PSD95 cluster density using immunocytochemistry did not allow separating

WT and KO preparations (Fig. 5*B*). Furthermore, no impact of the mutation on mEPSC frequency or amplitude recorded in LA principal cells could be detected (Fig. 5*C*), thus suggesting that the amygdala neuropile was not strongly affected by the removal of Il1rapl1.

Then, taking benefit of differential VGLUT1/VGLUT2 expression in amygdala-projecting brain structures (Fremeau et al., 2001), we specifically examined the morphology of thalamo–LA (expressing VGLUT2) synapses by analyzing the intensity of apposed VGLUT2/PSD95 clusters (Fig. 5*D*) (see Materials and Methods). Strikingly, in PSD95/VGLUT2 appositions, the VGLUT2 levels were significantly lower in *il1rapl1* KO mice (−35% of integrated intensity; Fig. 5D_2, bottom, $p < 0.05$), whereas PSD95 clusters were unaffected (Fig. 5D_2). As these results point to an impact of the mutation at the presynaptic level, we compared paired pulse recordings at thalamo–LA synapses but failed to detect changes in presynaptic release probability (Fig. 5*E*). Thus, our data suggest that Il1rapl1 controls both functional and morphological parameters at thalamo–LA excitatory synapses.

Ubiquitous distribution of *il1rapl1* mRNA in neuronal populations of amygdala

To get some insights on the rationale to *il1rapl1* −/y induced I/E imbalance, we then set out to examine the distribution of *il1rapl1* mRNA in the brain. Previous work raised some evidence for *il1rapl1* expression in olfactory bulb, hippocampus, and cortex (Carrié et al., 1999). However, no robust and detailed demonstration of *il1rapl1* expression pattern has yet been published. We thus performed *in situ* hybridization of *il1rapl1*, together with *vglut1* and *gad67*, to allow for the comparison of its relative expression in inhibitory and excitatory brain regions. Indeed, *vglut1* labels the major glutamatergic population of cells in the cortical forebrain regions (Fig. 6*A*,*C*), whereas *gad67* labels all GABAergic neurons in the brain (Fig. 6*A*,*B*). Slides were first exposed to phosphor imager screen (Fig. 6*A*), and then the cellular resolution was obtained through dipping into photographic emulsion combined with toluidine blue counter staining (see Materials and Methods). *il1rapl1* was probed using 7 oligonucleotides spread over the different exons of the gene. All probes provided the same profile of expression. As expected, probe number 6 (data not shown) and 7 raised within the deleted exon 5 provided no signal when incubated over *il1rapl1* −/*y* slices (Fig. 6*A*). Overall, *il1rapl1* expression was very low compared with that of *vglut1* or *gad67*. Higher expression levels were recurrently seen in olfactory bulbs (data not shown) and in dentate gyrus of the hippocampus (Fig. 6*A*). In the amygdaloid complex, expression spans all excitatory (basolateral amygdala) and inhibitory (intercalated cells and central amygdala) regions homogeneously. Regional observations were confirmed by the investigations on slides at the cellular levels (for better visualization, silver dots were converted to red in Fig. 6*B–D*). Although GABAergic and glutamatergic territories are well delineated in Figure 6*B*, *C*, *il1rapl1* specific pattern appeared homogeneously distributed ruling out the possibility for a selective lack of expression in one or the other subclass of neurons (see quantifications in Fig. 6*B–D*). However, a specific lack of expression in a subclass of interneurons cannot be ruled out.

Cued fear learning is rescued by preconditioning infusion of GABAA-R blockers in the LA of *il1rapl1*-deficient mice

Yet, a scenario emerges in which *il1rapl1* KO mice's impairment in associative learning is the result of exacerbated I/E balance in the LA during CS/US association. *Ex vivo* experiments suggest that this could in turn lead to lower LTP induction in *il1rapl1* KO animals. The next series of experiments aimed at normalizing behavior in KO mice by restoring I/E balance before learning. In this line, previous studies used local or systemic treatment increasing GABAergic transmission to interfere with the acquisition or expression of the conditioned fear response (Sanger and Joly, 1985).

We thus depressed intra-LA GABAA-R-mediated inhibition during the CS/US association (Fig. 7) by infusing the specific antagonist bicuculline into the LA of *il1rapl1*−/*y* and +/*y* littermates before conditioning (Fig. 7). To that end, mice were chronically implanted above the LA (guide cannula positions in Fig. 7*B*), and local infusion of bicuculline was performed bilaterally 30–60 min before the fear conditioning session (see Materials and Methods). Importantly, first attempts using doses previously used in rats (50 ng/200 nl per side) were readily leading to epileptic seizures immediately after infusion (Berlau and McGaugh, 2006). We thus lowered the dose to 20 ng/200 nl and retained only the animals in which the guide cannula tips were immediately above the LA to avoid unspecific effects (Fig. 7*B*). With these safeguards, no obvious seizures were observed during the drug treatment, although we noticed a slight effect of drug treatment on animal locomotor activity (ANOVA, $F_{(1,53)} = 8{,}115$; $p = 0.006$) (Fig. 7*C*). However, there was no difference in general locomotion between WT and KO-treated animals (SNK *post hoc*, $p = 0.706$), thus allowing comparing the behavioral consequences of the treatment in both genotypes. We then compared the freezing levels obtained during and 24 h after the fear conditioning session and compared with nonimplanted mice (Fig. 7*D*,*E*). Although we present the whole acquisition curve, bicuculline treatment did not reach significance until the fifth CS presentation, and comparisons between groups were done at this time point. Two-way ANOVA revealed an interaction effect between genotype and treatment (ANOVA, $F_{(1,57)} = 5{,}043$; $p = 0.029$). In control animals, as shown before, the fear response exhibited by KO mice at the fifth CS/US presentation during the conditioning session was lower than their WT littermates (SNK *post hoc*, $p = 0.011$) (Figs. 1*A*, 7*D*). Strikingly, in bicuculline-treated animals, freezing levels at the fifth CS/US presentation were found indistinguishable between genotypes (SNK *post hoc*, $p = 0.399$), and a significant effect of the treatment was found in KO (SNK *post hoc*, $p = 0.002$) but not WT animals (SNK *post hoc*, $p = 0.850$). When looking at freezing levels during recall, we noticed a significant interaction between genotype and drug treatment (ANOVA, $F_{(1,57)} = 4{,}820$; $p = 0.032$), leading to a normalization of the freezing deficit (control, SNK *post hoc*, $p = 0.008$; treated, SNK *post hoc*, $p = 0.479$; Fig. 7*E*). Normalization of acquisition only became significant at the fifth CS presentation, probably because of incomplete blockade of inhibitory system or a lack of excitation by incoming inputs at initial CS/US associations. However, together, these observations convincingly show a normalization of cued fear acquisition and recall after *in vivo* pharmacological manipulations of the LA ionotropic GABAergic system at the time of CS/US association.

Accordingly, bicuculline treatment in conditioned *il1rapl1* −/*y* mice also restored thalamo–LA LTP occlusion (*il1rapl1*−/*y*: LTP_{naive}, 161 ± 18%, $LTP_{5CS/US+bicu}$, 88 ± 8%, $p < 0.05$; Fig. 7*F*). These results indicate that restoring I/E balance before learning may suffice to allow LTP induction *in vivo* in *il1rapl1* KO animals. We thus propose the existence of a causal link between the deficit in associative learning, the failure of LTP induction, and I/E imbalance within the lateral amygdala.

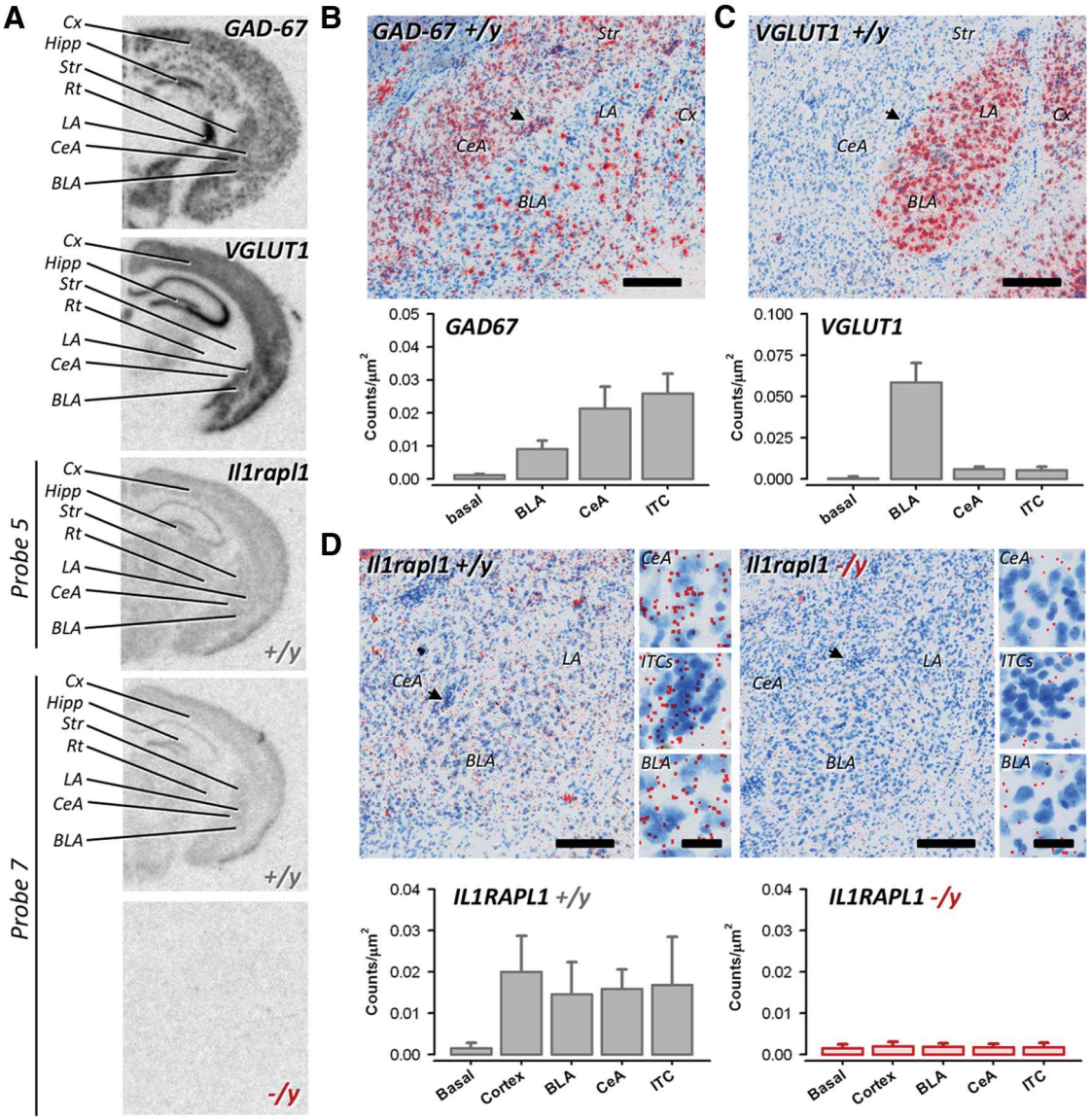

Figure 6. Ubiquitous distribution of *il1rapl1* mRNA in amygdala neurons. ***A***, Regional distribution of *gad67*, *vglut1*, and *il1rapl1*. *il1rapl1* was probed with 7 oligonucleotides; here probe 5 and 7 are shown. Probe 7 is specific of the exon 5, deleted in the knockout model. There is absence of signal when probe 7 is incubated on −/*y* slices. ***B–D***, Emulsion dipping of slices from ***A***. Silver dots were systematically masked and converted to red for display purpose. ***B***, Cellular distribution of *gad67* mRNA in the amygdala. There is dense labeling in the central nucleus, whereas sparse interneurons are depicted in the basolateral divisions. ***C***, Cellular distribution of *vglut1* mRNA in the amygdala. There is dense labeling of neurons in the basolateral division, whereas the central nucleus is devoid of labeling. ***D***, Cellular distribution of *il1rapl1* mRNA in the amygdala. Lower expression levels are detected compared with *gad67* and *vglut1*, but −/y slices display much lower background signals (right panels). *il1rapl1* expression covers all divisions of amygdala. Arrows point to ITCs. Scale bars: 250 μm; insets, 30 μm. Cx, Cortex; hipp, hippocampus; Str, striatum; Rt, reticular nucleus of the thalamus; LA, lateral amygdala; CeA, central amygdala; BLA, basolateral amygdala; ITC, intercalated cells.

Direct optical activation of LA cells during acquisition of associative cued fear normalizes fear learning in *il1rapl1*-deficient mice

During associative fear learning, US is thought to act as a detonator inducing depolarization and firing of LA principal cells, instructing plasticity at synapses conveying the CS onto the same cells (Rosenkranz and Grace, 2002; Maren, 2005). This phenomenon was spectacularly demonstrated recently by Johansen et al. (2010): by pairing auditory CS with optical activation of LA principal cells, they showed that direct activation of LA principal cells was sufficient to drive cued associative fear conditioning. We implemented a similar strategy to bypass an eventual fading of the US "detonation" in *il1rapl1*-deficient mice (Fig. 8). To this aim, LA cells were transfected with AAV2/9.CAG.ChR2-Venus.W.SV40-p1468 (U-Penn vector core) introduced through chronically implanted cannula, which also permitted the delivery of timely controlled light pulses within the LA via an optical fiber (see Materials and Methods) (Fig. 8*B–G*).

First, to control for the efficacy of the opsin strategy, we tested the light activation of LA principal neurons *in vitro* (Fig. 8*A*). In all transfected neurons, we observed that continuous 1 s, 460 nm light-applications were leading to continuous AP discharge (Fig. 8*A*). We also tested the capability of transfected neurons to respond to repeated short (2 ms long) flashes of 460 nm light, a condition previously used *in vivo* in the amygdala (Johansen et al., 2010). By varying flash frequencies, we observed that most ChR2-expressing neurons were able to strictly follow flashes up to 20 Hz before exhibiting discharge failures (Fig. 8*A*). Thus, 20 Hz trains were retained for *in vivo* experiments.

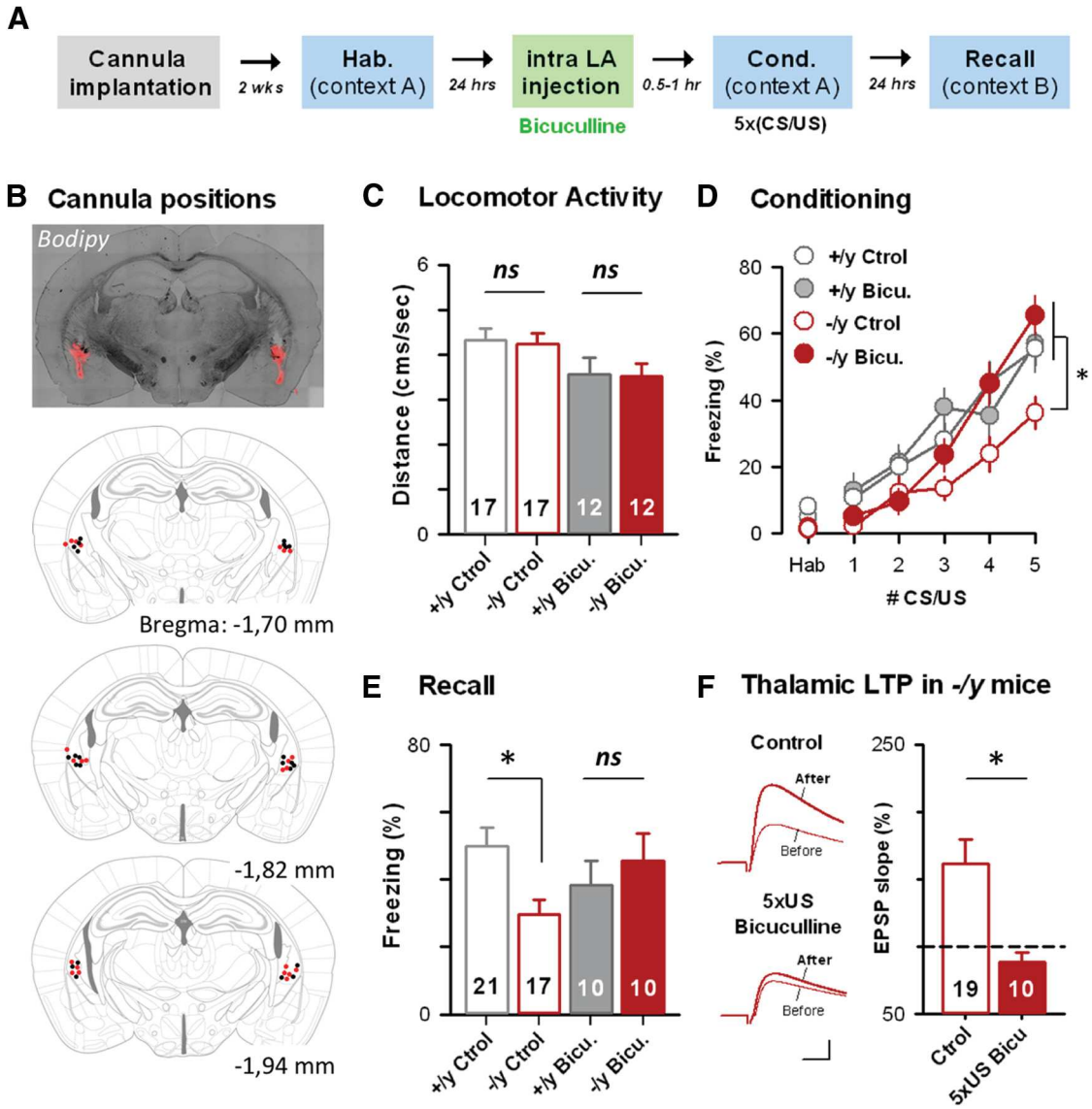

Figure 7. Cued fear learning deficit is restored by preconditioning infusion of the GABAA-R blocker bicuculline in the lateral amygdala. ***A***, Experimental paradigm. ***B***, Mice were bilaterally implanted above the LA to allow drug application in awake animals just before the fear conditioning. Top, Bodipy (500 nl each side) diffusion allowing assessment of drug diffusion in the amygdala region. Bottom, Cannula positions for all +/*y* (black dots) and −/*y* (red dots) animals considered for statistics. ***C***, Locomotor activity in control and bicuculline-injected animals was measured by tracking of animal movement before the acquisition phase (2 first minutes in Context A). ***D***, ***E***, Freezing levels exhibited by bicuculline injected *il1rapl1* +/*y* and −/*y* animals were measured during conditioning (***D***) and recall (***E***) and compared with nontreated, control KO, and WT mice. *ns*, Not significant. *$p < 0.05$. Number of animals is indicated. ***F***, Fear learning induced complete thalamo–LA LTP occlusion in bicuculline-treated *il1rapl1* −/*y* mice. Left, Typical EPSPs recorded before and after pairing in naive and conditioned control (Ctrl) and bicuculline-treated (5 × US bicu) KO mice. Calibration: 4 mV, 5 ms. Right, Mean LTP in *il1rapl1* −/*y* naive (Ctrl) and conditioned (5 × US Bicu) bicuculline-treated adult mice. Number of recorded cells is indicated.

Then, a first cohort of 7 ChR2-transduced mice of each genotype was exposed to an associative fear learning (CS/US) + light delivery procedure (Fig. 8*B–D*). During conditioning sessions, light applications (unilateral, 460 nm, 2 ms flashes at 20 Hz during 30 s, 6–8 mW output light power) were repeatedly applied together with CS^+/US presentations (Fig. 8*B*, *C*). Importantly, our *in vivo* light stimulations were proven to be efficient in activating LA neurons as the expression of the activity-reporter C-fos was specifically increased at the illuminated side (data not shown). We then score the freezing levels exhibited by WT and KO mice during CS^+ presentations within the conditioning phase (Fig. 8*C*). Strikingly, both KO and WT cohorts then exhibited very similar freezing levels, comparable with the one observed in WT animals submitted to CS/US pairings (Fig. 1). Interestingly, at the recall test, WT and KO mice did exhibit a high level of freezing reaction at the CS^+ presentation (WT light, 44 ± 13%; KO light, 54 ± 11%), indicating that the improvement of fear memory was maintained (Fig. 8*D*). However, KO mice also displayed a high degree of generalization (KO light CS^-, 55 ± 11%), suggesting that CS/US/Light protocol might have abnormally activated the amygdala, leading to a CS^-/US association. Importantly, we controlled that the light-application effect was depending on the presence of the US (Fig. 8*E–G*). Indeed, it has been previously shown that repeated Light/CS presentation could lead to the generation of an associative conditioned response to the CS (Johansen et al., 2010). Thus, in another implanted cohort of 8 +/*y* and 8 −/*y* animals, we could show that the application of 5 CS^+/Light was not able to induce robust conditioned fear response (Fig. 8*E–G*).

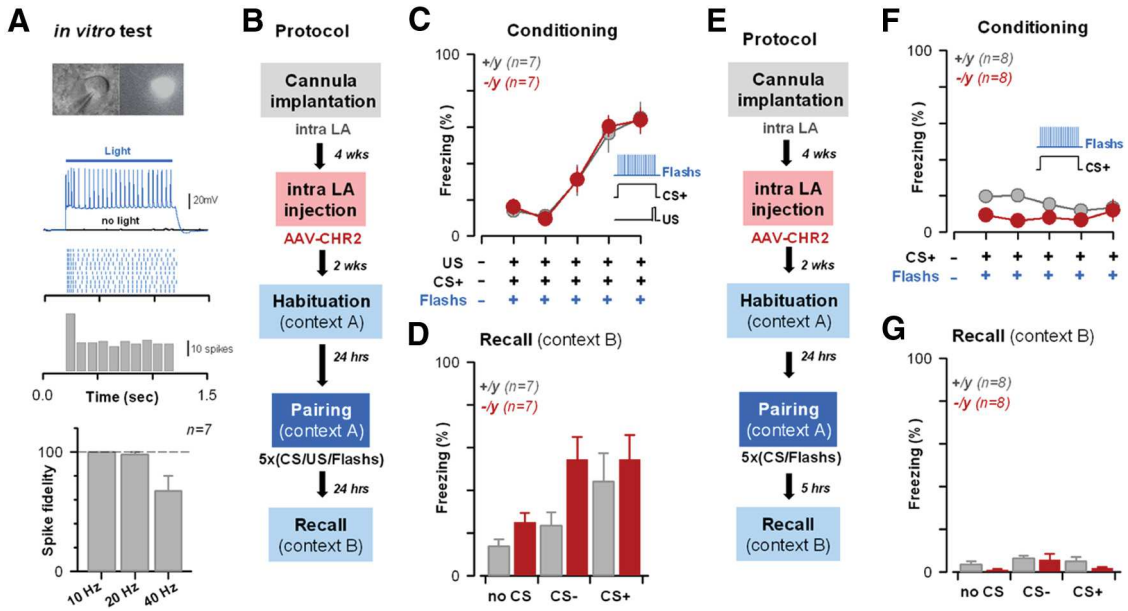

Figure 8. Direct optical activation of LA cells induces comparable associative cued fear learning in normal and *il1rapl1*-deficient mice. ***A***, Light activation of LA neuronal cells using opsin-based strategy. Top, Light flashes (1-s-long, 460 nm) induced continuous spiking discharge in AAV-ChR2-transfected LA cells. Bottom, Short flashes (5 ms) were applied at different frequencies, and discharge fidelity was measured. No failure in LA principal cell spiking was observed up to 20 Hz. ***B***, Experimental paradigm used for opsin-based conditioning protocol. It includes chronic cannula implantation, LA infection with AAV-ChR2 constructs, and 460 nm blue light/CS/US paired applications (see Materials and Methods). ***C***, ***D***, Freezing levels observed during the conditioning (***C***) and the recall (***D***) sessions in CS/US/light conditioned WT and KO mice. ***E–G***, Same presentation as in ***B–D***, but for CS/light pairings.

Collectively, pharmacological (Fig. 7) and opsin-based strategies (Fig. 8) led us to conclude that, once bypassing the requirement of postsynaptic depolarization in LA principal cells, *il1rapl1*-deficient and their WT littermates exhibited comparable amygdala-related learning capabilities. LA-targeted *in vivo* strategies correcting or bypassing the I/E imbalance at the time of CS/US associations seem successful in normalizing cued fear learning in *il1rapl1* mutant mice, pointing to the crucial role of this structure in generating the observed deficit.

Discussion

Using a combined approach at behavioral, cellular, and synaptic levels, we provide a thorough characterization of the consequences of *il1rapl1* deletion on cued fear related amygdala neuronal networks. Several lines of evidence indicate that the mutation impacts specifically excitatory synapses onto glutamatergic cells, leaving connections to GABAergic cells intact. The working model, strengthened here by *in vivo* approaches, proposes that local I/E imbalances in amygdala neuronal circuits led to deficits in the acquisition of cued fear memory by lowering LA PN activation, thereby decreasing associative LTP induction. Thus, discrete behavioral deficits may arise from the heterogeneous vulnerability of excitatory synapses to ID gene deficiency.

I/E imbalance and behavioral consequences after *il1rapl1* deletion

We propose here that *il1rapl1* deficiency leads to an I/E imbalance in the LA, perturbing cued fear memory formation, but not cued fear memory expression. Indeed, LA-dedicated experiments aiming at depressing or bypassing the LA-GABAergic system immediately before the CS/US association (i.e., at the exact timing of associative synaptic plasticity induction) were efficiently normalizing for the cued fear deficit during the recall tests (Figs. 7 and 8), long after that correcting treatments were passed. This indicates that, once properly acquired, cued fear memory expression is not impaired in *il1rapl1*-deficient mice. Thus, we propose that, after *il1rapl1* mutation, I/E imbalance in LA impairs cued fear memory formation by preventing associative LTP gating at major excitatory entries conveying CS and US modalities (Ehrlich et al., 2009). In addition, our data suggest that LA I/E balance may not be of crucial importance in the reactivation of LA neurons participating to the cued fear memory trace stored in the LA (Han et al., 2009). In this line, former *in vivo* observations pointed to a depression of the amygdala GABAergic system after cued fear conditioning (Chhatwal et al., 2005). However, because some modalities of the conditioned fear (i.e., $CS^+/CS-$ discrimination during recall; Fig. 8) and the kinetic of freezing behavior during acquisition (Fig. 7) are not entirely corrected by our *in vivo* treatments, we cannot exclude that additional mechanisms upstream or downstream to LA integration contribute to the observed cued fear learning phenotype.

The possible impairment of LTP induction in *il1rapl1* KO mice is reminiscent of previous observations made on hippocampal memory formation in a Down syndrome mouse model (Kleschevnikov et al., 2004) and more generally in line with an increasing number of reports linking ID/ASD mutations with discrete I/E imbalance in specific networks (Chao et al., 2010; Baroncelli et al., 2011; Pizzarelli and Cherubini, 2011; Yizhar et al., 2011). For Il1rapl1-dependent mechanisms, our view is that associative memory formation may be mainly impaired in the brain areas in which (1) the presence of Il1rapl1 in association with specific molecular partners is crucial for the maintenance/consolidation/function of excitatory synapses onto principal cells (see below), and (2) in which induction of associative LTP is strongly depending on feedforward inhibition and more globally on local I/E balance.

I/E imbalance is induced by the heterogeneous synaptic vulnerability to *il1rapl1* removal

Interestingly, our results pointed the differential vulnerability of excitatory synapses to *il1rapl1* mutation, especially regarding the identity (e.g., GABAergic or glutamatergic) of the postsynaptic cell (Figs. 3 and 4). Our efforts to better characterize the expression pattern of *il1rapl1* led to the identification of a specific but ubiquitous expression of weak levels of the mRNA in most likely all neuron types of the basolateral amygdala complex (Fig. 6). Thereby, the simplistic explanation of *il1rapl1* −/*y* phenotype through the differential expression in interneuron and principal cells is ruled out. Interestingly, Il1rapl1 protein recently emerged through the efforts of several groups as a new trans-synaptic adhesion and signaling molecule entering an heterophilic interaction with presynaptic PTP-∂ (Valnegri et al., 2011; Yoshida et al., 2011). This interaction promotes the aggregation of presynaptic (bassoon and VGLUT1) and postsynaptic (PSD95 and Shank2) proteins at excitatory, but not at inhibitory, contacts in dissociated neuron cultures and in cortical slices (Valnegri et al., 2011; Yoshida et al., 2011). In addition, a recent study proposed that the modulation of RhoA/ROCK signaling by the IL1RAPL1 TIR domain, through an interaction with Mcf2l (Hayashi et al., 2013), mediates both IL1RAPL1-mediated spinogenesis and control of AMPAR trafficking (Hayashi et al., 2013), possibly linking functional and morphological phenotypes. In the amygdala, feedforward inhibition is elicited through the activation of AMPAR- and NMDAR-containing postsynapses on low-spiny GABAergic interneurons (Szinyei et al., 2000, 2003; Spampanato et al., 2011). Taking this into account, one can imagine that *il1rapl1* mutation does not affect interneurons the same way it does principal cells. In this line, recent work strikingly brought evidence for a mirror role of the postsynaptic protein Erbin only at excitatory synapse formed with GABAergic neurons (Tao et al., 2013). Further work will be necessary to understand whether there is a causal relationship between the absence of dendritic spine and the absence of functional consequence of *il1rapl1* mutation. Indeed, one may anticipate that the impact of many ID gene mutations may not be ubiquitous at central synapses and that similar functional I/E imbalance generated by this heterogeneity may also be found in other ID models.

Recently, the emergence of several families of trans-synaptic adhesion molecules important for synapse specification raised a lot of interest by pointing to an unexpected possible wealth of heterogeneity in synaptic functions and plasticity (McMahon and Díaz, 2011; Siddiqui and Craig, 2011). Beyond the diversity in genes, many splice variants were also shown to occur at these loci (Missler and Südhof, 1998a). Additionally, secreted binding partners (e.g., neurexophilins) exist that can alter trans-synaptic adhesions (Missler and Südhof, 1998b). More striking is the activity-dependent regulation of neurexin1 binding through alternative splicing (Iijima et al., 2011). Thus, the synaptic code determining the balance of expression of this mixture of molecules at a given synapse is of key importance to understand how complex brain circuits are wired. Clearly, our work points to the functional heterogeneity of excitatory synaptic inputs involved in the fulfillment of complex behavioral functions. Although *il1rapl1* mRNA seems to be expressed at all cell types of amygdala, additional experiments will be required to understand the molecular rational behind the differential vulnerability of excitatory synapses to *il1rapl1* deletion.

We further show that deletion of *il1rapl1* results in fading of excitatory transmission and morphological impairments at thalamo–LA Vglut2-PSD95 (Fig. 5). Indeed, medial geniculate medial part and postintralaminar thalamic nuclei that project to LA both express robust levels of *vglut2* mRNA (Fremeau et al., 2001). Although we bring here convincing *in situ* hybridization of *il1rapl1* mRNA, the lack of comprehensive morphological description of the Il1rapl1 and PTP-∂ distributions hampers our ability to fully overview the system we dissected. Nevertheless, our data suggest that either the functional Il1rapl1/PTP-∂ complex is formed mainly at thalamo–LA synapses, or that it is formed at all excitatory synapses but is only critical at the thalamo–LA connection. In the latter scenario, functional redundancy may blur the phenotype of the deletion at most other synapses. Alternatively, we cannot rule out that our observations result from Il1rapl1-induced extrasynaptic alterations that in turn unravel existing presynaptic heterogeneity to neuromodulation. Indeed, Chu et al. (2012) recently illustrated the target-specific suppression of GABAergic transmission by dopamine.

Interestingly, we did not observe a loss of dendritic spines in LA pyramidal neurons from *il1rapl1* −/y animals (Fig. 5*A*), somehow contrasting with the I/O curves showing a functional disappearance of these long range connections (Fig. 3). Further, we also observed very little effects of the mutation on miniature EPSCs recorded in LA principal cells (Fig. 5). This paradox opens the interesting possibility that the mutation introduces a switch from long range to local synaptic connectivity, a model also proposed for neurodevelopmental disorders (Geschwind and Levitt, 2007). The neurodevelopmental disorder theory states that neurons are hyperconnected at the local network level, but in contrast, show decreased long-range connectivity between cortical brain circuits. For example, prominent hyperconnectivity was recently shown in local medial prefrontal cortical networks of a genetic mouse model for intellectual disability and autism (Testa-Silva et al., 2012). Addressing this question would require assessment of LA-LA principal cell connectivity in *il1rapl1* KO mice. Hyperconnectivity observations would then redefine *il1rapl1* mutations as causing a neurodevelopmental disorder syndrome.

In conclusion, our work unravels heterogeneity in synaptic dependency to Il1rapl1 function and its role in the fine-tuning of I/E balance in discrete circuits of the brain. We suggest that constitutive absence of Il1rapl1 disrupts this balance, possibly explaining the deficit in LTP induction *in vivo* and the behavioral deficits observed in KO mice. Beyond providing a first mechanistic explanation to I/E imbalance, a phenotype frequently associated with cognitive disorders, our results force one to not only examine the impact of a particular ID mutation onto a single synaptic type but rather to consider all physiological determinants driving a functional neuronal circuit. Conversely, the use of ID/ASD models may also allow identifying new sources of behaviorally relevant synaptic heterogeneity.

References

Baroncelli L, Braschi C, Spolidoro M, Begenisic T, Maffei L, Sale A (2011) Brain plasticity and disease: a matter of unhibition. Neural Plast 2011: 1–11. CrossRef Medline

Berlau DJ, McGaugh JL (2006) Enhancement of extinction memory consolidation: the role of the noradrenergic and GABAergic systems within the basolateral amygdala. Neurobiol Learn Mem 86:123–132. CrossRef Medline

Bissière S, Humeau Y, Lüthi A (2003) Dopamine gates LTP induction in lateral amygdala by suppressing feedforward inhibition. Nat Neurosci 6:587–592. CrossRef Medline

Bliss TV, Lomo T (1973) Long-lasting potentiation of synaptic transmission in the dentate area of the anaesthetized rabbit following stimulation of the perforant path. J Physiol 232:331–356. Medline

Carrié A, Jun L, Bienvenu T, Vinet MC, McDonell N, Couvert P, Zemni R, Cardona A, Van Buggenhout G, Frints S, Hamel B, Moraine C, Ropers

HH, Strom T, Howell GR, Whittaker A, Ross MT, Kahn A, Fryns JP, Beldjord C, et al. (1999) A new member of the IL-1 receptor family highly expressed in hippocampus and involved in X-linked mental retardation. Nat Genet 23:25–31. CrossRef Medline

Chao HT, Chen H, Samaco RC, Xue M, Chahrour M, Yoo J, Neul JL, Gong S, Lu HC, Heintz N, Ekker M, Rubenstein JL, Noebels JL, Rosenmund C, Zoghbi HY (2010) Dysfunction in GABA signalling mediates autism-like stereotypies and Rett syndrome phenotypes. Nature 468: 263–269. CrossRef Medline

Chhatwal JP, Myers KM, Ressler KJ, Davis M (2005) Regulation of gephyrin and GABAA receptor binding within the amygdala after fear acquisition and extinction. J Neurosci 25:502–506. CrossRef Medline

Chu HY, Ito W, Li J, Morozov A (2012) Target-specific suppression of GABA release from parvalbumin interneurons in the basolateral amygdala by dopamine. J Neurosci 32:14815–14820. CrossRef Medline

Dani VS, Chang Q, Maffei A, Turrigiano GG, Jaenisch R, Nelson SB (2005) Reduced cortical activity due to a shift in the balance between excitation and inhibition in a mouse model of Rett syndrome. Proc Natl Acad Sci U S A 102:12560–12565. CrossRef Medline

Ehrlich I, Humeau Y, Grenier F, Ciocchi S, Herry C, Lüthi A (2009) Amygdala inhibitory circuits and the control of fear memory. Neuron 62:757–771. CrossRef Medline

Fremeau RT Jr, Troyer MD, Pahner I, Nygaard GO, Tran CH, Reimer RJ, Bellocchio EE, Fortin D, Storm-Mathisen J, Edwards RH (2001) The expression of vesicular glutamate transporters defines two classes of excitatory synapse. Neuron 31:247–260. CrossRef Medline

Gabernet L, Jadhav SP, Feldman DE, Carandini M, Scanziani M (2005) Somatosensory integration controlled by dynamic thalamocortical feed-forward inhibition. Neuron 48:315–327. CrossRef Medline

Gambino F, Pavlowsky A, Béglé A, Dupont JL, Bahi N, Courjaret R, Gardette R, Hadjkacem H, Skala H, Poulain B, Chelly J, Vitale N, Humeau Y (2007) IL1-receptor accessory protein-like 1 (IL1RAPL1), a protein involved in cognitive functions, regulates N-type Ca^{2+}-channel and neurite elongation. Proc Natl Acad Sci U S A 104:9063–9068. CrossRef Medline

Gambino F, Kneib M, Pavlowsky A, Skala H, Heitz S, Vitale N, Poulain B, Khelfaoui M, Chelly J, Billuart P, Humeau Y (2009) IL1RAPL1 controls inhibitory networks during cerebellar development in mice. Eur J Neurosci 30:1476–1486. CrossRef Medline

Gambino F, Khelfaoui M, Poulain B, Bienvenu T, Chelly J, Humeau Y (2010) Synaptic maturation at cortical projections to the lateral amygdala in a mouse model of Rett syndrome. PLoS One 5:e11399. CrossRef Medline

Geschwind DH, Levitt P (2007) Autism spectrum disorders: developmental disconnection syndromes. Curr Opin Neurobiol 17:103–111. CrossRef Medline

Han JH, Kushner SA, Yiu AP, Hsiang HL, Buch T, Waisman A, Bontempi B, Neve RL, Frankland PW, Josselyn SA (2009) Selective erasure of a fear memory. Science 323:1492–1496. CrossRef Medline

Hayashi T, Yoshida T, Ra M, Taguchi R, Mishina M (2013) IL1RAPL1 associated with mental retardation and autism regulates the formation and stabilization of glutamatergic synapses of cortical neurons through RhoA signaling pathway. PLoS One 8:e66254. CrossRef Medline

Herry C, Ciocchi S, Senn V, Demmou L, Müller C, Lüthi A (2008) Switching on and off fear by distinct neuronal circuits. Nature 454:600–606. CrossRef Medline

Hong I, Kim J, Lee J, Park S, Song B, Kim J, An B, Park K, Lee HW, Lee S, Kim H, Park SH, Eom KD, Lee S, Choi S (2011) Reversible plasticity of fear memory-encoding amygdala synaptic circuits even after fear memory consolidation. PLoS One 6:e24260. CrossRef Medline

Humeau Y, Herry C, Kemp N, Shaban H, Fourcaudot E, Bissière S, Lüthi A (2005) Dendritic spine heterogeneity determines afferent-specific hebbian plasticity in the amygdala. Neuron 45:119–131. CrossRef Medline

Humeau Y, Reisel D, Johnson AW, Borchardt T, Jensen V, Gebhardt C, Bosch V, Gass P, Bannerman DM, Good MA, Hvalby Ø, Sprengel R, Lüthi A (2007) A pathway-specific function for different AMPA receptor subunits in amygdala long-term potentiation and fear cconditioning. J Neurosci 27:10947–10956. CrossRef Medline

Humeau Y, Gambino F, Chelly J, Vitale N (2009) X-linked mental retardation: focus on synaptic function and plasticity. J Neurochem 109: 1–14. CrossRef Medline

Iijima T, Wu K, Witte H, Hanno-Iijima Y, Glatter T, Richard S, Scheiffele P (2011) SAM68 regulates neuronal activity-dependent alternative splicing of neurexin-1. Cell 147:1601–1614. CrossRef Medline

Johansen JP, Hamanaka H, Monfils MH, Behnia R, Deisseroth K, Blair HT, LeDoux JE (2010) Optical activation of lateral amygdala pyramidal cells instructs associative fear learning. Proc Natl Acad Sci U S A 107:12692–12697. CrossRef Medline

Kleschevnikov AM, Belichenko PV, Villar AJ, Epstein CJ, Malenka RC, Mobley WC (2004) Hippocampal long-term potentiation suppressed by increased inhibition in the Ts65Dn mouse, a genetic model of Down syndrome. J Neurosci 24:8153–8160. CrossRef Medline

LeDoux JE (2000) Emotion circuits in the brain. Annu Rev Neurosci 23: 155–184. CrossRef Medline

Maren S (2005) Synaptic mechanisms of associative memory in the amygdala. Neuron 47:783–786. CrossRef Medline

McDonald AJ (1982) Neurons of the lateral and basolateral amygdaloid nuclei: a Golgi study in the rat. J Comp Neurol 212:293–312. CrossRef Medline

McMahon SA, Díaz E (2011) Mechanisms of excitatory synapse maturation by trans-synaptic organizing complexes. Curr Opin Neurobiol 21:221–227. CrossRef Medline

Missler M, Südhof TC (1998a) Neurexins: three genes and 1001 products. Trends Genet 14:20–26. CrossRef Medline

Missler M, Südhof TC (1998b) Neurexophilins form a conserved family of neuropeptide-like glycoproteins. J Neurosci 18:3630–3638. Medline

Moutsimilli L, Farley S, Dumas S, El Mestikawy El S, Giros B, Tzavara ET (2005) Selective cortical VGLUT1 increase as a marker for antidepressant activity. Neuropharmacology 49:890–900. CrossRef Medline

Pavlowsky A, Gianfelice A, Pallotto M, Zanchi A, Vara H, Khelfaoui M, Valnegri P, Rezai X, Bassani S, Brambilla D, Kumpost J, Blahos J, Roux MJ, Humeau Y, Chelly J, Passafaro M, Giustetto M, Billuart P, Sala C (2010) A postsynaptic signaling pathway that may account for the cognitive defect due to IL1RAPL1 mutation. Curr Biol 20:103–115. CrossRef Medline

Pavlowsky A, Chelly J, Billuart P (2011) Emerging major synaptic signaling pathways involved in intellectual disability. Mol Psychiatry 17: 682–693. CrossRef Medline

Piton A, Michaud JL, Peng H, Aradhya S, Gauthier J, Mottron L, Champagne N, Lafrenière RG, Hamdan FF, Hamdan FF, Joober R, Fombonne E, Marineau C, Cossette P, Dubé MP, Haghighi P, Drapeau P, Barker PA, Carbonetto S, Rouleau GA (2008) Mutations in the calcium-related gene IL1RAPL1 are associated with autism. Hum Mol Genet 17:3965–3974. CrossRef Medline

Pizzarelli R, Cherubini E (2011) Alterations of GABAergic signaling in autism spectrum disorders. Neural Plast 2011:1–12. CrossRef Medline

Pouille F, Scanziani M (2001) Enforcement of temporal fidelity in pyramidal cells by somatic feed-forward inhibition. Science 293:1159–1163. CrossRef Medline

Purpura DP (1974) Dendritic spine "dysgenesis" and mental retardation. Science 186:1126–1128. CrossRef Medline

Rodriguez A, Ehlenberger DB, Dickstein DL, Hof PR, Wearne SL (2008) Automated three-dimensional detection and shape classification of dendritic spines from fluorescence microscopy images. PLoS One 3:e1997. CrossRef Medline

Rosenkranz JA, Grace AA (2002) Dopamine-mediated modulation of odour-evoked amygdala potentials during Pavlovian conditioning. Nature 417:282–287. CrossRef Medline

Rumpel S, LeDoux J, Zador A, Malinow R (2005) Postsynaptic receptor trafficking underlying a form of associative learning. Science 308:83–88. CrossRef Medline

Sanger DJ, Joly D (1985) Anxiolytic drugs and the acquisition of conditioned fear in mice. Psychopharmacology (Berl) 85:284–288. CrossRef Medline

Siddiqui TJ, Craig AM (2011) Synaptic organizing complexes. Curr Opin Neurobiol 21:132–143. CrossRef Medline

Sosulina L, Meis S, Seifert G, Steinhäuser C, Pape HC (2006) Classification of projection neurons and interneurons in the rat lateral amygdala based upon cluster analysis. Mol Cell Neurosci 33:57–67. CrossRef Medline

Sosulina L, Graebenitz S, Pape HC (2010) GABAergic interneurons in the mouse lateral amygdala: a classification study. J Neurophysiol 104:617–626. CrossRef Medline

Spampanato J, Polepalli J, Sah P (2011) Interneurons in the basolateral amygdala. Neuropharmacology 60:765–773. CrossRef Medline

Szinyei C, Heinbockel T, Montagne J, Pape HC (2000) Putative cortical and

thalamic inputs elicit convergent excitation in a population of GABAergic interneurons of the lateral amygdala. J Neurosci 20:8909–8915. Medline

Szinyei C, Stork O, Pape HC (2003) Contribution of NR2B subunits to synaptic transmission in amygdaloid interneurons. J Neurosci 23:2549–2556. Medline

Tamamaki N, Yanagawa Y, Tomioka R, Miyazaki J, Obata K, Kaneko T (2003) Green fluorescent protein expression and colocalization with calretinin, parvalbumin, and somatostatin in the GAD67-GFP knock-in mouse. J Comp Neurol 467:60–79. CrossRef Medline

Tao Y, Chen YJ, Shen C, Luo Z, Bates CR, Lee D, Marchetto S, Gao TM, Borg JP, Xiong WC, Mei L (2013) Erbin interacts with TARP γ-2 for surface expression of AMPA receptors in cortical interneurons. Nat Neurosci 16:290–299. CrossRef Medline

Testa-Silva G, Loebel A, Giugliano M, de Kock CP, Mansvelder HD, Meredith RM (2012) Hyperconnectivity and slow synapses during early development of medial prefrontal cortex in a mouse model for mental retardation and autism. Cereb Cortex 22:1333–1342. CrossRef Medline

Vaillend C, Poirier R, Laroche S (2008) Genes, plasticity and mental retardation. Behav Brain Res 192:88–105. CrossRef Medline

Valnegri P, Montrasio C, Brambilla D, Ko J, Passafaro M, Sala C (2011) The X-linked intellectual disability protein IL1RAPL1 regulates excitatory synapse formation by binding PTP and RhoGAP2. Hum Mol Genet 20:4797–4809. CrossRef Medline

van Bokhoven H (2011) Genetic and epigenetic networks in intellectual disabilities. Annu Rev Genet 45:81–104. CrossRef Medline

Yizhar O, Fenno LE, Prigge M, Schneider F, Davidson TJ, O'Shea DJ, Sohal VS, Goshen I, Finkelstein J, Paz JT, Stehfest K, Fudim R, Ramakrishnan C, Huguenard JR, Hegemann P, Deisseroth K (2011) Neocortical excitation/inhibition balance in information processing and social dysfunction. Nature 477:171–178. CrossRef Medline

Yoshida T, Yasumura M, Uemura T, Lee SJ, Ra M, Taguchi R, Iwakura Y, Mishina M (2011) IL-1 receptor accessory protein-like 1 associated with mental retardation and autism mediates synapse formation by trans-synaptic interaction with protein tyrosine phosphatase. J Neurosci 31:13485–13499. CrossRef Medline

3. Unpublished work

3.1. Behavioral and cellular deficits in Il1rapl1 KO mouse are rescued by α5IA treatment

3.1.1. Context

In different neurodevelopmental diseases, either inhibitory or excitatory synapse function is impaired. Even if the origin of these disorders is very heterogeneous, synapse impairments result in changes in the excitation/inhibition (E/I) balance, that can be translated into behavioral changes (Kleschevnikov et al. 2004; Dani et al. 2005; Houbaert et al. 2013). GABAergic interneurons represent just ~10-20 % of neuronal population, but if the inhibition is disturbed, excessive excitation results in an unbalance of the E/I ratio and consequently, in a dysfunction of cognitive processes or in an increase of seizures susceptibility. Since GABAergic system is commonly disturbed in many neurodevelopmental disorders, a proposed strategy for reestablish normal brain function consist of the use of drugs that target specifically GABAergic signaling (Braat & Kooy 2014; Braat & Kooy 2015b).

$GABA_A$ receptors are ligand-gated chloride ion channels that mediate most of the GABA actions. Functional receptors consist of hetero tetramers from 19 known receptor subunits: α1–6, β1–3, γ1–3, δ, ε, θ, π, and ρ1–3. This give rise to a complex heterogeneity of $GABA_A$ receptor subtypes, where each subtype has a distinct physiological and pharmacological profile, and a specific regional, cellular, and subcellular expression pattern (Olsen & Sieghart 2009). However, the majority of $GABA_A$ receptors present in the brain are composed of α, β, and γ subunits (Pirker et al. 2000).

$GABA_A$ receptors containing α1–3, β, and γ2 subunits are mainly synaptic and mediate fast phasic inhibition, whereas α4–6 and δ-containing receptors are mainly located extra-synaptically where they produce persistent tonic inhibition by GABA spillover into the extracellular space (Farrant & Nusser 2005). $GABA_A$ receptors can be targeted by a wide variety of pharmacological compounds that bind to different regions of the receptor to mediate subunit-specific effects (Rudolph & Knoflach 2011). So, depending on the characteristics and the nature of the GABAergic system abnormalities, different drugs can be applied. The most studied compounds able to modulate $GABA_A$ receptor

activity are the benzodiazepines. These are allosteric modulators that bind to the interface between α and γ subunits (known as the benzodiazepine binding site) and enhance GABA inhibitory effects. The benzodiazepines, whose therapeutic effects were discovered in the 1950s, exert their different actions through influencing $GABA_A$ receptor activity depending on its subunit composition. The function of some $GABA_A$ receptors subtypes in the brain has been identified by introducing a point mutation into the genes of each α subunit rendering the respective receptors insensitive to allosteric modulation by benzodiazepines (Rudolph & Möhler 2004). Using this approach, it was demonstrated that α1 receptors mediate the sedative, anterograde amnestic and in part the anticonvulsant actions of benzodiazepines, α2 subunit mediates the anxiolytic activity and some of the muscle relaxant activities, α3 subunit seem to mediate the anti-absence effects, and that the α5 subunit influences learning and memory.

With this latter respect, it is interesting to note that mice lacking α5 $GABA_A$ receptor subunit show an enhanced performance in an hippocampal-dependent test of spatial learning, the Morris water maze (Collinson et al. 2002). This can be due to a decrease of spontaneous inhibitory post-synaptic currents (sIPSC), and thus a decrease of inhibition in the hippocampus (Collinson et al. 2002). The hippocampal-specificity of behavioral enhancement may be due to the higher expression of α5 subunit in the hippocampus than in other brain regions (Pirker et al. 2000; Crestani et al. 2002; Collinson et al. 2002). Results observed in the *Gabra5* KO mice suggested that the selective inhibition of α5-containing $GABA_A$ receptors may be suitable as a drug-enhancing cognitive function. A large amount of benzodiazepine-derived molecules have been synthetized for their use as an α5 subunit inverse agonists, binding to the benzodiazepine site but mediates the opposite pharmacologic effect (Street et al. 2004; Sternfeld et al. 2004). Treatment of wild-type mice with an α5-specific inverse agonist, α5IA, improved their performance in hippocampal-dependent memory tasks and enhanced LTP in hippocampal slices (Dawson et al. 2006; Atack et al. 2009). However, this LTP enhancement is not observed in *Gabra5* KO mice suggesting that α5-containig $GABA_A$ receptors play a role in the pharmacological enhancement of LTP, but has a minor impact in physiological LTP (Dawson et al. 2006; Collinson et al. 2002). Moreover, this inverse agonist does not produce the adverse effects induced by GABA antagonists or non-specific $GABA_A$ inverse agonists or antagonists, that are known to have proconvulsant and anxiogenic effects (Dawson et al. 2006; Atack et al. 2009). α5IA pre-clinical and clinical trials in healthy individuals demonstrated that in human

α5IA may be effective at increasing cognitive performance under certain conditions (Atack 2010).

Blocking α5-containing $GABA_A$ with α5IA is a strategy used to down regulate the increased inhibition present in some ID mouse models, like Ts65Dn mice model for Down syndrome. Down syndrome is the most common genetic cause of ID and is characterized by varying degrees of cognitive impairments (Silverman 2007). Ts65Dn mice have cognitive impairments, like hippocampal-dependent learning (Escorihuela et al. 1995; Kleschevnikov et al. 2004; Braudeau, Delatour, et al. 2011), and treatment of those mice with α5IA improves their cognitive deficits. However, the cellular mechanisms of these behavioral changes are not clear.

It was demonstrated *in vitro* and *in vivo* that in the absence of *Il1rapl1* there is a decrease of excitatory synapses in the cortex and the hippocampus, while there is no effect on inhibitory ones. Even if those structural changes were not observed in other brain regions, for instance lateral amygdala, functional defects were also observed in this structure that result in a perturbed excitation/inhibition (E/I) ratio in favor to inhibition (Houbaert et al. 2013). The origin of this unbalance is different from the Down syndrome, but attempts to rescue *Il1rapl1* KO mice cognitive impairment were carried out by two strategies. The first one is described in the first article presented as part of this thesis, and consists on the local infusion of a non-specific $GABA_A$ antagonist, bicuculline, into the lateral amygdala (Houbaert et al. 2013). After this treatment, the deficits in associative memory of *Il1rapl1* KO mice were corrected.

The second strategy was carried out by Hamid Meziane and Yann Hérault (IGBMC, Illkirch), and consisted in the treatment of *Il1rapl1* KO mice with the α5 $GABA_A$ receptor subunit inverse agonist, α5IA. This treatment was able to correct the hippocampal-dependent cognitive deficits observed in those mice.

With the aim of understanding the cellular and molecular mechanism underlying the cognitive improvement after α5IA treatment, Geoffroy Goujon and I measured the cellular effect of this $GABA_A$ inverse agonist in neuronal cultures. We started this study by evaluating the effect of α5IA on the synaptic phenotype described in neurons lacking *Il1rapl1* co-cultured with wild-type (WT) neurons, a decrease of PSD-95 clusters (Pavlowsky, Gianfelice, et al. 2010). This read-out appears to be a good candidate because the PSD-95 decrease, together with dendritic spine reduction, are not dramatically changed in the absence of *Il1rapl1* but could be enough for disturbing the

E/I balance the hippocampus. In addition, the effect of α5IA on excitatory synapses that could result from the modification of the inhibitory transmission has never been assessed. This work in collaboration with Hamid Meziane and Yann Hérault will be the subject of an upcoming publication.

3.1.2. Material and methods

Animals and hippocampal- dependent memory tasks

Two cohorts of *Il1rapl1* +/y and *Il1rapl1* -/y male mice in C57BL/6j genetic background were used for this study (the results presented here correspond only to the first cohort, 5-7 mice per condition). Mice were housed in a room with controlled temperature (21-22°C) under a 12-12 light-dark cycle (light on at 07:00 a.m.), with food and water available *ad libitum*. At 18-20 weeks of age, mice were probed for contextual memory in a Morris water maze. The water maze consisted of a white circular tank (1.50 m diameter) filled with opaque water (temperature adjusted to 21±1°C). The walls surrounding the maze were hung with visual cues and were visible during all stages of training and testing. Animals were first trained to locate the escape platform (10 cm diameter), that was positioned 1 cm below water level in the center of one of the maze quadrants, by using only extra-maze cues (spatial learning). Each mouse received 4 training trials per day over five consecutive days in which they were placed in the pool at one of four randomized start positions, and allowed to locate the hidden platform. Trials lasted for a maximum of 120 s and were separated by 15-20 min intervals. If a mouse failed to find the platform within this period, it was guided to its position by the experimenter. The latency, distance and the average speed were used to evaluate performance during training trials. Spatial learning performance was assessed during a probe trial 7 days after training, and for which the target platform was removed from the pool. For the probe trial, the percentage of time spent in each quadrant and the number of platform position crosses were used as index of spatial learning performance. Mice received an intraperitoneal injection of either 5mg/kg α5IA dissolved in a mixture of DMSO, Cremophor El and hypotonic water (10:15:75) or vehicle only, 40 minutes before tests (days 1-5) but not before probe test. All experimental procedures on animals were approved by the local ethical committee.

Hippocampal neuronal cultures from wild-type and Il1rapl1 KO mice and treatments

Hippocampal neuronal cultures were obtained from E16.5 C57Bl/6j or *Il1rapl1* KO mouse embryos (Gambino et al. 2009). Hippocampi were dissected and pooled by genotype, the tissue was dissociated by chemical and mechanical methods, and 100 000 cells were seeded in Poly-L lysine and laminin-coated coverslips. Cells were maintained in Neurobasal medium supplemented with B27 (Life Technologies), and transfected at 11 days *in vitro* (DIV) with 800 ng of a GFP-coding plasmid using Lipofectamine 2000 (Life Technologies). For immunocytochemistry experiments, cells were treated at 15 DIV with α5IA (kindly provided by Marie Claude Poitier, ICM, Paris) dissolved in DMSO. At 18 DIV neurons were fixed with 4% PFA plus 4% sucrose at room temperature for 20 min, and with 100% methanol at -20°C for 10 min. After permeabilization (0.2% TritonX-100, 15 minutes) and blocking (3% BSA + 0.2% Tween-20), coverslips were incubated with primary antibodies diluted in blocking buffer overnight. After PBS washes, coverslips were incubated with secondary antibodies (1:200, Jackson ImmunoResearch Labs) and mounted on glass slides (Fluoromount). Images were obtained using a Leica DMI6000 Spinning disk microscope and a 63x objective. 10-12 neurons per condition were imaged. The primary antibodies and the dilutions used were: mouse anti-PSD-95 (1:200, Neuromab), rabbit anti-synaptophysin (1:400, Cell Signaling) and mouse anti-GFP (1:1000, Abcam). PSD-95 and synaptophysin cluster number was assessed with ImageJ (Rasband, W.S., ImageJ, U.S. National Institutes of Health, Bethesda, Maryland, USA, http://imagej.nih.gov/ij/, 1997–2014) and NeuronJ plugin to normalize clusters by the length of dendrites.

RNA isolation and real time quantitative PCR

For real time quantitative PCR experiments, 18 DIV neurons were treated with 40 µM bicuculline, DMSO or α5IA during 1.5 hours prior of harvesting for RNA isolation. RNA was isolated from hippocampus or cell cultures using RNA Plus (Qbiogene) according to manufacturer's instructions, and integrity was assessed by Nanodrop (Thermo Scientific). cDNA was synthetized from 1 µg of RNA using Maxima reverse transcriptase (Thermo Scientific). Real time quantitative PCR using SYBR Green I and a LightCycler (Roche Diagnostics) was used to determine the relative abundance of mouse *Gabra5* and *c-Fos*. All pairs of primers used were designed to encompass an exon-exon junction and were controlled for optimal efficacy. The primers used were: *Gabra5*_F tcttggacggactcttggatggct, *Gabra5*_R tcgcacctgcgtgattcgct, *c-Fos*_F

cagagcgcagagcatcggca, *c-Fos*_R cgattccggcacttggctgc. *Actin* (F_ ccagttggtaacaatgccatg and R_ ctgtattcccctccatcgtg) and *Gapdh* (F_aagagaggccctatcccaac and R_ gcagcgaactttattgatgg) were both used as reference genes. mRNA relative abundance was calculated using the $2^{-\Delta\Delta C_T}$ method (Livak & Schmittgen 2001).

3.1.3. Results

α5IA treatment restores the cognitive deficits of Il1rapl1 KO mice

Il1rapl1 KO mice are known to have different cognitive deficits, especially hippocampal-dependent behaviors. We evaluated the effect of α5IA on the spatial learning performance (spatial memory) of those mice and compared them with wild-type (WT) mice. Mice were probed 7 days after training, and Figure 20 shows the index of spatial memory in terms of the percentage of time spent in each quadrant in wild-type or *Il1rapl1* KO mice, treated with vehicle or with α5IA. WT mice (white bars) passed more time in the pool quadrant were the platform used to be (Target), indicating a good contextual memory performance. As expected, *Il1rapl1* KO mice (black bars) had no preference for the target quadrant but interestingly, α5IA treatment improved their performance to the same levels than WT mice.

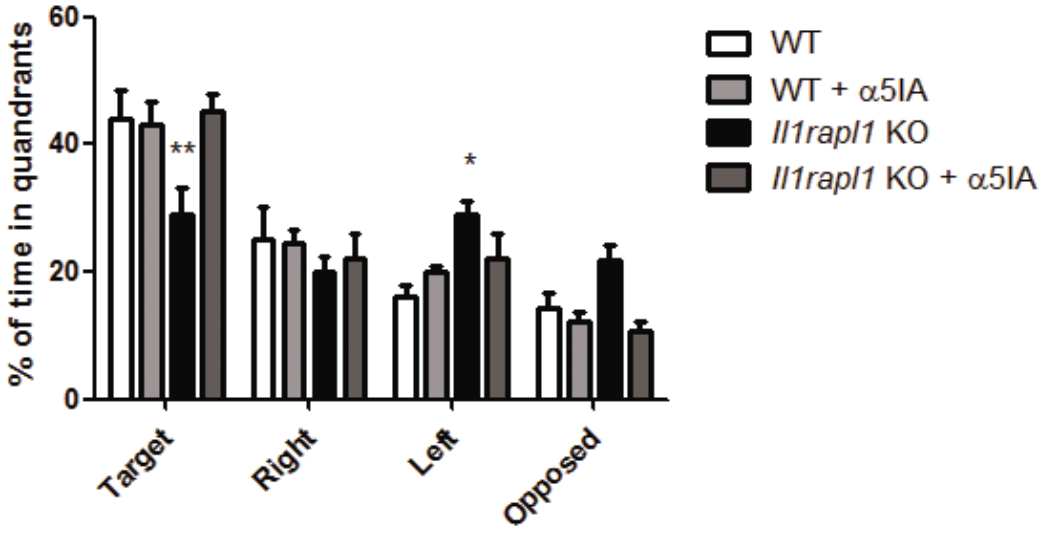

Figure 20. Effect of α5IA on contextual memory in wild-type and *Il1rapl1* KO mice. Bars show mean and standard error of the mean (SEM) of the % of time spent in each maze quadrant during the probe test. Target quadrant is where the platform used to be during training, 7 days before. ** p <0.01 * p<0.05 compared to WT. Two-ways ANOVA. n = 5-7 animals per group. WT: wild-type.

α5IA treatment restores the abundance of the immediate early gene c-Fos in Il1rapl1 KO neurons in culture

In order to elucidate the cellular mechanisms involved in the cognitive effect of α5IA in *Il1rapl1* KO mice, we treated hippocampal neurons in culture with this inverse agonist. We first evaluated at the mRNA level if the *Gabra5* subunit was present in our mature (18 DIV) hippocampal neuronal cultures. We found that this subunit is present at the same level in neurons from both WT and *Il1rapl1* KO mice (Figure 21) and the protein was previously shown to be present at all differentiation stages *in vitro*, in particular at 14 DIV (Killisch et al. 1991; Swanwick et al. 2006). We also evaluated *Gabra5* mRNA expression in adult hippocampus from WT and *Il1rapl1* KO mice, and obtained the same results (not shown).

The 30 and 300 nM doses correspond to ~50 and ~500 times the Ki of α5IA for α5 subunit. These doses were chosen because α5IA effect on LTP was observed at 30 and 100 nM in hippocampal slices (Dawson et al. 2006). As this is the first study of the sub-cellular effects of α5IA treatment, we wanted to be sure that the concentrations used would have an effect *in vitro*.

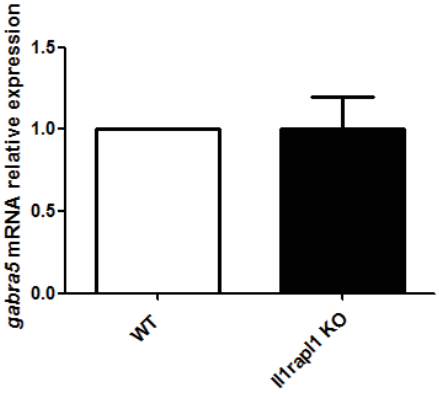

Figure 21. Gabra5 mRNA relative abundance in wild-type and *Il1rapl1* KO hippocampal neurons in culture. Bars represent the mean and SEM from 3 independent cultures 18 DIV. WT: wild-type.

Taking into account that α5IA has an effect on immediate early gene (IEG) transcription (Braudeau, Dauphinot, et al. 2011; Braudeau, Delatour, et al. 2011), we assessed if *c-Fos* mRNA was up regulated by a short (1.5h) α5IA treatment (Figure 22). This time window is optimal for *c-Fos* up regulation in neurons following to the exposure to 40 μM bicuculline (J. Renaud, personal communication). The effect of both α5IA concentrations in WT neurons was modest, compared with bicuculline treated samples. Interestingly, in non-treated neurons, there was a slight but significant

decrease of *c-Fos* mRNA abundance in *Il1rapl1* KO neurons (~30% decrease, p<0.05 paired t test) and this difference was no longer observed when *Il1rapl1* KO neurons were treated with α5IA.

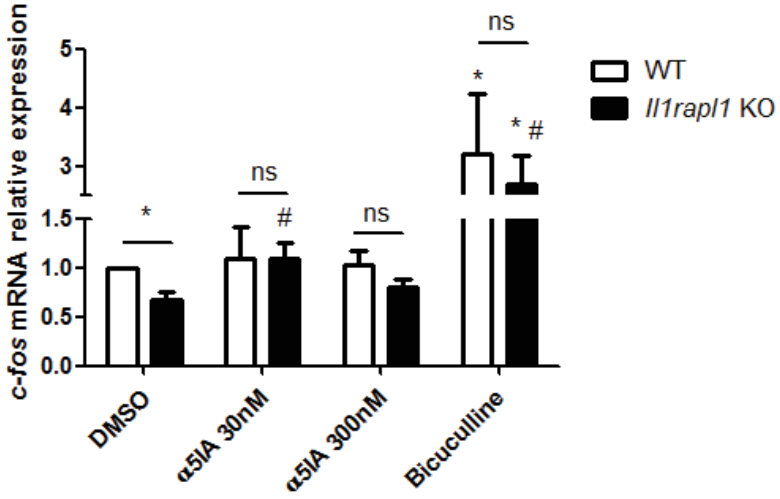

Figure 22. c-Fos mRNA relative abundance in hippocampal neurons after bicuculline or α5IA treatment (1.5 h). Bars represent the mean and SEM from 3 independent cultures. * p<0.05 compared with DMSO-treated wild-type (WT) neurons; # p<0.05 compared with DMSO-treated *Il1rapl1* KO neurons. 18 DIV.

α5IA treatment has different effects on the number of PSD-95 clusters in Il1rapl1 KO neurons

We then treated wild-type and *Il1rapl1* KO neurons with 30 and 300 nM α5IA for 2 or 72h and counted the PSD-95 clusters present in those cells. We chose those times of treatment because an effect of the drug has been observed after few minutes or hours of treatment and we also wanted to assess the “synaptic remodeling” that could take place after chronic treatment with this inverse agonist (Dawson et al. 2006; Braudeau, Delatour, et al. 2011; Braudeau, Dauphinot, et al. 2011). I only present here the effect on excitatory synapses of the 72h treatment (Figure 23 and 24).

As reported before, we observed a slight decrease (~25%) of PSD-95 clusters on *Il1rapl1* KO compared with WT neurons (Pavlowsky, Gianfelice, et al. 2010). This phenotype is specific for excitatory postsynapses, since the non-specific presynaptic protein synaptophysin is not changed in *Il1rapl1* KO neurons (Figure 24). Surprisingly, 30 and 300 nM α5IA treatments had different genotype-dependent effects on PSD-95 clusters. None of the treatments had an effect on the wild-type cells. In *Il1rapl1* KO neurons, the 30 nM treatment substantially increased the number of clusters (~50%

compared with DMSO-treated *Il1rapl1* KO neurons), whereas the 300 nM treatment reestablished the PSD-95 clusters to the same level that WT neurons. Once again, this PSD-95 cluster regulation by α5IA is specific of PSD-95 and does not have any effect on synaptophysin clusters.

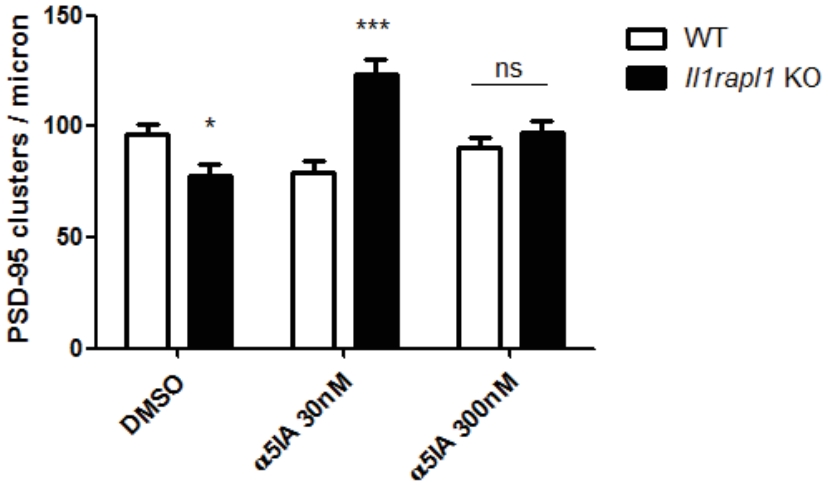

Figure 23. Postsynaptic changes after α5IA treatment. Bars show the mean and SEM of PSD-95 clusters per micron after 72h of treatment with α5IA, normalized by DMSO-treated wild-type (WT) neurons. 50 neurons from 4 independent cultures were analyzed. * p<0.05, *** p<0.001 compared with the WT neuron for each treatment. # p<0.05, ### p<0.001, compared with DMSO-treated *Il1rapl1* KO neurons.

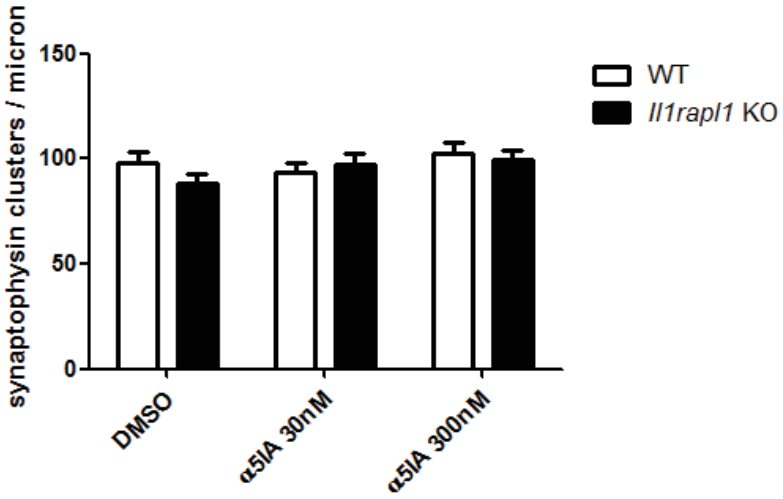

Figure 24. Presynapses are not altered after α5IA treatment. The number of synaptophysin clusters per micron is normalized by DMSO-treated wild-type (WT) neurons. Bars represent the mean and SEM from 50 neurons from 4 independent cultures.

DISCUSSION AND CONCLUSIONS

Intellectual disability (ID) is a genetically and clinically heterogeneous disorder. Total or partial deletions of *IL1RAPL1* gene, as well as duplications and frameshifts leading to premature stop codons were found in patients with ID. This gene encodes a synaptic protein and, due to its structural similarity, it was classified as part of the interleukin 1 receptor family of proteins. Nowadays, the role if this ID protein in interleukin 1 signaling remains unclear, but its synaptogenic role receives much attention since ID is often associated with synapse perturbations, and that synaptic connectivity resulting from the formation and elimination of synapses is critical for learning, memory and behavior function in developing and adult brain.

The studies realized during my PhD allowed to understand how specific *IL1RAPL1* mutations found in ID patients affect its synaptogenic activity, as well as which are the consequences of the absence of *IL1RAPL1* for synaptic function and cognition. Thanks to different enriching collaborations I could shed light on the importance of IL1RAPL1/PTPδ interaction for synapse formation, and on that not every cell/synapse is equally affected by IL1RAPL1 absence. This heterogeneous susceptibility lead to perturbations of the excitatory/inhibitory (E/I) balance that are translated into cognitive impairments. These observations were the basis to propose a treatment looking forward to reestablish the E/I balance and in consequence, the cognitive deficits in the absence of *IL1RAPL1*.

1. Importance of IL1RAPL1 - PTPδ interactions for synapse formation

Synaptogenesis is a well-orchestrated process, that in rodent hippocampus starts at the post-natal (P) period and stabilizes at adulthood (Steward & Falk 1986; Harris et al. 1992). Similarly, in hippocampal neurons in culture, synaptogenesis starts around 7 days *in vitro* (DIV), and reaches a peak after 21 DIV (Harrill et al. 2015) (Figure 25).

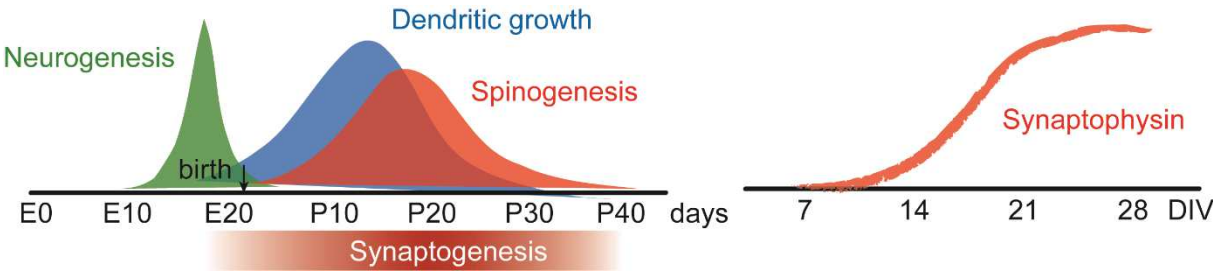

Figure 25. Synaptogenesis period in rat hippocampus and in hippocampal neurons in culture. Synaptogenesis in rat hippocampus is compared with other neurodevelopment processes (left), and in hippocampal neurons in culture (right) synaptophysin puncta was used as a marker to measure synapse abundance. E: embryonic, P: post-natal, DIV: days in vitro. Modified from Ben-Ari et al. 2007 and Harrill et al. 2015.

The discovery of IL1RAPL1/PTPδ interaction was a great advance in the understanding of the role of IL1RAPL1 in synaptogenesis. As confirmed by crystallography data, this interaction is specific to a subset of PTPδ isoforms generated by alternative splicing. Are IL1RAPL1-interacting PTPδ isoforms present at the same space and time that IL1RAPL1 during the development of synapses? Can other proteins, including a soluble isoform of IL1RAPL1 impair this interaction? These are questions that remain unanswered, but our preliminary results suggest that no major changes of the mRNA abundance of both partners are observed throughout hippocampal development (P1-30). An *Il1rapl1* short transcript predicted to lead to a protein containing only the Il1rapl1 extracellular domain was identified in the mouse, and the putative alternative splicing site was defined by Henriette Skala in our laboratory. The existence of a soluble IL1RAPL1 protein is an attractive possibility of signaling regulation, and it has been already reported for other members of IL1R family. A synthetic protein coding for IL1RAPL1 soluble protein prevents IL1RAPL1/PTPδ interaction both *in vitro* and *in vivo* (Yoshida et al. 2011) which evokes the possibility of regulating this interaction in physiological conditions. The biological relevance of this transcript is still unknown, since this putative mRNA was hardly observed in our experimental conditions.

Full length *Il1rapl1* expression is 4 times higher in mature (18 DIV) than in immature (2 DIV) neurons in culture, which coincides with maximal synapse presence in culture (Figure 25). The same increase was observed for the IL1RAPL1-interacting PTPδ isoform (meA+meB+), but not for the meA-meB- isoform, that shows a two-fold increase at 10 DIV that is maintained until 18 DIV. These observations suggest that

through isoform generation, PTPδ has different roles during synaptogenesis *in vitro*. However these results are semi-quantitative and protein expression levels should be evaluated in order to confirm the presence of both IL1RAPL1 and PTPδ in those periods.

Il1rapl1 and *Il1rapl2* mRNAs appear to have different expression patterns in the developing hippocampus, the first having a relative increase of expression at the peak of synaptogenesis (P20), and the latter's maximal expression is rather before this peak (P7-10, unpublished observations). Since IL1RAPL2 was shown to interact with PTPδ, those different expression patterns could mean differential regulation of PTPδ effects. It is important to emphasize that the PTPδ isoforms interacting with IL1RAPL2 have not been described yet. The major PTPδ isoform containing meA and meB that interacts with IL1RAPL1, can interact also with Slitrk3, although maybe with different affinities (Takahashi et al. 2012). This suggests that differential splicing of PTPδ in glutamatergic versus GABAergic axons contributes to selectivity in partner binding and function, similar to splicing in neurexins (Krueger et al. 2012). In addition, IL1RAcP was shown to interact with a different isoform of PTPδ and to induce excitatory but also inhibitory presynaptic increase. In contrast to IL1RAPL1, IL1RAcP protein does not appear to be particularly enriched in dendritic spines and it does not co-localize with PSD-95, which suggest its presence at inhibitory synapses or that the synaptogenic effects are due to overexpression of this protein (Gardoni et al. 2011; Yoshida et al. 2012).

The role of IL1RAPL1 as an adhesion and synaptogenic protein appears to be clearer than its involvement in interleukin 1 signaling. In neurons, the absence of Il1rapl1 impairs the IL1β-triggered JNK activation (Pavlowsky, Zanchi, et al. 2010). Our preliminary results suggest that this is not the case in astrocytes, since IL1β is still able to increase JNK phosphorylation in the absence of Il1rapl1. We were not able to detect Il1rapl1 protein in astrocytes, even if the mRNA abundance was not so different from neurons in culture. This observation could account for the lack of IL1RAPL1- regulated signaling in astrocytes.

Is IL1RAPL1 an accessory protein for IL1R1? This question remains to be answered. In one hand, IL1RAPL1 was shown to be unable to trigger classic IL1β signaling, like NFκB, ERK1/2 or p38 activation, but in the other hand it is unknown if the IL1RAPL1-regulated JNK activation by IL1β in neurons is also dependent on IL1R1 (Pavlowsky, Zanchi, et al. 2010). In order to elucidate if IL1RAPL1 can interact with IL1R1, we used

the bioluminescence resonance energy transfer (BRET) system, in collaboration with Julie Dam and Ralph Jockers (Institut Cochin, France). The procedure involves heterologous co-expression of fusion proteins, linking the proteins of interest to a bioluminescent donor enzyme or acceptor fluorophore. Energy transfer between these proteins can then be detected to monitor protein-protein interactions in real time (Pfleger et al. 2006). BRET assays were carried out in HEK293 cells in the presence or absence of IL1β, and in our experimental conditions, we were not able to detect any interaction between IL1R and IL1RAPL1. As this lack of interaction may be due to technical reasons, further experiments should be carried on to elucidate if IL1RAPL1 can act as an accessory protein.

It is now known that the intracellular domain of IL1RAPL1 is responsible for IL1RAPL1-induced spine formation. This is mediated by its interaction with two regulators of small GTPases: the RacGAP RhoGAP2 and the Rho and Cdc42 GEF Mcf2l. Interfering with IL1RAPL1/RhoGAP2 interaction affects dendritic spine shape, rendering them immature (Valnegri et al. 2011). Knocking down Mcf2l in neurons do not have any effect on spines *per se*, but abolishes two IL1RAPL1-dependent processes, the increase of dendritic spine number and the insertion of AMPA receptor subunits to the membrane (Hayashi et al. 2013). Both, RhoGAP2 and Mcf2l, interact with IL1RAPL1 TIR domain, but it is not known if their interaction is subjected to the same cellular conditions, and if they share the same effectors. For instance, Mcf2l effects are mediated through ROCK kinase, and RhoGAP2 is recruited to synapses by the IL1RAPL1/PTPδ interaction. However, it is possible that multiple signaling pathways mediate the IL1RAPL1-induced spine increase.

On the light of these observations, we wondered if some IL1RAPL1 mutations resulting in slight modifications of IL1RAPL1 extracellular domain, caused a decreased interaction with IL1RAPL1 partners, like PTPδ. The study of the functional consequences of Δex6 and C31R is interesting because it gives insight on how small protein modifications lead to IL1RAPL1 misfunction and thus ID. In HEK293 cells overexpressing C31R mutant, IL1RAPL1 protein levels were significantly reduced compared with L1RAPL1 wild-type protein. However, C31R substitution does not affect protein expression in neurons. In addition, C31R mutant is correctly expressed on the neuronal surface, and is found in both, dendritic spines and shafts. Strikingly, the

substitution of a single amino acid, Cys31 to Arg, is enough to severely reduce IL1RAPL1/PTPδ interaction. This is supported by a recent crystallographic study, in which Yamagata and collaborators mapped the interaction between the Ig1 domain of Il1rapl1 with both Ig2 and Ig3 domains of PTPδ (Yamagata, Yoshida, et al. 2015) (Figure 14). Due to the critical roles of IL1RAPL1 Asp37 and Trp34 on IL1RAPL1/PTPδ interaction, Cys31 change to Arg is very likely to affect this interaction (see Figure 18), which was confirmed by cell aggregation assays and co-immunoprecipitation. As a result, IL1RAPL1/PTPδ-mediated synaptogenesis is severely reduced by C31R mutation.

An in-frame deletion of *IL1RAPL1* exon6 was found in ID patients from two unrelated families, P72 and BMC. The only common clinical features between affected patients from both families are mild ID as well as motor and language delay. The in-frame deletion of *IL1RAPL1* exon 6 is predicted to lead to a slightly shorter protein, lacking 25 amino acids between the Ig1 and Ig2 domains. In both HEK293 cells and hippocampal neurons overexpressing IL1RAPL1 Δex6, we observed a reduction of the mutated protein. As a consequence, IL1RAPL1-induced synaptogenic activity is decreased in neurons overexpressing Δex6 mutant. We also observed a reduction of interaction with PTPδ, but this is likely due to the decrease in protein expression, rather than a loss of affinity. All this data suggests a loss of function after the deletion of exon 6. The protein decrease may be caused by mRNA degradation by the nonsense-mediated decay system, or protein degradation caused by its miss-folding (Miller & Pearce 2014; Caramelo & Parodi 2015). Our preliminary data suggest that *IL1RAPL1* Δex6 mRNA is expressed at the same levels than wild-type *IL1RAPL1* mRNA. This was assessed in RNA isolated from neural precursor cells (NPCs) obtained from patient's fibroblasts (patient III-2 of family P72). We measured *IL1RAPL1* mRNA relative abundance by real time quantitative PCR using a pair of primers upstream of *IL1RAPL1* exon 6 deletion. We observed that the relative abundance of *IL1RAPL1* mRNA in patient's NPCs was the same than in NPCs from a healthy individual ruling out the hypothesis of IL1RAPL1 mRNA degradation. Altogether, our data leads us to conclude that the loss of synaptogenic activity of IL1RAPL1 Δex6 is due to protein degradation.

The case of patient III-2 of family P72 is of particular interest because it is a female presenting with ID, and in this type of X-linked gene transmission female carriers do not always express the phenotype. In addition to the IL1RAPL1 exon 6 deletion, exome sequencing of genomic DNA from this patient showed that she also has a point mutation in the gene *FLNA*, located also in the X chromosome. Unlike *IL1RAPL1* Δex6, *FLNA* mutation was inherited from her mother who presents with an intellectual deficit. X-inactivation studies at the *FMR2* locus revealed a strong bias with major expression of the variant allele in fibroblasts from the mother, but there was not a bias in patient III-2. In both cases we cannot exclude a skewed X chromosome inactivation in their brain. *FLNA* gene was described as responsible for periventricular heterotopia (PVH) characterized by nodules lining the ventricular surface produced by a defect on neuronal migration (Fox et al. 1998). This gene encodes filamin 1, an actin-binding/crosslinking phosphoprotein involved in cytoskeleton-plasma membrane interaction. Most PVH patients with nonsense mutations leading to truncated filamin 1 protein or point mutations in splicing sites are heterozygous females with only mild ID to normal IQ whereas hemizygous males show early mortality (Fox et al. 1998). The variant found in our study was predicted to be probably damaging by *in silico* analysis (Polyphen2). However, the patient III-2 in our study did not present any brain structural abnormalities, so we think that the deletion on *IL1RAPL1* is the only cause of ID in this patient. However we cannot discard the contribution of *FLNA* mutation to the phenotype, since it could affect unexplored filamin 1 functions other that neuronal migration.

The remaining synaptogenic activity in brain lacking IL1RAPL1 is carried out by different proteins. As mentioned earlier in this discussion, PTPδ not only interacts with IL1RAPL1, but also with other related proteins with potential synaptogenic activity, like IL1RAPL2 and IL1RAcP. Can other IL1RAPL1-related proteins compensate the lack of IL1RAPL1 in ID patients? *IL1RAPL2* is also located in the X chromosome, and it codes for a protein very similar to IL1RAPL1. It interacts with PTPδ, suggesting that in the absence of IL1RAPL1, IL1RAPL2/PTPδ could induce synaptogenesis. Not all IL1RAPL1 functions are shared by IL1RAPL2, for example, in the absence of IL1RAPL1 the JNK-triggered signaling dependent on IL1RAPL1 would not be relieved by IL1RAPL2. However, the contribution of JNK activity regulation by IL1RAPL1 in ID phenotype needs to be further elucidated.

A recent report showed that expression of *IL1RAPL1* mRNA was reduced by 92% in fibroblasts from a patient with a homozygous deletion of *PTPRD* (Choucair et al. 2015). The authors of the study suggest that *IL1RAPL1* down regulation could explain the ID in this patient, but the mechanism of how the loss of PTPδ would decrease IL1RAPL1 at the transcriptional level remains to be clarified. We have observed almost undetectable levels of *IL1RAPL1* transcripts in fibroblasts, and this was also reported by others. The differences in *IL1RAPL1* expression between the patient and the control fibroblasts observed by Choucair and collaborators could be related to either inter individual differences or to the limits of the assay at low transcript expression.

2. Role of IL1RAPL1 in synapse formation and in E/I balance

To date, most of the *IL1RAPL1* mutations described in ID patients likely result in the loss of function of IL1RAPL1 protein. This makes the *Il1rapl1* KO mice a convenient tool that allows the study of the consequences of Il1rapl1 loss of function in complete circuits and even on behavior.

The spatial memory and fear conditioning are impaired in *Il1rapl1* KO mice, but it is noteworthy that they can perform some of these tasks if they are trained for long enough ((Houbaert et al. 2013; Zhang et al. 2014; Yasumura et al. 2014) and Hamid Meziane unpublished observation). Moreover, the underlying mechanisms are impaired in the brain structures involved in these cognitive tasks. In the hippocampus of *Il1rapl1* KO mice, long-term potentiation (LTP) is reduced when elicited by theta burst stimulation but not by high frequency stimulation, indicating stimulus- or mechanism-dependent effects (Pavlowsky, Gianfelice, et al. 2010). Similarly, thalamo-lateral amygdala (LA) LTP is also impaired in those mice. Different steps of the cognitive process can be affected in different circuits in the absence of Il1rapl1. For example, *Il1rapl1* KO mice have defects in contextual memory expression rather than memory formation, while they have deficits in cued fear memory formation but not expression (Zhang et al. 2014).

Establishing and maintaining the appropriate ratio of excitatory versus inhibitory synapses (E/I ratio) are critical factors that define circuit threshold and output responsiveness. Disruption of the E/I beyond an acceptable point leads to aberrant

transmission states that, when maintained chronically, cause severe dysfunctions (Gatto & Broadie 2010). Dysregulation of E/I balance is proposed to impair neural processing and underlie cognitive deficits in ID. The factors that may contribute to the imbalance include the selective loss of either excitatory or inhibitory synapses, the favoring of formation or maintenance of one class of synapse relative to the other, or the heterogeneity of vulnerability of synapses. Such imbalance may arise during initial neural circuit formation, or later as an inability to maintain the E/I ratio in mature circuits and leading to plasticity impairments. By stimulating the thalamo-lateral amygdala projections, the anatomic substrate for cued fear conditioning, we observed a decrease of excitation while inhibition remained unchanged in the *Il1rapl1* KO mice (Figure 19). This leads to an imbalance of E/I ratio, that was also observed in hippocampo-basolateral amygdala projections (Zhang et al. 2014).

Similarly, Gambino and collaborators showed that in the absence of Il1rapl1 the E/I balance was altered in the early post-natal development of the cerebellum (P10 to P14, see Figure 26). This was evidenced by a disinhibition of deep cerebellar nuclei (DCN) neurons, controlled by Purkinje cells (PC). As shown in Figure 26, PC activity is regulated by the E/I balance of cerebellar cortex circuits: The excitatory circuit is principally composed by granule cells (G) whose axons are known as parallel fibers that establishes synapses with PC and interneurons in the molecular layer. The inhibitory local circuit is formed by those interneurons (In).

When assessing the impact of parallel fibers excitation on interneurons and Purkinge cells in the absence of Il1rapl1, excitatory inputs on PC are preserved but interneurons are more susceptible to stimulation by parallel fibers. These results in PC silencing and consequently in DCN disinhibition, that occurs latter in normal cerebellum development. This E/I balance impairment is reestablished at later developmental stages (from P28) so the impact, if any, of this imbalance on cerebellar development of *Il1rapl1* KO mouse is not clear. Altogether, those observations suggest that E/I balance disruption is a functional signature of Il1rapl loss of function, at different developmental stages, in different circuits, and underlying different cognitive impairments.

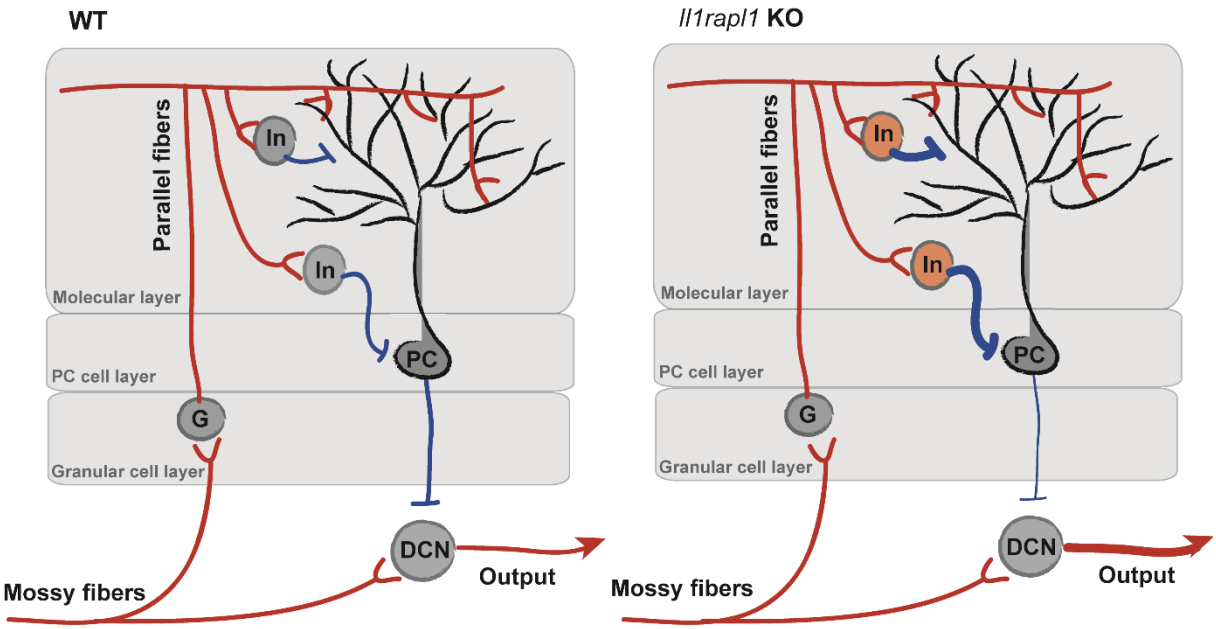

Figure 26. Cerebellar circuits are affected during development in the absence of Il1rapl1. In normal conditions (WT, left), parallel fibers form synapses into interneurons (In), as well as in GABAergic Purkinge cells (PC). PCs negatively regulate the output of deep cerebellar nuclei (DCN). In the absence of Il1rapl1 (*Il1rapl1* KO, right), inhibitory neurons are more sensitive to activation by parallel fibers (In, orange), which increases PC inhibition, and thus DPC disinhibition. Excitatory and inhibitory input are shown in red and blue, respectively. G: granule cells, In: interneurons, PC: Purkinge cells, DCN: deep cerebellar nucleus. Modified from Pavlowsky 2009.

These studies also suggest that not every synapse is equally affected by Il1rapl1 absence. This is supported by *in vivo* studies that reveal that neurons in different brain structures have different phenotypes in the absence of Il1rapl1. For example, in *Il1rapl1* KO mice a decrease of dendritic spines was observed in cortical and hippocampal neurons, but not in principal cells of lateral amygdala (Pavlowsky, Gianfelice, et al. 2010; Yasumura et al. 2014; Houbaert et al. 2013). Similarly, dendrite branching is increased in hippocampal but not in cortical neurons in the absence of Il1rapl1 (Caterina Montani, unpublished observations). These differences could reflect either the abundance of Il1rapl1 itself, or of its molecular partners. *Il1rapl1* mRNA seems to be present at the same low expression level in all types of neurons and in all brain regions, but differences may reside in Il1rapl1 protein expression. Evaluating the protein distribution in the mouse brain has been addressed several times, with non-satisfactory results due to the lack of sensitive tools.

Heterogeneous synaptic distribution of Il1rapl1 partners or differences in the composition of synaptic machinery are also cues to explain the different susceptibility

of synapses in the absence of Il1rapl1. In the case of E/I imbalance in the cerebellum, it was suggested that regulation of excitability by NCS-1 is impaired in interneurons in the absence of *Il1rapl1*. This is supported by the fact that NCS-1 is expressed in those cells and not in all Purkinje cells, which are not affected by Il1rapl1 absence (Jinno et al. 2002; Gambino et al. 2009). Moreover, as mentioned before, not every neuron possesses the same AMPA receptors subunits composition, and the particular subset expressed in the synapses on LA or cerebellar interneurons may be less or more sensitive respectively to Il1rapl1 and may change upon circuits maturity (Isaac et al. 2007; Tóth & McBain 1998).

Among the Il1rapl1 interactions that remain unexplored, the interaction with CFTR is particularly interesting. This protein (cystic fibrosis transmembrane conductance regulator or ATP-binding cassette sub-family C, member 7) is a chloride channel and even if the interaction with IL1RAPL1 was observed in an intestinal cell line, this protein is expressed in neurons (Wang et al. 2006; Guo et al. 2009). In epithelial cells, CFTR interacts directly or indirectly with protein phosphatase-2A (PP2A), AMP kinase (AMPK), syntaxin-1A (SYN1A), synaptosome-associated protein 23 kDa (SNAP23) and Munc-18a. These proteins inhibit channel activity and reduce CFTR-mediated chloride secretion across the apical plasma membrane in epithelial cells. Other CFTR-interacting proteins that enhance its activity, either directly or indirectly, include Na^+/H^+ exchanger regulatory factor isoform-1 (NHERF1), protein kinase A (PKA), receptor for activated C-kinase-1 (RACK1), protein kinase C (PKC), and ezrin (Guggino & Stanton 2006). All those proteins are expressed in the brain, and some are directly linked to synaptic vesicle fusion and interact directly with CFTR (syntaxin and Munc-18 are members of the SNARE complex, Figure 5). In neurons, chloride channels mediate passive chloride transport along the chloride concentration gradient capable to modulate chloride homeostasis and neuronal excitability. The particular function of CFTR in neurons, its interaction with IL1RAPL1 and its potential contribution on E/I balance in these cells remain to be elucidated.

The presynaptic consequences of Il1rapl1 loss of function in the hippocampus were assessed by electron microscopy (Pavlowsky, Gianfelice, et al. 2010). The measure of presynaptic terminal area, total synaptic vesicles density, and docked synaptic vesicles density was not changed in *Il1rapl1* KO mice. This was confirmed by paired pulse

facilitation in the hippocampus, whose responses showed no difference at any interstimulus intervals recorded compared with wild-type mice. Those observations demonstrate that neither the structure nor the plasticity of presynaptic terminals is affected in the hippocampus by Il1rapl1 absence. Whether there are consequences of Il1rapl1 absence at the presynaptic level in different brain areas remains to be investigated. For this purpose, conditional *Il1rapl1* KO mice could allow to selectively abolish Il1rapl1 expression in projecting neurons, while leaving intact the postsynaptic neurons. This mice model was generated in our laboratory and is already available for further studies. In the other hand, restoring IL1RAPL1 expression in particular brain areas in *Il1rapl1* KO mice can also help in the dissection of the circuits and cells affected by Il1rapl1 loss.

Conditional *Il1rapl1* KO mice would also allow to investigate the role of Il1rapl1 during development. As for the cerebellum, some defects on certain brain circuits may occur early during development. Being able to knockdown Il1rapl1 or reestablish its expression in a particular developing time can shed light on the precise moments where the presence of Il1rapl1 is important. Moreover, generation of better tools that permit a more direct study of the physiological role of this protein will be crucial to avoid overexpression of IL1RAPL1, and will allow mapping of protein Il1rapl1 expression in different cell types.

3. Towards a treatment for restoring E/I balance and improve cognitive deficits in ID mouse models

As mentioned earlier, the impairment of E/I balance is a feature shared by different ID mouse models, and GABAergic system is a commonly disturbed pathway in many neurodevelopmental disorders. For example, studies in the mice model for Fragile X syndrome (*Fmr1* KO) showed an overall downregulation of GABAergic system that is brain region- and age-dependent, and the cognitive impairments in a mice model for Down Syndrome (Ts65Dn) are thought to be due to an excess of inhibition (Braat & Kooy 2015a; Martínez-Cué et al. 2014). Targeting $GABA_A$ receptors to inhibit or increase their function has been proposed and starts to be widely explored in both mice models: Increasing GABAergic signaling in *Fmr1* KO and decreasing it in Ts65Dn mice is able to restore some behavioral phenotypes.

Our results suggest that blocking $GABA_A$ receptor function improves the cognitive deficits in *Il1rapl1* KO mice, presumably by restoring the E/I balance. The recall deficit observed in *Il1rapl1* KO mice was improved by local infusion of a non-selective $GABA_A$ receptor antagonist (bicuculline) into the LA before cued fear conditioning. Surprisingly, the same strategy was not able to correct the lack of contextual fear reaction in the same mice. Since both tasks involve different projection and targets in the amygdala, these observations suggest that targeting deficits in different circuits may take into account the intrinsic properties of each of them. However, due to its low selectivity and high side-effects unless locally delivered, bicuculline cannot be used as a treatment. In this line, α5IA appears to be a good treatment that targets selectively α5-containing $GABA_A$ receptors that crosses the brain-blood barrier and does not have any undesirable side effects in mice and rats (Dawson et al. 2006).
In healthy normal elderly volunteers (from 65-79 years), administration of α5IA did not improve paired associate learning (Atack 2010). This result may be due to the fact that connectivity in certain brain regions, as well as synaptic plasticity is decreased with age (Kelly et al. 2006). However, α5IA attenuates the ethanol-induced deficits in word-list learning (Nutt et al. 2007). Unfortunately, preclinical renal toxicity prevented further clinical development of this inverse agonist (Atack 2010).

α5 subunit is mostly expressed in the hippocampus, but its expression in other brain structures has been also observed (Collinson et al. 2002; Pirker et al. 2000). We observed that the treatment of *Il1rapl1* KO mice with this drug enhanced hippocampal-dependent memory, as assessed with the Morris water maze. In the present study, the inverse agonist does not have an effect on the performance of the WT mice. This is surprising because cognitive improvement has been associated with the blockage of α5 $GABA_A$ subunit, and for instance, *Gabra5* KO mice and α5IA-treated rats perform better hippocampal-dependent cognitive tasks that WT or vehicle treated animals (Collinson et al. 2002; Dawson et al. 2006). On the other hand, our data demonstrate that α5IA is able to improve the cognitive deficits in *Il1rapl1* KO mice, presumably by restoring the E/I balance.

To our knowledge, the signaling mechanism triggered by this inverse agonist is unknown. α5IA treatment increases the abundance of some IEG, like *c-Fos*, *in vivo*

and *in vitro* (Braudeau, Dauphinot, et al. 2011). The basal decrease of *c-Fos* mRNA levels reported in Ts65Dn mice was increased by α5IA treatment, and we observed the same phenomena in *Il1rapl1* KO neurons. This IEG is considered as a plasticity gene which could give cues to understand the cellular signaling triggered by α5IA (Miyashita et al. 2008).

Besides the pharmacological effect on α5-containing $GABA_A$ receptors, α5IA induces an increase of the excitatory scaffolding protein PSD-95 (Figure 27). PSD-95 is extremely abundant in the postsynaptic density (PSD) with an estimate of 300 copies of this protein in a purified PSD, compared with for example, 120 copies of AMPA and NMDA receptors (Sheng & Kim 2011). Indeed PSD-95 family proteins have many interactors in synapses which makes of these scaffolding proteins a major synaptic element with a strong influence on synaptic transmission and plasticity (Kim & Sheng 2004).

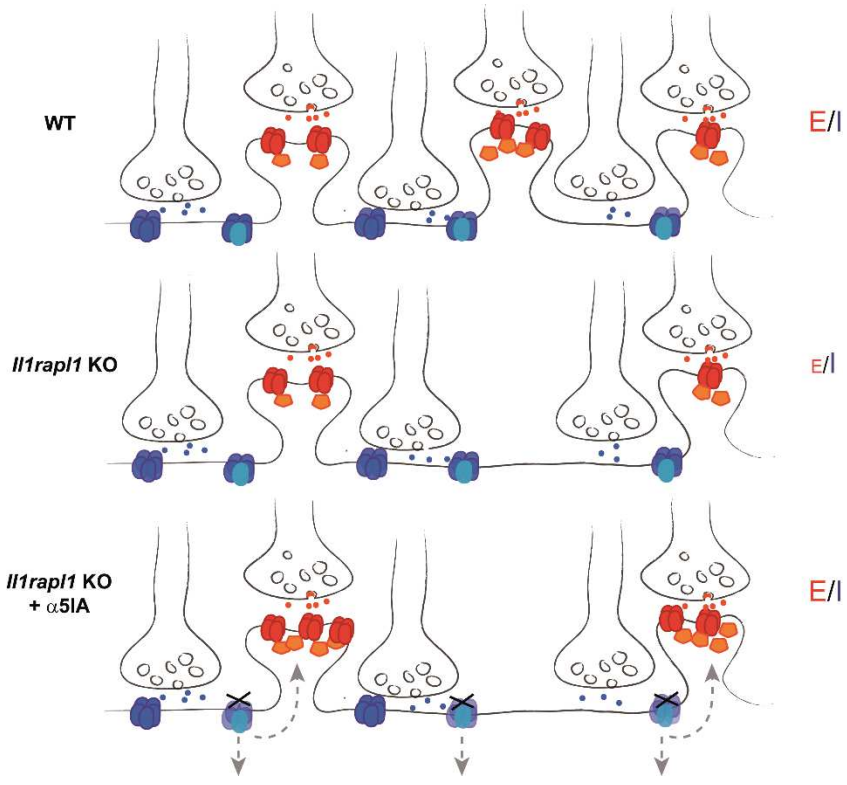

Figure 27. Possible mechanism for α5IA-induced improvement in hippocampal-dependent tasks in Il1rapl1 KO mice. In WT hippocampal neurons (up), the E/I balance is maintained by excitatory (red) and inhibitory (blue) synapses. In the absence of Il1rapl1 (middle), there is a decrease of excitatory synapses that generates an E/I imbalance and deficits in hippocampal-dependent cognitive tasks. When *Il1rapl1* KO mice are treated with α5IA, an improvement of the performance on these tasks is observed. One possible mechanism is restoring the E/I balance, and may include changes in PSD-95 scaffolding protein (PSD-95, orange) among others.

As observed in Morris water maze, α5IA treatment increased PSD-95 clusters in *Il1rapl1* KO, but not in WT neurons. Even if the precise signaling leading to these changes was not further studied, we can hypothesized that this PSD-95 cluster increase would participate to the reestablishment of the E/I balance in Il1rapl1-deficient mice (Figure 27).

In *Il1rapl1* KO neurons, we observed a surprising differential effect of α5IA treatment on PSD-95 clusters depending of the dose used. This could be explained by non-specific mechanisms. For example, α5IA was found to be either a low-efficacy partial inverse agonist, antagonist, or very weak partial agonist at other $GABA_A$ receptor subunits (Dawson et al. 2006). This drug acts as a modest inverse agonist of α1 that could produce *in vivo* effects, especially given the greater abundance of the α1 compared with α5 subunits. However the α1 subtype is known to mediate the proconvulsant effects of benzodiazepines (Rudolph et al. 1999), and since no effects of this nature were observed after α5IA treatment, this hypothesis can be ruled out. Similarly the very weak efficacy at the α2 and α3 subunits do not seem to have an effect *in vivo* since these subtypes are associated with anxiolytic-like activity (Atack et al. 2006) and α5IA had no obvious effect on anxiety. However, we cannot rule out that the effect on other subunits could participate to the observed PSD-95 clustering changes *in vitro* after α5IA treatment.

Our results on *Il1rapl1* KO mice together with the observations in other ID mice models, support the advantageous effect of targeting α5 $GABA_A$ receptor subunit to treat the cognitive deficits associated with neurodevelopmental disorders. It would be fundamental to treat the animals at different developmental stages in order to evaluate the capacity of the inverse agonist to correct cognitive deficits when applied during the establishment of specific brain circuits.

APENDIX

Table 1. Reported mutations on IL1RAPL1 in ID patients and their consequences for protein function. It is also indicated if ID is accompanied of other clinical features in these patients.

References	Mutation / exons	Protein	Functional consequences	ID/ASD
Nonsense mutations				
(Carrié et al. 1999; Pavlowsky, Gianfelice, et al. 2010; Valnegri et al. 2011)	nonsense, exon 11	Y459X predicted to lead to a protein lacking part of the TIR domain and the entire C-terminal domain.	ΔC does not increase dendritic spines number nor changes their length and width, increases the number of active presynaptic compartments and fails to target RhoGAP2 to synapses.	ID
(Kozak et al. 1993; Tabolacci et al. 2006)	nonsense, exon 11	W487X predicted to produce a protein lacking half of the TIR domain and the entire C-terminal domain.		ID
(Piton et al. 2008)	nonsense, exon 9	I367SX6, predicted to produce a protein lacking part of the trans-membrane domain as well as the entire intracellular domain.	Not targeted to the membrane, does not rescue neurite number and length phenotype after *Il1rapl1* knockdown.	ASD
Missense mutations				
(Tarpey et al. 2009; Ramos-Brossier et al. 2014)	missense, exon 3	One amino acid change before the first Ig-like domain (C31R). *In silico* analysis predicts damage to the structure and function.	C31R is targeted to the membrane and to dendritic spines. Fails to increase dendritic spines and functional excitatory synapses. Impaired interaction with PTPδ, but induces basal JNK activation.	ID
(Butler et al. 2015)	missense, exon 11	P478Q, localized in TIR domain. Damaging by *in silico* prediction.		ASD
Exon deletions				
(Behnecke et al. 2011)	deletion, exon 2	Probably not produced.		ID
(Franek et al. 2011)	deletion, exons 1-5	Probably not produced.		ID
(Carrié et al. 1999)	deletion exon 3-5	Probably not produced.		ID
(Nawara et al. 2008)	deletion exons 3-6 *	Probably not produced.		ID
(Behnecke et al. 2011)	deletion, exon 3-5	Probably not produced.		ID
(Whibley et al. 2010)	deletion, exons 3-5	Probably not produced.		ID

References	Mutation / exons	Protein	Functional consequences	ID/ASD
Exon deletions (continued)				
(Mikhail et al. 2011)	deletion exons 2-6	Probably not produced.		ID
(Youngs et al. 2012)	deletion, exons 3-11	Probably not produced.		ASD/ID
(Barone et al. 2013; Tucker et al. 2013)	deletion, exon 3	Out of frame deletion leading to a premature stop codon A28EfxX7. Protein is probably not produced.		ID
(Franek et al. 2011; Valnegri et al. 2011)	deletion, exons 3-6 *	In frame deletion p.28_259del, predicted to produce a shorter protein devoid of the two first Ig-like domains.	ΔN does not increase dendritic spine density, nor changes spine length and width. Fails to increase functional excitatory synapses, lacks interaction with PTPδ and fails to target RhoGAP2 to synapses.	ID
(Mignon-Ravix et al. 2014)	deletion, exons 3-5	In frame deletion of 207 amino acids (N29_A235del) predicted to produce a protein devoid of the 2 first Ig-like domains.		ID
(Ramos-Brossier et al. 2014)	deletion, exon 6	In frame deletion that results in a shorter extracellular domain. Protein instability.	Maintains the capacity to activate JNK.	ID
(Piton et al. 2008)	deletion, exons 3-7	Frame shift A28EfxX15, predicted to produce a short protein containing only 8 amino acids in addition to the signal peptide.		ID/ASD
(Redin et al. 2014)	deletion , exon 7	Predicted to produce a truncated protein containing only the first two Ig-like domains.		ID
(Jin et al. 2000)	deletion exons 9-11	Predicted to produce a truncated protein containing only the extracellular domain.		ID, MD, GKD, CAH
(Sasaki et al. 2003)	deletion , exons 7#-11	Predicted to produce a shorter protein containing part of extracellular domain.		ID and AHC

References	Mutation / exons	Protein	Functional consequences	ID/ASD
Deletion by chromosome inversion				
(Bhat et al. 2008)	X chromosome inversion with breakpoint in intron 2	Probably not produced.		ASD
(Leprêtre et al. 2003)	X chromosome inversion with breakpoint in exon 6	Predicted to produce a truncated protein, containing the entire extracellular domain.		ID
Large deletions containing the entire IL1RAPL1 gene				
(Zhang et al. 2004)	Xp22.1-p21.3 IL1RAPL1 and DAX1			ID and GKD
(Marshall et al. 2008)	CNV reported, but no information available			ASD
(Dinopoulos et al. 2014)	Xp21.2-p21.3 microdeletion #			ID and SE
Duplications				
(Utine et al. 2014)	Duplication, exons 4-5			ID
J. Lauer, personal communication	duplication Xp22.11-p21.2, including IL1RAPL1			ID
(Honda et al. 2010)	duplication, exon 2			ID and WS
Chromosome translocations				
(Moysés-Oliveira et al. 2015)	Translocation chromosomes X and 19 with breakpoint in *IL1RAPL1* intron 2, generates a *ZNF611-IL1RAPL1* fusion transcript.	Probably not produced.		ID and AHC
SNP in coding regions				
(Piton et al. 2008; Ramos-Brossier et al. 2014)	missense, exon 11	Ileu643Val variant produces a full length protein. *In silico* analysis predicts it to be tolerated by the protein.	No changes in protein function	-
(Piton et al. 2008)	missense, exon 10	Lys379Arg *In silico* analysis predicts it to be probably damaging for the protein.		-
(Piton et al. 2008)	missense, exon 11	Gln618Hys *In silico* analysis predicts it to be tolerated by the protein.		-

References	Mutation / exons	Protein	Functional consequences
SNP in coding regions (continued)			
(Piton et al. 2008)	missense, exon 11	Thr637Ser *In silico* analysis predicts it to be tolerated by the protein.	

* Modified from original article, in accordance with hg38 assembly. # Not precisely mapped. SNP: single nucleotide polymorphism. ID: intellectual disability, ASD: autism spectrum disorder, WS: West syndrome, SE: Startle epilepsy, AHC: adrenal hypoplasia congenital, GKD: glycerol kinase deficiency, MD: muscular dystrophy. *In silico* prediction of protein damage was performed with Pholyphen2

BIBLIOGRAPHY

Abidi, F.E., Holinski-Feder, E., Rittinger, O., F, K., Lubs, H.A., Stevenson, R.E., Schwartz, C.E., 2002. A novel 2 bp deletion in the TM4SF2 gene is associated with MRX58. *J. Med. Genet.*, **39**: 430–433.

Ackley, B.D., Harrington, R.J., Hudson, M.L., Williams, L., Kenyon, C.J., Chisholm, A.D., Jin, Y., 2005. The two isoforms of the Caenorhabditis elegans leukocyte-common antigen related receptor tyrosine phosphatase PTP-3 function independently in axon guidance and synapse formation. *J. Neurosci.*, **25**: 7517–7528.

Adzhubei, I.A., Schmidt, S., Peshkin, L., Ramensky, V.E., Gerasimova, A., Bork, P., Kondrashov, A.S., Sunyaev, S.R., 2010. A method and server for predicting damaging missense mutations. *Nat. Methods*, **7**: 248–249.

Aligianis, I. a, Johnson, C. a, Gissen, P., Chen, D., Hampshire, D., Hoffmann, K., Maina, E.N., Morgan, N. V, Tee, L., Morton, J., Ainsworth, J.R., Horn, D., Rosser, E., Cole, T.R.P., Stolte-Dijkstra, I., Fieggen, K., Clayton-Smith, J., Mégarbané, A., Shield, J.P., Newbury-Ecob, R., Dobyns, W.B., Graham, J.M., Kjaer, K.W., Warburg, M., Bond, J., Trembath, R.C., Harris, L.W., Takai, Y., Mundlos, S., Tannahill, D., Woods, C.G., Maher, E.R., 2005. Mutations of the catalytic subunit of RAB3GAP cause Warburg Micro syndrome. *Nat. Genet.*, **37**: 221–223.

Allen-Brady, K., Cai, G., Cannon, D., Robison, R., McMahon, W.M., Coon, H., Buxbaum, J.D., 2011. No evidence for IL1RAPL1 involvement in selected high-risk autism pedigrees from the AGRE data set. *Autism Res.*, **4**: 293–296.

Andre, R., Lerouet, D., Kimber, I., Pinteaux, E., Rothwell, N.J., 2005. Regulation of expression of the novel IL-1 receptor family members in the mouse brain. *J. Neurochem.*, **95**: 324–330.

Andre, R., Pinteaux, E., Kimber, I., Rothwell, N.J., 2005. Differential actions of IL-1 alpha and IL-1 beta in glial cells share common IL-1 signalling pathways. *Neuroreport*, **16**: 153–157.

Atack, J.R., 2010. Preclinical and clinical pharmacology of the GABAA receptor alpha5 subtype-selective inverse agonist alpha5IA. *Pharmacol. Ther.*, **125**: 11–26.

Atack, J.R., Maubach, K.A., Wafford, K.A., Connor, D.O., Rodrigues, A.D., Evans, D.C., Tattersall, F.D., Chambers, M.S., Macleod, A.M., Eng, W., Ryan, C., Hostetler, E., Sanabria, S.M., Gibson, R.E., Krause, S., Burns, H.D., Hargreaves, R.J., Agrawal, N.G.B., Mckernan, R.M., Murphy, M.G., Gingrich, K., Dawson, G.R., Musson, D.G., Petty, K.J., 2009. In vitro and in vivo properties of 3-tert-butyl-7-(5-methylisoxazol-3-yl)-2-(1-methyl-1H-1,2,4-triazol-5-ylmethoxy)-pyrazolo[1,5-d]-[1,2,4]triazine (MRK-016), a GABAA receptor alpha5 subtype-selective inverse agonist. *J. Pharmacol. Exp. Ther.*, **331**: 470–484.

Atack, J.R., Wafford, K.A., Tye, S.J., Cook, S.M., Sohal, B., Pike, A., Sur, C., Melillo, D., Bristow, L., Bromidge, F., Ragan, I., Kerby, J., Street, L., Carling, R., Castro, J.L., Whiting, P., Dawson, G.R., McKernan, R.M., 2006. TPA023 [7-(1,1-dimethylethyl)-6-(2-ethyl-2H-1,2,4-triazol-3-ylmethoxy)-3-(2-fluorophenyl)-1,2,4-triazolo[4,3-b]pyridazine], an agonist selective for alpha2- and alpha3-containing GABAA receptors, is a nonsedating anxiolytic in rodents and primates. *J. Pharmacol. Exp. Ther.*, **316**: 410–422.

Avital, A., Goshen, I., Kamsler, A., Segal, M., Iverfeldt, K., Richter-Levin, G., Yirmiya, R., 2003. Impaired interleukin-1 signaling is associated with deficits in hippocampal memory processes and neural plasticity. *Hippocampus*, **13**: 826–834.

Ba, W., van der Raadt, J., Nadif Kasri, N., 2013. Rho GTPase signaling at the synapse: implications for intellectual disability. *Exp. Cell Res.*, **319**: 2368–2374.

Bahi, N., Friocourt, G., Carrié, A., Graham, M.E., Weiss, J.L., Chafey, P., Fauchereau, F., Burgoyne, R.D., Chelly, J., 2003. IL1 receptor accessory protein like, a protein involved in X-linked mental retardation, interacts with Neuronal Calcium Sensor-1 and regulates exocytosis. *Hum. Mol. Genet.*, **12**: 1415–1425.

Ban, E.M., Sarlière, L.L., Haour, F.G., 1993. Interleukin-1 binding sites on astrocytes. *Neuroscience*, **52**: 725–733.

Barone, C., Bianca, S., Luciano, D., Di Benedetto, D., Vinci, M., Fichera, M., 2013. Intragenic ILRAPL1 deletion in a male patient with intellectual disability, mild dysmorphic signs, deafness, and behavioral problems. *Am. J. Med. Genet. A*, **161A**: 1381–1385.

Bassani, S., Cingolani, L. a., Valnegri, P., Folci, A., Zapata, J., Gianfelice, A., Sala, C., Goda, Y., Passafaro, M., 2012. The X-linked intellectual disability protein TSPAN7 regulates excitatory synapse development and AMPAR trafficking. *Neuron*, **73**: 1143–1158.

Bayés, À., Collins, M.O., Croning, M.D.R., van de Lagemaat, L.N., Choudhary, J.S., Grant, S.G.N., 2012. Comparative study of human and mouse postsynaptic proteomes finds high compositional conservation and abundance differences for key synaptic proteins. *PLoS One*, **7**: e46683.

Bayés, À., Lagemaat, L.N. Van De, Collins, M.O., Croning, M.D.R., Ian, R., Choudhary, J.S., Grant, S.G.N., 2011. Characterisation of the proteome , diseases and evolution of the human postsynaptic density. *Nat. Neurosci.*, **14**: 19–21.

Behnecke, A., Hinderhofer, K., Bartsch, O., Nümann, A., Ipach, M.-L.L., Damatova, N., Haaf, T., Dufke, A., Riess, O., Moog, U., 2011. Intragenic deletions of IL1RAPL1: Report of two cases and review of the literature. *Am. J. Med. Genet. A*, **155A**: 372–379.

Bellinger, F.P., Madamba, S., Siggins, G.R., 1993. Interleukin 1β inhibits synaptic strength and long-term potentiation in the rat CA1 hippocampus. *Brain Res.*, **628**: 227–234.

Ben-Ari, Y., Gaiarsa, J., Tyzio, R., Khazipov, R., 2007. GABA: a pioneer transmitter that excites immature neurons and generates primitive oscillations. 1215–1284.

Berkel, S., Marshall, C.R., Weiss, B., Howe, J., Roeth, R., Moog, U., Endris, V., Roberts, W., Szatmari, P., Pinto, D., Bonin, M., Riess, A., Engels, H., Sprengel, R., Scherer, S.W., Rappold, G. a, 2010. Mutations in the SHANK2 synaptic scaffolding gene in autism spectrum disorder and mental retardation. *Nat. Genet.*, **42**: 489–491.

Bhalla, K., Luo, Y., Buchan, T., Beachem, M. a., Guzauskas, G.F., Ladd, S., Bratcher, S.J., Schroer, R.J., Balsamo, J., DuPont, B.R., Lilien, J., Srivastava, A.K., 2008. Alterations in CDH15 and KIRREL3 in patients with mild to severe intellectual disability. *Am. J. Hum. Genet.*, **83**: 703–713.

Bhat, S.S., Ladd, S., Grass, F., Spence, J.E., Brasington, C.K., Simensen, R.J., Schwartz, C.E., DuPont, B.R., Stevenson, R.E., Srivastava, A.K., 2008. Disruption of the IL1RAPL1 gene associated with a pericentromeric inversion of the X chromosome in a patient with mental retardation and autism. *Clin. Genet.*, **73**: 94–96.

Bienvenu, T., des Portes, V., McDonell, N., Carrié, A., Zemni, R., Couvert, P., Ropers, H.H., Moraine, C., Van Bokhoven, H., Fryns, J.P., Allen, K., Walsh, C.A., Boué, J., Kahn, A., Chelly, J., Beldjord, C., 2000. Missense mutation in PAK3, R67C, causes X-linked nonspecific mental retardation. *Am. J. Med. Genet.*, **93**: 294–298.

Billuart, P., Bienvenu, T., Ronce, N., des Portes, V., Vinet, M.C., Zemni, R., Roest Crollius, H., Carrié, A., Fauchereau, F., Cherry, M., Briault, S., Hamel, B., Fryns, J.P., Beldjord, C., Kahn, A., Moraine, C., Chelly, J., 1998. Oligophrenin-1 encodes a rhoGAP protein involved in X-linked mental retardation. *Nature*, **392**: 923–926.

Blasi, F., Riccio, M., Brogi, a, Strazza, M., Taddei, M.L., Romagnoli, S., Luddi, a, D'Angelo, R., Santi, S., Costantino-Ceccarini, E., Melli, M., 1999. Constitutive expression of interleukin-1beta (IL-1beta) in rat oligodendrocytes. *Biol. Chem.*, **380**: 259–264.

Boda, B., Alberi, S., Nikonenko, I., Node-Langlois, R., Jourdain, P., Moosmayer, M., Parisi-Jourdain, L., Muller, D., 2004. The mental retardation protein PAK3 contributes to synapse formation and plasticity in hippocampus. *J. Neurosci.*, **24**: 10816–10825.

Van Bokhoven, H., 2011. Genetic and epigenetic networks in intellectual disabilities. *Annu. Rev. Genet.*, **45**: 81–104.

Born, T.L., Smith, D.E., Garka, K.E., Renshaw, B.R., Bertles, J.S., Sims, J.E., 2000. Identification and characterization of two members of a novel class of the interleukin-1 receptor (IL-1R) family. Delineation of a new class of IL-1R-related proteins based on signaling. *J. Biol. Chem.*, **275**: 29946–29954.

Braat, S., Kooy, R.F., 2014. Fragile X syndrome neurobiology translates into rational therapy. *Drug Discov. Today*, **19**: 510–519.

Braat, S., Kooy, R.F., 2015a. Insights into GABAAergic system deficits in fragile X syndrome lead to clinical trials. *Neuropharmacology*, **88**: 48–54.

Braat, S., Kooy, R.F., 2015b. The GABAA receptor as a therapeutic target for neurodevelopmental disorders. *Neuron*, **86**: 1119–1130.

Braudeau, J., Dauphinot, L., Duchon, A., Loistron, A., Dodd, R.H., Hérault, Y., Delatour, B., Potier, M.C., 2011. Chronic treatment with a promnesiant GABA-A α5 -selective inverse agonist increases immediate early genes expression during memory processing in mice and rectifies their expression levels in a Down syndrome mouse model. *Adv. Pharmacol. Sci.*, **2011**: 1–11.

Braudeau, J., Delatour, B., Duchon, A., Pereira Lopes, P., Dauphinot, L., de Chaumont, F., Olivo-Marin, J.-C., Dodd, R.H., Hérault, Y., Potier, M.-C., 2011. Specific targeting of the GABA-A receptor α5 subtype by a selective inverse agonist restores cognitive deficits in Down syndrome mice. *J. Psychopharmacol.*, **25**: 1030–1042.

Butler, M., Rafi, S., Hossain, W., Stephan, D., Manzardo, A., 2015. Whole exome sequencing in females with autism implicates novel and candidate genes. *Int. J. Mol. Sci.*, **16**: 1312–1335.

Caramelo, J.J., Parodi, A.J., 2015. A sweet code for glycoprotein folding. *FEBS Lett.* 1–9.

Carrié, A., Jun, L., Bienvenu, T., Vinet, M.C., McDonell, N., Couvert, P., Zemni, R., Cardona, A., Van Buggenhout, G., Frints, S., Hamel, B., Moraine, C., Ropers, H.H., Strom, T., Howell, G.R., Whittaker, A., Ross, M.T., Kahn, A., Fryns, J.P., Beldjord, C., Marynen, P., Chelly, J., 1999. A new member of the IL-1 receptor family highly expressed in hippocampus and involved in X-linked mental retardation. *Nat. Genet.*, **23**: 25–31.

Castets, M., Schaeffer, C., Bechara, E., Schenck, A., Khandjian, E.W., Luche, S., Moine, H., Rabilloud, T., Mandel, J.L., Bardoni, B., 2005. FMRP interferes with the Rac1 pathway and controls actin cytoskeleton dynamics in murine fibroblasts. *Hum. Mol. Genet.*, **14**: 835–844.

Chen, C., Yu, L., Zhang, P., Jiang, J., Zhang, Y., Chen, X., Wu, Q., Wu, Q., Zhao, S., 2002. Human neuronal calcium sensor-1 shows the highest expression level in cerebral cortex. *Neurosci. Lett.*, **319**: 67–70.

Chen, X.L., Zhong, Z.G., Yokoyama, S., Bark, C., Meister, B., Berggren, P.O., Roder, J., Higashida, H., Jeromin, A., 2001. Overexpression of rat neuronal calcium sensor-1 in rodent NG108-15 cells enhances synapse formation and transmission. *J. Physiol.*, **532**: 649–659.

Chin, L.S., Nugent, R.D., Raynor, M.C., Vavalle, J.P., Li, L., 2000. SNIP, a novel SNAP-25-interacting protein implicated in regulated exocytosis. *J. Biol. Chem.*, **275**: 1191–1200.

Cho, K.O., Hunt, C.A., Kennedy, M.B., 1992. The rat brain postsynaptic density fraction contains a homolog of the Drosophila discs-large tumor suppressor protein. *Neuron*, **9**: 929–942.

Choucair, N., Mignon-Ravix, C., Cacciagli, P., Abou Ghoch, J., Fawaz, A., Mégarbané, A., Villard, L., Chouery, E., 2015. Evidence that homozygous PTPRD gene microdeletion causes trigonocephaly, hearing loss, and intellectual disability. *Mol. Cytogenet.*, **8**: 39.

Clement, J., Aceti, M., Creson, T.K., Ozkan, E.D., Shi, Y., Reish, N.J., Almonte, A.G., Miller, B.H., Wiltgen, B.J., Miller, C.A., Xu, X., Rumbaugh, G., 2012. Pathogenic SYNGAP1 mutations impair cognitive development by disrupting the maturation of dendritic spine synapses. *Cell*, **151**: 709–723.

Coffey, E.T., 2014. Nuclear and cytosolic JNK signalling in neurons. *Nat. Rev. Neurosci.*, **15**: 285–299.

Collinson, N., Kuenzi, F.M., Jarolimek, W., Maubach, K.A., Cothliff, R., Sur, C., Smith, A., Otu, F.M., Howell, O., Atack, J.R., Mckernan, R.M., Seabrook, G.R., Dawson, G.R., Whiting, P.J., Rosahl, T.W., 2002. Enhanced learning and memory and altered GABAergic synaptic transmission in mice lacking the alpha 5 subunit of the GABAA receptor. *J. Neurosci.*, **22**: 5572–5580.

Crestani, F., Keist, R., Fritschy, J.-M., Benke, D., Vogt, K., Prut, L., Blüthmann, H., Möhler, H., Rudolph, U., 2002. Trace fear conditioning involves hippocampal alpha5 GABA(A) receptors. *Proc. Natl. Acad. Sci. U. S. A.*, **99**: 8980–8985.

Cullinan, E.B., Kwee, L., Nunes, P., Shuster, D.J., Ju, G., McIntyre, K.W., Chizzonite, R.A., Labow, M.A., 1998. IL-1 receptor accessory protein is an essential component of the IL-1 receptor. *J. Immunol.*, **161**: 5614–5620.

D'Adamo, P., Menegon, A., Lo Nigro, C., Grasso, M., Gulisano, M., Tamanini, F., Bienvenu, T., Gedeon, A.K., Oostra, B., Wu, S.K., Tandon, A., Valtorta, F., Balch, W.E., Chelly, J., Toniolo, D., 1998. Mutations in GDI1 are responsible for X-linked non-specific mental retardation. *Nat. Genet.*, **19**: 134–139.

Dani, V.S., Chang, Q., Maffei, A., Turrigiano, G.G., Jaenisch, R., Nelson, S.B., 2005. Reduced cortical activity due to a shift in the balance between excitation and inhibition in a mouse model of Rett syndrome. *Proc. Natl. Acad. Sci. U. S. A.*, **102**: 12560–12565.

Davis, C.N., Tabarean, I., Gaidarova, S., Behrens, M.M., Bartfai, T., 2006. IL-1b induces a MyD88-dependent and ceramide-mediated activation of Src in anterior hypothalamic neurons. *J. Neurochem.*, **98**: 1379–1389.

Dawson, G.R., Maubach, K.A., Collinson, N., Cobain, M., Everitt, B.J., MacLeod, A.M., Choudhury, H.I., McDonald, L.M., Pillai, G., Rycroft, W., Smith, A.J., Sternfeld, F., Tattersall, F.D., Wafford, K.A., Reynolds, D.S., Seabrook, G.R., Atack, J.R., 2006. An inverse agonist selective for alpha5 subunit-containing GABAA receptors enhances cognition. *J. Pharmacol. Exp. Ther.*, **316**: 1335–1345.

Dinopoulos, A., Stefanou, M.-I., Attilakos, A., Tsirouda, M., Papaevangelou, V., 2014. A case of startle epilepsy associated with IL1RAPL1 gene deletion. *Pediatr. Neurol.*, **51**: 271–274.

Durand, C.M., Betancur, C., Boeckers, T.M., Bockmann, J., Chaste, P., Fauchereau, F., Nygren, G., Rastam, M., Gillberg, I.C., Anckarsäter, H., Sponheim, E., Goubran-Botros, H., Delorme, R., Chabane, N., Mouren-Simeoni, M.-C., de Mas, P., Bieth, E., Rogé, B., Héron, D., Burglen, L., Gillberg, C., Leboyer, M., Bourgeron, T., 2007. Mutations in the gene encoding the synaptic scaffolding protein SHANK3 are associated with autism spectrum disorders. *Nat. Genet.*, **39**: 25–27.

El-Husseini, A.E., Schnell, E., Chetkovich, D.M., Nicoll, R.A., Bredt, D.S., 2000. PSD-95 involvement in maturation of excitatory synapses. *Science*, **290**: 1364–1368.

Elia, J., Gai, X., Xie, H.M., Perin, J.C., Geiger, E., Glessner, J.T., D'arcy, M., DeBerardinis, R., Frackelton, E., Kim, C., Lantieri, F., Muganga, B.M., Wang, L., Takeda, T., Rappaport, E.F., Grant, S.F.A., Berrettini, W., Devoto, M., Shaikh, T.H., Hakonarson, H., White, P.S., 2010. Rare structural variants found in attention-deficit hyperactivity disorder are preferentially associated with neurodevelopmental genes. *Mol. Psychiatry*, **15**: 637–646.

Elias, G.M., Elias, L.A.B., Apostolides, P.F., Kriegstein, A.R., Nicoll, R.A., 2008. Differential trafficking of AMPA and NMDA receptors by SAP102 and PSD-95 underlies synapse development. *Proc. Natl. Acad. Sci. U. S. A.*, **105**: 20953–20958.

Elias, G.M., Funke, L., Stein, V., Grant, S.G., Bredt, D.S., Nicoll, R.A., 2006. Synapse-specific and developmentally regulated targeting of AMPA receptors by a family of MAGUK scaffolding proteins. *Neuron*, **52**: 307–320.

Elzinga, B.M., Twomey, C., Powell, J.C., Harte, F., McCarthy, J. V, 2009. Interleukin-1 receptor type 1 is a substrate for gamma-secretase-dependent regulated intramembrane proteolysis. *J. Biol. Chem.*, **284**: 1394–1409.

Emes, R.D., Pocklington, A.J., Anderson, C.N.G., Bayes, A., Collins, M.O., Vickers, C.A., Croning, M.D.R., Malik, B.R., Choudhary, J.S., Armstrong, J.D., Grant, S.G.N., 2008. Evolutionary expansion and anatomical specialization of synapse proteome complexity. *Nat. Neurosci.*, **11**: 799–806.

Endele, S., Rosenberger, G., Geider, K., Popp, B., Tamer, C., Stefanova, I., Milh, M., Kortüm, F., Fritsch, A., Pientka, F.K., Hellenbroich, Y., Kalscheuer, V.M., Kohlhase, J., Moog, U., Rappold, G., Rauch, A., Ropers, H.-H., von Spiczak, S., Tönnies, H., Villeneuve, N., Villard, L., Zabel, B., Zenker, M., Laube, B., Reis, A., Wieczorek, D., Van Maldergem, L., Kutsche, K., 2010. Mutations in GRIN2A and GRIN2B encoding regulatory subunits of NMDA receptors cause variable neurodevelopmental phenotypes. *Nat. Genet.*, **42**: 1021–1026.

Endris, V., Wogatzky, B., Leimer, U., Bartsch, D., Zatyka, M., Latif, F., Maher, E.R., Tariverdian, G., Kirsch, S., Karch, D., Rappold, G.A., 2002. The novel Rho-GTPase activating gene MEGAP/ srGAP3 has a putative role in severe mental retardation. *Proc. Natl. Acad. Sci. U. S. A.*, **99**: 11754–11759.

Escorihuela, R.M., Fernández-Teruel, A., Vallina, I.F., Baamonde, C., Lumbreras, M.A., Dierssen, M., Tobeña, A., Flórez, J., 1995. A behavioral assessment of Ts65Dn mice: a putative Down syndrome model. *Neurosci. Lett.*, **199**: 143–146.

Farrant, M., Nusser, Z., 2005. Variations on an inhibitory theme: phasic and tonic activation of GABA(A) receptors. *Nat. Rev. Neurosci.*, **6**: 215–229.

Ferrante, M.I., Ghiani, M., Bulfone, A., Franco, B., 2001. IL1RAPL2 maps to Xq22 and is specifically expressed in the central nervous system. *Gene*, **275**: 217–221.

Fox, J.W., Lamperti, E.D., Ekşioğlu, Y.Z., Hong, S.E., Feng, Y., Graham, D.A., Scheffer, I.E., Dobyns, W.B., Hirsch, B.A., Radtke, R.A., Berkovic, S.F., Huttenlocher, P.R., Walsh, C.A., 1998. Mutations in filamin 1 prevent migration of cerebral cortical neurons in human Periventricular heterotopia. *Neuron*, **21**: 1315–1325.

Franek, K.J., Butler, J., Johnson, J., Simensen, R., Friez, M.J., Bartel, F., Moss, T., DuPont, B., Berry, K., Bauman, M., Skinner, C., Stevenson, R.E., Schwartz, C.E., 2011. Deletion of the immunoglobulin domain of IL1RAPL1 results in nonsyndromic X-linked intellectual disability associated with behavioral problems and mild dysmorphism. *Am. J. Med. Genet. A*, **155A**: 1109–1114.

Gambino, F., Kneib, M., Pavlowsky, A., Skala, H., Heitz, S., Vitale, N., Poulin, B., Khelfaoui, M., Chelly, J., Billuart, P., Humeau, Y., 2009. IL1RAPL1 controls inhibitory networks during cerebellar development in mice. *Eur. J. Neurosci.*, **30**: 1476–1486.

Gambino, F., Pavlowsky, A., Béglé, A., Dupont, J.-L., Bahi, N., Courjaret, R., Gardette, R., Hadjkacem, H., Skala, H., Poulain, B., Chelly, J., Vitale, N., Humeau, Y., 2007. IL1-receptor accessory protein-like 1 (IL1RAPL1), a protein involved in cognitive functions, regulates N-type Ca2+-channel and neurite elongation. *Proc. Natl. Acad. Sci. U S A.*, **104**: 2–7.

Gardoni, F., Boraso, M., Zianni, E., Corsini, E., Galli, C.L., Cattabeni, F., Marinovich, M., Di Luca, M., Viviani, B., 2011. Distribution of interleukin-1 receptor complex at the synaptic membrane driven by interleukin-1β and NMDA stimulation. *J. Neuroinflammation*, **8**: 14.

Gatto, C.L., Broadie, K., 2010. Genetic controls balancing excitatory and inhibitory synaptogenesis in neurodevelopmental disorder models. *Front. Synaptic Neurosci.*, **2**: 1–19.

Gayle, D., Ilyin, S.E., Plata-Salamán, C.R., 1997. Central nervous system IL-1 beta system and neuropeptide Y mRNAs during IL-1 beta-induced anorexia in rats. *Brain Res. Bull.*, **44**: 311–317.

Gécz, J., Barnett, S., Liu, J., Hollway, G., Donnelly, a, Eyre, H., Eshkevari, H.S., Baltazar, R., Grunn, a, Nagaraja, R., Gilliam, C., Peltonen, L., Sutherland, G.R., Baron, M., Mulley, J.C., 1999. Characterization of the human glutamate receptor subunit 3 gene (GRIA3), a candidate for bipolar disorder and nonspecific X-linked mental retardation. *Genomics*, **62**: 356–368.

Giannandrea, M., Bianchi, V., Mignogna, M.L., Sirri, A., Carrabino, S., D'Elia, E., Vecellio, M., Russo, S., Cogliati, F., Larizza, L., Ropers, H.H., Tzschach, A., Kalscheuer, V., Oehl-Jaschkowitz, B., Skinner, C., Schwartz, C.E., Gecz, J., Van Esch, H., Raynaud, M., Chelly, J., de Brouwer, A.P.M., Toniolo, D., D'Adamo, P., 2010. Mutations in the small GTPase gene RAB39B are responsible for X-linked mental retardation associated with autism, epilepsy, and macrocephaly. *Am. J. Hum. Genet.*, **86**: 185–195.

Gilmore, J.H., Jarskog, L.F., Vadlamudi, S., Lauder, J.M., 2004. Prenatal infection and risk for schizophrenia: IL-1beta, IL-6, and TNFalpha inhibit cortical neuron dendrite development. *Neuropsychopharmacology*, **29**: 1221–1229.

Gordon, S.L., Cousin, M.A., 2013. X-linked intellectual disability-associated mutations in synaptophysin disrupt synaptobrevin II retrieval. *J. Neurosci.*, **33**: 13695–13700.

Goshen, I., Kreisel, T., Ounallah-Saad, H., Renbaum, P., Zalzstein, Y., Ben-Hur, T., Levy-Lahad, E., Yirmiya, R., 2007. A dual role for interleukin-1 in hippocampal-dependent memory processes. *Psychoneuroendocrinology*, **32**: 1106–1115.

Grant, S.G.N., 2012. Synaptopathies: diseases of the synaptome. *Curr. Opin. Neurobiol.*, **22**: 522–529.

Guggino, W.B., Stanton, B.A., 2006. New insights into cystic fibrosis: molecular switches that regulate CFTR. *Nat. Rev. Mol. Cell Biol.*, **7**: 426–436.

Guo, Y., Su, M., McNutt, M.A., Gu, J., 2009. Expression and distribution of cystic fibrosis transmembrane conductance regulator in neurons of the human brain. *J. Histochem. Cytochem.*, **57**: 1113–1120.

Hackett, A., Tarpey, P.S., Licata, A., Cox, J., Whibley, A., Boyle, J., Rogers, C., Grigg, J., Partington, M., Stevenson, R.E., Tolmie, J., Yates, J.R., Turner, G., Wilson, M., Futreal, A.P., Corbett, M., Shaw, M., Gecz, J., Raymond, F.L., Stratton, M.R., Schwartz, C.E., Abidi, F.E., 2010. CASK mutations are frequent in males and cause X-linked nystagmus and variable XLMR phenotypes. *Eur. J. Hum. Genet.*, **18**: 544–552.

Hamdan, F.F., Daoud, H., Piton, A., Gauthier, J., Dobrzeniecka, S., Krebs, M.O., Joober, R., Lacaille, J.C., Nadeau, A., Milunsky, J.M., Wang, Z., Carmant, L., Mottron, L., Beauchamp, M.H., Rouleau, G.A., Michaud, J.L., 2011. De novo syngap1 mutations in nonsyndromic intellectual disability and autism. *Biol. Psychiatry*, **69**: 898–901.

Hamdan, F.F., Gauthier, J., Araki, Y., Lin, D.T., Yoshizawa, Y., Higashi, K., Park, A.-R., Spiegelman, D., Dobrzeniecka, S., Piton, A., Tomitori, H., Daoud, H., Massicotte, C., Henrion, E., Diallo, O., Shekarabi, M., Marineau, C., Shevell, M., Maranda, B., Mitchell, G., Nadeau, A., D'Anjou, G., Vanasse, M., Srour, M., Lafrenière, R.G., Drapeau, P., Lacaille, J.C., Kim, E., Lee, J.R., Igarashi, K., Huganir, R.L., Rouleau, G.A., Michaud, J.L., 2011. Excess of de novo deleterious mutations in genes associated with glutamatergic systems in nonsyndromic intellectual disability. *Am. J. Hum. Genet.*, **88**: 306–316.

Hamdan, F.F., Gauthier, J., Spiegelman, D., Noreau, A., Yang, Y., Pellerin, S., Dobrzeniecka, S., Côté, M., Perreau-Linck, E., Carmant, L., D'Anjou, G., Fombonne, É., Addington, A.M.,

Rapoport, J.L., Delisi, L.E., Krebs, M.-O., Mouaffak, F., Joober, R., Mottron, L., Drapeau, P., Marineau, C., Lafrenière, R.G., Lacaille, J.C., Rouleau, G.A., Michaud, J.L., 2009. Mutations in SYNGAP1 in autosomal nonsyndromic mental retardation. *N Engl J Med*, **360**: 599–605.

Hamdan, F.F., Piton, A., Gauthier, J., Lortie, A., Dubeau, F., Dobrzeniecka, S., Spiegelman, D., Noreau, A., Pellerin, S., Côté, M., Henrion, E., Fombonne, É., Mottron, L., Marineau, C., Drapeau, P., Lafrenière, R.G., Lacaille, J.C., Rouleau, G.A., Michaud, J.L., 2009. De novo STXBP1 mutations in mental retardation and nonsyndromic epilepsy. *Ann. Neurol.*, **65**: 748–753.

Handley, M.T.W., Lian, L.-Y., Haynes, L.P., Burgoyne, R.D., 2010. Structural and functional deficits in a neuronal calcium sensor-1 mutant identified in a case of autistic spectrum disorder. *PLoS One*, **5**: e10534.

Harrill, J. a, Chen, H., Streifel, K.M., Yang, D., Mundy, W.R., Lein, P.J., 2015. Ontogeny of biochemical, morphological and functional parameters of synaptogenesis in primary cultures of rat hippocampal and cortical neurons. *Mol. Brain*, **8**: 1–15.

Harris, K.M., Jensen, F.E., Tsao, B., 1992. Three-dimensional structure of dendritic spines and synapses in rat hippocampus (CA1) at postnatal day 15 and adult ages: implications for the maturation of synaptic physiology and long-term potentiation. *J. Neurosci.*, **12**: 2685–2705.

Hata, Y., Butz, S., Südhof, T.C., 1996. CASK: a novel dlg/PSD95 homolog with an N-terminal calmodulin-dependent protein kinase domain identified by interaction with neurexins. *J. Neurosci.*, **16**: 2488–2494.

Hayashi, T., Yoshida, T., Ra, M., Taguchi, R., Mishina, M., 2013. IL1RAPL1 associated with mental retardation and autism regulates the formation and stabilization of glutamatergic synapses of cortical neurons through RhoA signaling pathway. *PLoS One*, **8**: e66254.

Honda, S., Hayashi, S., Imoto, I., Toyama, J., Okazawa, H., Nakagawa, E., Goto, Y.-I., Inazawa, J., 2010. Copy-number variations on the X chromosome in Japanese patients with mental retardation detected by array-based comparative genomic hybridization analysis. *J. Hum. Genet.*, **55**: 590–509.

Horii, Y., Beeler, J.F., Sakaguchi, K., Tachibana, M., Miki, T., 1994. A novel oncogene, ost, encodes a guanine nucleotide exchange factor that potentially links Rho and Rac signaling pathways. *EMBO J.*, **13**: 4776–4786.

Houbaert, X., Zhang, C.-L.L., Gambino, F., Lepleux, M., Deshors, M., Normand, E., Levet, F., Ramos, M., Billuart, P., Chelly, J., Herzog, E., Humeau, Y., 2013. Target-specific vulnerability of excitatory synapses leads to deficits in associative memory in a model of intellectual disorder. *J. Neurosci.*, **33**: 13805–13819.

Houge, G., Rasmussen, I.H., Hovland, R., 2012. Loss-of-function CNKSR2 mutation is a likely cause of non-syndromic X-linked intellectual disability. *Mol. Syndromol.*, **2**: 60–63.

Hu, H., Haas, S.A., Chelly, J., Van Esch, H., Raynaud, M., de Brouwer, a P.M., Weinert, S., Froyen, G., Frints, S.G.M., Laumonnier, F., Zemojtel, T., Love, M.I., Richard, H., Emde, A.-K., Bienek, M., Jensen, C., Hambrock, M., Fischer, U., Langnick, C., Feldkamp, M., Wissink-Lindhout, W., Lebrun, N., Castelnau, L., Rucci, J., Montjean, R., Dorseuil, O., Billuart, P., Stuhlmann, T., Shaw, M., Corbett, M.A., Gardner, A., Willis-Owen, S., Tan, C., Friend, K.L., Belet, S., van Roozendaal, K.E.P., Jimenez-Pocquet, M., Moizard, M.-P., Ronce, N., Sun, R., O'Keeffe, S., Chenna, R., van Bömmel, A., Göke, J., Hackett, A., Field, M., Christie, L., Boyle,

J., Haan, E., Nelson, J., Turner, G., Baynam, G., Gillessen-Kaesbach, G., Müller, U., Steinberger, D., Budny, B., Badura-Stronka, M., Latos-Bieleńska, A., Ousager, L.B., Wieacker, P., Rodríguez Criado, G., Bondeson, M.-L., Annerén, G., Dufke, A., Cohen, M., Van Maldergem, L., Vincent-Delorme, C., Echenne, B., Simon-Bouy, B., Kleefstra, T., Willemsen, M., Fryns, J.-P., Devriendt, K., Ullmann, R., Vingron, M., Wrogemann, K., Wienker, T.F., Tzschach, A., van Bokhoven, H., Gecz, J., Jentsch, T.J., Chen, W., Ropers, H.-H., Kalscheuer, V.M., 2015. X-exome sequencing of 405 unresolved families identifies seven novel intellectual disability genes. *Mol. Psychiatry* [Epub ahead of print].

Huang, Y., Smith, D.E., Ibáñez-Sandoval, O., Sims, J.E., Wilma Friedman, J., Huang, Y., Smith, D.E., Ibáñez-Sandoval, O., Sims, J.E., Friedman, W.J., 2011. Neuron-specific effects of interleukin-1β are mediated by a novel isoform of the IL-1 receptor accessory protein. *J. Neurosci.*, **31**: 18048–18059.

Hui, H., McHugh, D., Hannan, M., Zeng, F., Xu, S.-Z., Khan, S.-U.-H., Levenson, R., Beech, D.J., Weiss, J.L., 2006. Calcium-sensing mechanism in TRPC5 channels contributing to retardation of neurite outgrowth. *J. Physiol.*, **572**: 165–172.

Humeau, Y., Gambino, F., Chelly, J., Vitale, N., 2009. X-linked mental retardation: Focus on synaptic function and plasticity. *J. Neurochem.*, **109**: 1–14.

Humeau, Y., Reisel, D., Johnson, A.W., Borchardt, T., Jensen, V., Gebhardt, C., Bosch, V., Gass, P., Bannerman, D.M., Good, M. a, Hvalby, Ø., Sprengel, R., Lüthi, A., 2007. A pathway-specific function for different AMPA receptor subunits in amygdala long-term potentiation and fear conditioning. *J. Neurosci.*, **27**: 10947–10956.

Isaac, J.T.R., Ashby, M., McBain, C.J., 2007. The Role of the GluR2 Subunit in AMPA Receptor Function and Synaptic Plasticity. *Neuron*, **54**: 859–871.

Ito, H., Atsuzawa, K., Sudo, K., Di Stefano, P., Iwamoto, I., Morishita, R., Takei, S., Semba, R., Defilippi, P., Asano, T., Usuda, N., Nagata, K.I., 2008. Characterization of a multidomain adaptor protein, p140Cap, as part of a pre-synaptic complex. *J. Neurochem.*, **107**: 61–72.

Jamain, S., Quach, H., Betancur, C., Råstam, M., Colineaux, C., Gillberg, I.C., Soderstrom, H., Giros, B., Leboyer, M., Gillberg, C., Bourgeron, T., 2003. Mutations of the X-linked genes encoding neuroligins NLGN3 and NLGN4 are associated with autism. *Nat. Genet.*, **34**: 27–29.

Jan, Y.-N., Jan, L.Y., 2010. Branching out: mechanisms of dendritic arborization. *Nat. Rev. Neurosci.*, **11**: 316–328.

Jaworski, J., Kapitein, L.C., Gouveia, S.M., Dortland, B.R., Wulf, P.S., Grigoriev, I., Camera, P., Spangler, S.A., Di Stefano, P., Demmers, J., Krugers, H., Defilippi, P., Akhmanova, A., Hoogenraad, C.C., 2009. Dynamic microtubules regulate dendritic spine morphology and synaptic plasticity. *Neuron*, **61**: 85–100.

Jensen, L.E., Muzio, M., Mantovani, A., Whitehead, A.S., 2000. IL-1 signaling cascade in liver cells and the involvement of a soluble form of the IL-1 receptor accessory protein. *J. Immunol.*, **164**: 5277–5286.

Jensen, L.E., Whitehead, A.S., 2004. The 3' untranslated region of the membrane-bound IL-1R accessory protein mRNA confers tissue-specific destabilization. *J. Immunol.*, **173**: 6248–6258.

Jin, H., Gardner, R.J., Viswesvaraiah, R., Muntoni, F., Roberts, R.G., 2000. Two novel members of the interleukin-1 receptor receptor gene family, one deleted in Xp22.1–Xp21.3 mental retardation. *Eur. J. Hum. Genet.*, **8**: 87–94.

Jinno, S., Jeromin, a., Roder, J., Kosaka, T., 2002. Immunocytochemical localization of neuronal calcium sensor-1 in the hippocampus and cerebellum of the mouse, with special reference to presynaptic terminals. *Neuroscience*, **113**: 449–461.

Jo, J., Heon, S., Kim, M.J., Son, G.H., Park, Y., Henley, J.M., Weiss, J.L., Sheng, M., Collingridge, G.L., Cho, K., 2008. Metabotropic glutamate receptor-mediated LTD involves two interacting Ca2+ sensors, NCS-1 and PICK1. *Neuron*, **60**: 1095–111.

John, G.R., Chen, L., Rivieccio, M. a, Melendez-Vasquez, C. V, Hartley, A., Brosnan, C.F., 2004. Interleukin-1beta induces a reactive astroglial phenotype via deactivation of the Rho GTPase-Rock axis. *J. Neurosci.*, **24**: 2837–2845.

Katsuki, H., Nakai, S., Hirai, Y., Akaji, K., Kiso, Y., Satoh, M., 1990. Interleukin-1 beta inhibits long-term potentiation in the CA3 region of mouse hippocampal slices. *Eur. J. Pharmacol.*, **181**: 323–326.

Kelly, M., Kelly, M., Nadon, L., Nadon, L., Morrison, H., Morrison, H., Thibault, O., Thibault, O., Barnes, A., Barnes, A., Blalock, M., Blalock, M., 2006. The neurobiology of aging. *Epilepsy Res.*, **68S**: S5–S20.

Khan, J.A., Brint, E.K., O'Neill, L.A.J., Tong, L., 2004. Crystal structure of the Toll/interleukin-1 receptor domain of human IL-1RAPL. *J. Biol. Chem.*, **279**: 31664–31670.

Khelfaoui, M., Denis, C., van Galen, E., de Bock, F., Schmitt, A., Houbron, C., Morice, E., Giros, B., Ramakers, G., Fagni, L., Chelly, J., Nosten-Bertrand, M., Billuart, P., 2007. Loss of X-linked mental retardation gene oligophrenin1 in mice impairs spatial memory and leads to ventricular enlargement and dendritic spine immaturity. *J. Neurosci.*, **27**: 9439–9450.

Khelfaoui, M., Pavlowsky, A., Powell, A.D., Valnegri, P., Cheong, K.W., Blandin, Y., Passafaro, M., Jefferys, J.G.R., Chelly, J., Billuart, P., 2009. Inhibition of RhoA pathway rescues the endocytosis defects in Oligophrenin1 mouse model of mental retardation. *Hum. Mol. Genet.*, **18**: 2575–2583.

Killisch, I., Dotti, C.G.C., Laurie, D.J., Lüddens, H., Seeburg, P.H., 1991. Expression patterns of GABAA receptor subtypes in developing hippocampal neurons. *Neuron*, **7**: 927–936.

Kim, E., Sheng, M., 2004. PDZ domain proteins of synapses. *Nat. Rev. Neurosci.*, **5**: 771–781.

Kim, M.J., Dunah, A.W., Wang, Y.T., Sheng, M., 2005. Differential roles of NR2A- and NR2B-containing NMDA receptors in Ras-ERK signaling and AMPA receptor trafficking. *Neuron*, **46**: 745–760.

Kim, M.J., Futai, K., Jo, J., Hayashi, Y., Cho, K., Sheng, M., 2007. Synaptic accumulation of PSD-95 and synaptic function regulated by phosphorylation of serine-295 of PSD-95. *Neuron*, **56**: 488–502.

Kleschevnikov, A.M., Belichenko, P. V, Villar, A.J., Epstein, C.J., Malenka, R.C., Mobley, W.C., 2004. Hippocampal long-term potentiation suppressed by increased inhibition in the Ts65Dn mouse, a genetic model of Down syndrome. *J. Neurosci.*, **24**: 8153–8160.

Kozak, L., Chiurazzi, P., Genuardi, M., Pomponi, M.G., Zollino, M., Neri, G., 1993. Mapping of a gene for non-specific X linked mental retardation : evidence for linkage to chromosomal region Xp21.1-Xp22.3. *J. Med. Genet.*, **30**: 866–869.

Kroon, T., Sierksma, M.C., Meredith, R.M., 2013. Investigating mechanisms underlying neurodevelopmental phenotypes of autistic and intellectual disability disorders : a perspective. *Front. Syst. Neurosci.*, **7**: 75.

Krueger, D.D., Tuffy, L.P., Papadopoulos, T., Brose, N., 2012. The role of neurexins and neuroligins in the formation, maturation, and function of vertebrate synapses. *Curr. Opin. Neurobiol.*, **22**: 412–422.

Kulkarni, V.A., Firestein, B.L., 2012. The dendritic tree and brain disorders. *Mol. Cell. Neurosci.*, **50**: 10–20.

Kwon, S.-K., Woo, J., Kim, S.-Y., Kim, H., Kim, E., 2010. Trans-synaptic adhesions between netrin-G ligand-3 (NGL-3) and receptor tyrosine phosphatases LAR, protein-tyrosine phosphatase delta (PTPdelta), and PTPsigma via specific domains regulate excitatory synapse formation. *J. Biol. Chem.*, **285**: 13966–13978.

Lai, A.Y., Swayze, R.D., El-Husseini, A., Song, C., 2006. Interleukin-1 beta modulates AMPA receptor expression and phosphorylation in hippocampal neurons. *J. Neuroimmunol.*, **175**: 97–106.

Laumonnier, F., Bonnet-Brilhault, F., Gomot, M., Blanc, R., David, A., Moizard, M.-P., Raynaud, M., Ronce, N., Lemonnier, E., Calvas, P., Laudier, B., Chelly, J., Fryns, J.-P., Ropers, H.-H., Hamel, B.C.J., Andres, C., Barthélémy, C., Moraine, C., Briault, S., 2004. X-linked mental retardation and autism are associated with a mutation in the NLGN4 gene, a member of the neuroligin family. *Am. J. Hum. Genet.*, **74**: 552–557.

Lebel, R.R., May, M., Pouls, S., Lubs, H. a, Stevenson, R.E., Schwartz, C.E., 2002. Non-syndromic X-linked mental retardation associated with a missense mutation (P312L) in the FGD1 gene. *Clin. Genet.*, **61**: 139–145.

Ledoux, J.E., 2000. Emotion circuits in the brain. *Annu. Rev. Neurosci.*, **23**: 155–184.

Lee, H.W., Choi, J., Shin, H., Kim, K., Yang, J., Na, M., Choi, S.Y., Kang, G.B., Eom, S.H., Kim, H., Kim, E., 2008. Preso, a novel PSD-95-interacting FERM and PDZ domain protein that regulates dendritic spine morphogenesis. *J. Neurosci.*, **28**: 14546–14556.

Leprêtre, F., Delannoy, V., Froguel, P., Vasseur, F., Montpellier, C., 2003. Dissection of an inverted X(p21.3q27.1) chromosome associated with mental retardation. *Cytogenet. Genome Res.*, **101**: 124–129.

Lesca, G., Till, M., Labalme, A., Vallee, D., Hugonenq, C., Philip, N., Edery, P., Sanlaville, D., 2011. De novo Xq11.11 microdeletion including ARHGEF9 in a boy with mental retardation, epilepsy, macrosomia, and dysmorphic features. *Am. J. Med. Genet. Part A*, **155**: 1706–1711.

Lim, J., Ritt, D.A., Zhou, M., Morrison, D.K., 2014. The CNK2 scaffold interacts with Vilse/ARHGAP39 and modulates Rac cycling during morphogenesis of dendritic spines. *Curr. Biol.*, **24**: 786–792.

Livak, K.J., Schmittgen, T.D., 2001. Analysis of relative gene expression data using real-time quantitative PCR and the 2(-Delta Delta C(T)) method. *Gene Expr.*, **408**: 402–408.

Lu, H.-L., Yang, C.-Y., Chen, H.-C., Hung, C.-S., Chiang, Y.-C., Ting, L.-P., 2008. A novel alternatively spliced interleukin-1 receptor accessory protein mIL-1RAcP687. *Mol. Immunol.*, **45**: 1374–1384.

Malhotra, D., McCarthy, S., Michaelson, J.J., Vacic, V., Burdick, K.E., Yoon, S., Cichon, S., Corvin, A., Gary, S., Gershon, E.S., Gill, M., Karayiorgou, M., Kelsoe, J.R., Krastoshevsky, O., Krause, V., Leibenluft, E., Levy, D.L., Makarov, V., Bhandari, A., Malhotra, A.K., McMahon, F.J., Nöthen, M.M., Potash, J.B., Rietschel, M., Schulze, T.G., Sebat, J., 2011. High frequencies of de novo cnvs in bipolar disorder and schizophrenia. *Neuron*, **72**: 951–963.

Marchler-Bauer, A., Derbyshire, M.K., Gonzales, N.R., Lu, S., Chitsaz, F., Geer, L.Y., Geer, R.C., He, J., Gwadz, M., Hurwitz, D.I., Lanczycki, C.J., Lu, F., Marchler, G.H., Song, J.S., Thanki, N., Wang, Z., Yamashita, R.A., Zhang, D., Zheng, C., Bryant, S.H., 2014. CDD: NCBI's conserved domain database. *Nucleic Acids Res.*, **43**: D222–D226.

Marco, E.J., Abidi, F.E., Bristow, J., Dean, W.B., Cotter, P., Jeremy, R.J., Schwartz, C.E., Sherr, E.H., 2008. ARHGEF9 disruption in a female patient is associated with X linked mental retardation and sensory hyperarousal. *J. Med. Genet.*, **45**: 100–105.

Marshall, C.R., Noor, A., Vincent, J.B., Lionel, A.C., Feuk, L., Skaug, J., Shago, M., Moessner, R., Pinto, D., Ren, Y., Thiruvahindrapduram, B., Fiebig, A., Schreiber, S., Friedman, J., Ketelaars, C.E.J., Vos, Y.J., Ficicioglu, C., Kirkpatrick, S., Nicolson, R., Sloman, L., Summers, A., Gibbons, C. a, Teebi, A., Chitayat, D., Weksberg, R., Thompson, A., Vardy, C., Crosbie, V., Luscombe, S., Baatjes, R., Zwaigenbaum, L., Roberts, W., Fernandez, B., Szatmari, P., Scherer, S.W., 2008. Structural variation of chromosomes in autism spectrum disorder. *J. Hum. Genet.*, **82**: 477–488.

Martínez-Cué, C., Delatour, B., Potier, M.-C.C., 2014. Treating enhanced GABAergic inhibition in Down syndrome: Use of GABA α5-selective inverse agonists. *Neurosci. Biobehav. Rev.*, **46**: 218–227.

Martone, M.E., Edelmann, V.M., Ellisman, M.H., Nef, P., 1999. Cellular and subcellular distribution of the calcium-binding protein NCS-1 in the central nervous system of the rat. *Cell Tissue Res.*, **295**: 395–407.

Matus, A., 2000. Actin-based plasticity in dendritic spines. *Science (80-.).*, **290**: 754–758.

Maurin, T., Zongaro, S., Bardoni, B., 2014. Fragile X Syndrome: From molecular pathology to therapy. *Neurosci. Biobehav. Rev.*, **46**: 242–255.

McCormack, S.G., Stornetta, R.L., Zhu, J.J., 2006. Synaptic AMPA receptor exchange maintains bidirectional plasticity. *Neuron*, **50**: 75–88.

Ben Menachem-Zidon, O., Avital, A., Ben-Menahem, Y., Goshen, I., Kreisel, T., Shmueli, E.M., Segal, M., Ben Hur, T., Yirmiya, R., 2011. Astrocytes support hippocampal-dependent memory and long-term potentiation via interleukin-1 signaling. *Brain. Behav. Immun.*, **25**: 1008–1016.

Mignon-Ravix, C., Cacciagli, P., Choucair, N., Popovici, C., Missirian, C., Milh, M., Mégarbané, A., Busa, T., Julia, S., Girard, N., Badens, C., Sigaudy, S., Philip, N., Villard, L., 2014. Intragenic rearrangements in X-linked intellectual deficiency: Results of a-CGH in a series of

54 patients and identification of TRPC5 and KLHL15 as potential XLID genes. *Am. J. Med. Genet. A*, **9999**: 1–7.

Mikhail, F.M., Lose, E.J., Robin, N.H., Descartes, M.D., Rutledge, K.D., Rutledge, S.L., Korf, B.R., Carroll, A.J., 2011. Clinically relevant single gene or intragenic deletions encompassing critical neurodevelopmental genes in patients with developmental delay, mental retardation, and/or autism spectrum disorders. *Am. J. Med. Genet. A*, **155A**: 2386–2396.

Miller, J.N., Pearce, D.A., 2014. Nonsense-mediated decay in genetic disease: Friend or foe? *Mutat. Res. Mutat. Res.*, **762**: 52–64.

Miller, L.G., Galpern, W.R., Dunlap, K., Dinarello, C.A., Turner, T.J., 1991. Interleukin-1 augments gamma-aminobutyric acidA receptor function in brain. *Mol. Pharmacol.*, **39**: 105–108.

Mishra, A., Kim, H.J., Shin, A.H., Thayer, S.A., 2012. Synapse loss induced by interleukin-1β requires pre- and post-synaptic mechanisms. *J. Neuroimmune Pharmacol.*, **7**: 571–578.

Miyashita, T., Kubik, S., Lewandowsky, G., Guzowski, J.F., 2008. Networks of neurons, networks of genes: an integrated view of memory consolidation. *Neurobiol. Learn. Mem.*, **89**: 269–284.

Molina-Holgado, E., Ortiz, S., Molina-Holgado, F., Guaza, C., 2000. Induction of COX-2 and PGE(2) biosynthesis by IL-1beta is mediated by PKC and mitogen-activated protein kinases in murine astrocytes. *Br. J. Pharmacol.*, **131**: 152–159.

Moysés-Oliveira, M., Guilherme, R.S., Meloni, V.A., Di Battista, A., de Mello, C.B., Bragagnolo, S., Moretti-Ferreira, D., Kosyakova, N., Liehr, T., Carvalheira, G.M., Melaragno, M.I., 2015. X-linked intellectual disability related genes disrupted by balanced X-autosome translocations. *Am. J. Med. Genet. Part B Neuropsychiatr. Genet.* [Epub ahead of print].

Nadif Kasri, N., Nakano-Kobayashi, A., Malinow, R., Li, B., Aelst, L. Van, 2009. The Rho-linked mental retardation protein oligophrenin-1 controls synapse maturation and plasticity by stabilizing AMPA receptors. *Genes Dev.*, **23**: 1289–1302.

Nakano-Kobayashi, A., Kasri, N.N., Newey, S.E., Aelst, L. Van, 2009. The Rho-linked mental retardation protein OPHN1 controls synaptic vesicle endocytosis via endophilin A1. *Curr. Biol.*, **19**: 1133–1139.

Nalivaeva, N.N., Rybakina, E.G., Pivanovich IYu, Kozinets, I.A., Shanin, S.N., Bartfai, T., 2000. Activation of neutral sphingomyelinase by IL-1beta requires the type 1 interleukin 1 receptor. *Cytokine*, **12**: 229–232.

Nawara, M., Klapecki, J., Borg, K., Jurek, M., Moreno, S., Tryfon, J., Bal, J., Chelly, J., Mazurczak, T., 2008. Novel mutation of IL1RAPL1 gene in a nonspecific X-linked mental retardation (MRX) family. *Am. J. Med. Genet. A*, **146A**: 3167–3172.

Newey, S.E., Velamoor, V., Govek, E.E., Van Aelst, L., 2005. Rho GTPases, dendritic structure, and mental retardation. *J. Neurobiol.*, **64**: 58–74.

Nguyen, L., Rothwell, N.J., Pinteaux, E., Boutin, H., 2011. Contribution of interleukin-1 receptor accessory protein B to interleukin-1 actions in neuronal cells. *Neurosignals.*, **19**: 222–230.

Nutt, D.J., Besson, M., Wilson, S.J., Dawson, G.R., Lingford-Hughes, A.R., 2007. Blockade of alcohol's amnestic activity in humans by an α5 subtype benzodiazepine receptor inverse agonist. *Neuropharmacology*, **53**: 810–820.

O'Neill, L.A.J., 2000. The Interleukin-1 Receptor / Toll-like Receptor Superfamily : Signal Transduction During Inflammation and Host Defense. *Sci. STKE*, **44**: 1–11.

Ohnishi, H., Murata, Y., Okazawa, H., Matozaki, T., 2011. Src family kinases: Modulators of neurotransmitter receptor function and behavior. *Trends Neurosci.*, **34**: 629–637.

Olafsson, P., Soares, H.D., Herzog, K.H., Wang, T., Morgan, J.I., Lu, B., 1997. The Ca2+ binding protein, frequenin is a nervous system-specific protein in mouse preferentially localized in neurites. *Mol. Brain Res.*, **44**: 73–82.

Olsen, R.W., Sieghart, W., 2009. GABA A receptors: subtypes provide diversity of function and pharmacology. *Neuropharmacology*, **56**: 141–148.

Parker, L.C., Luheshi, G.N., Rothwell, N.J., Pinteaux, E., 2002. IL-1 beta signalling in glial cells in wildtype and IL-1RI deficient mice. *Br. J. Pharmacol.*, **136**: 312–320.

Pavlowsky, A., 2009. Mécanismes physiopathologiques du déficit cognitif associé aux mutations du gène IL-1 receptor accessory protein like -1. Univeristé Pierre et Marie Curie. *Thèse Dr.*, **Paris**: 220.

Pavlowsky, A., Gianfelice, A., Pallotto, M., Zanchi, A., Vara, H., Khelfaoui, M., Valnegri, P., Rezai, X., Bassani, S., Brambilla, D., Kumpost, J., Blahos, J., Roux, M.J., Humeau, Y., Chelly, J., Passafaro, M., Giustetto, M., Billuart, P., Sala, C., 2010. A postsynaptic signaling pathway that may account for the cognitive defect due to IL1RAPL1 mutation. *Curr. Biol.*, **20**: 103–115.

Pavlowsky, A., Zanchi, A., Pallotto, M., Giustetto, M., Chelly, J., Sala, C., Billuart, P., 2010. Neuronal JNK pathway activation is mediated through IL1RAPL1 , a protein required for development of cognitive functions. *Commun. Integr. Biol.*, **10**: 245–247.

Perronnet, C., Vaillend, C., 2010. Dystrophins, utrophins, and associated scaffolding complexes: Role in mammalian brain and implications for therapeutic strategies. *J. Biomed. Biotechnol.*, **2010**: 970749.

Pfleger, K.D.G., Seeber, R.M., Eidne, K.A., 2006. Bioluminescence resonance energy transfer (BRET) for the real-time detection of protein-protein interactions. *Nat. Protoc.*, **1**: 337–345.

Pinteaux, E., Parker, L.C., Rothwell, N.J., Luheshi, G.N., 2002. Expression of interleukin-1 receptors and their role in interleukin-1 actions in murine microglial cells. *J. Neurochem.*, **83**: 754–763.

Pinto, D., Pagnamenta, A.T., Klei, L., Anney, R., Merico, D., Regan, R., Conroy, J., Magalhaes, T.R., Correia, C., Abrahams, B.S., Almeida, J., Bacchelli, E., Bader, G.D., Bailey, A.J., Baird, G., Battaglia, A., Berney, T., Bolshakova, N., Bölte, S., Bolton, P.F., Bourgeron, T., Brennan, S., Brian, J., Bryson, S.E., Carson, A.R., Casallo, G., Casey, J., Chung, B.H.Y., Cochrane, L., Corsello, C., Crawford, E.L., Crossett, A., Cytrynbaum, C., Dawson, G., de Jonge, M., Delorme, R., Drmic, I., Duketis, E., Duque, F., Estes, A., Farrar, P., Fernandez, B. a, Folstein, S.E., Fombonne, E., Freitag, C.M., Gilbert, J., Gillberg, C., Glessner, J.T., Goldberg, J., Green, A., Green, J., Guter, S.J., Hakonarson, H., Heron, E. a, Hill, M., Holt, R., Howe, J.L., Hughes, G., Hus, V., Igliozzi, R., Kim, C., Klauck, S.M., Kolevzon, A., Korvatska, O., Kustanovich, V., Lajonchere, C.M., Lamb, J. a, Laskawiec, M., Leboyer, M., Le Couteur, A., Leventhal, B.L.,

Lionel, A.C., Liu, X.-Q., Lord, C., Lotspeich, L., Lund, S.C., Maestrini, E., Mahoney, W., Mantoulan, C., Marshall, C.R., McConachie, H., McDougle, C.J., McGrath, J., McMahon, W.M., Merikangas, A., Migita, O., Minshew, N.J., Mirza, G.K., Munson, J., Nelson, S.F., Noakes, C., Noor, A., Nygren, G., Oliveira, G., Papanikolaou, K., Parr, J.R., Parrini, B., Paton, T., Pickles, A., Pilorge, M., Piven, J., Ponting, C.P., Posey, D.J., Poustka, A., Poustka, F., Prasad, A., Ragoussis, J., Renshaw, K., Rickaby, J., Roberts, W., Roeder, K., Roge, B., Rutter, M.L., Bierut, L.J., Rice, J.P., Salt, J., Sansom, K., Sato, D., Segurado, R., Sequeira, A.F., Senman, L., Shah, N., Sheffield, V.C., Soorya, L., Sousa, I., Stein, O., Sykes, N., Stoppioni, V., Strawbridge, C., Tancredi, R., Tansey, K., Thiruvahindrapduram, B., Thompson, A.P., Thomson, S., Tryfon, A., Tsiantis, J., Van Engeland, H., Vincent, J.B., Volkmar, F., Wallace, S., Wang, K., Wang, Z., Wassink, T.H., Webber, C., Weksberg, R., Wing, K., Wittemeyer, K., Wood, S., Wu, J., Yaspan, B.L., Zurawiecki, D., Zwaigenbaum, L., Buxbaum, J.D., Cantor, R.M., Cook, E.H., Coon, H., Cuccaro, M.L., Devlin, B., Ennis, S., Gallagher, L., Geschwind, D.H., Gill, M., Haines, J.L., Hallmayer, J., Miller, J., Monaco, A.P., Nurnberger, J.I., Paterson, A.D., Pericak-Vance, M. a, Schellenberg, G.D., Szatmari, P., Vicente, A.M., Vieland, V.J., Wijsman, E.M., Scherer, S.W., Sutcliffe, J.S., Betancur, C., 2010. Functional impact of global rare copy number variation in autism spectrum disorders. *Nature*, **466**: 368–372.

Pirker, S., Schwarzer, C., Wieselthaler, A., Sieghart, W., Sperk, G., 2000. GABA(A) receptors: Immunocytochemical distribution of 13 subunits in the adult rat brain. *Neuroscience*, **101**: 815–850.

Piton, A., Michaud, J.L., Peng, H., Aradhya, S., Gauthier, J., Mottron, L., Champagne, N., Lafrenière, R.G., Hamdan, F.F., Joober, R., Fombonne, E., Marineau, C., Cossette, P., Dubé, M.-P.P., Haghighi, P., Drapeau, P., Barker, P. a., Carbonetto, S., Rouleau, G.A., 2008. Mutations in the calcium-related gene IL1RAPL1 are associated with autism. *Hum. Mol. Genet.*, **17**: 3965–3974.

Pizzi, M., Goffi, F., Boroni, F., Benarese, M., Perkins, S.E., Liouand, H.C., Spano, P., 2002. Opposing roles for NF-kB/Rel factors p65 and c-Rel in the modulation of neuron survival elicited by glutamate and interleukin-1b. *J. Biol. Chem.*, **277**: 20717–20723.

Pugh, C.R., Fleshner, M., Watkins, L.R., Maier, S.F., Rudy, J.W., 2001. The immune system and memory consolidation: A role for the cytokine IL-1b. *Neurosci. Biobehav. Rev.*, **25**: 29–41.

Pulido, R., Krueger, N.X., Serra-Pagès, C., Saito, H., Streuli, M., 1995. Molecular characterization of the human transmembrane protein-tyrosine phosphatase delta. Evidence for tissue-specific expression of alternative human transmembrane protein-tyrosine phosphatase delta isoforms. *J. Biol. Chem.*, **270**: 6722–6728.

Pulido, R., Serra-Pagès, C., Tang, M., Streuli, M., 1995. The LAR/PTP delta/PTP sigma subfamily of transmembrane protein-tyrosine-phosphatases: multiple human LAR, PTP delta, and PTP sigma isoforms are expressed in a tissue-specific manner and associate with the LAR-interacting protein LIP.1. *Proc. Natl. Acad. Sci. U. S. A.*, **92**: 11686–11690.

Qin, J., Qian, Y., Yao, J., Grace, C., Li, X., 2005. SIGIRR inhibits interleukin-1 receptor- and Toll-like receptor 4-mediated signaling through different mechanisms. *J. Biol. Chem.*, **280**: 25233–25241.

Raemaekers, T., Peric, A., Baatsen, P., Sannerud, R., Declerck, I., Baert, V., Michiels, C., Annaert, W., 2012. ARF6-mediated endosomal transport of Telencephalin affects dendritic filopodia-to-spine maturation. *EMBO J.*, **31**: 3252–3269.

Ramos-Brossier, M., Montani, C., Lebrun, N., Gritti, L., Martin, C., Seminatore-Nole, C., Toussaint, A., Moreno, S., Poirier, K., Dorseuil, O., Chelly, J., Hackett, A., Gecz, J., Bieth, E., Faudet, A., Heron, D., Kooy, R.F., Loeys, B., Humeau, Y., Sala, C., Billuart, P., 2014. Novel IL1RAPL1 mutations associated with intellectual disability impair synaptogenesis. *Hum. Mol. Genet.*, **24**: 1106–1118.

Redin, C., Gerard, B., Lauer, J., Herenger, Y., Muller, J., Quartier, A., Masurel-Paulet, A., Willems, M., Lesca, G., El-Chehadeh, S., Le Gras, S., Vicaire, S., Philipps, M., Dumas, M., Geoffroy, V., Feger, C., Haumesser, N., Alembik, Y., Barth, M., Bonneau, D., Colin, E., Dollfus, H., Doray, B., Delrue, M.-A., Drouin-Garraud, V., Flori, E., Fradin, M., Francannet, C., Goldenberg, A., Lumbroso, S., Mathieu-Dramard, M., Martin-Coignard, D., Lacombe, D., Morin, G., Polge, A., Sukno, S., Thauvin-Robinet, C., Thevenon, J., Doco-Fenzy, M., Genevieve, D., Sarda, P., Edery, P., Isidor, B., Jost, B., Olivier-Faivre, L., Mandel, J.-L., Piton, A., 2014. Efficient strategy for the molecular diagnosis of intellectual disability using targeted high-throughput sequencing. *J. Med. Genet.*, **51**: 724–736.

Reissner, C., Stahn, J., Breuer, D., Klose, M., Pohlentz, G., Mormann, M., Missler, M., 2014. Dystroglycan binding to α-neurexin competes with ceurexophilin-1 and ceuroligin in the brain. *J. Biol. Chem.*, **289**: 27585–27603.

Reutlinger, C., Helbig, I., Gawelczyk, B., Subero, J.I.M., Tönnies, H., Muhle, H., Finsterwalder, K., Vermeer, S., Pfundt, R., Sperner, J., Stefanova, I., Gillessen-Kaesbach, G., Von Spiczak, S., Van Baalen, A., Boor, R., Siebert, R., Stephani, U., Caliebe, A., 2010. Deletions in 16p13 including GRIN2A in patients with intellectual disability, various dysmorphic features, and seizure disorders of the rolandic region. *Epilepsia*, **51**: 1870–1873.

Rock, F.L., Hardiman, G., Timans, J.C., Kastelein, R.A., Bazan, J.F., 1998. A family of human receptors structurally related to Drosophila Toll. *Proc. Natl. Acad. Sci. U. S. A.*, **95**: 588–593.

Romero-Pozuelo, J., Dason, J.S., Atwood, H.L., Ferrús, A., 2007. Chronic and acute alterations in the functional levels of Frequenins 1 and 2 reveal their roles in synaptic transmission and axon terminal morphology. *Eur. J. Neurosci.*, **26**: 2428–2443.

Ropers, H.H., 2010. Genetics of early onset cognitive impairment. *Annu. Rev. Genomics Hum. Genet.*, **11**: 161–187.

Ross, F.M., Allan, S.M., Rothwell, N.J., Verkhratsky, A., 2003. A dual role for interleukin-1 in LTP in mouse hippocampal slices. *J. Neuroimmunol.*, **144**: 61–67.

Rudolph, U., Crestani, F., Benke, D., Brünig, I., Benson, J.A., Fritschy, J.M., Martin, J.R., Bluethmann, H., Möhler, H., 1999. Benzodiazepine actions mediated by specific gamma-aminobutyric acid(A) receptor subtypes. *Nature*, **401**: 796–800.

Rudolph, U., Knoflach, F., 2011. Beyond classical benzodiazepines: Novel therapeutic potential of GABAA receptor subtypes. *Nat. Rev. Drog Discov.*, **10**: 685–697.

Rudolph, U., Möhler, H., 2004. Analysis of GABAA receptor function and dissection of the pharmacology of benzodiazepines and general anesthetics through mouse genetics. *Annu. Rev. Pharmacol. Toxicol.*, **44**: 475–498.

Rumpel, S., LeDoux, J., Zador, A., Malinow, R., 2005. Postsynaptic receptor trafficking underlying a form of associative learning. *Science*, **308**: 83–88.

Saitsu, H., Kato, M., Mizuguchi, T., Hamada, K., Osaka, H., Tohyama, J., Uruno, K., Kumada, S., Nishiyama, K., Nishimura, A., Okada, I., Yoshimura, Y., Hirai, S., Kumada, T., Hayasaka, K., Fukuda, A., Ogata, K., Matsumoto, N., 2008. De novo mutations in the gene encoding STXBP1 (MUNC18-1) cause early infantile epileptic encephalopathy. *Nat. Genet.*, **40**: 782–788.

Sana, T.R., Debets, R., Timans, J.C., Bazan, J.F., Kastelein, R.A., 2000. Computational identification, cloning, and characterization of IL-1R9, a novel interleukin-1 receptor-like gene encoded over an unusually large interval of human chromosome Xq22.2-q22.3. *Genomics*, **69**: 252–262.

Sasaki, R., Inamo, Y., Saitoh, K., Hasegawa, T., Kinoshita, E., Ogata, T., 2003. Mental retardation in a boy with congenital adrenal hypoplasia: a clue to contiguous gene syndrome involving DAX1 and IL1RAPL. *Endocr. J.*, **50**: 303–307.

Sasaki, T., Takai, Y., 1998. The Rho small G protein family-Rho GDI system as a temporal and spatial determinant for cytoskeletal control. *Biochem. Biophys. Res. Commun.*, **245**: 641–645.

Schneider, H., Pitossi, F., Balschun, D., Wagner, A., del Rey, A., Besedovsky, H.O., 1998. A neuromodulatory role of interleukin-1beta in the hippocampus. *Proc. Natl. Acad. Sci. U. S. A.*, **95**: 7778–7783.

Schormair, B., Kemlink, D., Roeske, D., Eckstein, G., Xiong, L., Lichtner, P., Ripke, S., Trenkwalder, C., Zimprich, A., Stiasny-Kolster, K., Oertel, W., Bachmann, C.G., Paulus, W., Högl, B., Frauscher, B., Gschliesser, V., Poewe, W., Peglau, I., Vodicka, P., Vávrová, J., Sonka, K., Nevsimalova, S., Montplaisir, J., Turecki, G., Rouleau, G., Gieger, C., Illig, T., Wichmann, H.-E., Holsboer, F., Müller-Myhsok, B., Meitinger, T., Winkelmann, J., 2008. PTPRD (protein tyrosine phosphatase receptor type delta) is associated with restless legs syndrome. *Nat. Genet.*, **40**: 946–948.

Schreuder, H., Tardif, C., Trump-Kallmeyer, S., Soffientini, A., Sarubbi, E., Akeson, A., Bowlin, T., Yanofsky, S., Barrett, R.W., 1997. A new cytokine-receptor binding mode revealed by the crystal structure of the IL-1 receptor with an antagonist. *Nature*, **386**: 194–200.

Sheng, M., Kim, E., 2011. The postsynaptic organization of synapses. *Cold Spring Harb. Perspect. Biol.*, **3**: a005678.

Shimojima, K., Okanishi, T., Yamamoto, T., 2011. Marfanoid hypermobility caused by an 862kb deletion of Xq22.3 in a patient with Sotos syndrome. *Am. J. Med. Genet. Part A*, **155**: 2293–2297.

Shoubridge, C., Tarpey, P.S., Abidi, F., Ramsden, S.L., Rujirabanjerd, S., Murphy, J.A., Boyle, J., Shaw, M., Gardner, A., Proos, A., Puusepp, H., Raymond, F.L., Schwartz, C.E., Stevenson, R.E., Turner, G., Field, M., Walikonis, R.S., Harvey, R.J., Hackett, A., Futreal, P.A., Stratton, M.R., Gécz, J., 2010. Mutations in the guanine nucleotide exchange factor gene IQSEC2 cause nonsyndromic intellectual disability. *Nat. Genet.*, **42**: 486–488.

Silverman, W., 2007. Down syndrome: Cognitive phenotype. *Ment. Retard. Dev. Disabil. Res. Rev.*, **13**: 228–236.

Sims, J.E., March, C.J., Cosman, D., Widmer, M.B., Macdonald, H.R., Mcmahan, C.J., Grubin, C.E., Wignall, J.M., Jackson, J.L., Call, S.M., Friend, D., Alpert, A.R., Gillis, S., Urdal, D.L.,

Dower, S.K., 1988. cDNA Expression Cloning of the IL-I Receptor, a Member of the Immunoglobulin Superfamily. *Science (80-.).*, **241**: 585–588.

Smeets, R.L., Joosten, L.A.B., Arntz, O.J., Bennink, M.B., Takahashi, N., Carlsen, H., Martin, M.U., Van Den Berg, W.B., Van De Loo, F.A.J., 2005. Soluble interleukin-1 receptor accessory protein ameliorates collagen-induced arthritis by a different mode of action from that of interleukin-1 receptor antagonist. *Arthritis Rheum.*, **52**: 2202–2211.

Smith, D.E., Lipsky, B.P., Russell, C., Ketchem, R.R., Kirchner, J., Hensley, K., Huang, Y., Friedman, W.J., Boissonneault, V., Plante, M.-M.M., Rivest, S., Sims, J.E., 2009. A central nervous system-restricted isoform of the interleukin-1 receptor accessory protein modulates neuronal responses to interleukin-1. *Immunity*, **30**: 817–831.

Smith, D.E., Renshaw, B.R., Ketchem, R.R., Kubin, M., Garka, K.E., Sims, J.E., 2000. Four new members expand the interleukin-1 superfamily. *J. Biol. Chem.*, **275**: 1169–1175.

Spangler, S.A., Schmitz, S.K., Kevenaar, J.T., De Graaff, E., De Wit, H., Demmers, J., Toonen, R.F., Hoogenraad, C.C., 2013. Liprin-a2 promotes the presynaptic recruitment and turnover of RIM1/CASK to facilitate synaptic transmission. *J. Cell Biol.*, **201**: 915–928.

Srinivasan, D., Yen, J.-H., Joseph, D.J., Friedman, W., 2004. Cell type-specific interleukin-1beta signaling in the CNS. *J. Neurosci.*, **24**: 6482–6488.

Srivastava, A.K., Schwartz, C.E., 2014. Intellectual disability and autism spectrum disorders: Causal genes and molecular mechanisms. *Neurosci. Biobehav. Rev.*, **46**: 1–14.

Sternfeld, F., Carling, R.W., Jelley, R.A., Ladduwahetty, T., Merchant, K.J., Moore, K.W., Reeve, A.J., Street, L.J., O'Connor, D., Sohal, B., Atack, J.R., Cook, S., Seabrook, G., Wafford, K., Tattersall, F.D., Collinson, N., Dawson, G.R., Castro, J.L., MacLeod, A.M., 2004. Selective, orally active gamma-aminobutyric acidA alpha5 receptor inverse agonists as cognition enhancers. *J. Med. Chem.*, **47**: 2176–2179.

Steward, O., Falk, P.M., 1986. Protein-synthetic machinery at postsynaptic sites during synaptogenesis: a quantitative study of the association between polyribosomes and developing synapses. *J. Neurosci.*, **6**: 412–423.

Street, L.J., Sternfeld, F., Jelley, R.A., Reeve, A.J., Carling, R.W., Moore, K.W., Mckernan, R.M., Sohal, B., Cook, S., Pike, A., Dawson, G.R., Bromidge, F.A., Wafford, K.A., Seabrook, G.R., Thompson, S.A., Marshall, G., Pillai, G. V, Castro, L., Atack, J.R., MacLeod, A.M., 2004. Synthesis and biological evaluation of 3-heterocyclyl-7,8,9,10-tetrahydro-(7,10-ethano)-1,2,4-triazolo[3,4-a]phthalazines and analogues as subtype-selective inverse agonists for the GABA(A)alpha5 benzodiazepine binding site. *J. Med. Chem.*, **47**: 3642–3657.

Südhof, T.C., 2008. Neuroligins and neurexins link synaptic function to cognitive disease. *Nature*, **455**: 903–911.

Südhof, T.C., 2012. The presynaptic active zone. *Neuron*, **75**: 11–25.

Sun, Q.L., Wang, J., Bookman, R.J., Bixby, J.L., 2000. Growth cone steering by receptor tyrosine phosphatase delta defines a distinct class of guidance cue. *Mol. Cell. Neurosci.*, **16**: 686–695.

Swanwick, C.C., Murthy, N.R., Mtchedlishvili, Z., Siegart, W., Kapur, J., 2006. Development of GABAergic synapses in cultured hippocampal neurons. *J. Comp. Neurol.*, **495**: 497–510.

Symons, J.A., Young, P.R., Duff, G.W., 1995. Soluble type II interleukin 1 (IL-1) receptor binds and blocks processing of IL-1 beta precursor and loses affinity for IL-1 receptor antagonist. *Proc. Natl. Acad. Sci. U. S. A.*, **92**: 1714–1718.

Tabolacci, E., Pomponi, M.G., Pietrobono, R., Terracciano, A., Chiurazzi, P., Neri, G., 2006. A truncating mutation in the IL1RAPL1 gene is responsible for X-linked mental retardation in the MRX21 family. *Am. J. Genet.*, **487**: 482–487.

Takahashi, H., Craig, A.M., 2013. Protein tyrosine phosphatases PTPδ, PTPσ, and LAR: presynaptic hubs for synapse organization. *Trends Neurosci.*, **36**: 522–534.

Takahashi, H., Katayama, K., Sohya, K., Miyamoto, H., Prasad, T., Matsumoto, Y., Ota, M., Yasuda, H., Tsumoto, T., Aruga, J., Craig, A.M., 2012. Selective control of inhibitory synapse development by Slitrk3-PTPδ trans-synaptic interaction. *Nat. Neurosci.*, **15**: 389–398.

Tarpey, P.S., Smith, R., Pleasance, E., Whibley, A., Edkins, S., Hardy, C., Meara, S.O., Latimer, C., Dicks, E., Menzies, A., Stephens, P., Blow, M., Greenman, C., Xue, Y., Tyler-smith, C., Thompson, D., Gray, K., Andrews, J., Barthorpe, S., Buck, G., Cole, J., Dunmore, R., Jones, D., Maddison, M., Mironenko, T., Turner, R., Turrell, K., Varian, J., West, S., Widaa, S., Wray, P., Teague, J., Butler, A., Jenkinson, A., Jia, M., Richardson, D., Shepherd, R., Wooster, R., Tejada, M.I., Martinez, F., Carvill, G., Goliath, R., Brouwer, A.P.M. De, Bokhoven, H. Van, Esch, H. Van, Chelly, J., Raynaud, M., Ropers, H.-H., Abidi, F.E., Srivastava, A.K., Cox, J., Luo, Y., Mallya, U., Moon, J., Parnau, J., Mohammed, S., Tolmie, J.L., Shoubridge, C., Corbett, M., Gardner, A., Haan, E., Rujirabanjerd, S., Shaw, M., Vandeleur, L., Fullston, T., Easton, D.F., Boyle, J., Partington, M., Hackett, A., Field, M., Skinner, C., Stevenson, R.E., Bobrow, M., Turner, G., Schwartz, C.E., Gecz, J., Raymond, F.L., Futreal, P.A., Stratton, M.R., 2009. A systematic, large scale resequencing screen of X-chromosome coding exons in mental retardation. *Nat. Genet.*, **41**: 535–543.

Tau, G.Z., Peterson, B.S., 2010. Normal development of brain circuits. *Neuropsychopharmacology*, **35**: 147–168.

Thomas, G.M., Lin, D.-T.T., Nuriya, M., Huganir, R.L., 2008. Rapid and bi-directional regulation of AMPA receptor phosphorylation and trafficking by JNK. *EMBO J.*, **27**: 361–372.

Thomassen, E., Renshaw, B.R., Sims, J.E., 1999. Identification and characterization of SIGIRR, a molecule representing a novel subtype of the IL-1R superfamily. *Cytokine*, **11**: 389–399.

Tomasoni, R., Repetto, D., Morini, R., Elia, C., Fabrizio, G., Luca, M. Di, Turco, E., Defilippi, P., Matteoli, M., 2013. SNAP-25 regulates spine formation through postsynaptic binding to p140Cap. *Nat. Commun.*, **4**: 2136.

Tonks, N.K., 2006. Protein tyrosine phosphatases: from genes, to function, to disease. *Nat. Rev. Mol. Cell Biol.*, **7**: 833–846.

Tóth, K., McBain, C.J., 1998. Afferent-specific innervation of two distinct AMPA receptor subtypes on single hippocampal interneurons. *Nat. Neurosci.*, **1**: 572–578.

Tsakiri, N., Kimber, I., Rothwell, N.J., Pinteaux, E., 2008. Interleukin-1-induced interleukin-6 synthesis is mediated by the neutral sphingomyelinase/Src kinase pathway in neurones. *Br. J. Pharmacol.*, **153**: 775–783.

Tucker, T., Zahir, F.R., Griffith, M., Delaney, A., Chai, D., Tsang, E., Lemyre, E., Dobrzeniecka, S., Marra, M., Eydoux, P., Langlois, S., Hamdan, F.F., Michaud, J.L., Friedman, J.M., 2013. Single exon-resolution targeted chromosomal microarray analysis of known and candidate intellectual disability genes. *Eur. J. Hum. Genet.*, **22**: 792–800.

Tyagarajan, S.K., Fritschy, J.-M., 2014. Gephyrin: a master regulator of neuronal function? *Nat. Rev. Neurosci.*, **15**: 141–156.

Tzschach, A., Menzel, C., Erdogan, F., Istifli, E.S., Rieger, M., Ovens-Raeder, A., Macke, A., Ropers, H.H., Ullmann, R., Kalscheuer, V., 2010. Characterization of an interstitial 4q32 deletion in a patient with mental retardation and a complex chromosome rearrangement. *Am. J. Med. Genet. Part A*, **152**: 1008–1012.

Uetani, N., Kato, K., Ogura, H., Mizuno, K., Kawano, K., Mikoshiba, K., Yakura, H., Asano, M., Iwakura, Y., 2000. Impaired learning with enhanced hippocampal long-term potentiation in PTPdelta-deficient mice. *EMBO J.*, **19**: 2775–2785.

Utine, G.E., Haliloğlu, G., Volkan-Salanci, B., Çetinkaya, A., Kiper, P.Ö., Alanay, Y., Aktaş, D., Anlar, B., Topçu, M., Boduroğlu, K., Alikaşifoğlu, M., Haliloğlu, G., Volkan-Salancı, B., Cetinkaya, A., Kiper, P.Ö., Alanay, Y., Aktaş, D., Anlar, B., Topçu, M., Boduroğlu, K., Alikaşifoğlu, M., 2014. Etiological yield of SNP microarrays in idiopathic intellectual disability. *Eur. J. Paediatr. Neurol.*, **18**: 1–11.

Vaillend, C., Poirier, R., Laroche, S., 2008. Genes, plasticity and mental retardation. *Behav. Brain Res.*, **192**: 88–105.

Valnegri, P., Montrasio, C., Brambilla, D., Ko, J., Passafaro, M., Sala, C., 2011. The X-linked intellectual disability protein IL1RAPL1 regulates excitatory synapse formation by binding PTPδ and RhoGAP2. *Hum. Mol. Genet.*, **20**: 4797–4809.

Verpelli, C., Montani, C., Vicidomini, C., Heise, C., Sala, C., 2013. Mutations of the synapse genes and intellectual disability syndromes. *Eur. J. Pharmacol.*, **719**: 112–116.

Vithlani, M., Terunuma, M., Moss, S.J., 2011. The dynamic modulation of GABA(A) receptor trafficking and its role in regulating the plasticity of inhibitory synapses. *Physiol. Rev.*, **91**: 1009–1022.

Viviani, B., Bartesaghi, S., Gardoni, F., Vezzani, A., Behrens, M.M., Bartfai, T., Binaglia, M., Corsini, E., Luca, M. Di, Galli, C.L., Marinovich, M., 2003. Interleukin-1 beta Enhances NMDA Receptor-Mediated Intracellular Calcium Increase through Activation of the Src Family of Kinases. , **23**: 8692–8700.

Volk, L., Chiu, S.-L., Sharma, K., Huganir, R.L., 2014. Glutamate Synapses in Human Cognitive Disorders. *Annu. Rev. Neurosci.*, **11**: 127–149.

Wald, D., Qin, J., Zhao, Z., Qian, Y., Naramura, M., Tian, L., Towne, J., Sims, J.E., Stark, G.R., Li, X., 2003. SIGIRR, a negative regulator of Toll-like receptor-interleukin 1 receptor signaling. *Nat. Immunol.*, **4**: 920–927.

Wang, G., Gilbert, J., Man, H.-Y., 2012. AMPA receptor trafficking in homeostatic synaptic plasticity: functional molecules and signaling cascades. *Neural Plast.* 825364.

Wang, J., Bixby, J.L., 1999. Receptor tyrosine phosphatase-delta is a homophilic, neurite-promoting cell adhesion molecular for CNS neurons. *Mol. Cell. Neurosci.*, **14**: 370–384.

Wang, S., Cheng, Q., Malik, S., Yang, J., 2000. Interleukin-1beta inhibits gamma-aminobutyric acid type A (GABA(A)) receptor current in cultured hippocampal neurons. *J. Pharmacol. Exp. Ther.*, **292**: 497–504.

Wang, X., Barone, F.C., Aiyar, N. V., Feuerstein, G.Z., del Zoppo, G.J., 1997. Interleukin-1 Receptor and Receptor Antagonist Gene Expression After Focal Stroke in Rats. *Stroke*, **28**: 155–162.

Wang, X., Venable, J., LaPointe, P., Hutt, D.M., Koulov, A. V., Coppinger, J., Gurkan, C., Kellner, W., Matteson, J., Plutner, H., Riordan, J.R., Kelly, J.W., Yates, J.R., Balch, W.E., 2006. Hsp90 Cochaperone Aha1 Downregulation Rescues Misfolding of CFTR in Cystic Fibrosis. *Cell*, **127**: 803–815.

Whibley, A.C., Plagnol, V., Tarpey, P.S., Abidi, F., Fullston, T., Choma, M.K., Boucher, C.A., Shepherd, L., Willatt, L., Parkin, G., Smith, R., Futreal, P.A., Shaw, M., Boyle, J., Licata, A., Skinner, C., Stevenson, R.E., Turner, G., Field, M., Hackett, A., Schwartz, C.E., Gecz, J., Stratton, M.R., Raymond, F.L., 2010. Fine-scale survey of X chromosome copy number variants and indels underlying intellectual disability. *Am. J. Hum. Genet.*, **87**: 173–188.

Wu, Y., Arai, A.C., Rumbaugh, G., Srivastava, A.K., Turner, G., Hayashi, T., Suzuki, E., Jiang, Y., Zhang, L., Rodriguez, J., Boyle, J., Tarpey, P., Raymond, F.L., Nevelsteen, J., Froyen, G., Stratton, M., Futreal, A., Gecz, J., Stevenson, R., Schwartz, C.E., Valle, D., Huganir, R.L., Wang, T., 2007. Mutations in ionotropic AMPA receptor 3 alter channel properties and are associated with moderate cognitive impairment in humans. *Proc. Natl. Acad. Sci. U. S. A.*, **104**: 18163–18168.

Xu, X., Miller, E.C., Pozzo-Miller, L., 2014. Dendritic spine dysgenesis in Rett syndrome. *Front. Neuroanat.*, **8**: 1–8.

Xu, Y., Tao, X., Shen, B., Horng, T., Medzhitov, R., Manley, J.L., Tong, L., 2000. Structural basis for signal transduction by the Toll / interleukin-1 receptor domains. *Nature*, **408**: 111–115.

Yamagata, A., Sato, Y., Goto-Ito, S., Uemura, T., Maeda, A., Shiroshima, T., Yoshida, T., Fukai, S., 2015. Structure of Slitrk2–PTPδ complex reveals mechanisms for splicing-dependent trans-synaptic adhesion. *Sci. Rep.*, **5**: 9686.

Yamagata, A., Yoshida, T., Sato, Y., Goto-Ito, S., Uemura, T., Maeda, A., Shiroshima, T., Iwasawa-Okamoto, S., Mori, H., Mishina, M., Fukai, S., 2015. Mechanisms of splicing-dependent trans-synaptic adhesion by PTPδ–IL1RAPL1/IL-1RAcP for synaptic differentiation. *Nat. Commun.*, **6**: 6926.

Yamamoto, T., Wilsdon, A., Joss, S., Isidor, B., Erlandsson, A., Suri, M., Sangu, N., Shimada, S., Shimojima, K., Le Caignec, C., Samuelsson, L., Stefanova, M., 2014. An emerging phenotype of Xq22 microdeletions in females with severe intellectual disability, hypotonia and behavioral abnormalities. *J. Hum. Genet.*, **59**: 300–306.

Yan, J., Leal, K., Magupalli, V.G., Nanou, E., Martinez, G.Q., Scheuer, T., Catterall, W. a., 2014. Modulation of CaV2.1 channels by neuronal calcium sensor-1 induces short-term synaptic facilitation. *Mol. Cell. Neurosci.*, **63**: 124–131.

Yang, Q., Li, L., Yang, R., Shen, G.Q., Chen, Q., Foldvary-Schaefer, N., Ondo, W.G., Wang, Q.K., 2011. Family-based and population-based association studies validate PTPRD as a risk factor for restless legs syndrome. *Mov. Disord.*, **26**: 516–519.

Yasumura, M., Yoshida, T., Yamazaki, M., Abe, M., Natsume, R., Kanno, K., Uemura, T., Takao, K., Sakimura, K., Kikusui, T., Miyakawa, T., Mishina, M., 2014. IL1RAPL1 knockout mice show spine density decrease, learning deficiency, hyperactivity and reduced anxiety-like behaviours. *Sci. Rep.*, **4**: 6613.

Yim, Y.S., Kwon, Y., Nam, J., Yoon, H.I., Lee, K., Kim, D.G., Kim, E., Kim, C.H., Ko, J., 2013. Slitrks control excitatory and inhibitory synapse formation with LAR receptor protein tyrosine phosphatases. *Proc. Natl. Acad. Sci. U. S. A.*, **110**: 4057–4062.

Yogev, S., Shen, K., 2014. Cellular and Molecular Mechanisms of Synaptic Specificity. *Annu. Rev. Cell Dev. Biol.*, **30**: 417–437.

Yoshida, T., Mishina, M., 2008. Zebrafish orthologue of mental retardation protein IL1RAPL1 regulates presynaptic differentiation. *Mol. Cell. Neurosci.*, **39**: 218–228.

Yoshida, T., Shiroshima, T., Lee, S.-J., Yasumura, M., Uemura, T., Chen, X., Iwakura, Y., Mishina, M., 2012. Interleukin-1 receptor accessory protein organizes neuronal synaptogenesis as a cell adhesion molecule. *J. Neurosci.*, **32**: 2588–2600.

Yoshida, T., Yasumura, M., Uemura, T., Lee, S.-J.S.J., Ra, M., Taguchi, R., Iwakura, Y., Mishina, M., 2011. IL-1 receptor accessory protein-like 1 associated with mental retardation and autism mediates synapse formation by trans-synaptic interaction with protein tyrosine phosphatase δ. *J. Neurosci.*, **31**: 13485–13499.

Youngs, E.L., Henkhaus, R., Hellings, J.A., Butler, M.G., 2012. IL1RAPL1 gene deletion as a cause of X-linked intellectual disability and dysmorphic features. *Eur. J. Med. Genet.*, **55**: 32–36.

Zemni, R., Bienvenu, T., Vinet, M.C., Sefiani, A., Carrié, A., Billuart, P., McDonell, N., Couvert, P., Francis, F., Chafey, P., Fauchereau, F., Friocourt, G., des Portes, V., Cardona, A., Frints, S., Meindl, A., Brandau, O., Ronce, N., Moraine, C., van Bokhoven, H., Ropers, H.H., Sudbrak, R., Kahn, A., Fryns, J.P., Beldjord, C., Chelly, J., 2000. A new gene involved in X-linked mental retardation identified by analysis of an X;2 balanced translocation. *Nat. Genet.*, **24**: 167–170.

Zhang, C.-L., Houbaert, X., Lepleux, M., Deshors, M., Normand, E., Gambino, F., Herzog, E., Humeau, Y., 2014. The hippocampo-amygdala control of contextual fear expression is affected in a model of intellectual disability. *Brain Struct. Funct.* [Epub ahead of print].

Zhang, Y., Luan, Z., Liu, A., Hu, G., 2001. The scaffolding protein CASK mediates the interaction between rabphilin3a and b-neurexins. *FEBS Lett.*, **497**: 99–102.

Zhang, Y.-H., Huang, B.-L., Niakan, K.K., McCabe, L.L., McCabe, E.R.B., Dipple, K.M., 2004. IL1RAPL1 is associated with mental retardation in patients with complex glycerol kinase deficiency who have deletions extending telomeric of DAX1. *Hum. Mutat.*, **24**: 273.

Zweier, C., de Jong, E.K., Zweier, M., Orrico, A., Ousager, L.B., Collins, A.L., Bijlsma, E.K., Oortveld, M.A.W., Ekici, A.B., Reis, A., Schenck, A., Rauch, A., 2009. CNTNAP2 and NRXN1 are mutated in autosomal-recessive Pitt-Hopkins-like mental retardation and determine the level of a common synaptic protein in Drosophila. *Am. J. Hum. Genet.*, **85**: 655–666.